

## **Nanotechnology: The magic bullet towards attainment of Kenya's Vision 2030 on industrialization**

**E. Gatebe**

*Jomo Kenyatta University of Technology and Agriculture, Nairobi, Kenya*

*Email: erastusgatebe@gmail.com*

Nanotechnology, which is the study of manipulating matter on atomic and molecular scales, involves developing materials or devices possessing at least one dimension sized from 1 to 100 nanometers. Nanomaterials (structures with at least one dimension between 1 and 100 nm) are revolutionizing the scientific world mainly on the account of their unique properties in comparison to the traditional micron-sized materials. There are a large number of new opportunities that could be realized by down-sizing currently existing structures into the regime of <100 nm, or making new types of nanostructures.

For Kenya, nanotechnology provides a new focus for research through her stated aim to manufacture from the 'bottom-up' approach that uses state of the art techniques and tools to make complete, high performance products, with its potential in the form of improved water purification systems, energy systems, healthcare, food production and communications, and in agriculture and health. Recent statistics lament on the lack of Kenyan scientists in applying research and technology in advancement of science due to lethargy in research. Although many reasons have been advanced for lack of growth in this field ranging from poor remuneration, lack of infrastructure as well as lack of well-trained researchers and scientists, the country has an opportunity for take-off through resource mobilization and restructuring. The STI Act 2012 and Education Act 2012 are efforts toward the right direction where the government envisages setting about 2% of the GDP on STI and this should enable our fledging scientists to embrace the new and emerging technologies such as nanotechnology. Also the development of Nanotechnology policy 2013 and creation of new Ministry of Industrialization and Enterprise Development shows the political will to industrialize the country as per Vision 2030 development blue print, otherwise it will remain a pipe dream without these concrete steps.

There are so many raw materials that can be improved through value addition in Kenya for example the rice husks that are normally burned can be used to recover silica which continue to revolutionize electrical and electronic engineering and the compost made into viable fertilizers if appropriate technology is applied such as nanotechnology. The Silicon Valley famed for use of silicon developed from simple concepts as is the case with Embraer in Brazil which has used technology to build the world's third most viable aircraft manufacturer. With the discovery of huge deposits of minerals in Kenya from coal in Mutomo, titanium in Kwale, all the way to oils in Turkana, Kenya has a chance to showcase the benefits of using

appropriate technology in efficient utilization of natural resources for wealth creation and poverty reduction. But for this to happen, the government must invest in quick succession on capacity building while emphasizing on technical and vocational training and desist from converting middle level colleges into universities. For example, by identifying institutions such as KIRDI, KARI and KEMRI among others as flag ship projects to drive the economy, the universities will be left with the tasks of teaching and research while these institutions will act as incubation centers and a link between innovators and end users.

Currently, every local university seeks attention as centers of excellence, incubation centers and research park but this at best remains in their charters with colorful vision and mission statements. Thus, for the jubilee government to achieve on her manifesto, it must empower few research centers with infrastructure such as state of the art equipment like transmission electron microscope(TEM), scanning electron microscope(SEM) which will enable researchers across disciplines benefit; audit existing programs and courses in our universities and TIVET institutions as well as set deliverable targets to CEOs in our local research institution in order to eliminate copycat duplications of programs and research. In line with this, the curricula in our universities and TIVET institutions must be made to embrace new and emerging technologies of delivering their contents. Some of them although have technical names are analog in their teaching and research methodologies. Some lecturers and tutors are computer illiterate yet every year they sign performance contracts. Going technology, nanotechnology will enable this country to industrialize at a quicker pace and catch up with emerging economies which have fully embraced the new thinking through manufacturing, drug delivery, farm input encapsulation which saves millions of dollars in wastage to paint industry thus mitigating on environmental pollution. Nanotechnology, unlike biotechnology, possesses no known serious environmental risks and the technology revolves around minimalization with maximum return. It is on this premise that we hope the new CEO at the ministry of industrialization and enterprise development will assemble a visionary leadership that can help him duplicate the corporate success he had at Barclays Plc.

The author is a senior lecturer at the Department of Chemistry.

## SMALLHOLDER DAIRYING IN KENYA: THE ASSESSMENT OF THE TECHNICAL EFFICIENCY USING THE STOCHASTIC PRODUCTION FRONTIER MODEL

***E. B. Majiwa<sup>1</sup>, M. M. Kavoi<sup>1</sup> and H. Murage<sup>1</sup>***

*<sup>1</sup>Jomo Kenyatta University of Agriculture and Technology*

*Email: eucamajiwa@gmail.com*

### **Abstract**

Dairying in Kenya remains a multi-purpose cattle system providing milk, manure and capital assets to the farmer. Dairy activities in Kenya are predominantly run by smallholders and are concentrated in the high and medium potential areas. Smallholders operating 1-3 dairy cows on small farms are predominant in Kenya. They produce 56% of the total milk in the country and supply 80% of Kenya's marketed milk. Estimated growth in the consumption of milk and dairy products in developing countries is 3.3%, which is in line with Kenya's 3% per year. National statistics show that milk production continues to decline. For example, since 2000 milk annual growth rate has been 1.4% compared to 9.2% experienced between 1980 and 1990. The main challenge of Kenya's dairy industry is how to confront growing milk demand and a highly competitive export environment when yields are as low as 195 litres per lactation. One of the key options is to develop a vibrant competitive dairy sector in Kenya by increasing the efficiency of production. Thus, this study examined the technical efficiency of smallholder dairy farms of rural Kenya. Data from a 2005 survey of smallholder farms in five provinces was utilized to examine the technical efficiency of smallholder farms. The Cobb-Douglas stochastic production frontier model was used to identify the determinants of technical inefficiency. The findings revealed that the mean efficiency was 79 percent, which suggested that 21 percent of production was lost due to technical inefficiency. The technical efficiency also varied across regions ranging from a mean of 83.9% in Central region and 72.5% in Nyanza region. Land size, access to extension service, infrastructure and the level of schooling were found to reduce inefficiency.

**Key words:** Smallholder dairy, technical efficiency, stochastic production frontier

## **1.0 Introduction**

Kenya is a developing country and the agricultural sector is particularly important for its large contribution to national income and employment. Kenya's economy is still heavily dependent on agriculture. The National statistics show that the agricultural sector currently contributes about 26% of Kenya's gross domestic product (GDP) and is a major source of livelihood for the majority of households, especially in the rural areas. The dairy industry is the single largest agricultural sub-sector contributing about 14% of agricultural GDP and 3.5% of total GDP respectively. Omore (1999) has shown that, milk production sustains about 800,000 small-scale farmers who account for 80 per cent of the country's total milk production and offers employment of about 350,000 jobs along the milk marketing chain. Milk sales are beneficial to farmers. Annual net earnings from milk cash income averages \$370 (Ngigi et. al, 2003). The stated Government policy in the National Food Policy and the Kenya Dairy Development Policy is to maintain a position of broad self-sufficiency in food crops, milk and meat production. The policy also seeks to establish reserve stocks that will ensure both the security of food supply and an equitable distribution of foodstuffs to each section of the community.

Currently, the demand for milk is growing because milk is an important part of the diet of both rural and urban Kenyans, with per capita milk consumption of 80-100 litres per year. It has been estimated that annual consumption of milk and dairy products in developing countries will more than double (i.e. from approximately 168 to 391 million tonnes) between 1993 and 2020 (Thorpe et al., 2000). Population growth, urbanization and increased purchasing power are expected to drive this increase in consumption. Estimated growth in the consumption of milk and dairy products in developing countries is 3.3%. This projection is closely in line with Kenya's annual population growth rate of 3%. However, Food and Agriculture Organization (FAO) statistics (2005a) show that the annual milk growth rate in Kenya continues to lag behind the projected consumption and population growth rates. For example since the year 2000 milk annual growth rate has been 1.4% as compared to 9.2% experienced between 1980 and 1990. The productivity per animal remains as low as 195 litres per lactation despite the availability of advanced dairy production technologies when compared with other developing countries like India whose productivity per cow is more than 2000 litres per lactation (Karanja, 2003).

Kenya was a net exporter of dairy products but since 1997, imports have grown and exports declined. The Common Market for Eastern and Southern Africa (COMESA) statistics indicate that currently the milk production in this region is estimated to be 12 million tonnes per year against a demand of 14 million tonnes. The demand for milk and milk products in this region is expected to rise to about 400 million metric tonnes of milk in the year 2020. Thus, given the massive

increases in the demand for food of animal origin that has been predicted for developing countries in the coming years, will the expected large increase in population and demand for milk be met by the current level production? To answer the above question, there was need to know the current efficiency of production of the smallholder dairy farms in rural Kenya since they are the majority of the producers of milk in East Africa as well as in the Sub Saharan region.

The main purpose of this paper was, therefore, to investigate the technical efficiency of smallholder dairy farms in rural Kenya. It also determined the socio economic factors influencing milk yields for small holders.

## **2.0 Methodology**

### **2.1 Data sources and variables**

Cross sectional data was used in this study. The data came from the REPEAT Research on Poverty and Environment and Agricultural Technology survey carried out in 2005 by Temengo Institute of Agricultural Policy and Development, Kenya and the Foundation of Advanced Studies in International Development (FASID), Japan. Stratified random sampling was used to select 900 agricultural households covering five (5) main agricultural provinces of Kenya i.e. Central, Rift Valley, Western, Nyanza and Eastern Provinces. The sample was a national representation of all crop and dairy keeping farmers in the main agricultural provinces. Then a survey of all the respondents was undertaken for the study. A structured questionnaire instrument was used to collect data on physical quantities of inputs, their costs and production of crops and livestock for the period. Household socio-economic variables were also collected during the survey, e.g. assets owned, education level, type of household head i.e. whether female headed or male headed and distance to the nearest urban centre. In the analysis of technical efficiency the regions were classified into the high potential areas (i.e. Central Province) and the medium potential areas (i.e. Rift Valley, Nyanza, Western and Eastern Province). Afterwards the dairy keeping households were selected from the sample. Then data cleaning ensued, removal of outliers was done and observations with missing values were discarded. Ultimately, 474 household cases were used for the stochastic frontier analysis.

Technical efficiency (TE) was estimated simultaneously along with its determinants. The level of efficiency was measured using Cobb Douglas production function; the output and input variables included in the production frontier are described below and summarized in Table 1. Output refers to the total quantity of milk produced measured in litres. The inputs included labor (sum of family and hired labor), number of milking cows, total costs for commercial feeds and veterinary services and the breed type of the cows. The variables for inefficiency model were mainly farm specific factors, farmers specific factors and

organizational factors. These variables included land size; education level of household male and female; off farm income; use of extension services and infrastructure. Land size was measured in acres, education level was measured by the number of years of schooling, off farm income was measured by the total revenue earned outside the farm in Kenyan shillings, infrastructure was captured by the amount of time in hours it took to get to the nearest urban Centre, a dummy variable was used to capture water infrastructure (i.e. 1 if there is water on the farm, 0 otherwise); a dummy variable was used to captures extension service provision using Artificial Insemination service (i.e. 1 if the farmer is served with A.I, 0 otherwise). Finally, a dummy variable was used to differentiate the potential in provinces (i.e. 1 for central province as a high potential area, 0 otherwise). The descriptive statistics are as presented in Table 1.

*Table 1: Descriptive statistics for the variables*

Variable	Units	Mean	Std. Dev	Min	Max
Milk Yield	Yield in litres	4077.66	4005.03	195	38635.82
Labor	Man hours	4.29	2037.07	553.20	13463
Milking cows	Number	4	2	1	18
Cost of feeds	Kenya Shilings	8175.97	6176.80	10	22550
Breed	Type (Improved or local)	0.467	0.423	0	1
Health costs	Kenya Shilings	2004.88	2327.10	0	26600
Land size	Hectares	4.57	4.37	0.2	38
Offincome	Kenya Shilings	19037.95	47795.35	0	440000
Travel time	Hours	0.52	0.23	0.15	1.62
Educ Male	Number of years of schooling	10.16	3.81	0	20
Educ Female	Number of years of schooling	9.14	4.16	0	19
Water	Dummy for yes=1, No =0	0.33	0.63	0	1
A.I Service	Dummy for yes=1, No=0	0.42	0.56	0	1

Source: Tegemeo Institute, Kenya, REPEAT Survey, 2007

The average yield of milk per cow per lactation of the sampled farms was 4077.66 litres while the minimum was 195 litres per lactation. This yield was relatively low compared to other milk producers who realize a minimum of 6000 litres of per cow per lactation such as Israel and South Africa. This yield was obtained by milking 4 cows on average which used: 4.29 Man-hours, expenditures of Kshs. 8175.97 on purchased feeds and Kshs 2004.88 veterinary services and 4.57 Hectares. In addition, farmers spent 30 (0.52\*60) minutes of travelling to the nearest shopping centre. Dairy farmers engaged in off-farm activities realized Kshs. 19037.95. About 47% of the farmers had improved breeds while about 42% had local breeds. Only 33% of the sampled farms had water on farm. About 42% of the farmers used Artificial Insemination service while 56% used bulls.

**2.2 Technical inefficiency effects model**

The technical efficiency of an individual is defined in terms of the ratio of the observed output of the corresponding frontier output conditioned on the level of inputs used by the farm. Technical inefficiency is therefore defined as the ratio of the amount by which the level of production for the farm is less to the frontier output. The use of stochastic frontier production approach is the most popular approach to measure technical efficiency. The stochastic production Frontier function that was first proposed by Aigner, and his colleagues (1977) and Meeuseen and Van den Broecl (1977) is defined as follows:

$$Y_i = f(x_i; \beta) + e_i \dots\dots\dots (1)$$

where  $i = 1, 2, \dots, N$ ,

$$e_i = v_i - u_i,$$

Where  $Y_i$  represents the output level of the  $i$ th sample farm;  $f(x; \beta)$  is a suitable function such as Cobb Douglas or translog production functions of vector  $X_i$  of inputs for the  $i$ th farm and vector  $\beta_i$  of unknown parameters;  $e_i$  is an error term made up of two components,  $v_i$  which is a random error having zero mean  $N(0; \sigma^2)$  associated with for example measurement errors in production and weather conditions which farmers do not have control over and  $u_i$  which is a non negative truncated half normal  $N(0; \sigma^2)$  random variable associated with farm specific factors which leads to the  $i$ th farm not attaining maximum efficiency of production. It is associated with technical efficiency and ranges between zero and one. Thus,

$$\hat{TE}_i = Y_i / Y_i^* \dots\dots\dots (2)$$

where,  $Y_i^* = f(x_i; \beta)$ , highest predicted output for the  $i$ th farm

$$\hat{TE}_i = \text{Exp}(-u_i) = \frac{Y_i}{Y_i^*} (\text{Actualoutput} / \text{Frontieroutput}) \dots\dots\dots (3)$$

$$\text{Technical Inefficiency} = 1 - \hat{TE}_i \dots\dots\dots (4)$$

**2.3 Empirical model specification**

The Cobb Douglas production Frontier was used to specify the stochastic production frontier hence forming the basis for deriving the technical efficiency and its related efficiency measures. The stochastic Cobb Douglas production function was chosen because this functional form has been widely used in farm efficiency analyses for both developing and developed countries. The first

application of the stochastic frontier model to farm-level agricultural data was presented by Battese and Corra (1977). Data from the 1973/74 Australian Grazing Industry Survey were used to estimate deterministic and stochastic Cobb-Douglas production frontiers for the three states included in the Pastoral Zone of Eastern Australia. The variance of the farm effects were found to be a highly significant proportion of the total variability of the logarithm of the value of sheep production in all states. The parameter estimates exceeded 0.95 in all cases, hence the stochastic frontier production functions were significantly different from their corresponding deterministic frontiers. Kalirajan (1981) estimated a stochastic frontier Cobb-Douglas production function using data from 70 rice farmers for the rabi season in a district in India. The variance of farm effects was found to be a highly significant component in describing the variability of rice yields. Bagi (1982a) used the stochastic frontier Cobb-Douglas production function model to determine whether there were any significant differences in the technical efficiencies of small and large crop and mixed-enterprise farms in West Tennessee. The variability of farm effects were found to be highly significant and the mean technical efficiency of mixed-enterprise farms was smaller than that for crop farms (about 0.76 versus 0.85, respectively). However, there did not appear to be significant differences in mean technical efficiency for small and large farms, irrespective of whether the farms were classified according to acreage or value of farm sales. Dawson and Lingard (1989) used a Cobb-Douglas stochastic frontier production function to estimate technical efficiencies of Philippine rice farmers using four years of data.

The individual technical efficiencies ranged between 0.10 and 0.99, with the means between 0.60 and 0.70 for the four years involved. In developing countries, studies on technical efficiency include that of Nega *et al.* (2006) who analyzed the inefficiency of smallholder dairy producers in the central Ethiopian highlands using the stochastic production frontier technique and confirmed the existence of systematic inefficiency in milk production. The average efficiency level of the farmers was only 79% implying that milk output would be attained on average by 21% with the existing technology by training dairy farmers on better production techniques. The study recommended training of farmers on proper feeding, calving, milking, cleaning of cows, storing milk, marketing as well as other management skills to improve efficiency in milk production. Kibaara (2005) analyzed the technical efficiency in Kenya's maize production using a translog production function. The results indicated that maize farmers were 49% efficient with a range of 8 to 98%. The number of years of formal schooling, age of household head, health of the household head, gender of the household head, use or non use of tractors and off-farm income were found to have an impact on technical efficiency.

In this study, the Frontier (4.1) software program was used to estimate the Stochastic Frontier Model. This program used the maximum likelihood technique



for estimation (Coelli 1996). The general non-log form model is specified as follows:

$$y = f(x_1, x_2) \dots\dots\dots (5)$$

The general log form model is specified as follows:

$$y_i = \alpha_0 + \sum_{k=1}^5 \alpha_k \ln x_{ki} + v_i - u_i \dots\dots\dots (6)$$

Where, ln denotes natural logarithms, y and x variables are defined in Table 1, α's are parameters to be estimated. The inefficiency model is estimated from the equation given below.

$$u_i = \delta_0 + \sum_{m=1}^8 \delta_m z_i \dots\dots\dots (7)$$

The variables z<sub>i</sub> are the variables in the inefficiency model. Equation 7 above shows a joint estimation of the stochastic frontier production function in Frontier 4.1.

$$\begin{aligned} \ln y = & \beta_0 + \beta_1 \ln \text{labour} + \beta_2 \ln \text{labour}^2 + \beta_3 \ln \text{cows} + \beta_4 \ln \text{feeds} + \beta_5 \ln \text{othercosts} \\ & + \beta_6 \text{Breed} + \delta_0 + \delta_1 \text{land} + \delta_2 \text{offincome} + \delta_3 \text{traveltime} + \delta_4 \text{schyrsmale} + \delta_5 \text{schyrsfemale} \\ & + \delta_6 \text{watersource} + \delta_7 \text{AIservice} + \delta_8 \text{regionaldummy} + v_i - u_i \end{aligned} \dots\dots\dots 8$$

Where :

- Y= milk yield in litres;
- Feeds = cost of feeds;
- Other costs = Veterinary costs;
- Cows = number of cows;
- Breed = Type of breed (improved or local)
- Labor = labor in man hrs;
- Land size= number of acres of land;
- Offinc = dummy for off farm income Yes =1 No = 0;
- Travel time= time in hrs to the nearest urban centre;
- Educmale = number of years of schooling for males;
- Educfemale = number of years of schooling for females;
- Water= dummy for source of water, has water on the farm: Yes = 1 No =0;
- AI = dummy for AI services, Uses AI: Yes = 1 No =0;
- Regional dummy = dummy for high potential region;
- v<sub>i</sub> - u<sub>i</sub> = error terms, and the former refers to normal statistical error while the latter concerns technical efficiency of farms.

### 3.0 Model estimation results

The estimated coefficients of the production frontier for smallholder dairy farms are presented in Table 2. Most of the estimates were found to be significant at the five percent significance level. The summary statistics on the technical efficiency of individual farms for the 474 smallholder farms are presented in Table 3, which presents the range of technical efficiency scores of the farms and the number of farms within each range.

The mean efficiency of the small dairy farms was 79%, with the highest efficiency value of 94% and the lowest farm efficiency value of 46%. These results clearly rejected the null hypothesis that there was no gap between potential and actual milk production of smallholders' dairy farming in rural Kenya meaning that most farmers had not yet attained full efficiency and there was still potential to increase milk production by 21% on average.

*Table 2: Results of the maximum likelihood estimates of stochastic production function*

Parameter	Coefficient	Standard Error	t-ratio
Beta0	10.359	1.399	7.395***
Labor	-1.109	0.353	-3.139***
labour^2	0.066	0.023	2.935***
Milking cows	0.964	0.044	21.721***
Cost of feeds	0.163	0.015	10.800***
Breed	0.815	0.033	8.213***
Health costs	-0.002	0.015	-0.158
Delta0	1.420	0.907	-1.565
Land size	-0.008	0.079	-0.099
Off farm income	0.017	0.019	0.899
Travel time	0.419	0.195	2.149**
Educ Male	0.385	0.194	1.994**
Educ Female	-0.006	0.095	-0.067
Water	-0.416	0.173	-2.398**
AI service	3.243	1.296	-2.617***
Regional	0.590	0.191	-3.097***
sigma^2	0.692	0.142	4.890***
gamma	0.812	0.049	16.297***

Log likelihood function=-0.27913653E+03

Source: Authors' Analytical Estimates, 2007.

Asterisk indicates: \*significant at 10%, \*\* significant at 5% and \*\*\*significant at 1%.

*Table 3: Results of summary statistics on technical efficiency of individual farms*

Technical Efficiency	Frequency	Percentage
<50	7	1.480
50-59	28	5.91
60-69	60	12.66
70-79	115	24.26
80-89	183	38.61
90-99	81	17.09
Total	474	100

Source: Authors' Analytical Estimates, 2007.

The summary statistics of technical efficiency for the smallholder farms in the five regions presented in Table 4 indicated the diversity of scores of efficiency among regions, which suggests that the diversity in socio economic factors can have different impacts on efficiency in milk production in different regions.

*Table 4: Results of scores of technical efficiency among regions*

Region	Observation	Mean	Std. Dev	Min	Max
Nyanza	73	0.725781	0.109076	0.456	0.906
Western	43	0.750442	0.085484	0.544	0.891
Rift Valley	140	0.768786	0.120632	0.464	0.94
Central	200	0.83924	0.090964	0.479	0.938
Eastern	18	0.7805	0.099433	0.577	0.913

Source: Authors' Analytical Estimates, 2007.

#### **4.0 Technical inefficiency and socio-economic characteristics**

Considering the detailed results, the coefficient of labor was significant at 1% though it had a negative sign, while when labor was squared; the coefficient became positive and statistically significant at 1%. This shows that when labor increased from the present level, milk production declined, but after some time milk production increases. The plausible explanation for this observation being that dairying requires some experience especially on management practices like feeding and not all the laborers may possess this experience. In the absence of such experience in the majority of employed labor, the coefficient tends to be negative. With an increase in experienced labor force, milk production tends to increase as shown by the squared labor term. Another possible explanation is that in most cases, family labor may be used which may not be restricted to only dairying and hence it may be difficult to correctly quantify the amount of time strictly spent on dairying activities.

The coefficient of feeds was positive and statistically significant at 1% as was expected meaning that feeds are critical in milk production and thus an increase in feeding increased milk production. The coefficient of cows was significant at 1% and had a positive sign as was expected, meaning that milk production increased

with the increase in the number of milking cows. The number of cows was a good proxy for farm size. Thus, the higher the number of cows a farmer owns, the higher the milk production.

The coefficient of breed was significant at 1% and had a positive sign as was expected, meaning that milk production increased with the type of breed, improved cows would give more milk than the local breeds. The coefficient of health costs was negative though it was not significant. Normally a high expenditure in health is a proxy for unhealthy animals or poor management and this reduces milk production.

Considering the estimates of the determinants of technical efficiency, the coefficient of land was negative, meaning that land size may reduce inefficiency due to economies of scale, though the coefficient was not statistically significant. The explanation is that in smallholder dairy farms, there is a tendency of integrating dairy and the growing of food or cash crops on the same piece of land; hence, economies of scale may not be realized. Furthermore, intensification of dairy, such as zero grazing, is enabling farmers to keep cows without necessarily having land as long as they have a source of feeds. Thus, land may not have an impact on efficiency.

The coefficient of off farm income was positive, meaning that an increase in off farm income may increase inefficiency, but this coefficient was not statistically significant. This may indicate that the surveyed farmers may solely be depending on farming and therefore the off farm activities do not affect their farm activities. The coefficient of years of schooling for males was positive and statistically significant at 5%, which clearly indicates that more years of schooling for males increases their inefficiency in milk production, while the coefficient of that of females was negative but was not statistically significant. The major argument is that with more years of schooling, males tend to get off farm employment and income activities, which may result in dairying inefficiency.

The coefficient of travel time to the nearest urban centre which was a proxy for infrastructure was positive and statistically significant at 1%, meaning that inefficiency increased when more time was taken in traveling to the nearest urban centre. Bad roads are evident in most rural areas of Kenya and thus it takes a lot of time to get milk to the market and to get the inputs to the farms especially the feeds. Bad roads also deter extension services from being effective, thus increasing inefficiency. Milk production requires speedy transportation to the market and requires easy access to commercial feeds and artificial insemination services which are obtainable from the nearest urban centres.

The dummy for source of water at the farm was negative and statistically significant at 1%, meaning that having water on the farm reduced inefficiency. Dairying requires water throughout and access to water on the farm cannot be overemphasized.

The dummy for artificial insemination was negative and statistically significant at 1%, meaning that it reduced inefficiency to use artificial insemination. Artificial insemination was a good proxy for extension service. Artificial insemination allows farmers to upgrade their animals and reduces fertility diseases such as brucellosis, which reduce milk production. Thus, Artificial Insemination helps in reducing inefficiency. The government provided this service to the farmers up to 1992 when the dairy industry was liberalized and the private agents started to offer this service.

The regional dummy that represented the high potential areas (i.e. Central Province) was negative and statistically significant at 1%. This means that being in a high potential region reduces technical inefficiency. This region is noticeable for its good infrastructure, high quality breeds and its close proximity to the capital city of Nairobi, where most of the milk is sold and inputs especially the commercial feeds are processed.

## **5.0 Policy implications and recommendations**

One of the important policy implications concerns technology. Feeds were found to reduce inefficiency. Technologies that will enable the farmers to produce feeds cheaply should be introduced as several farmers depend on manufactured feeds besides grazing land to feed milking cows, it is thus imperative to facilitate easy access to manufactured feeds at affordable prices. The government needs to encourage production of manufactured feeds by promoting industrial activities.

Another policy implication is to make the artificial insemination services affordable to farmers since it reduces inefficiency. This will help the farmers to upgrade their dairy cows without using the traditional bulls that may have low quality genetic potential and are capable of transmitting breeding diseases.

Importantly, the government needs to improve infrastructure especially rural roads, which in most cases are in a deplorable condition. This will enable the farmers to access the inputs and to market their produce with ease. This is not only beneficial to the milk producers but also to the other agricultural activities. Water is an important input in dairy production and its supply on farms cannot be overemphasized. The supply can be piped water or borehole water and this will greatly reduce the inconvenience and the time that the farmers have to take to fetch water for their animals. This will also save useful labor time that can be used in other farming activities.

### Acknowledgements

We acknowledge the Japan International Cooperation Agency (JICA) for the financial assistance to undertake a Masters Degree Program and a Thesis in National Graduate Institute of Policy Studies, Japan from which this research article was extracted. We are also grateful to Tegemeo Institute of Agricultural Policy and Development for providing household survey data used in this study. Finally, special thanks go to Prof. Kaliappa Kalirajan for his input in this paper.

### References

- Ahmad M. and Bravo-Ureta B. (1995). "Technical efficiency measures for US dairy farms using panel data: A comparison of alternative model specifications". *American Journal of Agricultural Economics*, **77**, pp. 914-921.
- Aigner D. K., Lovell C. K. and Schmidt P. (1977). "Formulation and Estimation of Stochastic: Frontier Production Function Models". *Journal of Econometrics*, **6**, pp. 21-37.
- Ali M. and Flinn J. (1989). "Profit efficiency among Basmati rice producers in Pakistan" *American Journal of Agricultural Economics*, **71**, pp. 303-310.
- Alvarez A. and Arias, C. (2004). "Technical efficiency and farm size: A conditional analysis of Spanish dairy farms". *American Journal of Agricultural Economics*, **30 (3)**, pp. 241-50.
- Bagi F. S. (1982a). "Relationship Between Farm Size and Technical Efficiency in West Tennessee Agriculture". *Southern Journal of Agricultural Economics*, **14**, pp. 139-144.
- Battese G.E. and Corra G.S. (1977). "Estimation of a Production Frontier Model: With Application to the Pastoral Zone of Eastern Australia". *Australian Journal of Agricultural Economics*, **21**, pp. 169-179.
- Central Bureau of Statistics (2002). "Economic Survey, 2002", Ministry of Finance and Planning, Nairobi, Kenya.
- Coelli T. J. 1995. "Recent development in frontier estimation and efficiency measurement", *Australia Journal of Agricultural Economics*, **39**, pp. 219-245.
- Dawson P. J. and J. Lingard (1989). "Measuring Farm Efficiency Over Time on Philippine Rice Farms", *Journal of Agricultural Economics*, **40**, pp. 168-177.
- Food and Agricultural Organization. (2005). FAOSTAT Data, Food and Agriculture Organization, Rome.
- Farrell M., (1957). "The measurement of productive efficiency". *Journal of Royal Statistical Society, Series A (General)*, **120 (3)**, pp. 253-282.
- Huang Y. and Kalirajan K. P. (1997). "Potential of China's grain production evidence from the household data". *Agricultural Economics Elsevier*, **17(2)**, pp. 191-199.

Jacoby H. G. (2000). "Access to markets and the benefits of rural roads", *Economic Journal* **110 (465)**, pp. 713-737.

Kalirajan K. (1981). "An Econometric Analysis of Yield Variability in Paddy Production". *Canadian Journal of Agricultural Economics*, **29**, pp. 283-294.

Kalirajan K. P and Shand R. T. (1994). "Economies in Disequilibrium: A view from the Frontier", Macmillan, New Delhi.

Karanja A. (2003). "The dairy industry in Kenya: Post liberalization agenda" Working Paper, Tegemeo Agricultural Monitoring and Policy Analysis Project.

Karanja D. D., Jayne S. T. and Strasberg P. (1998). "Maize productivity and impact of market liberalization in Kenya" Working Paper, Tegemeo Agricultural Monitoring and Policy Analysis Project.

Kategile J. A and Mubi S. (1992). "Future of livestock industries in East and southern Africa". Proceedings of a workshop held at Kadoma Ranch Hotel, Zimbabwe, July 20-23.

Kompas T. and Tuong N. C. (2004). Production and technical efficiency on Australian dairy farms. International and Development Economics Paper 04-1.

Kopp R. J. and Diewert W. E. (1982). "The Decomposition of Frontier Cost Function Deviations into Measures of Technical and Allocative Efficiency". *Journal of Econometrics*, **19**, pp. 319-332.

Kopp R. J. (1981). "The Measurement of Productive Efficiency: A Reconsideration". *Quarterly Journal of Economics* **96**, pp. 477-503.

Kumbhakar S. C., Ghosh S. and McGuckin J. (1991). "A generalized production frontier approach for estimating determinants of inefficiency in United States dairy farms". *Journal of Business, Economics and Statistics*, **9**, pp. 279-286.

Kumbhakar S. C., Biswas B. and Bailey D. (1989). "A study of Economic Efficiency of Utah Dairy Farmers: A system Approach". *The review of Economics and Statistics*, MIT Press, **71 (4)**, pp. 595

Leibenstein H. (1966). "Allocative Efficiency vs. 'X-Efficiency". *American Economic Review* **56**(June): pp. 392-415.

Meeusen W and Vaden Broeck J. (1977). "Efficiency estimation from Cobb Douglas production function with composed error" *International Economics Review*, **18**, pp. 435-444.

Ministry of Agriculture, Livestock Development and Marketing, Kenya. (1993a). Sessional Paper on National Food Policy, **3**, pp. 53.

Muriuki H. G. (2002). "Smallholder dairy production and marketing in Kenya: Regional synthesis". Proceedings of a South-South workshop on Smallholder dairy production and marketing-Opportunities and constraints held at NDDDB, Anand, India, 13-16 March 2001.

Mwangi D. M. and Staal S. J. (2004). "Understanding the role of dairy in smallholder system and the effect of intensification". Paper presented at the 9th KARI Biennial Scientific Conference/Kenya Agricultural Research Forum, Nairobi, November 8-12.

Yamano T., Otsuka K., Place F., Kijima, Y and Nyoro J. (2005). "The 2005 REPEAT (Research on Poverty and Environment and Agricultural Technology) survey in Kenya".

Nega W. and Simeon E. (2006). Technical Efficiency of Smallholder Dairy Farmers in the Central Ethiopian Highlands. Paper presented at the International Association of Agricultural Economists Conference, Gold Coast, Australia, August 12-18, 2006

Ngigi M. (2003). "The case of smallholder Dairying in Eastern Africa". Paper presented at the 2003 InWEnt, IFPRI, NEPAD, CTA conference "Successes in African Agriculture" Pretoria, December 1-3.

Omoro A., Muriuki H., Kenyanjui M., Owango, M. and Staal S. (1999). "The Kenya Dairy Sub-Sector: A Rapid Appraisal". Smallholder Dairy (Research & Development) Project Report, 51.

Peeler E. J. and Omoro A. (1997). "Manual of livestock production systems in Kenya". 2nd edition. KARI (Kenya Agricultural Research Institute), Nairobi, Kenya, 138.

Romney D., Kaitho R., Biwott J., Wambugu M., Chege L., Omoro A., Staal S., Wanjohi P. and Thorpe W. (2000). "Technology Development and Field Testing: Access to credit to allow smallholder dairy farmers in central Kenya to reallocate concentrates during lactation". Paper presented at the 11th Conference of the Egyptian Society of Animal Production, Alexandria, Egypt, November 6-9.

Romney D. L., Njubi D., Njoroge L., Nyangaga J., Waithaka, M., Muriuki, H.G. Wokabi A., Staal J., Waithaka M., Njoroge L., Mwangi D. M., Njubi D. and Wokabi, A. (2003). "Costs of milk production in Kenya": Estimates from Kiambu, Nakuru and Nyandarua districts. Smallholder Dairy (R&D) Project, Report 1.

Tangka F., Ouma E. A., Staal S. J. and Shapiro B. (1999). "Women and the sustainable development of market-oriented dairying: Evidence from the highlands of East Africa". Paper presented at the International Sustainable Development Research Conference held at University of Leeds, Leeds, UK, March 25 - 26.

Thorpe W., Muriuki, H. G., Omoro, A., Owango, M.O. and Staal, S. (2000). "Dairy Development in Kenya: The past, the present and the future". Paper presented at the Annual Symposium of the Animal Production Society of Kenya, Nairobi, March 22-23.



## EFFECT OF RAIN WATER HARVESTING AND DRIP IRRIGATION ON CROP PERFORMANCE IN AN ARID AND SEMI-ARID ENVIRONMENT

**J. W. Kaluli<sup>1</sup>, K. Nganga<sup>1</sup>, P. G.Home<sup>1</sup>, J. M. Gathenya<sup>1</sup>, A.W. Muriuki<sup>2</sup> and A. W. Kihurani<sup>1</sup>**

<sup>1</sup>Jomo Kenyatta University of Agriculture and Technology, Kenya

<sup>2</sup>Kenya Agricultural Research Institute (KARI)

Email: wambuak@gmail.com

### Abstract

Rainwater harvesting and drip irrigation are possible interventions to enhance crop performance in Arid and Semi-Arid Lands (ASAL). Work was undertaken to evaluate the feasibility of rainwater harvesting for bean production under an ASAL environment in Kaiti Watershed, Makueni District, Kenya. Treatments comprised two rainwater harvesting methods, Zai pits and contour ridges; bucket-kit drip irrigation and a control. No intervention was made to enhance water availability in the crop root zone in the control. The experiment was arranged in a Randomized Complete Block Design with three replicates. Each of the 12 experimental plots was planted with beans (*Phaseolus vulgaris* L.), variety GLP 2. Soil moisture content and pan evaporation were measured daily for 100 days and runoff after every rainfall event. Crop height was measured once a week and grain and biomass yield were determined at the end of the growing season. Soil moisture content and crop performance were significantly influenced by drip irrigation but not by rainwater harvesting. In drip irrigated plots, grain and biomass yield, were 4 tonnes ha<sup>-1</sup> and 9 tonnes ha<sup>-1</sup> respectively compared to 3.5 tonnes ha<sup>-1</sup> and 7.5 tonnes ha<sup>-1</sup> respectively, in the control plots. Drip irrigation effectively maintained adequate soil moisture resulting in better crop performance while rain water harvesting methods failed to significantly enhance soil moisture content and crop performance. This study indicated that rainwater harvesting makes a difference in runoff when the 14 Day Antecedent Precipitation (14DAP) exceeds 80 mm. However, the grain yield obtained in all the plots was higher than the national average of 0.36 tonnes Ha<sup>-1</sup>. It is recommended that further research be done under different rainfall conditions to confirm the conditions under which the benefits of rainwater harvesting using contour ridges and zai pits can be realized in the enhancement of crop performance in ASAL conditions.

**Key words:** ASAL, soil moisture content, *Phaseolus vulgaris* L, Zai pits, contour ridges drip irrigation, rainwater harvesting

## 1.0 Introduction

Water that is held in the spaces between soil particles is referred to as soil moisture. Surface soil moisture is the water stored in the upper 10 cm of soil. The root zone depth, depending on the crop varies between 60 cm for shallow rooted crops like cabbage to about 200 cm for deep rooted crops such as citrus (Michael, 1978). Compared to other components of the hydrologic cycle, the volume of soil moisture is small; nonetheless, it is of fundamental importance to many hydrological, biological and biogeochemical processes. Soil moisture information is valuable to those who are concerned with weather and climate, runoff potential and flood control, soil erosion and slope failure, reservoir management, geotechnical engineering, and water quality.

Arid and Semi Arid Lands (ASAL) are those areas characterized by low, poorly distributed, and highly variable rainfall within 100-600 mm per year (Mugwe et al, 1999). The ASAL in Kenya covers over 80 % of the country. These vast lands are generally poor and experience food scarcity. Accurate knowledge of soil water content, in ASAL areas is essential for proper soil water management, irrigation scheduling and crop production. However, the data necessary for sound agricultural water management is often scarce.

Studies have shown that agriculture in the ASALs of East Africa is mostly rain-fed (Hatibu and Mahoo, 2000; Critchley, *et al.* 1999). Therefore, moisture stress is a major constraint against food production in these areas. Demand for water use in agriculture will continue to increase as a result of growing population and economic growth (Rosegrant, 2009). This is a threat to food security. To guarantee food security, sound Agricultural Water Management (AWM) is necessary. AWM includes all deliberate human actions designed to optimize the availability and utilization of water for agricultural purposes (Mati, 2007). AWM include practices such as irrigation (supplemental or full), drainage, soil and water conservation, rainwater harvesting, soil fertility management, conservation agriculture and wastewater reuse among others. Sound agricultural management should ensure that available rainwater becomes useful to crops and that it is not used for negative impacts such as soil erosion. Wei *et al.* (2007) showed that surface runoff depends on the antecedent moisture conditions, and that when it rains during wet conditions, much of the rainwater is likely to be lost as runoff. Soil and water conservation with water harvesting, is one of the techniques for supporting rain-fed agriculture in the ASAL (Hai, 1998; Mati, 2006), where bean crop failure is observed during 3 out of every 10 seasons (Jaetzold (2007). On-farm rainwater harvesting using structures such as pits, bunds, basins and contour ridges preserve soil moisture and result in improved crop yields (Kaluli *et al.*, 2005; Gathenya and Kaluli, 2004). Zai pits, usually with a diameter of 0.3-0.6 m and 0.3 m deep, are used to harvest rain water at farm level. Manure may be put into the pits to improve soil fertility. Retaining the water in a pit prevents it from running off the farm and makes water available for crops. Another way of making water available for crop production is through the use of contour ridges and trenches. Ridging is the construction of furrows along a contour at a spacing of 1-2 m (Mati, 2007). In East and Southern Africa ridging is done for high value crops such as potatoes, groundnuts and

maize. Ridging and pits retard surface runoff, improve infiltration, and reduce soil erosion.

This project was conducted in Kaiti watershed which receives between 300 to 500 mm of rainfall annually (Nderitu, 2006). Dry spells of 2 weeks to 1 month during the growing season are a common feature in this area. Furthermore, soil erosion and degradation of organic matter, soil physical characteristics and soil fertility in Kaiti watershed make crops susceptible to water deficits. Information on soil water availability and the relationships between crop production and crop water use during the growing season is needed to assess crop water requirements and make good schedules for irrigation (Michael, 1978). This knowledge can be used to improve water use efficiencies and increase returns to the producer. Such information can also help farmers and the government to make better plans for development. Using the common bean (*Phaseolus vulgaris* L.), as the test crop, the effect of on-farm rain water harvesting on soil moisture and crop yield in the ASAL environment of Kaiti watershed was investigated, with the objective of providing information on the most suitable rainwater management technologies for arid

## **2.0 Materials and methods**

### **2.1 Location of the study site**

The research site, Kaiti watershed (1°44'1.5"S to 1°47'19.3"S; 37°13'13.4"E to 37°41'25.2"E), is located within the greater Makueni District, which borders Kajiado District to the west, Taita Taveta to the southeast, Kitui to the east and Machakos District to the North (Figure 1). It is typically ASAL with minimum monthly mean temperature of 10°C in July and a maximum of about 30°C in February. The rainfall pattern is bimodal, but generally scarce, with significant differences in distribution during different years. Average annual rainfall ranges from slightly over 1000 mm in the higher rainfall areas to less than 500 mm in the low lying south and southeastern parts of the district (Gichuki, 2000). The dry season falls between the months of January and February and between August and September. The average slope is 15-30% and the soil is deep sandy clay loam.

### **2.2 Experimental design**

The study was carried out for 100 days from October 1, 2005 to January 8, 2006. Treatments comprised two rainwater harvesting methods, Zai pits and contour ridges, bucket-kit drip irrigation and a control. The Zai pits had a diameter of 30 cm and a depth of 30 cm. They were dug at a spacing of 90 cm between rows and 60 cm within the row. The contour ridges were 25 cm high and they were constructed at a spacing of 100 cm. The bucket-kit drip irrigation was set up at 1.0 m high on a wooden stand placed at the highest point of the plot. The water was filtered to remove sediments before being placed in the bucket to prevent clogging of the drip emitters. In the control no intervention was applied to enhance water availability.

The treatments were randomly allocated to experimental plots that were 3 m wide, along the contour, and 10 m long. The experiment was arranged in a Randomized

Complete Block Design (RCBD) with three replicates (Figure 2). To reduce interference between plots, galvanized iron sheets were placed around individual plots and placed at 30 cm below the ground and extended 30 cm above the ground. A 2 m buffer zone was also created between blocks. Each plot was planted with a bean crop (*Phaseolus vulgaris* L.), variety GLP 2 popularly known as “nyayo”. In each treatment the beans were spaced at 15 cm to give a plant population of 17 per m<sup>2</sup>. Farm yard manure was applied at the rate of 10 ton ha<sup>-1</sup> and Diammonium phosphate (DAP) fertilizer at 200 kg ha<sup>-1</sup>.

### **2.3 Land preparation**

Land preparation, which involved digging using a hoe followed by harrowing, was carried out in late September and early October, 2005, before the onset of the rains. The land was then graded to achieve uniform slope within each block.

### **2.4 Drip irrigation and runoff measurement**

Drip irrigation is a method of watering plants through devices called emitters (Figure 3). Drops of water come out one at a time to wet the soil around the roots of the plant. The “bucket drip kit” used in this study is a simple drip system commonly used by farmers in home gardens. It is made up of a bucket, a filter, connectors and a drip tape. Some 4 mm of water was applied daily through drip irrigation from November 20, 2005 to December 13, 2005. By this time the crop had matured to the point that it would not be affected by lack of irrigation water. For all treatments, a 50 mm PVC pipe was fixed at the outfall of each plot and directed into a 20 litre plastic container. The amount of runoff collected in the containers was measured at the end of each rainfall event.

### **2.5 Measurement of rainfall, evaporation and soil moisture**

Soil moisture content and pan evaporation were measured daily during the study period with the help of a tensiometer placed at a depth of 15 cm, and Class A Evaporation pan, respectively. A rain gauge was used to measure daily rainfall.

### **2.6 Measurement of crop performance**

The crop data collected included crop height, measured once a week; and grain and biomass yield for each treatment measured at the end of the experiment. Biomass was measured by uprooting randomly selected mature plants and weighing them. The beans were then threshed and the grain separated from the straws. Further weighing was then done. This gave the weight of grain as well as the weight of total biomass. At least twelve plants were sampled from every plot. To ease identification of the sampled plants the selected plants were tagged.

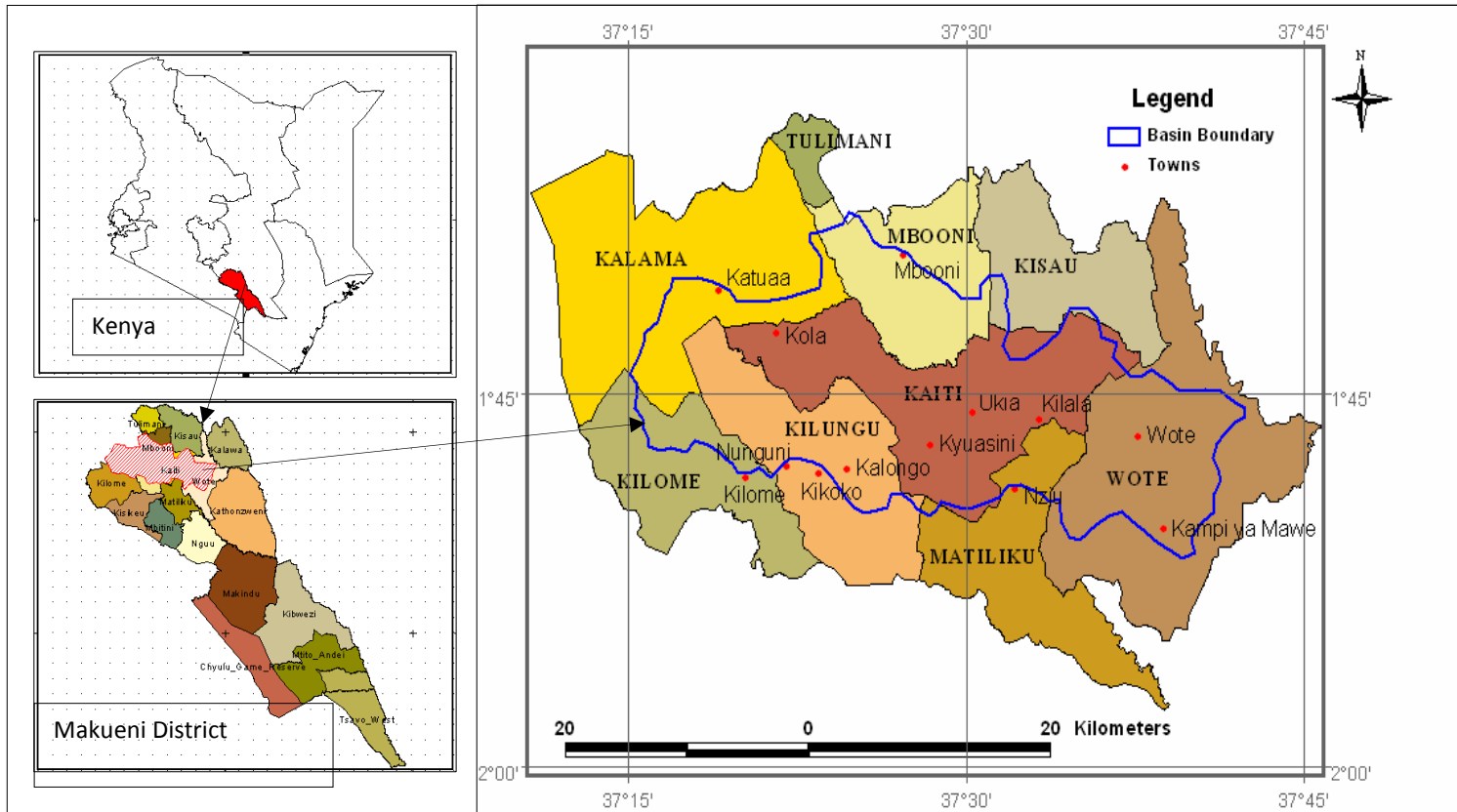


Figure 1: Location map of Kaiti watershed  
Source: Nderitu, 2006

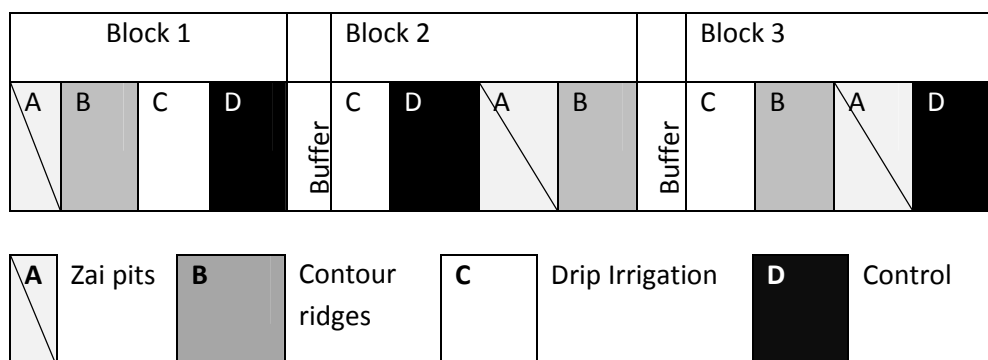


Figure 2: A sketch of experimental layout



Figure 3: Drip irrigation and use of tensiometers for soil moisture monitoring Statistical analysis

## 2.7 Statistical analysis

The Statistical Package for the Social Sciences (SPSS) was used for the statistical analysis on mean soil moisture content, mean crop height, and bean biomass yield. Analysis of variance (ANOVA) was chosen to analyze the data. The model for each analysis included the treatments; drip irrigation, ridging, zai pits and the control. The hypothesis of normal distribution of the residuals was verified.

## 3.0 Results and discussion

During the data collection period, 171 mm of rainfall occurred and was spread over the 100 days. During this period there were 24 wet days. For most of December 2005, the weather was dry and pan evaporation varied between 3 and 7 mm/day. The total pan evaporation for the study period was 359 mm, which translated to a

daily average rate of about 3.6 mm. The highest daily rate of evaporation was 7.8 mm which was recorded on 17th January 2006. The lowest evaporation rate of about 2 mm/day was recorded in early November 2005 (Figure 4).

### **3.1 Effect of rainfall and evaporation on soil moisture**

To evaluate the effect of rainfall and evaporation on soil moisture only the data for the control treatment was considered. Soil moisture content was highest between November 24, 2005 and December 14, 2005. This was the period with the most rainfall, when the weather was cooler, tending to reduce the rate of evaporation.

Most of December was dry and pan evaporation increased from 2.5 mm/day to about 7.0 mm/day, causing soil moisture content to decrease from about 14% to about 2% (Figure 4 and Figure 5). The rainfall received over a 14 day period, prior to a certain date is referred to as the 14 Day Antecedent Precipitation (14DAP). There was a strong linear relationship between the 14DAP and soil moisture content, suggesting that rainfall is the main factor affecting soil moisture content in this farm (Figure 6). Peaks of the 14DAP corresponded to soil moisture content peaks for different treatments (Figure 7).

### **3.2 Effect of rainwater harvesting and drip irrigation on soil moisture and crop performance**

Zai pits and contour ridges did not significantly increase soil moisture when compared to the control. The pits and contour ridges failed to collect and store rain water and provide adequate moisture to crops even after the rain had stopped. Because rainfall was insufficient during most of the study period, there was hardly any surface runoff even from the control and drip irrigated plots. Soil moisture in drip irrigated plots was significantly higher than in the control plots, even after irrigation was discontinued (Figure 7).

The wettest period of the growing season was the last week of November 2007. After the rainfall event of November 27, when the 14DAP was about 80 mm, the control and drip irrigated plots yielded surface runoff of 2.5 – 2.6 mm. However, plots under Zai pits and contour ridges had less surface runoff of 0.8-0.9 mm. This suggests that a minimum 14DAP of 80 mm is required for runoff to be produced. However, there is need for further research to confirm the conditions under which rainwater harvesting would be effective in preventing runoff and enhancing root zone soil moisture. Crop performance was assessed in terms of crop height, biomass yield, and bean grain yield. Rainwater harvesting did not influence crop development in terms crop height (Figure 8). This is could have been because the rainfall received during the vegetative stage of plant growth was just enough for the purposes of plant growth. By end of November 2005, the bean crop had reached maximum height. The fastest growth occurred during the second month after planting.

The bean crop was harvested after 100 days and the highest biomass yield was 9 tonnes ha<sup>-1</sup> realized in drip irrigated plots. However, biomass yield for drip irrigated plots was not different from the control treatment. Biomass yield from zai pits and contour ridges was significantly lower than the yield from drip irrigated plots at 5% level of significance (Figure 9). Although Mati (2006) found that contour ridges increased the yield of maize in semi-arid climate, in this study, beans planted in contour ridges did not perform as well. This was contrary to expectations. Bean yields were higher than the national average of 0.36 tonnes ha<sup>-1</sup> (Ministry of Agriculture, 2009) and higher than the average bean yield for Makueni District (0.4 tonnes ha<sup>-1</sup>) (Jaetzold, 2007) for all the treatments. Drip irrigated plots had the highest average bean grain yield of 4.0 Ton ha<sup>-1</sup>.

Reasons for lack of rainwater harvesting impact on bean yield are unknown. The fact that there was minimal runoff suggests that most of the rainfall went into the soil uniformly in all the plots, and hence the reason crop yield from plots that were not irrigated was nearly the same, irrespective of rainwater harvesting.

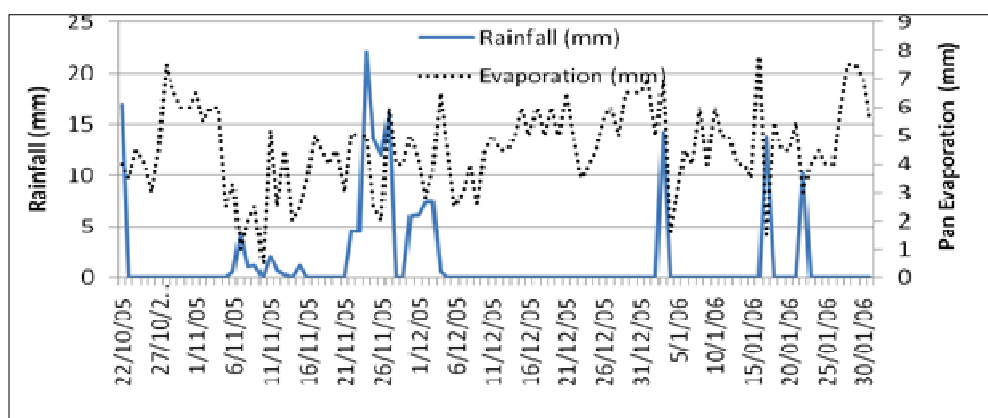


Figure 4: Temporal variation of rainfall and pan evaporation data during the study period

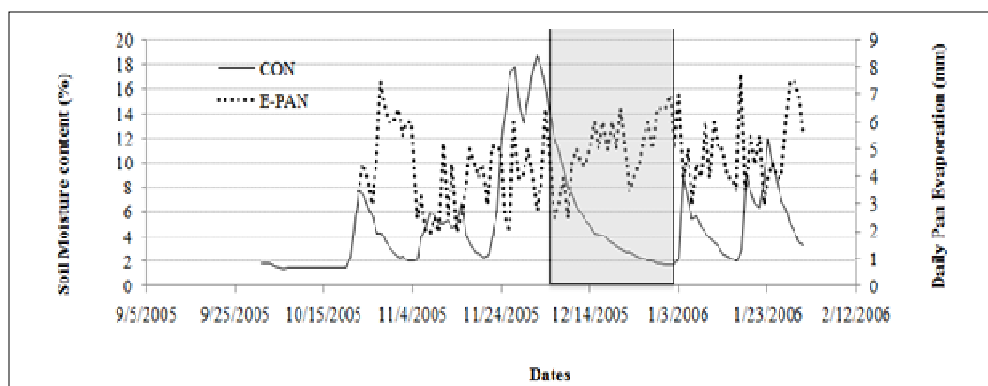


Figure 5: Soil moisture and evaporation data for the experimental period



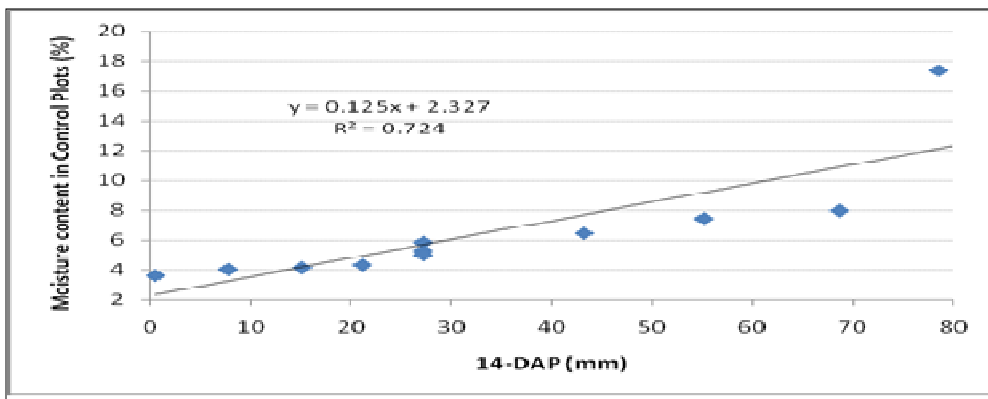


Figure 6: Soil moisture and evaporation data for the study period

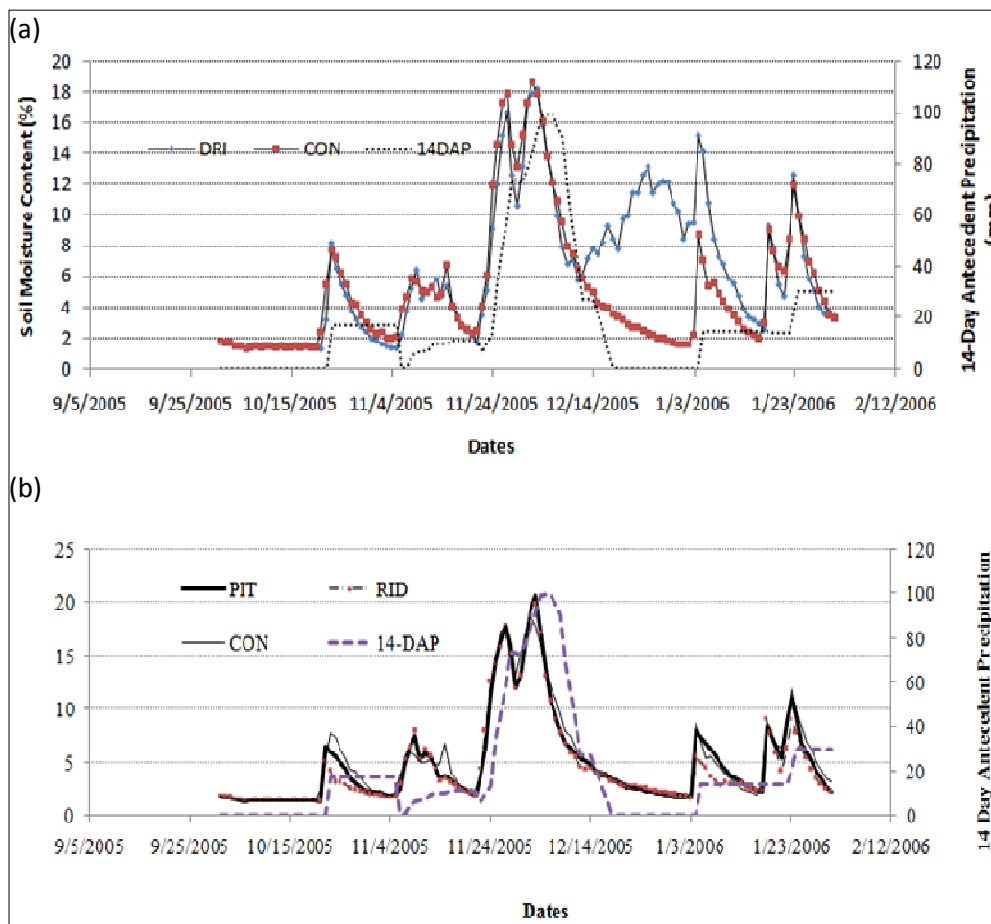


Figure 7(a-b): Effect of rainfall on Soil moisture content: (a) Control versus Drip; (b) Control versus Zai Pits and Contour ridges

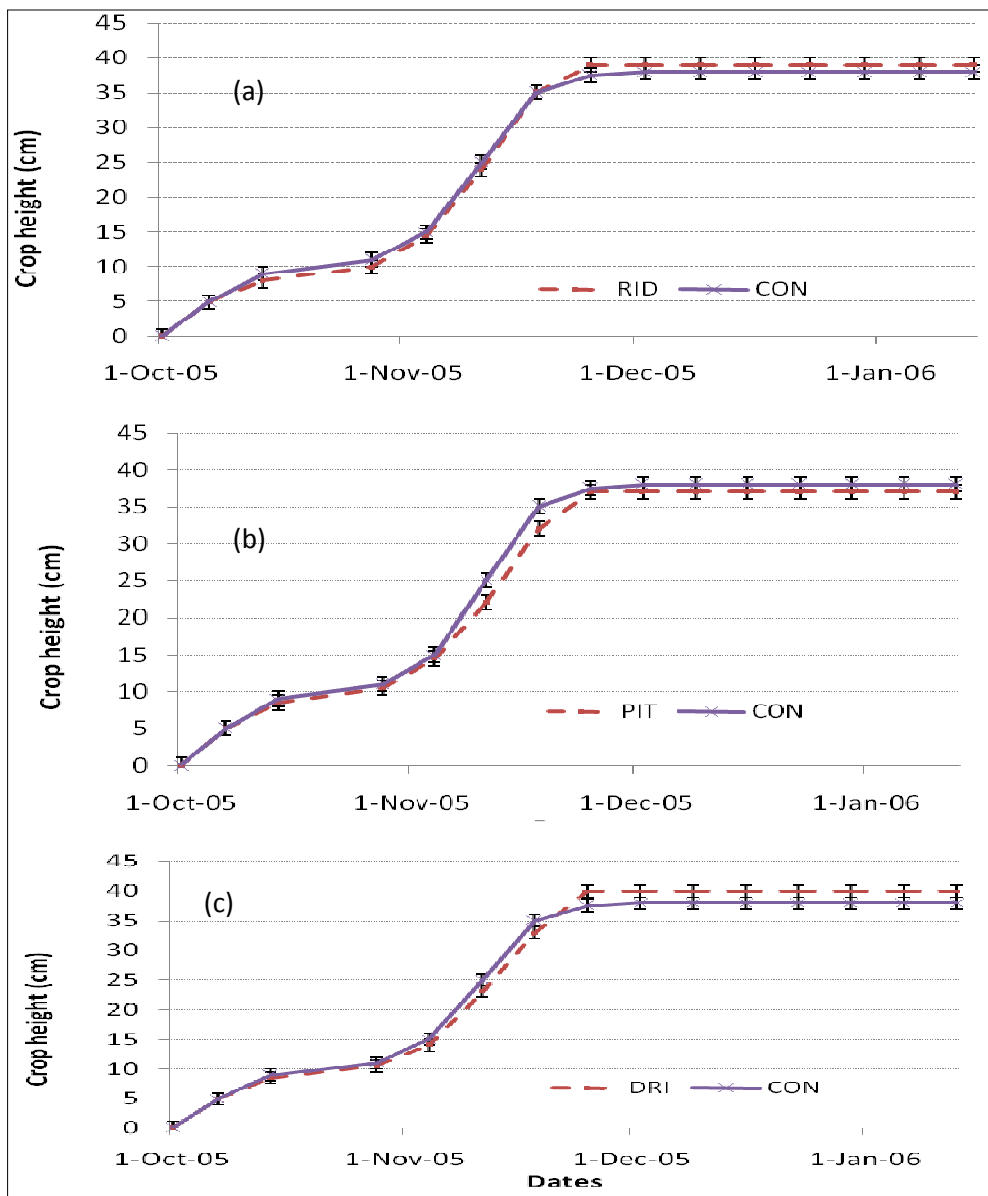


Figure 8 (a-c): Effect of water harvesting and drip irrigation on crop height: (a) Contour ridges versus control; (b) Zai pits versus control and (c) Drip irrigation versus control

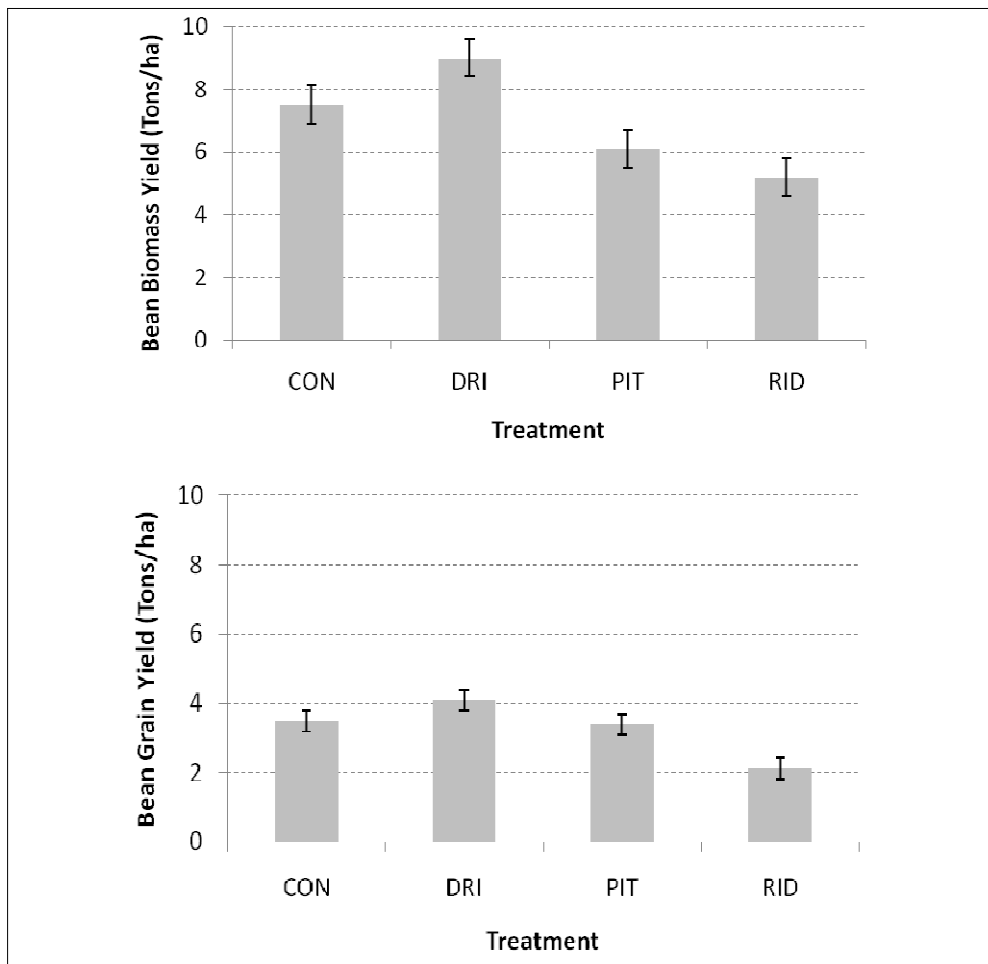


Figure 9: Bean grain and biomass yield

**4.0 Conclusions and recommendations**

The strong linear relationship between the 14 Day Antecedent Precipitation (14DAP) and soil moisture content indicates that rainfall is the main factor affecting soil moisture content and crop performance. Under the soil and crop conditions used in this study, a minimum 14DAP of 80 mm is necessary for surface runoff to be produced, and therefore for the impact of rainwater harvesting on soil moisture to be observed. Further research, under various rainfall and soil conditions should be undertaken to confirm the conditions under which the benefits of rainwater harvesting using contour ridges and zai pits can be realized in the enhancement of crop performance in ASAL conditions.

### Acknowledgements

The authors would like to recognize the contributions of various colleagues. The watershed map of the study area was developed by Anthony Nderitu, a graduate student in the Department of Biomechanical and Environmental Engineering. We wish thank Mr. Stephen King'atya who assisted with data collection in the field. Mr. Peter Mwirigi of the Research, Production and Extension Division of JKUAT, helped with the statistical analysis of the data. Dr. D.N. Sila of the Food Science and Post-Harvest Technology, JKUAT, proofread the paper. Sincere thanks and recognition go to the African Institute for Capacity Development (AICAD) who provided some of the funds used in buying rainfall and evaporation equipment.

### References

- Critchley W. Reij C. and Seznec A. (1999). Water harvesting for plant production. Volume II: Case studies and conclusions for sub-Saharan Africa. World Bank Technical Paper Number 157. Africa Technical Department series.
- Gathenya M. and Kaluli W. (2004). Hydrological Data Availability for Water Resources Planning in Makueni District. Paper presented at the 17th WAITRO International Conference held from 6th –11th of September 2004.
- Gichuki F. N., (2000). Makueni District Profile: Water Management, 1989-1998. Drylands Research. Crewkerne, Somerset, UK.
- Hai M. T., (1998). Water Harvesting. An Illustrative Manual for Development of Microcatchment Techniques for Crop Production in Dry Areas. Technical Handbook no. 16. Published by SIDA's regional land management Unit, RELMA, 1998.
- Hatibu N. and Mahoo H. F., (2000). Rainwater Harvesting for Natural Resources Management for Tanzania. Technical Handbook No. 22 RELMA, Nairobi.
- Jaetzold R. (2007). Farm Management Handbook Vol II for Eastern Kenya. 2<sup>nd</sup> Edition. Ministry of Agriculture, Kenya.
- Kaluli W., Ng'ang'a S. K., Gathenya M., Kihoro J. and Muriuki A., (2005). Water harvesting for Household and Agricultural Water Supply: Kaiti Watershed Case Study. *Proceedings of 2005 Scientific Technological and Industrialisation conference on Leveraging Indegenous Products and Technologies through research for Industrialisation and Development.* October 2005. Nairobi, Kenya. pp 287- 298.
- Mati B. M. (2006). Overview of Water and Soil Nutrient Management Under Smallholder Rain-fed Agriculture in East Africa. *Working Paper 105.* Colombo, Sri Lanka: International Water management Institute (IWMI).
- Mati B. M. (2007). 100 ways to manage water for small holder agriculture in East and Southern Africa. SWMnet Working Paper 13. Improved Management in Eastern and Southern Africa (IMAWESA).

Michael A.M. (1978). Irrigation theory and practice. Vikas Publishing House PVT Ltd, India.

Ministry of Agriculture. (2009). Economic Review of Agriculture. Central Planning and project monitoring Unit/MoA. Nairobi, Kenya

Mugwe J., Oneill M., Gachanja S., Muriuki J. and Mwangi J., (1999). Participatory Evaluation of Water Harvesting Techniques for Establishing Improved Mangoes varieties in Small holder Farms in Mbeere District. 10th International Soil Conservation organization; Sustaining the Global Farm, pp. 1152-1157.

Nderitu A. (2006). Hydrologic modeling as a tool for water resources planning in ASAL watersheds: Kaiti watershed case study. M.Sc. Thesis, JKUAT.

Rosegrant M., Ringler C., and Zhu T., (2009). Water for Agriculture: Maintaining Food Security under Growing Scarcity. *Annual Rev. Environ. Resources*. 2009., **34**, pp. 205-222.

Wei L., Zhang B. and Wang M. (2007). Effects of antecedent soil moisture on runoff and soil erosion in alley cropping systems. *Agricultural Water Management*, **94**, pp. 54-62.

**THE INFLUENCE OF NITROGEN APPLICATION ON THE GROWTH AND MINERAL CONTENT OF TWO AFRICAN NIGHTSHADE SPECIES (*SOLANUM SPP.*) CULTIVATED IN KENYA**

**P. W. Masinde<sup>1</sup> and S. G. Agong<sup>2</sup>**

<sup>1</sup>Jomo Kenyatta University of Agriculture and Technology, Kenya

<sup>2</sup>Bondo University College, Bondo, Kenya

Email: masindepeter@hotmail.com

**Abstract**

Plant growth, leaf nitrogen and nitrate-N, and chemical content of two African nightshades, *Solanum villosum* and *S. sarrachoides* under different nitrogen levels was investigated in field experiments in 2001 and 2004. Plants were supplied with 0, 1.3, 2.6 and 5.2 g N/plant. Both African nightshade species responded similarly to nitrogen supply. Leaf area and dry matter production of plants supplied with nitrogen was 4-8 times that of plants not supplied with nitrogen. Plants supplied with nitrogen had significantly higher specific leaf area but had a lower leaf to stem ratio ( $p \leq 0.05$ ). Leaf nitrogen concentration was significantly higher ( $p \leq 0.05$ ) in plants supplied with nitrogen. However, when expressed on a leaf area basis, the differences in the leaf nitrogen content between nitrogen treatments were minimal. Leaf blade nitrate-N tended to be high in young plants especially those that were supplied with nitrogen. The species showed significant differences ( $p \leq 0.05$ ) in the mineral content. It was concluded that African nightshade responded to limited nitrogen by drastic reduction in leaf area to maintain the leaf nitrogen content.

**Key words:** Leaf nitrogen, leaf to stem ratio, mineral content, nitrates, *Solanum sarrachoides*, *Solanum villosum*

## 1.0 Introduction

African nightshades are grown and consumed as leafy vegetable crops in Kenya and various parts of Africa (Chweya and Eyzaguirre, 1999; Smith and Eyzaguirre, 2007). They are promising alternative cash crops considering their increasing availability in retail and supermarkets and have been recently ranked second to amaranth in priority among indigenous vegetables in Kenya (Agong and Masinde, 2006; Ndegwa et al., 2011). Limited agronomic technologies have been identified as a constraint facing African nightshade production (Ndegwa et al., 2011). The application of nitrogen to increase yield in leafy vegetables is a well-recognized practice. It is known that nitrogen deficiency exerts its effects on plant growth through reduced leaf area index and hence low light interception and low dry matter production (Jones, 1992). Also, the leaf nitrogen content correlates well with the leaf chlorophyll content, hence N deficiency leads to reduced photosynthesis resulting in lower biomass accumulation (Zhao et al., 2005). Under limited nitrogen supply, plants may respond by reducing leaf area and hence maintain the leaf nitrogen concentration as has been shown in potato (*Solanum tuberosum* L.) (Vos and van der Putten, 1998). Another strategy is to maintain a high leaf area, but adapt the leaf nitrogen concentration to nitrogen availability as demonstrated in maize (*Zea mays* L.) (Vos et al., 2005). A clear understanding of the response of African nightshades to limited nitrogen supply is vital in the efforts to integrate them into the mainstream agriculture. Growers may apply excessive N to realise high leaf yield and presumably high economic returns but this can lead to environmental contamination as well as nitrate accumulation in the vegetables, thereby posing health hazards to consumers (Gashaw and Mugwira, 1981; Wright and Davison, 1964).

Some agronomic studies to develop optimal cultivation practices for improved yield and nutritive quality of African nightshades have been conducted (Murage, 1990; Khan et al., 1995; Opiyo, 2004). These studies have shown that production of leafy *Solanum* spp. required high amounts of nitrogen application with recommendations of upto 5 g N/plant under field conditions. This study focuses on *Solanum villosum* Mill. subsp. *miniatum* (Bernh. ex Willd.) Edmonds and *S. sarrachoides* Sendtn. (Edmonds and Chweya, 1997; Schippers, 2000). The objective of this study was to evaluate the mechanisms of adaptation to nitrogen stress by these species and assess the influence of nitrogen application on the nutrient content of the two African nightshade species.

## 2.0 Materials and methods

### 2.1 Experimental site and plant materials

Field experiments were conducted in July - October 2001 and December 2003 - March 2004 at Jomo Kenyatta University of Agriculture and Technology (JKUAT) farm, Juja, Kenya (1525 m above sea level). The plant materials consisted of two African nightshade species; *Solanum sarrachoides* Sendtn. obtained from

Genebank of Kenya (GBK 028726) and also from IPK Genebank, Gatersleben, Germany (Sol 262/97) and *S. villosum* Mill. subsp. *miniatum* (Bernh. ex Willd.) Edmonds purchased from Kenya Seed Company, Nairobi, Kenya.

## 2.2 Experimental design and crop culture

The experiments were carried out as split plots in a completely randomised block design with three replications. The experimental factors consisted of 0, 2.6, 5.2 g N/plant in 2001 and 0, 1.3, 2.6 and 5.2 g N/plant in 2003, and two African nightshade species. The main plots comprised of the nitrogen levels, while the sub-plots consisted of the two species. The sub-plots, each measuring 2 m × 2.5 m were prepared by raising the soil about 15 cm above the ground. Seedlings were first raised in pots (10 cm diameter) in July 2001 and December 2003. The field was ploughed and harrowed and sub-plots raised about 15 cm were made to fine tilth. Soil samples were taken for nitrogen analysis using the Kjeldahl method (Okalebo et al., 1992). Transplanting to the field was done in August 2001 and January 2004 at a spacing of 40 x 40 cm in 2001 and 30 x 30 cm in 2004. The crops were irrigated using sprinklers 2-3 times in a week depending on weather conditions. Nitrogen treatments consisting of Calcium Ammonium Nitrate (CAN, 26%N) were applied one week after transplanting using. The fertilizer was weighed and applied uniformly by hand along drills ensuring that each plant row had drills on either side. Phosphorus was applied at planting along the drills at levels of 92 kg P<sub>2</sub>O<sub>5</sub>/ha using triple superphosphate (TSP, 46% P<sub>2</sub>O<sub>5</sub>).

## 2.3 Harvesting

At transplanting time, some seedlings were excised to determine the initial plant size in terms of leaf area, plant height and shoot dry weight. Subsequent harvests were carried out 5-16 days interval to quantify plant size over time. Harvesting was ended when plants were flowering profusely. At each harvest, one plant in a central row from each plot was cut at the base and partitioned into leaf blade, petioles and stems. Plant leaf area was measured using a leaf area meter model AAM-8, Hayashi Denko Co. LTD., Tokyo for 2001 crop, and model 3100, LI-COR, Lincoln, Nebr. for 2004 crop. The shoot parts were dried at 100°C for 48 hours in the oven for dry weight measurement. Dried leaf blades were ground and used for nutrient analysis. Nitrogen content was analysed using the Kjeldahl method (Okalebo et al., 2002). Nitrate content was analysed using the colorimetric method while determination of Ca and Fe contents was done by dry ashing followed by use of atomic absorption spectrophotometer for Ca and Fe (Okalebo et al., 2002).

## 2.4 Data analyses

Statistical analysis was done using the GLM procedure of SAS (SAS, 1999). An ANOVA was executed with a split plot design for the field experiments for each date separately for the parameters; leaf area, dry weights, nitrogen and nitrate contents and mineral contents. Significance level was set at P≤0.05.



### 3.0 Results

#### 3.1 Effect of nitrogen and species on growth of African nightshade

The soils nitrogen content at 0.10% N, which was low. The interactions between nitrogen applied and species were not significant. Nitrogen application significantly increased leaf area from the age of 16 and 15 days after transplanting in 2001 and 2004, respectively (Figure 1). In 2001, plants supplied with 2.6 and 5.2 g N/plant had similar leaf area in all the harvests except at 53 days after transplanting when the 5.2 g N/plant treatments plants had significantly higher leaf area. Similarly, in 2004 plants supplied with 5.2 g N/plant had significantly higher leaf areas followed by plants in the 1.3 and 2.6 g N/plant treatments, while plants in the 0 g N/plant had the lowest leaf area. Leaf area was generally higher in *sarrachoides* as compared to *villosum* but this was significant only at 53 days after transplanting in 2001 and beyond 15 days after transplanting in 2004. At the time of terminating the experiments, the leaf area of *sarrachoides* ranged 6029.83-10448.41 cm<sup>2</sup> while that of *villosum* ranged 3050.06-6930.74 cm<sup>2</sup>.

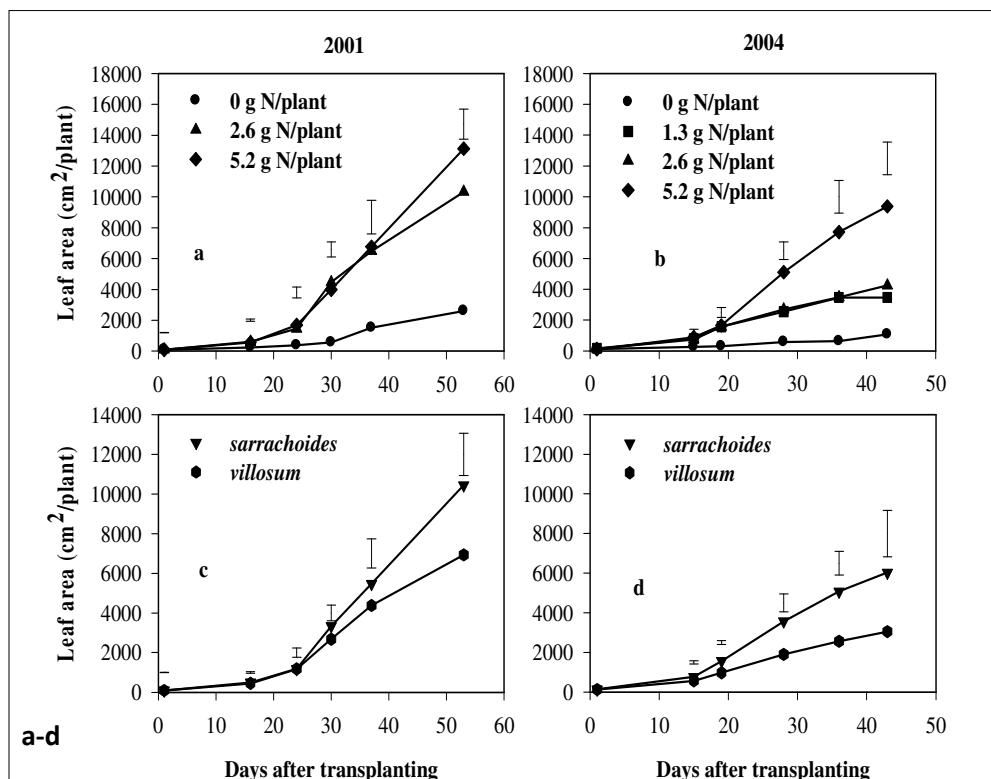


Figure 1(a-d): The leaf area as influenced by nitrogen rates (a, b) and species (c, d) for African nightshade grown at JKUAT farm in August-October 2001 and January-March 2004. Vertical bars show LSD0.05.

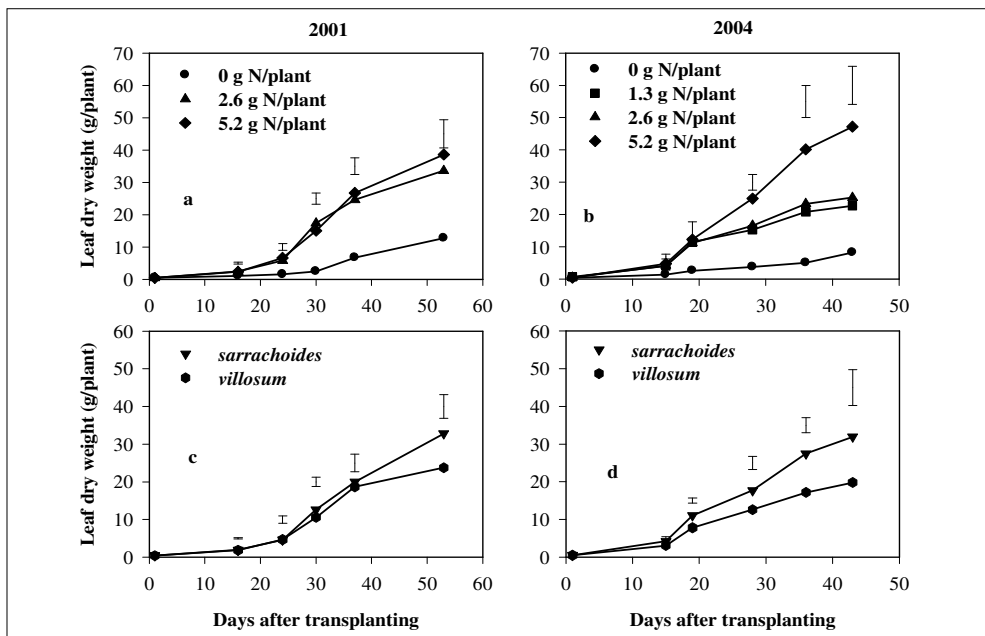


Figure 2(a-d): The leaf dry weight as influenced by nitrogen rates (a, b) and species (c, d) for African nightshade grown at JKUAT farm in August-October 2001 and January-March 2004 Vertical bars show LSD0.05

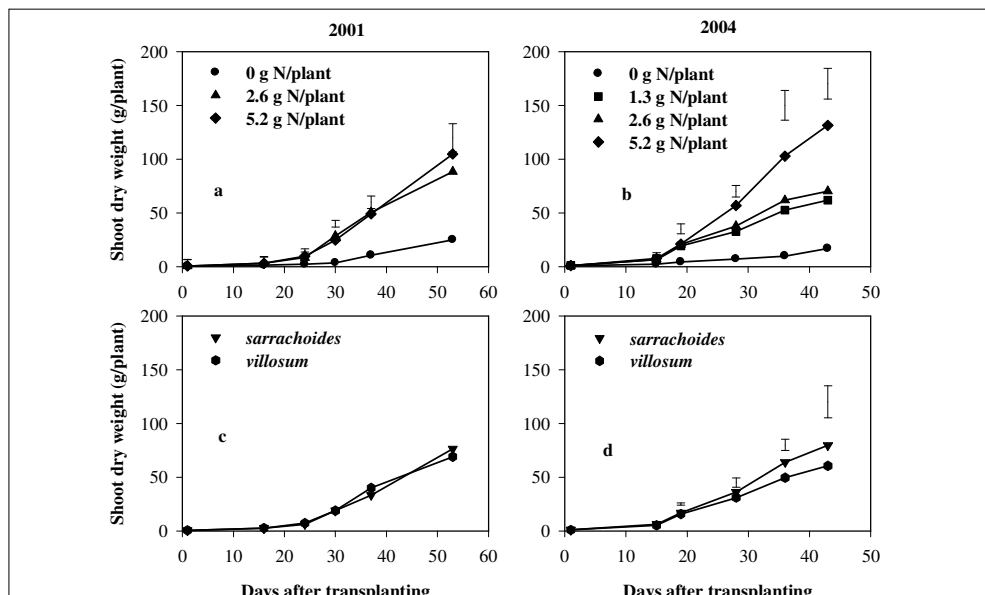


Figure 3(a-d): The shoot dry weight as influenced by nitrogen rates (a, b) and species (c, d) for African nightshade grown at JKUAT farm in August-October 2001 and January- March 2004 Vertical bars show LSD0.05

Leaf dry weights followed similar patterns as leaf areas. Nitrogen application gave significantly higher leaf dry weights from 16 and 15 days after transplanting in 2001 and 2004, respectively (Figure 2). In 2001, there was no difference in the leaf dry weight between plants supplied with 2.6 g and 5.2 g N/plant while in 2004, plants in the 5.2 g N/plant treatment gave consistently higher leaf dry weight. The influence of the species on leaf dry weight corresponded closely to that of leaf area with *S. sarrachoides* having significantly higher weights than *S. villosum* in older plants.

The influence of nitrogen application on shoot dry weight was similar to leaf area and leaf dry weight (Figure 3). On the other hand, the shoot dry weight was not significantly different between the two species except at 36 days after transplanting in 2004 when *S. sarrachoides* had higher shoot dry weight than *S. villosum*.

### 3.2 Effect of nitrogen and species on the specific leaf area (SLA) and dry matter partitioning of African nightshade

Plants supplied with nitrogen maintained a higher specific leaf area (SLA) in both species than plants, which did not receive any nitrogen, and this difference was significant in mature plants (Figure 4). In both years, treatment 5.2 g N/plant gave the highest SLA but this was significantly different from the other nitrogen treatments only at 53, and 28 to 43 days after transplanting in 2001 and 2004, respectively. *Solanum sarrachoides* had significantly higher SLA ranging 179.57-328.94 cm<sup>2</sup>/g compared to 156.56-264.53 cm<sup>2</sup>/g for *S. villosum* in the mature plants.

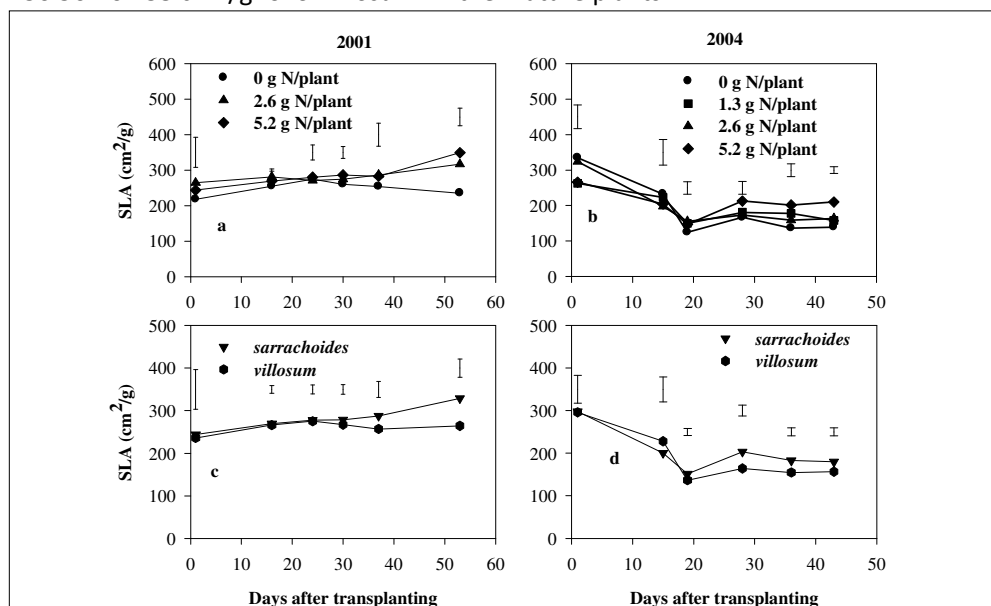


Figure. 4(a-d): The specific leaf area as influenced by nitrogen rates (a, b) and species (c, d) for African nightshade grown at JKUAT farm in August-October 2001 and January-March 2004. Vertical bars show LSD0.05

Leaf to stem ratios declined over time in both years. Plants supplied with nitrogen had significantly lower leaf to stem ratios from 22 and 28 days after transplanting in 2001

and 2004, respectively (Figure 5). The differences in the leaf to stem ratio between the nitrogen treatments 1.3 - 5.2 g N/plant were minimal. *Solanum sarrachoides* maintained a significantly higher leaf to stem ratio than *S. villosum* for all or most of the harvesting period in both years.

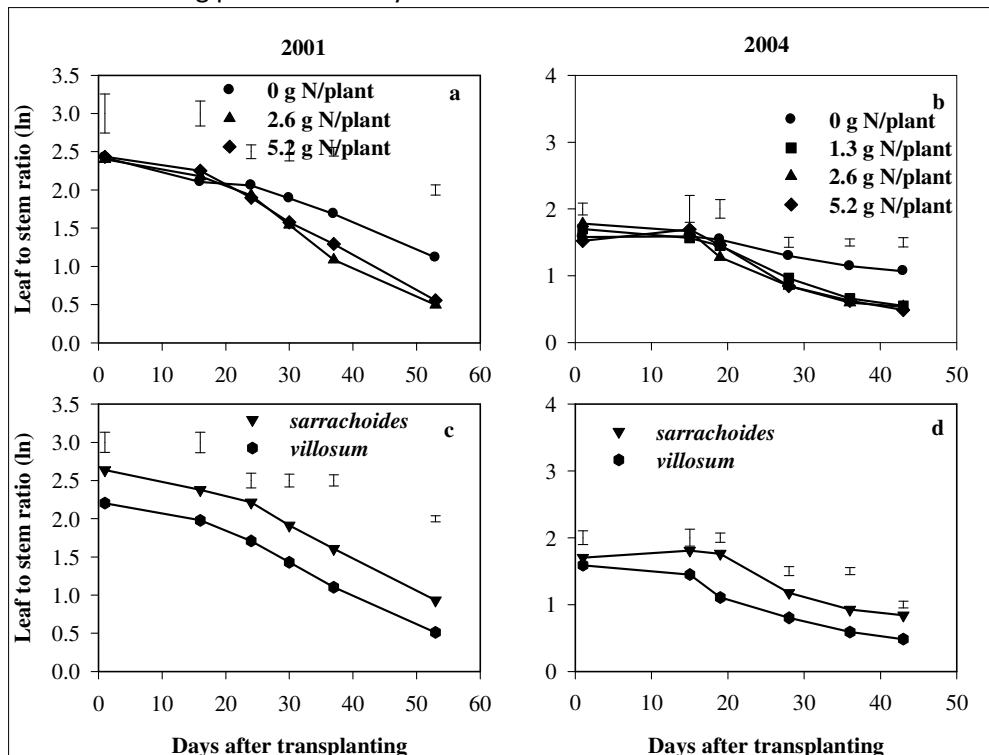


Figure. 5(a-d). Leaf (harvestable part, blade+petiole) to stem ratio in natural logarithms as influenced by nitrogen rates (a, b) and species (c, d) for African nightshade grown at JKUAT farm in August-October 2001 and January-March 2004. Vertical bars show LSD0.05.

The leaf blade to stem ratio in 2001 declined with increasing plant height (Figure 6). The power function fitted well to the data for *S. sarrachoides* only in 2001, and for *S. villosum* in both years. The two species had similar coefficients in 2001, while *S. villosum* had a significantly higher power coefficient in 2004 as compared to in 2001 (Table 1). Nitrogen treatments had no significant effect on the leaf blade to stem ratio as a function of plant height.

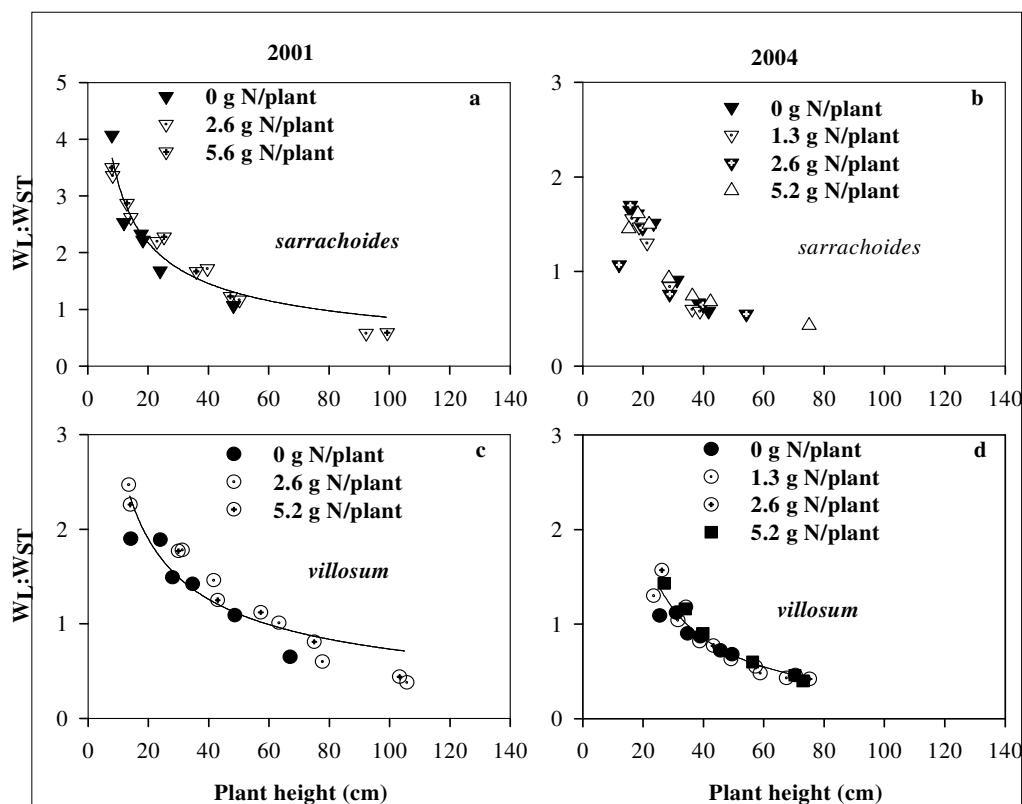


Figure. 6(a-d) The blade to stem (stem+petiole) ratio as functions of plant height for African nightshade species *S. sarrachoides* (a, b) and *S. villosum* (c, d) under different nitrogen levels grown at JKUAT farm in August-October 2001 and January-March 2004. Lines show power function  $y=ax^{-b}$  where the coefficients are significant. The coefficients  $a$  and  $b$  are shown in Table 2.

Table 1: Coefficients and their 95 % confidence intervals for the blade to stem ratio as functions of plant height

Species	Year	a (95%CI)	b (95% CI)	R2
<i>S. sarrachoides</i>	2001	12.3 (7.1, 17.5)	-0.58 (-0.73, -0.42)	0.95
	2004	14.9 (-11.7, 41.5)	-0.80 (-1.39, -0.22)	n.s.*
<i>S. villosum</i>	2001	11.1 (0.6, 21.5)	-0.59 (-0.88, -0.30)	0.99
	2004	45.9 (18.3, 73.6)	-1.08 (-1.25, -0.91)	0.99

### 3.3 Effect of nitrogen and species on the mineral contents of African nightshade leaf blades

The leaf blade nitrogen concentration was significantly higher in plants supplied with 5.2 g N/plant as compared to plants that received no nitrogen (Figure 7). Plants that received 2.6 g N/plant had intermediate leaf blade nitrogen concentration. The nitrogen concentration ranged 3.26-5.37%, 3.84-6.09% and 5.33-6.29% in control, 2.6, and 5.2 g N/plant treatments. Similarly, plants supplied

with 5.2 g N/plant had higher leaf blade nitrate concentration, significant at 16 and 37 days after transplanting (Figure 7). The nitrate concentrations declined in more less the same ways as leaf blade nitrogen concentration, with the decline being highest in the 2.6 and 0 g N/plants treatments. For both leaf blade nitrogen and nitrate concentrations, there were no differences between the species.

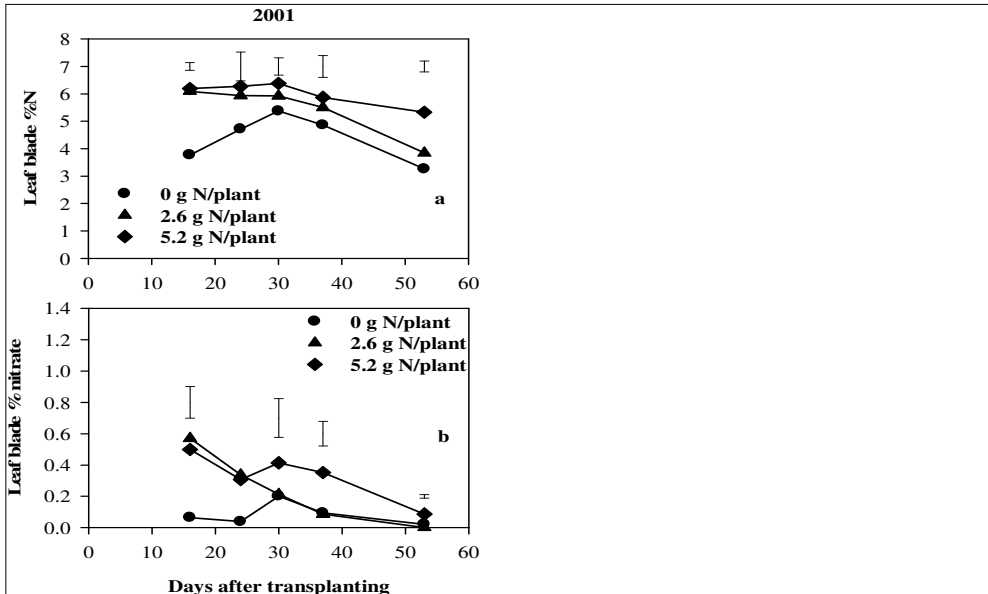


Figure 7: The leaf blade nitrogen (a) and nitrate (b) contents of African nightshade grown at JKUAT farm in July-October 2001 as influenced by nitrogen rates. Vertical bars show LSD0.05.

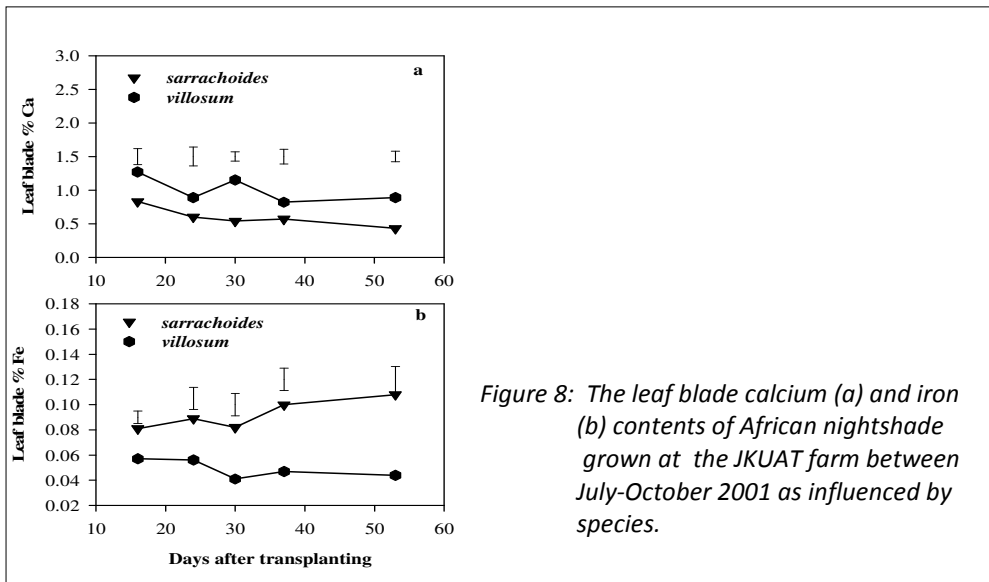


Figure 8: The leaf blade calcium (a) and iron (b) contents of African nightshade grown at the JKUAT farm between July-October 2001 as influenced by species.

Application of nitrogen had limited influence on the % Ca and % Fe content in leaf blades. Significant differences were observed only at 53 days after transplanting where plants supplied with 5.2 g N/plant had higher % Ca while those supplied with 0 and 2.6 g N/plant had higher % Fe (data not shown). On the other hand, *S. villosum* had significantly higher % Ca in leaf blades as compared to *S. sarrachoides* while *S. sarrachoides* had significantly higher % Fe as compared to *S. villosum* (Figure 8).

#### 4.0 Discussion

The objective of this study was to evaluate the growth characteristics leaf nitrogen concentration and mineral nutrient content of *Solanum villosum* and *S. sarrachoides* under different nitrogen levels. In both years, the two species responded similarly to nitrogen supply as shown by lack of significant interactions between the species and nitrogen levels. Leaf area in mature plants was 5-8 times higher in plants supplied with 5.2 g N/plant than in plants that were not supplied with nitrogen. Potato, which has a similar strategy, was shown to vary the leaf area 4-fold between non-limiting and limiting nitrogen supplies (Vos and Van der Putten, 1998). On the other hand, maize, which does not have this response, increased leaf area only by 30% in plants supplied with non-limiting nitrogen rates as compared to those in the limiting rates (Vos *et al.*, 2005).

Dry matter production response corresponded with that of the leaf area. Both leaf and shoot dry weights were 4-8 times higher in the plants supplied with non-limiting nitrogen than plants in the nitrogen limiting treatment. This can be attributed to the reuction in leaf area, which results in reduction in the cumulative light interception (Jones, 1992). It has been shown that in tomato (*Lycopersicon esculentum* Mill.), increasing nitrogen supply led to an increase in the accumulated absorbed photosynthetically active radiation through increase in leaf area index (Tei *et al.*, 2002). Nitrogen supply has been shown to increase dry matter production in crops such as soybean (*Glycine max* (L.) Merr) (Taylor *et al.*, 2005), sunflower (*Helianthus annuus* L. var. CATISSOL-01) (Cechin and de F`atima Fumis, 2004) and safflower (*Carthmus trinctorious* L.) (Dordas and Sioulas, 2009). The leaf area and leaf dry weight being higher in *S. sarrachoides* suggests that it would be a better leaf yielder as compared to *S. villosum*. Differences in the shoot dry weight between the two species were minimal or absent due to a bigger stem in *S. villosum*.

The specific leaf area (SLA) was higher in plants that were supplied with higher levels of nitrogen. This could be explained by the higher leaf area in these plants, which may imply a higher leaf expansion as well as leaf appearance. The low SLA in the African nightshades under nitrogen stress suggests that plants were restricting leaf area probably to maintain a high leaf nitrogen concentration. Meziane and Shipley (2001) working on 22 herbaceous species have shown that increased

nutrient supply increased specific leaf area at low irradiance. Similarly, higher nutrient additions resulted in higher SLA in *Arabidopsis thaliana* (Bonser *et al.*, 2010). A low SLA suggests thicker leaves as opposed to thinner leaves which have a high SLA. Whereas thicker leaves have a greater concentration of the photosynthetic apparatus per unit leaf area, broad thinner leaves can intercept more light (White and Consuelo Montes, 2005). The higher SLA in *S. sarrachoides* as compared to *S. villosum* especially in mature plants may suggest a higher light interception and photosynthetic activity in the former species. However, photosynthesis was not measured in this study. In addition, there was no clear evidence of differences in shoot dry matter production between the species.

The partitioning of dry matter in the two species was considered through the leaf to stem ratio and the leaf blade to stem ratio. The former is a measure of the harvest index, in which case the leaf consisted of the leaf blade and petiole, which comprise the harvestable part. The latter is an indication of partitioning of dry matter between the photosynthetic tissues (leaf blades) and the support structures (stems and petioles). It seems that application of nitrogen while increasing overall leaf growth, increases stem growth relatively more, hence the low leaf to stem ratios. The differences emerged at 22-28 days after transplanting and widened with time. In mature plants, the dry matter allocated to the leaves was about 60% of that allocated to stems in plants that were supplied with nitrogen. In comparison, mature plants that received no nitrogen supply had similar dry matter allocation between the leaves and stems. In this regard, nitrogen supply could be seen as having reduced the harvest index.

In the second consideration of dry matter partitioning, the leaf blade to stem ratio was fitted as a function of plant height. It is recognized that as the plant leaf area increases, a greater proportion of new dry matter needs to be invested in structural material (mainly stems) to maintain the plant's integrity and strength (Stützel *et al.*, 1988). Thus, the leaf blade to stem ratio declines with increase in plant size in a power function. In this study, attempts were made to evaluate the effect of nitrogen application and species on the function. Both factors had no significant effect on the function. This suggests that the partitioning of new above-ground dry matter was directly dependent on plant size rather than nitrogen level or species.

Leaf nitrogen concentration is an important physiological parameter that indicates the plants nitrogen status. In this study, plants supplied with the highest nitrogen level that is 5.2 g N/plant maintained higher leaf nitrogen as compared to other treatments. Such a response has been reported in soybean (Taylor *et al.*, 2005), and 22 herbaceous species and wheat (Sinclair *et al.*, 2000; Meziane and Shipley, 2001). However, the leaf nitrogen concentration in plants supplied with no nitrogen ranged 61%-84% of the concentration in plants supplied with 5.2 g



N/plant. The differences therefore were much smaller than those in leaf area and dry matter production. Moreover, when the leaf nitrogen concentration was expressed per unit leaf area, the range of leaf nitrogen content in plants not supplied with nitrogen was 64%-95% of that in plants supplied with 5.2 g N/plant. This suggests that the African nightshade species under nitrogen stress tried to maintain a high leaf nitrogen concentration. This was probably through reduction in leaf growth. It has been shown that the maximum canopy photosynthesis in cauliflower, maize and rice was correlated to leaf nitrogen concentration (Vos *et al.*, 2005).

Supplying nitrogen to African nightshade can increase the nitrate content in blades significantly. In this study, the equivalent NO<sub>3</sub> content in fresh blades using the observed moisture content of 88% ranged 2652-3029 mg/kg to 5-462 mg/kg in plants supplied with nitrogen, and 1063 mg/kg to 112 mg/kg in plants not supplied with nitrogen, in young to mature plants, respectively. It therefore appears that in the early vegetative stages, African nightshade can be classified together with crop species that accumulate moderate nitrates up to 2500 mg/kg such as endives (*Cichorium endivia* L.), leeks (*Allium ampeloprasum* var *porrum* (L.) J. Gay), parley (*Petroselinum crispum*) and rhubarb (*Rheum rhabarbarum*) (Hill 1991, Santamaria and Elia 1997). However, in cases where high nitrogen has been supplied, the young plants have high amounts of nitrates (above 2500 mg/kg), similar to high accumulating species like celery (*Apium graveolens* L.), lettuce (*Lactuca sativa* L.) and spinach (*Spinacia oleracea* L.) (Van Der Boon *et al.*, 1990; Hill, 1991; Andersen and Nielsen, 1992; Behr and Wiebe, 1992; Martignon *et al.*, 1994; Jaworska, 2005; Prasad and Chetty, 2008). Mature plants have relatively low nitrates in the leaf blades irrespective of whether nitrogen was supplied or not. The European Commission Regulation (EC) No 1881/2006 has established maximum levels (MLs) for nitrate in lettuces and spinach at 2500-3500 mg mg/kg for summer harvest and 3000-4500 mg/kg for winter harvest (Cited in Correia *et al.*, 2010). Thus there is always the risk of accumulating nitrates more than the acceptable levels especially in young African nightshades, which have been supplied with high nitrogen levels. The differences in the mineral content between the two species means they can play complementary roles in meeting the consumers nutrient requirement. *Solanum sarrachoides* will be valued for its high iron content while *S. villosum* provides high calcium content.

## 5.0 Conclusion

The two species of African nightshade responded to limited nitrogen supply by drastic reduction in leaf area. This could be seen as a strategy to maintain a high leaf nitrogen content and therefore keep photosynthesis high. On the contrary, this led to a similar drastic reduction in dry matter production which could be attributed to reduced light interception. To avoid these reductions and keep the leaf yield high, it is recommended that growers may need to supply up to 5.2 g

N/plant, although the risk of nitrate accumulation has also to be considered. Nitrate fertilizer levels that may lead to toxic nitrates levels need further investigation.

### Acknowledgements

We are grateful to the Germany Academic Exchange Service (DAAD) for providing the scholarship to the senior author and the department of Horticulture, Jomo Kenyatta University of Agriculture and Technology for availing facilities that enabled this research work to be done.

### References

- Agong S. G. and Masinde P. W. (2006). Improvement of indigenous/traditional plants utilized as vegetables and medicinal plants in Kenya. AICAD Research Abstracts Pilot Second and Third Call Final Reports volume 3, pp 33.
- Andersen L., and Nielsen N. E. (1992). A new cultivation method for the production of vegetables with low content of nitrate. *Scientia Horticulturae*, **49**, pp. 167-171.
- Behr U., and Wiebe H. J. (1992). Relationship between photosynthesis and nitrate content of lettuce cultivars. *Scientia Horticulturae*, **49**, pp. 175-179.
- Bonser S. P., Ladd B., Monro K., Hall M. D. and Forst M. A. (2010). The adaptive value of functional and life-history traits across fertility treatments in an annual plant. *Annals of Botany*, **106**, pp. 979-988.
- Cechin I. and de F`atima Fumis T. (2004). Effect of nitrogen supply on growth and photosynthesis of sunflower plants grown in greenhouse. *Plant Science*, **166**, pp. 1379-1385.
- Chweya J. A. and Eyzaguirre P. B. (1999). The biodiversity of traditional leafy vegetables. International Plant Genetic Resources Institute, Rome, Italy. pp. 52-83.
- Correia M., Barroso A., Barroso M. F., Soares D., Oliveira M.B.P.P. and Delerue-Matos C. (2010). Contribution of different vegetable types to exogenous nitrate and nitrite exposure. *Food Chemistry*, **120**, pp. 960-966.
- Dordas C. A. and Sioulas C. (2009). Dry matter and nitrogen accumulation, partitioning, and retranslocation in safflower (*Carthamus tinctorius* L.) as affected by nitrogen fertilization. *Field Crops Research*, **110**, pp. 35-43.
- Edmonds J. M. and Chweya J. A. (1997). Black nightshades. *Solanum nigrum* L. and related species. Promoting the conservation and use of underutilized and neglected crops. Institute of Plant Genetics and Crop Plant Research, Gatersleben/International Plant genetic resources Institute, Rome, Italy, pp. 112
- Gashaw L. and Mugwira L. M. (1981). Ammonium-N and Nitrate-N effects on the growth and mineral compositions of triticale, wheat and rye. *Agronomy Journal*, **73**, pp. 47-51.

Hill M.J. (1991). Nitrates and nitrites in food and water. Ellis Horwood Limited, pp. 93-96, pp. 131-194.

Jaworska G. (2005). Content of nitrates, nitrites, and oxalates in New Zealand spinach. Food Chemistry, **89**, pp. 235-242.

Jones H. G. (1992). Plants and microclimate: A quantitative approach to environmental plant physiology. 2nd edition, Cambridge University press.

Khan M.M., Samiullah A., Afaq S. H. and Afridi R. M. (1995). Response of black nightshade (*Solanum nigrum* L.) to nitrogen application. Journal of Agronomy and Crop Science, **174**, pp. 91-98.

Martignon G., Casarotti D., Venezia A., Schiavi M., and Malorgio F. (1994). Nitrate accumulation in celery as affected by growing system and N content in the nutrient solution. Acta Horticulturae, **361**, pp. 583-587.

Meziane D. and Shipley B. (2001). Direct and indirect relationships between specific leaf area, leaf nitrogen and leaf gas exchange. Effects of irradiance and nutrient supply. Annals of Botany, **88**, pp. 915-927.

Murage E. N. (1990). The effect of nitrogen rates on growth, leaf yield and nutritive quality of black nightshade (*Solanum nigrum* L.). M.Sc. Thesis, University of Nairobi.

Ndegwa A. M. M., Kimani A. W., Kirigua V., Kiuru P. D., Menza M. K., Muchui M. N. Omwenga J.Q., Wasike V. W., Wasilwa L., Waturu C. N. (2011). Report on Vegetable APVC Stakeholders Workshop, Held at KARI-Thika, 6th to 8th December 2010 pp. 23-29

Okalebo J. R., Gathua K. W., Woomer P. L. (2002) Laboratory Methods of Soil Analysis: A working Manual, 2nd Edition. TSBF-CIAT and SACRED Africa, Nairobi, Kenya. pp 29-32

Opiyo A. M. (2004). Effect of nitrogen application on leaf yield and nutritive quality of black nightshade (*Solanum nigrum* L.). Outlook on Agriculture 33:209-214.

Prasad S. and Chetty A. A. (2008). Nitrate-N determination in leafy vegetables: Study of the effects of cooking and freezing. Food Chemistry, **106**, pp. 772-780.

Santamaria P. and Elia A. (1997). Producing nitrate-free endive heads: Effects of nitrogen form on growth, yield and ion composition of endive. Journal of American Society of Horticultural Science, **122**, pp. 140-145.

SAS (1999). Statistical Analysis System. SAS Institute Inc. SAS/STAT Users guide.

Schippers R.R. (2000). African Indigenous Vegetables. An overview of the cultivated species, Revised CD-ROM edition, Horticultural Development Services, Chatham, UK, pp. 25-31, 147-192.

Sinclair T. R., Pinter P.J., Kimball B. A., Adamsen F. J., LaMorte R. L., Wall G. W., Hunsaker D. J., Adam N., Brooks T. J., Garcia R. L., Thompson T., Leavitt S. and Mathias A. (2000). Leaf nitrogen concentration of wheat subjected to elevated CO<sub>2</sub> and either water or N deficits. *Agricultural Ecosystems and Environment*, **79**, pp. 53-60

Smith I. F. and Eyzaguirre P. (2007) African Leafy Vegetables: Their role in the World health organization's global fruit and vegetables initiative. *African Journal of Food Agriculture Nutrition and Development*, **7(3)**, pp. 1-17.

Stützel H., Charles-Edwards D. A. and Beech D.F. (1988). A model of partitioning of new above-ground dry matter. *Annals of Botany*, **61**, pp. 481-487.

Taylor R. S., Weaver D. P., Wood C. W. and van Santen E. (2005). Nitrogen application increases yield and early dry matter accumulation in late-planted soybean. *Crop Science*, **45**, pp. 854-858.

Tei F., Benincasa P., Guiducci M. (2002). Critical nitrogen concentration in processing tomato. *European Journal of Agronomy*, **18**, pp. 45-55.

Van Der Boon J., Steenhuizen J. W., and Steingröver E. G. (1990). Growth and nitrate concentration of lettuce as affected by total nitrogen and chloride concentration, NH<sub>4</sub>/NO<sub>3</sub> ratio and temperature of the recirculating nutrient solution. *Journal of Horticultural Science*, **65**, pp. 309-321.

Vos J. and van der Putten P. E. I. (1998). Effect of nitrogen supply on leaf growth, leaf nitrogen economy and photosynthetic capacity in potato. *Field Crops Research*, **59**, pp. 63-72.

Vos J. van der Putten P. E. L. and Birch C. J. (2005). Effect of nitrogen supply on leaf appearance, leaf growth, leaf nitrogen economy and photosynthetic capacity in maize (*Zea mays* L.). *Field Crops Research*, **93**, pp. 64-73.

White J. W. and Consuelo Montes R. (2005). Variation in parameters related to leaf thickness in common bean (*Phaseolus vulgaris* L.). *Field Crops Research*, **91**, pp. 7-21.

Wright M. T. and Davison K. L. (1964). Nitrate accumulation in crops and nitrate poisoning. *Advances in Agronomy*, **16**, pp. 197-247.

Wright M. T. and Davison K. L. (1964). Nitrate accumulation in crops and nitrate poisoning. *Advances in Agronomy*, **16**, pp. 197-247.

Zhao D., Reddy K. R., Kakani V. G. and Reddy V.R. (2005). Nitrogen deficiency effects on plant growth, leaf photosynthesis, and hyperspectral reflectance properties of sorghum. *European Journal of agronomy*, **22**, pp. 391-403.

## PHYSICOCHEMICAL CHARACTERISTICS OF UNDRAINABLE WATER DAMS UTILIZED FOR FISH REARING IN THE SEMI-ARID NAROMORU AREA, CENTRAL KENYA

T. C. Ndiwa<sup>1</sup>, B. M. Mwangi<sup>1</sup>, E. Kairu<sup>1</sup>, J. W. Kaluli<sup>2</sup> and D. Nyingi<sup>3</sup>

<sup>1</sup>Kenyatta University, Nairobi, Kenya

<sup>2</sup>Jomo Kenyatta University for Agriculture and Technology, Nairobi, Kenya

<sup>3</sup>National Museums of Kenya

Email: ndiwatitus@yahoo.com

### Abstract

Naromoru is a semiarid area in Central Kenya, occurring on the leeward side of Mt. Kenya. Its water sources include a few permanent rivers such as Nairobi River, intermittent streams and a large number of undrainable water reservoirs. Most of the undrainable water resources have been stocked with fish but their utilization for fish rearing has generally remained very low. The purpose of this study was therefore to examine the water quality status of the dams to assess their suitability and potential for fish production. pH, electro-conductivity and total dissolved solutes (TDS) were measured *in-situ* from three reservoirs (Gathathini, Lusoi and Kianda dams) differing in their habitat characteristics. Water samples were collected for determination of the ionic concentrations of the reservoirs. Water quality status differed markedly between sites, with electric conductivity ranging from 350 $\mu\text{Scm}^{-1}$  at Gathathini dam to over 1350 $\mu\text{Scm}^{-1}$  at Lusoi dam. pH however showed only a slight variation from 8-9.6. Water temperature and transparency varied significantly between the sites, while cationic constituents ( $\text{Ca}^{2+}$ ,  $\text{K}^+$ ,  $\text{Mg}^{2+}$  and  $\text{Na}^+$ ), anions ( $\text{SO}_4^{2-}$ ,  $\text{HCO}_3^{2-}$ , and  $\text{Cl}^{-1}$ ), heavy metals ( $\text{Pb}^{2-}$  and  $\text{Cu}^{2+}$ ) and nutrients ( $\text{NO}_3^-$  and  $\text{PO}_4^{2-}$ ) were all within the recommended WHO levels for fish production. Generally the water quality status was within the standards recommended for fisheries production.

**Key words:** Mt. Kenya, limnology, fisheries, productivity

## 1.0 Introduction

Undrainable dams in general are relatively small, perennial water bodies, varying in size from 0.02 to 25ha in area, with depths rarely exceeding 2.5 m. They have been constructed in many countries that lack natural lakes to trap run off water to meet future water demands and enhance food security (Sena de Silva, 1988). Because of their location in semi-arid areas, they experience extensive water level fluctuations due to water run-off, direct precipitation, ground water discharge, evaporation and most importantly human interference (Kemdirim, 2005). Their fisheries productivity is mainly influenced by prevailing physical and chemical characteristics (Chapman, 1996). Chapman (1996) and Dorstch (1981) noted that water temperature in dams affects their physical, chemical and biological processes. Different types of pollutants that end up in dams can also influence water by changing its temperature, light penetration, pH and electrical conductivity (Kinyua & Pacini, 1991). Similarly, high concentrations of certain minerals in water bodies cause problems both to the ecosystem and human health (Chapman, 1996; Masloomi *et al.*, 2009). In semi-arid areas, water bodies are largely affected by high evaporation rates that may result in high concentration of mineral salts.

The Naromoru area is generally a semi-arid area with few natural water bodies, although there are numerous small community owned dams. In the year 2003 for example, a project initiated by Waterman Foundation and Self Help Centre constructed several large reservoirs (25,000 m<sup>3</sup>) and three sub reservoirs (5,000 m<sup>3</sup>) to supply farmers with water for irrigation. The older dams were however constructed by white settlers to provide water for irrigation and domestic use. Some of the constructed undrainable dams have been stocked with fish, mainly tilapias, although fisheries development has remained low. This paper assesses the suitability of these dams for future fisheries production by presenting data on their physical and chemical characteristics.

## 2.0 Materials and methods

Naromoru area is located on the western leeward side of Mt. Kenya (Figure 1) and upper Ewaso Ng'iro River basin (Gichuki *et al.*, 1998). The area receives a bimodal rainfall pattern with the long rains received from March to May and the short rains from October to December. Rainfall received is usually low averaging 800 mm with a range of 500 mm to 1200 mm per annum. Because of the low rainfall, the main economic activity in the area is marginal mixed farming. Temperatures in the area vary from 20°C to 25°C during the day and from 10°C to 15°C at night (Mathooko, 1992). Fisheries development in the area is largely practised on small aquaculture ponds with little focus on the large undrainable water dams in the area.

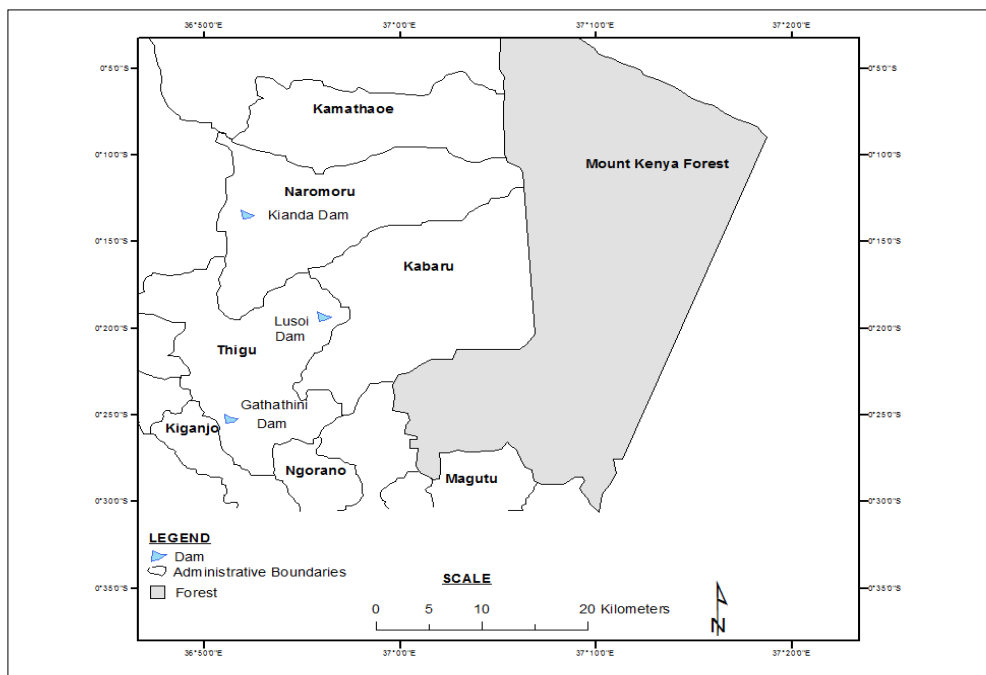


Figure 1: Location of the undrainable water reservoirs (Gathathini, Lusoi and Kianda) in Naromoru area, Central Kenya

Sampling was carried out bi-monthly from September, 2008 to February, 2009. Three dams were purposively selected for sampling, representing the different localities of Naromoru, namely Gathathini (co-ordinates  $S00^{\circ}22.173'$  and  $E037^{\circ}00.699'$ ), Lusoi (co-ordinates  $S00^{\circ}16.528'$  and  $E037^{\circ}03.096'$ ) and Kianda dams (co-ordinates  $S00^{\circ}05.713'$  and  $E037^{\circ}00.107'$ ). Gathathini dam (1782m asl) was developed from a disused quarry but had broken down three years prior to the start of the study and was subsequently rehabilitated. Much of the banks had been overgrazed although the western shores were more vegetated with tussocky grass. The dam is fed by water from Nairobi River, which passes through irrigated vegetable farmlands. During the dry season, the dam's water volume declines significantly due to low inflows although it never dries out completely. Lusoi dam (1989m asl) receives water from a permanent stream and its water level remains largely constant. The dam was constructed in the early 1960s but had been recently desilted. It is well protected with heavy tussocky grass and shrubs growing along the shores. The dam's inlet is characterized by massive growth of emergent macrophytes such as *Typha* species, which prevents excessive inflows of pollutants from the surrounding farmlands.

Kianda dam (1880m asl) is located in a more dryer area. It was recently renovated having broken down in 2003. The dam is fed by a seasonal stream which similarly flows through an intensive agricultural area. During the dry season the inflowing stream dries up and the dam's volume decreases massively. The dam's shores are

bare with little grassy vegetation although large acacia trees surround the dam. The local community has started farming around the dam posing a great danger to the water quality of the dam.

In each of the three dams, the major physical and chemical descriptors of water quality were measured. Water temperature was measured using a pocket thermometer while transparency was estimated by a 20-cm diameter secchi disc (Wetzel, 1983). The secchi disc was gently lowered into the water until it disappeared and then slowly raised until it reappeared. Secchi depth was computed as an average of the depth at which it disappeared and reappeared. Maximum depth of each reservoir was measured using a long straight pole and a tape measure. Water pH, conductivity and total dissolved solids (TDS) were measured in-situ using a calibrated portable pH/Conductivity/TDS probe meter (model PCT: 40). Dissolved oxygen (DO) was measured using a calibrated portable HI 9146 dissolved oxygen meter. Duplicate water samples were collected from the inlet, the shores, dam centre and outlet for analysis of major cations and anions. In total, five samples were collected from dam during the sampling period. Samples were transported in well-rinsed sample bottles to the Department of Mines and Geology, Kenya Government, where concentrations of all ions were determined using an electron spectrophotometer (APHA, 1998).

### 3.0 Results

Surface water temperature, averaged for the whole the study period, was generally higher at Gathathini dam, averaging  $21.9 \pm 0.52^\circ\text{C}$  as compared to  $20.3 \pm 0.43^\circ\text{C}$  and  $20.8 \pm 0.49^\circ\text{C}$  at Lusoi and Kianda dams, respectively (Table 1) although the differences were not significant ( $K=3.638$ ,  $P>0.05$ , Kruskal-Wallis test). The water temperature remained fairly stable at Gathathini dam, ranging from  $21.0$  to  $24.3^\circ\text{C}$ , while at Lusoi dam, water temperature showed greater fluctuation ranging from  $19.3$  to  $21.3^\circ\text{C}$ .

Water transparency was lower at Kianda dam as compared to Lusoi and Gathathini dams (Table 1), but the differences were not significant ( $K=4.028$ ,  $P<0.05$ , Kruskal-Wallis). Gathathini dam was significantly deeper ( $K=6.25$ ,  $P<0.05$ , Kruskal-Wallis) than Lusoi and Kianda dams, with an average depth of  $1.7 \pm 0.38\text{m}$ . The increased depth of water at Gathathini dam was due to the desilting that occurred after the 1997-98 El Nino rains. Kianda dam recorded the least mean depth of  $0.8 \pm 0.08\text{m}$  as compared to Lusoi dam with a mean of  $0.9 \pm 0.03\text{m}$ . Water depth at Gathathini dam was also noted to experience high fluctuations which ranged from  $1.21\text{m}$  to  $4.91\text{m}$ , while Lusoi and Kianda dams had relatively stable water depths.

Water pH was higher at Lusoi dam averaging  $9.6 \pm 0.05$ , as compared to Gathathini and Kianda dams with mean pH values of  $8.3 \pm 0.11$  and  $8.6 \pm 0.05$ , respectively (Table 1).



Table 1: Physical-chemical characteristics of the three reservoirs of Naromoru

Reservoir	Temp (°C)	Transparency (cm)	Depth (m)	pH	TDS (mg/l)	Conductivity (µS/cm)	DO (mg/l)
Gathathini	21.9±0.5	20.4±0.87	1.7±0.	8.3±0	221±4.	312±41.	5.3±0
	2		38	.11	41	3	.01
Lusoi	20.3±0.4	20.5±0.98	0.9±0.	9.6±0	833±3	1283±4	6.7±0
	3		003	.05	5.3	8.1	.06
Kianda	20.8±0.4	7.4±0.03	0.8±0.	8.6±0	530±5	730±10	5.9±0
	9		08	.05	0		.06

However, the differences were not significant ( $K=5.139$ ,  $P>0.05$ , Kruskal-Wallis test). Gathathini dam recorded high fluctuations in water pH ranging from 7.53 to 8.64. Lusoi and Kianda dams had stable water pH that ranged from 9.46 to 9.73 and 8.5 to 8.69, respectively. Lusoi dam had significantly higher TDS ( $K=6.25$ ,  $P>0.05$ , Kruskal-Wallis test) than Gathathini and Kianda dams. TDS at Gathathini dam was low and fairly constant throughout the study period, probably because of low entry of solutes into the dam as the dam is entirely dependent on rain water and its banks are well protected. Lusoi and Kianda dams, however, received stream inflows from extensive agricultural catchments. Water electrical conductivity was significantly higher at Lusoi dam ( $K=6.25$ ,  $P<0.05$ , Kruskal-Wallis), averaging  $1283\mu\text{S}/\text{cm}$ , with a range of 1190 to  $1350\mu\text{S}/\text{cm}$ , probably because of ionic concentration due to the long period it has existed as it was constructed in 1960's. At Gathathini and Kianda dams, electrical conductivity was low averaging  $312\pm 1.11\mu\text{S}/\text{cm}$  and  $730\pm 10\mu\text{S}/\text{cm}$ , respectively. These dams were newly constructed.

Dissolved oxygen (DO) concentration was generally high (Table 1) in the three dams and did not differ significantly between the dams ( $K=1.111$ ,  $P>0.05$ , Kruskal-Wallis test). Lusoi dam had the highest DO concentration that averaged  $6.7\pm 0.06\text{ mg l}^{-1}$ , and relatively higher fluctuations ranging from 5.13 to  $8.31\text{ mg l}^{-1}$ . The high level of oxygen concentration is attributed to the low water temperatures and the location of the dam at high altitude (1989 m) as oxygen solubility increases with decreasing temperature as altitude rises (APHA, 2005). Gathathini and Kianda dams were located at lower altitudes (1782 m and 1880 m) and consequently had higher water temperatures and lower DO concentrations, averaging  $5.3\pm 0.01\text{ mg l}^{-1}$  and  $5.9\pm 0.06\text{ mg l}^{-1}$ , with ranges of 4.91-5.50  $\text{mg l}^{-1}$  and 5.15 to 6.67  $\text{mg l}^{-1}$ , respectively.

Mean concentration of calcium ions ( $123.9\pm 41.71\text{ mg l}^{-1}$ ) was significantly higher at Kianda dam ( $K=6.14$ ,  $P<0.05$ , Kruskal-Wallis test), with Gathathini and Lusoi dams having means of  $18.2\pm 0.79\text{ mg l}^{-1}$  and  $77.4\pm 14.99\text{ mg l}^{-1}$ , respectively (Figure 2).

Unlike calcium, however, sodium ion concentration was significantly higher in Lusoi Dam ( $K=19.65$ ,  $P<0.05$ , Kruskal-Wallis test), averaging  $202.2\pm 9.86 \text{ mg l}^{-1}$  than at Kianda ( $105.9\pm 8.25 \text{ mg l}^{-1}$ ) and Gathathini ( $21.2\pm 0.89 \text{ mg l}^{-1}$ ). Potassium ion concentration at Kianda dams was significantly higher ( $K=12.75$ ,  $P<0.05$ , Kruskal-Wallis test) than the concentrations at Gathathini and Lusoi dams (Figure 2).

The concentrations of heavy metals commonly used in agricultural chemicals and equipment (mainly copper and lead) were generally very low in all the three dams, ranging from  $0.001$  to  $0.134 \text{ mg l}^{-1}$  (Figure 4). Like the major cations, however, Lusoi dam had significantly higher concentrations (Kruskal-Wallis test,  $K=10.66$ ,  $P<0.05$ ), averaging  $0.01\pm 0.002 \text{ mg l}^{-1}$ ,  $0.007\pm 0.002 \text{ mg l}^{-1}$  and  $0.003\pm 0.002 \text{ mg l}^{-1}$  of copper at Lusoi, Kianda and Gathathini dams, respectively. Similarly, lead concentration averaged  $0.048\pm 0.05 \text{ mg l}^{-1}$ ,  $0.02\pm 0.003 \text{ mg l}^{-1}$  and  $0.04\pm 0.009 \text{ mg l}^{-1}$  at Lusoi, Gathathini and Kianda dams, respectively. All the three dams were generally rich in nutrients, particularly phosphates which ranged from  $1.2$  to  $6.0 \text{ mg l}^{-1}$  (Figure. 5). Nitrate levels were significantly higher at Gathathini dam ( $K=14.17$ ,  $P<0.05$ , Kruskal-Wallis test), averaging  $2.0\pm 1.66 \text{ mg l}^{-1}$ ,  $1.3\pm 0.27 \text{ mg l}^{-1}$  and  $0.07\pm 0.01 \text{ mg l}^{-1}$  at Gathathini, Lusoi and Kianda dams, respectively. The concentrations of phosphate ions however had no significant differences ( $K=3.362$ ,  $P>0.05$ , Kruskal-Wallis test) between the three dams, with averages being  $6.0\pm 2.75 \text{ mg l}^{-1}$ ,  $4.7\pm 1.42 \text{ mg l}^{-1}$  and  $1.2\pm 0.81 \text{ mg l}^{-1}$  at Kianda, Lusoi and Gathathini dams, respectively.

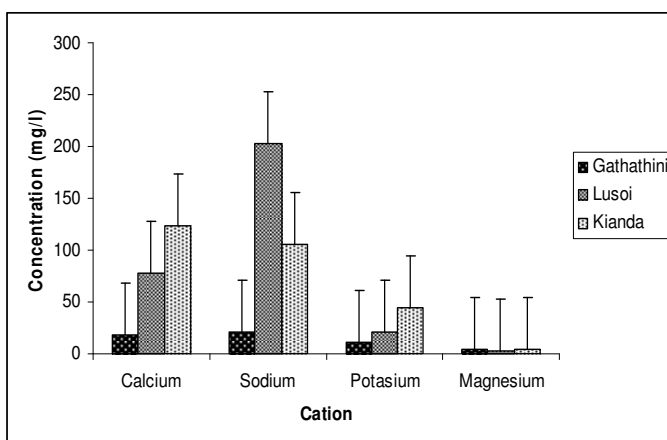


Figure 2: Mean concentration of the major cations in the three undrainable reservoirs of Naromoru

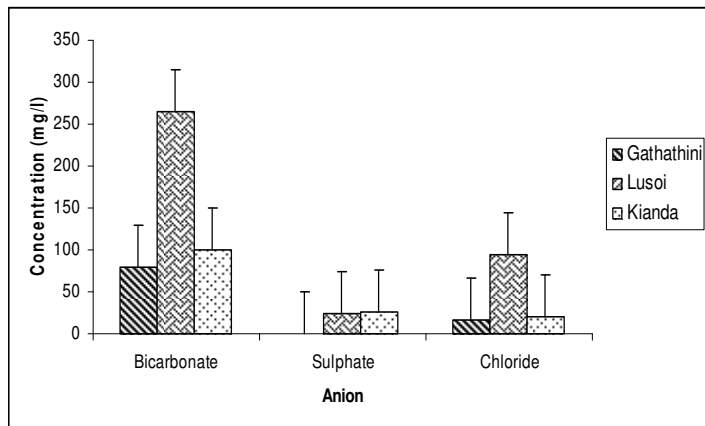


Figure 3: Variation in concentrations of the major anions in the three undrainable reservoirs of Naromoru

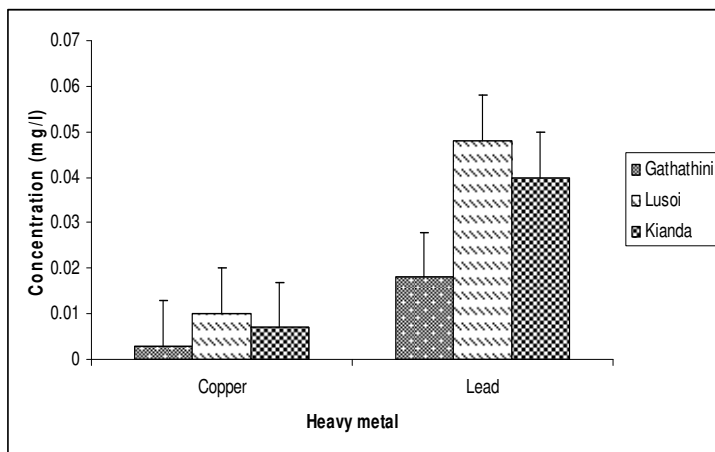


Figure 4: Variations in concentration of heavy metals in the three reservoirs of Naromoru

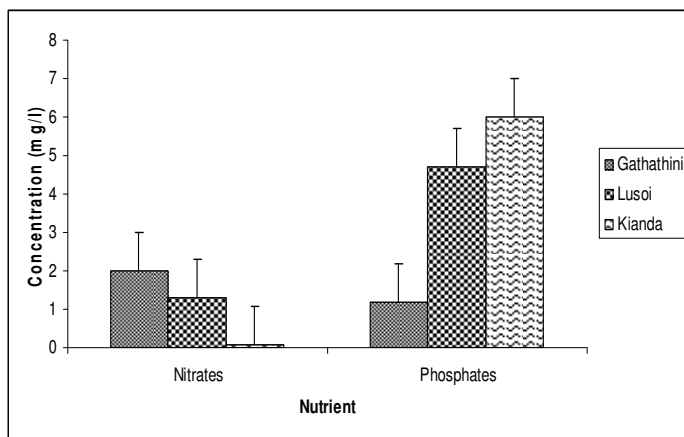


Figure 5: Variation of the major nutrients in the three dams of Naromoru

#### 4.0 Discussion

Undrainable dams generally differ in their characteristics based on location, form and operations (Chapman, 1996). The three undrainable dams differed markedly in their physical and chemical characteristics in relation to their location. Gathathini dam, for example, located at an altitude of 1756m, experienced in average higher temperatures than Lusoi and Kianda dams, which were located on higher altitudes of 1960m and 1852m, respectively. Water dams in Naromoru were generally highly turbid, with turbidity's ranging from 7.32cm at Kianda dam to 22.5cm at Lusoi dam, due to siltation from surrounding catchment areas. Among the three dams, Kianda Dam had more turbid waters than Lusoi and Gathathini dams, as it was open to extensive erosion by surface run-off and disturbance by catfish, *C. gariepinus*. The shores of the dams had extensively cleared shoreline, which had been subdivided by the local community for agricultural purposes. Catfish are bottom dwellers, which extensively stir the bed sediments of a water body while searching for benthic invertebrates, which are their key food items (Koekemoer and Steyn, 2005). High turbidity prevents light penetration into the water thereby reducing primary productivity (Bruckner, 2009). According to Datta (2010), transparencies ranging from 20 to 40cm are suitable for fish production. And while Gathathini and Lusoi dams were within this range, Kianda dam fell below the range. The undrainable dams of Naromoru were generally very shallow, possibly because they have been in existence over a long period and have therefore suffered from extensive siltation. Recently, however, the Government began renovating them and Gathathini dam was reconstructed after the 1997/1998 El Nino rains. As such, Gathathini dam was the deepest of all the three. Kumar (1992) also reported that most undrainable dams in India have shallow depths arising from siltation. Siltation rates of undrainable dams in semi-arid areas are generally high as such areas potentially generate and transport large quantities of sediments during rainy seasons as they are characterised by scanty vegetation cover (Ampofo *et al.*, 2001).

Dissolved oxygen (DO) concentration in the three undrainable dams of Naromoru ranged from 5.0mg<sup>l</sup><sup>-1</sup> at Gathathini dam to 8.71mg<sup>l</sup><sup>-1</sup> at Lusoi dam, which was greater than the minimum concentration of 5mg<sup>l</sup><sup>-1</sup> required for survival of aquatic organisms (Chapman, 1996). The low DO concentration at Gathathini Dam was attributed to the high water temperatures that were experienced in the dam, reducing DO solubility (Ebbert, 2003). Lusoi dam on the other hand had high DO concentration, due to strong waves that occurred in the dam constantly aerating the water. The three undrainable dams of Naromoru had slightly alkaline waters with pH ranging from 7.53 at Gathathini dam to 9.73 at Lusoi dam, which was within the reported ranges of undrainable dams (Chapman, 1996). Kumar (1992), for example, studying the undrainable dams of India found their pH ranging from 7.0 to 9.0. The pH range recorded in all the three dams is within the tolerance

levels of most aquatic organisms (Mukherjee *et al.*, 1992), with maximum fish production occurring with the pH ranges of 6.5 to 8.5 (Alabaster and Lloyd, 1980).

Measurements of total dissolved solutes showed Lusoi dam to have significantly higher ionic concentration, indicating that the dam was much more fertile than the other two. Similarly, the dam also had significantly higher conductivity than the other two, again confirming the higher fertility status of the dam. TDS and conductivity have been shown to have a positive and significant correlation (Kutty, 1987), which supports the findings reported in this study. The high concentration of TDS and electrical conductivity at Lusoi dam was attributed to accumulation of ions in the dam over a long period of time (since the creation of the dam in early 1960's). Gathathini and Kianda dams, which were constructed later recorded lower TDS and electrical conductivities. Generally, undrainable dams tend to have high salinities and conductivities due to lack or less outflow of water (UNEP, 2006), and high evaporation rates, which tend to concentrate dissolved minerals (Gordy, 2001). The predominant ions in all the three dams were sodium and calcium, although highest concentrations were recorded in Lusoi dam. The observation is in agreement to the measurements of conductivity and TDS, which were also highest in Lusoi dam. Studies by Purandara *et al.* (2004) along Malaprabha River in India reported that water bodies with high electrical conductivity values are predominant with sodium and chloride ions. Unexpectedly, the dams though occurring in intensively cultivated areas, had very low heavy metal concentrations, far below the recommended WHO guide for safe water levels (WHO, 2008). This result was surprising as most farmers around the area frequently use pesticides to spray their vegetables against pests. Nitrate levels were significantly higher in Gathathini Dam as expected as the reservoir had been recently fertilized using farm manure. It is concluded that the water quality of the dams is suitable for fish farming.

#### **Acknowledgements**

We are grateful to Kenya Agricultural Productivity Project (KAPP), Kenyatta University and the Department of Geology and Mines which supported us both financially and by providing equipments and services that ensured successful completion of this study.

#### **References**

- Alabaster J. S and Lloyd R. (1980). Water quality criteria for fresh water fish. *International Review of Hydrobiology*, **66**(3), pp. 443.
- Ampofo E. A, Muni R. K. and Bonsu M. (2001). An assessment of sediment loading into an agricultural reservoir in a semi-arid region of Kenya. *West African Journal of Applied Ecology*, **2**, pp. 37-47.

APHA. (2005). American Public Health Association, Standard Methods for the Examination of Water and Wastewater (22nd Ed), American Public Health Association, Washington D.C., USA.

Bruckner M. Z. (2009). Measuring lake turbidity using a secchi disk: Science education resource centre. Carleton College.

Chapman D. (1996). Water quality assessment: A guide to the use of biota, sediments and water in environmental monitoring. E & FN spon publishers, London, pp. 650.

Datta S. (2010). Water analysis and management for fish culture. Coldlake city, Kolkata. Retrieved from <http://www.scribd.com/doc/23536285/Water-Analysis-and-Management-for-Fish-Culture>.

Dortsch, M.S. (1981). Destratification of lakes and reservoirs to improve water quality: Australian publishing service.

Dortsch M. S. (1981). Destratification of lakes and reservoirs to improve water quality: Australian publishing service.

Ebbert J. C. (2003). Water temperature, specific conductance, pH, and dissolved oxygen in the lower White River and the Puyallup River estuary, Washington, August-October 2002. Water resource investigation report 03-4177.

Gichuki F. N., Liniger H., Macmillan L. C. Schwilch G. and Gikonyo J. K. (1998). Scarce water: Exploring resource availability, use and improved management. *East and Southern Africa journal*. Vol. 8, Special number.

Gordy G. E (2001). A primer on water quality. United States Geological Survey (USGS), USA FS-027-01.

Kemdirim E. C. (2005). Studies on hydrochemistry of Kangimi reservoir, Kaduna state, Nigeria. *African Journal of Ecology*. 43, pp. 7-13.

Kinyua A. M. and Pacini M. (1991) Impact of Pollution on the Ecology of Nairobi-Athi river System in Kenya. *International Journal of Biochemistry and Biophysiology*. 1, pp. 5-7.

Koekemoer J. H and Meyn G. J. (2005). Fish community study of Hartbeespoort Dam. Research report by the Department of Agriculture, Environment and Tourism, North West Province, South Africa. Final report No. 67/2004.

Kumar D. (1992). Fish culture in undrainable ponds: A manual of extension FAO fisheries technical report No. 325. Rome, FAO, 1992, pp. 239.

Kutty M. N (1987). Site selection for aquaculture; biological productivity of water bodies. FAO publication Report No: FAO-FI--RAF/82/009; FAO-FI--ARAC/87/WP/12/1-2, Port Harcourt, Nigeria, pp 9.

Maslooni S., Deghani M. H., Norouzi M., Davil M. F., Amarluie A., Tardast A and Karamitabar Y. (2009). Physical and chemical water quality of Ilam water treatment plant. *World applied Science Journal*, **6(12)**, pp. 1660-1664.

Mathooko J. M. (1992). A survey to establish the nature and composition of benthos along Narumoru, a tropical river in Central Kenya. Msc. Thesis.

Mukherjee T. K., Moi P. S., Parandam J. M and Yang Y. S. (1992). Integrated livestock-fish production. FAO/IPT workshop in Kuala Lumpur.

Purandara B. K., Varadarajan N. and Kumar C. P. (2004). Application of chemical mass balance to water quality data of Malaprabha River. *Journal of Spatial Hydrology*, **4(2)**, pp. 1-23.

Sena de Silva. (1988). Reservoirs of Sri-Lanka and their fisheries, FAO technical paper No. 298:128.

Thornton J. A and Rast W. (1993). A test of hypothesis relating to the comparative limnology and assessment of eutrophication in semi-arid and man-made lakes: Development in hydrobiology. Klumer academic publishers, pp. 1-24.

UNEP (2006). Water quality for ecosystem and human health. United Nations Environmental Programme Global Monitoring System (GEMS)/ water programme. Ontario, Canada. Technical Advisory Paper No. 3-September 2006.

Wetzel R. G. (1983). Limnology, 2<sup>nd</sup> edition. Saunders, Philadelphia, pp 767.

World Health Organization. (2008). Guidelines for drinking water quality: Third edition incorporating first and second addenda, Vol. 1. Recommendations, Geneva, Switzerland, pp. 297-460.

**DISTRIBUTION OF COMMERCIAL MOBYDICK (*GOMPHOCARPUS SPP*)  
GROWN IN KENYA AS REVEALED BY MORPHOLOGICAL CHARACTERIZATION**

**S. M. Saggafu<sup>1</sup>, A. O. Watako<sup>1</sup> and G. E. Mamati<sup>1</sup>**

<sup>1</sup>Jomo Kenyatta University of Agriculture and Technology, Kenya

Email: saggasito@gmail.com

**Abstract**

The genus *Asclepias* of *Gomphocarpus* subspecies commonly known as mobydick is currently grown commercially as a cutflower in Kenya. *Asclepias* refers to milkweed species grown in America and other Western worlds while *Gomphocarpus* refers to *Asclepias* species in Africa and Arabia continents. The varieties are distinguished mainly by boll characteristics which include size, shape, and plant height. In the farmers' fields, *Gomphocarpus physocarpus* and *Gomphocarpus fruticosus* integrate to form a continuum and are difficult to distinguish. However, there is no precise data on the available commercial varieties of *Gomphocarpus* species grown and exported from Kenya. The species has recently been domesticated in Kenya but characterization has not been done. The objective of the study was to determine the distribution of major *Gomphocarpus* varieties in Kenya. A preliminary survey was done using the morphological characteristic of height to determine the prevalent type among farmers. The survey was conducted between April and June, 2011. The sampled areas were Machakos, Murang'a, Nandi, Nyeri, Bomet, Embu, Laikipia, Kisumu, Meru, Kajiado, Migori and Makueni districts. In order to get accurate information on the data collection sites, each farm was mapped by Global Positioning System (GPS) receiver; this instrument gave the altitudes (elevations), latitudes and longitudes of the sampled areas. A line level was used to establish the slope of the various sampled sites. Using boards graduated in the metric system, a distance of 10 metres between the boards was used. The board was moved up and down the slope until the spirit level showed that the string was horizontal. In this case, a difference in height of 10 cm would mean a slope of 1 %, whereas a height difference of 5 cm meant a gradient of 0.5% and 2.5 cm difference in height represented 0.25% gradient. A total of 145 farmers were selected at random and interviewed using a questionnaire. Soil samples were collected from sampled farms and analyzed in JKUAT laboratory using the hydrometer method. Materials used for soil structural analysis were water, sieves, hydrometer, sodium hexametaphosphate solution, amyl alcohol, soil dispersing stirrer, reciprocating shaker and soil textural triangle. The results showed that of the 145 farmers, 84.8% grew tall mobydick variety while 15.6 % grew the short variety. The results also indicate that 30.9% of all farmers growing the tall variety are in Machakos, Muranga (6.5 %), Nandi (11.4 %), Nyeri (14.6 %), Bomet( 7.3%), Embu (4.9 %), Laikipia ( 6.5%) , Kisumu (4.1%) , Meru (11.4 %) and the least were in Kajiado, Migori and Makueni each recording 0.8 %. As regards altitude, 84.8 % of all mobydick farmers grow the tall variety between 887-1388 m above sea level. Data collected on agro-ecological zones indicate that mobydick grows across UM4, LU4, UM2, LM4, SU3, LM3, LM1 and LM5 with 84.8 % of all farmers growing the tall variety. In conclusion, the tall variety is the most dominant of the commercial mobydick varieties among the Kenya farmers. The variety also dominates all agro-ecological zones at the current status.

**Key words:** *Asclepias*, characterization, cutflower, distribution, Mobydick



## 1.0 Introduction

The milkweeds or *Gomphocarpus* genus consists of over 140 species. The term *Gomphocarpus* is derived from the Greek *gomphos* meaning a club, and *karpos*, fruit. *Asclepias* is used to refer to milkweed species grown in America and other Western worlds while *Gomphocarpus* refers to *Asclepias* species found in Africa and Arabia continents (Hodkiss, 2009). *Gomphocarpus* comprises about twenty two (22) species in tropical Africa and Peninsular Arabia. *Gomphocarpus fruticosus* grows wild throughout in African countries (Gurib-Fakim et al., 2011). These countries include East Africa, Southern Africa and South Africa, Senegal, Guinea, Côte d'Ivoire, Cameroon, Sudan, Madagascar and Mauritius. The plant also occurs in Yemen, northern Africa, southern Europe, eastern Australia, Oman and Saudi Arabia. *Gomphocarpus cancellatus* and *Gomphocarpus filiformis* occur in Namibia and South Africa. *Gomphocarpus glaucophyllus* occurs from Uganda south to South Africa. *Gomphocarpus semilunatus* occurs from Nigeria east to Ethiopia, East Africa to southern Congo, Zambia and Angola. *Gomphocarpus solstitialis* occurs throughout West Africa. *Gomphocarpus stenophyllus* appears in the semi-arid regions of southern Ethiopia, Kenya and Tanzania. *Gomphocarpus tomentosus* appears throughout southern Africa (Baerts and Lehmann, 2009).

On the other hand, *Gomphocarpus physocarpus* is widespread in America, Europe, Asia and Africa. Although naturalised and widespread in South Africa for some time, it is an introduced weed native to tropical Africa (Muller, 2005).

Both *Gomphocarpus fruticosus* and *Gomphocarpus physocarpus* occur in well-drained, dry sandy soils. They are also found in grasslands, along road sides, railway lines and abandoned fields; they are frequently on river banks, in full sun or partial shade. However, some species are also found in shady forest understories although these are few (Eigenbrode and Espelie, 1995). The two grow from sea-level up to 887-2191 m altitude.

Cutflower constitutes a major section of the horticultural export market in Kenya. Over the years, the cutflower industry has undergone rapid expansion placing Kenya as the biggest supplier of cutflowers in the international market. However, the market is still dominated by traditional flowers while the indigenous ornamentals account for 0.01% of the Kenya cutflowers market (Waiganjo et al., 2008). Over dependence on traditional flowers is unsustainable because of stiff market competition, production challenges and breeders rights requirements in the global market. So far, research activities have mainly concentrated on exotic crops for many years in Kenya. Studies have revealed that most indigenous crops have fewer challenges in the field compared to the existing traditional crops (Waiganjo et al., 2008). Thus, extra efforts are essential in order to increase the diversity of cutflower exports and remain competitive in the international market through collection, domestication and development of production packages for indigenous cutflower.

Some visits were made before the year 2008 headed by the Kenya Agricultural Research institute (KARI), Thika researchers in collaboration with the wildlife officers to the Mount Kenya forest, bush lands in central Kenya, Aberdares and Coast Province. The aim of this mission was to look for plants with outstanding ornamental features for possible domestication.

Commonly known as Mobydick, *Gomphocarpus* is currently grown commercially as a cutflower in Kenya. In the farmers' fields, *G. physocarpus* and *Gomphocarpus fruticosus* integrate to form a continuum and are difficult to distinguish. The species could be distinguished mainly by boll characteristics which include size, shape, and plant height. Some *Gomphocarpus* have relatively large green bolls while others have small green bolls.

*Gomphocarpus physocarpus* is known to hybridize with *Gomphocarpus fruticosus* (Goyder, 2001). When *Gomphocarpus* was introduced into the export market in central Kenya in the year 2001 as cutflower, it became particularly popular among consumers. The crop has had phenomenal growth in export markets from 13 kg valued at Ksh.1287 in the year 2001 to 288,707kg valued at Kshs. 50,000,000 in the year 2006 (Waiganjo *et al.*, 2008).

However, there is no precise data on the available commercial varieties of *Gomphocarpus* species grown and exported from Kenya. The species has recently been domesticated in Kenya but characterization of the useful lines has not been done. The species is also grown commercially and therefore there is need to improve it and develop varieties with better utility locally and at international market.

An investigation was carried out between April and June 2011 in the famers' fields to study the major *Gomphocarpus* variety grown in Kenya. The main objectives of the project were to determine the distribution of major *Gomphocarpus* among small scale growers in Kenya. The information obtained from this study shall be used for the documentation of the *Gomphocarpus* germplasm available in Kenya and determine their distribution in the various growing regions.

## 2.0 Materials and methods

A survey was conducted to collect information on the distribution of commercial Mobydick in Kenya between April and June, 2011. In order to get accurate information on the data collection sites, each farm was mapped by Global Positioning System (GPS) receiver; this instrument gave the altitudes (elevations), latitudes and longitudes of the sampled areas. The sampled areas were selected at random to give a more realistic statistic data on the distribution of commercial mobydick grown in Kenya. A line level was used to establish the slope of the various sampled sites. A line level was used to establish the slope of the various sampled sites. Using boards graduated in the metric system, a distance of 10 metres between the boards was used. The board was moved up and down the

slope until the spirit level showed that the string was horizontal. In this case, a difference in height of 10 cm would mean a slope of 1 %, whereas a height difference of 5 cm meant a gradient of 0.5% and 2.5 cm difference in height represented 0.25% gradient. In total, 145 farmers were selected and later interviewed. Soil samples were also collected from sampled farms and analyzed at Jomo Kenyatta University of Agriculture and Technology (JKUAT) laboratory using the hydrometer method. Materials used for soil structural analysis were water, sieves, hydrometer, sodium hexametaphosphate solution, amyl alcohol, soil dispersing stirrer, reciprocating shaker and soil textural triangle. A soil sample weighing 50g collected from each sampled farm was subjected to analysis using Bouyoucos method. The survey was carried out in twelve mobydick growing areas namely, Machakos, Murang'a, Nandi, Nyeri, Bomet, Embu, Laikipia, Kisumu, Meru, Kajiado, Migori and Makueni districts of Kenya.

### **2.1 Sampling**

A targeted sampling procedure was used in which farmers growing Mobydick were identified. In the survey, consultation with local *Gomphocarpus* farmers was used as a guide to accurately locate sampled sites.

### **2.2 Data collection**

Data collection involved individual interviews of Mobydick-growing farmers at targeted sites. A semi-structured questionnaire was used as a tool in the study to get relevant information from the respondents. The sampled farms were mapped using Global Positioning System (GPS) receiver to get accurate position of the mobydick farms. Soil samples were also collected at random from various positions on the farms. These samples were then analysed for soil mapping at JKUAT laboratory to establish the soil textures of mobydick growing areas. To establish the gradient of the sampled farms, a line level consisting of two sticks (boards) was used. Using boards graduated in the metric system a distance of 10 metres between the boards was used. Information concerning the mobydick varieties grown by the farmers, acreage under each variety, constraints to mobydick production, altitude, longitude and latitude was collected using a questionnaire. Data on planting materials (seed sources), soil textures, gradient (%) of sampled farms and market for Mobydick were also captured.

### **2.3 Data analysis**

Data analysis was carried out using Statistical Package for the Social Sciences (SPSS). This package produced percentages of the Mobydick varieties found grown by farmers in the sampled farms. Descriptive characteristics were obtained for various attributes. Such attributes included altitude, soil texture and agro-ecological zones. A likelihood ratio test or chi-square probability distribution was employed to determine whether the distribution of Mobydick varies significantly or not across agro-ecological zones, districts, altitude and soil texture.

### 3.0 Results

#### 3.1 Mobydick distribution in Kenya

This distribution is displayed in the map (Figure 1). Farmers in these districts grew either of two commercial mobydick varieties or both. The two varieties were a six month and three months long maturity types (Table 1).

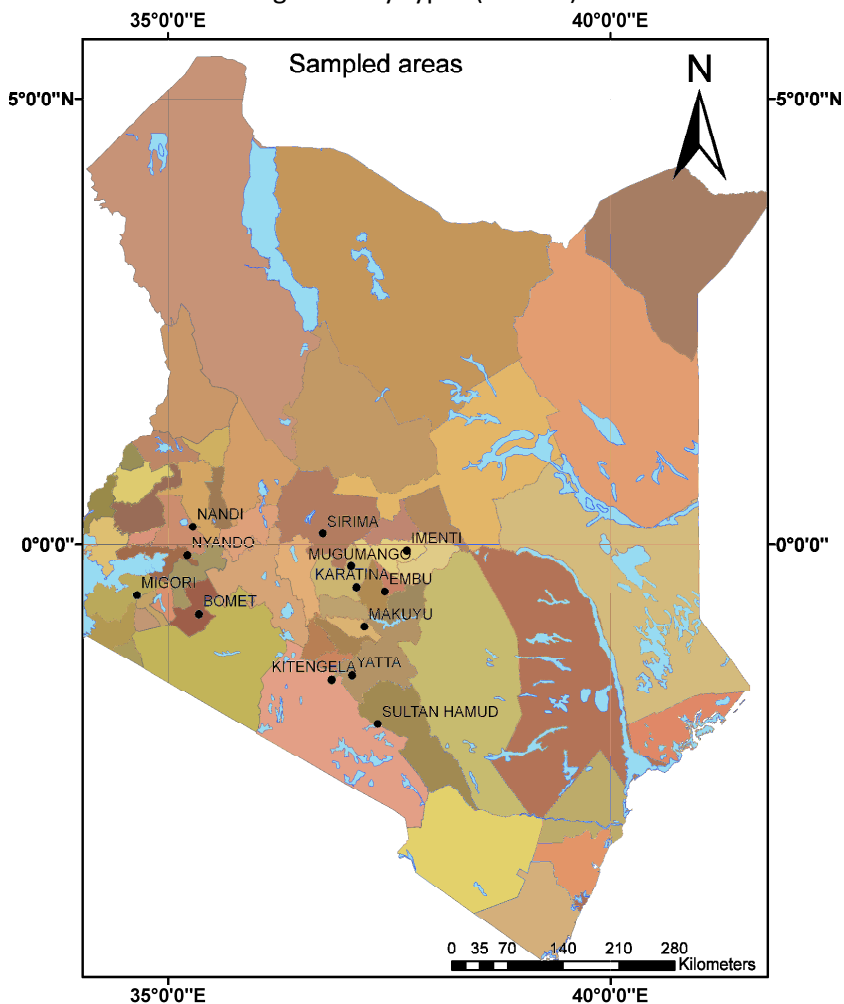



Figure 1: Map showing prevalent areas commercial Mobydick are currently grown in Kenya

Key: The colors represent different administrative boundaries and water points

 Water points (rivers, streams, lakes)

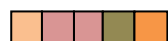
 All other colors inclusive referring to administrative boundaries

Table 1: Mobydick variety frequencies in sampled district farms

Locality	variety	Mobydick count
Machakos	Tall, short	* ( 38 , 4 )
Muranga	Tall, short	(8, 2 )
Nandi	Tall, short	(14, 4 )
Nyeri	Tall, short	(18, 3 )
Bomet	Tall, short	(9, 2 )
Embu	Tall, short	( 6 , 1)
Laikipia	Tall, short	( 8 , 2 )
Kisumu	Tall, short	( 5 , 1 )
Meru	Tall, short	(14, 3 )
Kajiado	Tall, short	(1, 0 )
Migori	Tall, short	(1, 0 )
Makueni	Tall, short,	(1, 0 )

*\*Number of farmers growing the Tall and Short Mobydick. The first and second figures in the brackets stand for Tall and Short varieties respectively*

In the survey, the six month varieties were identified to be more popular than the three months type in all visited farms (Table 1). The three months Mobydick was relatively shorter in height compared to the six months variety. The bolls of the six months variety were globular unlike the three months variety bolls which had a tapered end.

The six months mobydick occupied 84.8 % of mobydick farms while the three months variety occupied 15.2 % only (Table 2). Survey results indicated that current mobydick farms range between 0.1 to 3 acres in size in which 97.2 % of farmers hold 0.1 to 1 acres of mobydick production (Table 3). The type of the planting material used by all the farmers was seed which were sourced from contracted commercial company/Wilmar (97.9%), farmer's own farm (1.4%) and from neighbors (0.7%) (Table 3). Constraints to mobydick farming were pests, diseases and capital (Table 3). Mobydick farming was prevalent at altitudes 887 to 1388 meters above sea level. Similarly, soil types ranged from sand to red loam while the popular gradient was moderate slope. The total percentage attribute against each parameter is shown in the last column (Table 3).

As shown in Table 4, there were no significant differences in the distribution of Mobydick varieties across agro-ecological zones, districts, altitudes and soil texture ( $P= 0.05$ ).

Table 2: Mobydick distribution across districts and agro-ecological zones (AEZ)

Attribute		% within Mobydick		% of Total		Gross %	
		Tall	Short	Tall	Short	Tall ( 6 Moths Variety)	Short (3 Moths Variety)
District	Machakos	30.9	18.2	26.2	2.8	84.8%	15.2%
	Muranga	6.5	9.1	5.5	1.4		
	Nandi	11.4	18.2	9.7	2.8		
	Nyeri	14.6	13.6	12.4	2.1		
	Bomet	7.3	9.1	6.2	1.4		
	Embu	4.9	4.5	4.1	0.7		
	Laikipia	6.5	9.1	5.5	1.4		
	Kisumu	4.1	4.5	3.4	0.7		
	Meru	11.4	13.6	9.7	2.1		
	Kajiado	0.8	0.0	0.7	0.0		
	Migori	0.8	0.0	0.7	0.0		
Makueni	0.8	0.0	0.7	0.0			
AEZ	UM4	44.7	36.4	37.9	5.5		
	LU4	10.6	18.2	9.0	2.8		
	UM2	20.3	18.2	17.2	2.8		
	LM4	12.2	13.6	10.3	2.1		
	SU3	4.1	4.5	3.4	0.7		
	LM3	6.5	9.1	5.5	1.4		
	LM1	0.8	0.0	0.7	0.0		
	LM5	0.8	0.0	0.7	0.0		

Table 3: Mobydick distribution and attributes in sampled districts

Attribute		% of gomphocarpus in attribute		Gross ( % of sub-attribute in main attribute )
Main attribute	Sub-attribute	Tall	Short	
soil texture	sand	81.8	18.2	7.6
	sand loam	84.1	15.9	30.3
	loam	86.1	13.9	24.8
	alluvial black	85.7	14.3	4.8
	clay loam	82.4	17.6	11.7
	black cotton	87.0	13.0	15.9
	red loam	85.7	14.3	4.8
Slope	Flat (0-1%)	100.0	0.0	2.1
	Gentle (1-2.5%)	84.6	15.4	18.1
	Moderate (2.5-5%)	84.3	15.7	79.9
Altitude(m)	887-1388	87.0	13.0	47.8
	1389-1690	81.0	19.0	14.5
	1691-2191	83.6	16.4	37.9
Farming duration(yrs)	1-5YRS	83.6	16.4	80.0
	6-10YR	89.7	10.3	20.0
Latitude(°)	-2.9 to -1	100.0	0.0	0.7
	-0.9 to 0	81.8	18.2	7.6
	0.1to 2	85.0	15.0	91.7
Longitude(°)	34.5 -35.9	80.6	19.4	24.8
	36 - 37.4	83.3	16.7	29.0
	37.5-38.9	88.1	11.9	46.2
Planting material source	One's own farm seeds	100.0	0.0	1.4
	Commercial company (Wilmar) seeds	84.5	15.5	97.9
	Neighbor seeds	100.0	0.0	0.7
Farm size(Acres)	0.1-1	85.1	14.9	97.2
	1.1-2	100.0	0.0	1.4
	2.1-3	50.0	50.0	1.4

Table 4: *Gomphocarpus* distribution test of significance across key attributes

Attribute	Chi-Square Tests value (Likelihood Ratio)	Pvalue
Altitude	0.542	0.762
Soil texture	0.310	0.999
Districts	3.298	0.986
Agro ecological zones	2.038	0.958

There was no significant difference in the distribution of Mobydick varieties across agro-ecological zones, districts, altitude and soil texture (P=0.05).

Table 5: Features of commercial *Gomphocarpus* varieties

Gomphocarpus species	Boll shape and size	Leaf shape	Canopy density	Duration to maturity	Plant height	Height range of tall and short varieties
<i>Gomphocarpus physorcarpus</i>	Larger more globular bolls	Broader leaf shape	Giant /bush canopy	Takes 6 months to mature	Has potential to grow to 2.5 m.	0.5m
<i>Gomphocarpus fruticosus</i>	Smaller bolls with tapering short curved beak.	Narrow leaved shape.	Light canopy	Takes 3 months to mature.	Grows up to 2 meters high.	

Adapted from Goyder and Nicholas (2001)

*Gomphocarpus fruticosa* bolls were smaller with curved beak end whereas the *Gomphocarpus physorcarpus* bolls were larger and globular in shape. The two Mobydick plants differed in their canopy appearance. *Gomphocarpus fruticosus* could grow to a height of 2.0 m with a light canopy compared to *Gomphocarpus physorcarpus* bush canopy having a potential to grow to a height of 2.5 metres, hence giving a height range of 0.5m between the tall and short Mobydick varieties (Table 5).

#### 4.0 Discussion

In order to determine the distribution of commercial Mobydick varieties in Kenya, a survey was conducted targeting the Mobydick growers in various areas. Results indicate that currently Mobydick is grown between 887m to 2191m above sea



level (Table 3). These results confirm previous findings on Mobydick growing areas giving an altitude range of between sea level up to 2500 m (Gurib-Fakim *et al.*, 2011). At least 62% of Mobydick farmers were concentrated in the lower hot altitude between 887 m-1690 m above sea level in Machakos, Migori, Kisumu, and Makueni. A few farmers, 38%, were in higher altitudes above 1700 m in cooler environments of Nandi, Nyeri, Laikipia and Embu. These altitude levels agree with Körner and Renhardt (1988) work that lower temperatures at higher altitudes delay plants growth thus fewer farmers preferring to grow this crop. The optimum growing temperatures for Mobydick are considered to be between 22-27°C (Waiganjo *et al.*, 2008). In cooler regions such as tea growing zones (over 1800m above sea level), it takes a longer time to mature.

Two commercial Mobydick varieties were found on farmers' fields, *Gomphocarpus physocarpa* and *Gomphocarpus fruticosus*. Farmers use duration to maturity as a criterion in describing the two Mobydick varieties. Hence, the six months variety is referred to as taller and takes a longer time to mature whereas the three months variety is dwarf and matures earlier. The six months variety was more superior against browning of the bolls, which is a big challenge in Mobydick industry (Waiganjo *et al.*, 2009). Over 68% of the narrow leaved variety was found in the drier agro-ecological zones 4 and 5, matching the results by Garnish (2004) that leaf size decreases with environmental aridity.

Both pests and diseases are common mostly on dry weather (Coakley *et al.*, 1999). Mobydick grew in a wide range of soil textures from sand, sandy loam, loam, alluvial black, clay loam, black cotton and red loam (Table 3). The survey results also showed that Mobydick was grown between latitude 2.90 South to 20 North and longitude 34.50 East to 38.90 East. According to survey results, most growers were small scale farmers with farm size ranging from 0.1 to 3 acres (Table 3). The tall or six month maturity variety was still prevalent from topographical point of view, which is at flat (0-2.5%) slope, gentle (2.5-5%) slope and moderate (2.5-5%) slope (Table 3). The results also showed that Mobydick farming has been in existence at least for the last 10 years in Kenya (Table 3). Analysis results revealed that there were no significant differences in the distribution of Mobydick varieties across agro-ecological zones, altitude, districts and soil texture (Table 4).

Morphological characteristics revealed that the tall and six months maturing variety had larger, more globular bolls with broader leaves. The canopy of the six months maturity variety was denser compared to the shallower three months maturity Mobydick (Table 5). This confirms similar findings by Goyder and Nicholas (2001) and similar description of morphological characteristics of giant swan or *Gomphocarpus physocarpus* (Lazarides and Hince, 1993). The three months variety is an erect narrow leaved plant, growing up to 2.5m high, with smaller bolls tapering into a short curved beak. These morphological features of the three

months variety matched Gurib-Fakim *et al.*, (2011) description of *Gomphocarpus fruticosus* or Swan plant; the six months variety is very similar to *Gomphocarpus fruticosus* except for its broader leaves and a more globular fruit that stands on a straight stalk; the fruit in the six months variety doesn't taper into the short curved beak. The six months variety has the potential to grow upto 2.5m (Coombs *et al.* 2008), giving a height difference of 0.5m between the short and tall Mobydick varieties (Table 5).

## 5.0 Conclusion and recommendations

The study aimed at determining the distribution of major Mobydick varieties in Kenya. Farmers commented that they chose to grow the six months variety because the variety seemed to be less affected by boll discolouration than the three months variety. The two Mobydick varieties have been identified as *Gomphocarpus physocarpus* and *Gomphocarpus fruticosus* for six months and three months maturing plants respectively.

*Gomphocarpus physocarpus*, the vigorous growing, broad leaved Mobydick was more prevalent in the field situation with an occurrence of 84.8% of the total commercial Mobydick count. *Gomphocarpus fruticosus*, the dwarf, narrow leaved swan plant, which was observed to be more susceptible to boll pigmentation but less prevalent occupied the remaining 15.2 %.

Since the distribution of Mobydick varieties was not significant across agro-ecological zones, districts, altitude and soil texture, it means that there were other covariants which could have better explained Mobydick distribution other than agro-ecological zones, districts, altitude and soil texture. There is an opportunity, therefore, to introduce Mobydick to other areas in Kenya where the crop has not been grown before.

## Acknowledgements

I would like to express my deep appreciation and gratitude to the Department of Horticulture (JKUAT) for the advice, guidance as well as to the National Council for Science and Technology (NCST) for the financial support.

## References

- Baerts M. and Lehmann J. (2009). *Gomphocarpus fruticosus*. Prelude Medicinal Plants Database. Metafro-Infosys, Royal Museum for Central Africa, Tervuren, Belgium.
- Coakley S. M., Scherm H and Chakraborty S. (1999). Climate Change and Disease Management. *Ann.Rev. Phytologist*, **37**, pp. 99-426.
- Coombs G., Peter C. I. and Johnson S. D. (2008). A test for Allee effects in the self-incompatible wasp-pollinated milkweed *Gomphocarpus physocarpus*. *Australia Ecology*, **34** (6), pp. 688-697.

Eigenbrode S. D. and Espelie K. E. (1995). Effects of plant epicuticular lipids on insect herbivores. *Annual Review of Entomology*, **40**, pp. 171–194.

Garnish T. J. (2004). Comparative studies of leaf form—assessing the relative roles of selective pressures and phylogenetic constraints. *New Phytologist*, **106**, pp. 131–160.

Goyder D. (2001). *Gomphocarpus* (Apocynaceae: Asclepiadaceae) in an African and a global context – an outline of the problem. *Biologiske Skrifter*, **54**, pp. 55-62, Netherlands.

Goyder D. J. and Nicholas A. (2001). A revision of *Gomphocarpus* R.Br. (Apocynaceae: Asclepiadeae). *Kew Bulletin*, **56**(4), pp. 769–836.

Gurib-Fakim A., Aiton W. T and Schmeltzer, G. H. (2011). *Medicinal plants/Plantes médicinales 2*. [CD-Rom]. PROTA, Wageningen, Netherlands.

Hodkiss R. J. (2009). *Asclepias* – International Asclepiad Society Journal; The succulent plant 106: 24-58

Körner, C. and Renhardt, U. (1988). Dry-matter partitioning and root length leaf-area ratios in herbaceous perennial plants with diverse altitudinal distribution. *Oecologia* **74**, pp. 11–418.

Lazarides M. and Hince B. (1993). *CSIRO handbook of economic plants of Australia*. (CSIRO, Melbourne). No. 136.2.

Muller J. F. (2005). Geographical distribution and seasonal variation of surface emissions and deposition velocities of atmospheric trace gases, *J. Geophys. Res.* 787–3804.

Waiganjo M. M., Gikaara D. N., Kamau E. and Muthoka N. M. (2008). Domestication of indigenous ornamentals and the crop production challenges in mobydick, *Asclepias* sp. in Kenya. *Acta Horticulture (ISHS)*, **813**, pp. 79-86.

Waiganjo M. M., Gikaara D. N., Kamau E. and Muthoka N. M. (2009). Domestication of indigenous ornamentals and the crop production challenges in mobydick, *Asclepias* sp. in Kenya. *Acta Horticulture (ISHS)*, **813**, pp.79-86

**EFFECTS OF EXPOSING ADULTS OF *AMBLYOMMA VARIEGATUM* TO NEEM CAKE EXTRACTS IN TRAPS BAITED WITH SEMIOCHEMICALS UNDER SEMI-LABORATORY CONDITIONS**

**A. Touré<sup>1</sup>, R. Maranga<sup>2</sup>, A. Hassanali<sup>3</sup>, S. Kubasu<sup>4</sup>, E. O. Osir<sup>3</sup> and E. Nyandat<sup>3</sup>**

<sup>1</sup> Ministère de l'Élevage, Dakar, Sénégal

<sup>2</sup> Jomo Kenyatta University of Agriculture and Technology, Kenya

<sup>3</sup> International Centre of Insect Physiology and Ecology (icipe), Nairobi, Kenya

<sup>4</sup> Kenyatta University, Kenya

Email : bellamaranga2010@yahoo.com

**Abstract**

The efficacy of a trap baited with an attractant blend comprising of attraction-aggregation-attachment pheromone (AAAP), 1-octen-3-ol and CO<sub>2</sub> and treated with Neem (*Azadirachta indica*) cake extracts (0.6% of azadirachtin) to attract and expose the ticks, *Amblyomma variegatum* (Fabricius) (Acari: Ixodidae) to the active constituents of the cake was evaluated in circular field plots. Ticks were released at various distances from trap placed at the center of the plots. Ticks that arrived at the trap (and exposed to the extracts) and those in control plots were collected and their mortality was monitored in the laboratory over a three-week period. All concentrations of the neem extracts caused mortality of *A. variegatum* adults with highest mortality rate (97.8%) recorded in the concentration of 30 % of extracts. The mortality of the ticks was also dependent upon the time ticks were exposed to the extracts. The findings suggest the possibility of using semiochemicals-baited traps in combination with neem extracts for off-host control of these ticks in small-holder farms.

**Key words:** *Amblyomma variegatum*, traps, *Azadirachta indica*, semiochemicals

## 1.0 Introduction

Trapping of ticks in vegetation has been known for many years. Eads *et al.* (1982) and Gray (1985) demonstrated the attraction effect of CO<sub>2</sub> on *Dermacentor andersoni* and *Ixodes ricinus* in sampling experiments. Subsequently, (Schöni *et al.*, 1984) reported that *Amblyomma variegatum* female was attracted from 1 m by the attraction-aggregation-attachment pheromone (AAP) and that ortho-nitrophenol induces orientation and dynamic aggregation while methyl salicylate and nonanoic acid, together with ortho-nitrophenol, induce mounting and clasping behaviour. Norval *et al.* (1989) showed in field experiments that ortho-nitrophenol is a long-range attractant used by the ticks to locate hosts and attached feeding males.

A combination of CO<sub>2</sub> and pheromones was later reported by Norval *et al.* (1989) to be attractive to *Amblyomma hebraeum*. They demonstrated that males and females were activated by carbon dioxide and attracted to AAP in the field. Maranga *et al.* (2003) reported the attraction of *Amblyomma variegatum* to carbon dioxide combined to AAP up to 5 m. The findings of these workers paved way for studies in the attraction of ticks by CO<sub>2</sub> and pheromones traps for the control of ticks. The use of pheromone/acaricide mixtures to control *Amblyomma hebraeum* has been reported (Norval *et al.*, 1991). Maranga *et al.* (2005) also investigated the efficacy of fungi traps baited with AAP for the control of *A. variegatum* under semi-laboratory conditions.

Neem derivatives are traditionally used by farmers in Asia and Africa to control insect pests of household, agricultural and medical importance (Kaaya, 2003) and could be useful in controlling ticks and therefore be incorporated in Integrated Tick Management.

Plants of the family Meliaceae have been evaluated against many tick species but most of the studies carried out so far targeted only *A. variegatum* larvae. Since the African 3-host ticks spend 95-97% of their life time in the vegetation (Punyua, 1992), an off-host control strategy using plants in baited traps would go along way in controlling ticks in the pastures. The aim of this study was to assess the effect of neem cake on adult *A. variegatum* attracted to traps baited with semiochemicals in an attempt to control the tick in vegetation.

## 2 Materials and methods

### 2.1 Study site

Field experiments were carried out at the Kenya Agriculture Research Institute, National Veterinary Research Centre, Muguga-KARI: latitude 1° 13' S, longitude 36° 18' E, altitude 2070 m (Obiri *et al.*, 1994). The climate in Muguga is a modified equatorial type with a mean monthly temperature of 18°C. Mean annual rainfall is 1005 mm, distributed bimodally with peaks in April and October (Obiri *et al.*, 1994).

## 2.2 Experimental plots

Twelve separate plots were prepared by measuring a circular plot of 8 m radius. The grass within each plot was cut to a height of 5cm (Maranga *et al.*, 2003). Each plot was marked from the centre using wooden pegs at intervals of 1 m in a straight line. The marking was done in straight lines prepared at 45° interval all around the plot. A small circle of 10 cm radius was made at the centre of the plot and all the grass removed for placement of the trap. Each plot had a barrier of 5 m un-cleared grass surrounding it (Maranga *et al.*, 2003).

## 2.3 Traps

The traps used were prepared according to Maranga *et al.* (2006). In brief they consisted of a pheromone dispenser, dry ice container and a contamination chamber in which the Neem Cake Extract (NCE) was placed. The semiochemical/pheromone dispenser consisted of a Petri dish (9 cm diameter) on which a Whatman's filter paper (9cm diameter) fixed on the bottom side using laboratory parafilm. The contamination chamber consisted of an aluminum tray fixed to the cylindrical aluminum tube carrying the dry ice.

## 2.4 Preparation of the Neem Cake Extracts (NCE)

The Neem cake was obtained from the ICIPE Neem factory. 500 g of cake ( 0.6% Azadirachtin) was mixed with hexane to cover the neem cake and left to stand for 3 days. The mixture was then filtered using a fine sieve and the solvent evaporated in an evaporator at 60°C until all the solvent was evaporated. The extract was then formulated as 10, 20 and 30% extracts using paraffin oil (Mwangi *et al.*, 1995b).

## 2.5 Semiochemicals/CO<sub>2</sub>

The synthetic AAAP pheromone components consisting of ortho-nitrophenol, methyl salicylate and nonanoic acid were obtained from Sigma-Aldrich Company (Ltd), UK. The equivalent to the AAAP pheromone produced by one attached feeding *A. variegatum* male (0.2mg of ortho-nitrophenol, 0.1mg of methyl salicylate and 0.8mg nonanoic acid) (Schoni *et al.*, 1984) was prepared by mixing 200mg of ortho-nitrophenol, 100mg of methyl salicylate and 800mg nonanoic acid in 1ml hexane. One microliter of this solution contained the three components in approximate amounts produced by one feeding male approximately 1.1mg of the pheromone. The source of CO<sub>2</sub> was dry ice obtained from Carbacid (Nairobi, Kenya) while 1-octen-3-ol was obtained from Sigma chemicals.

A blend of 2.2 mg of AAAP and 16 ng of 1-octen-3-ol (dissolved in dichloromethane) that attracted the highest number of *A. variegatum* ticks in previous studies (Toure, 2005) was used as the attractant. The blends were placed on Whatman's filter paper fixed on a Petri dish using laboratory parafilm (Maranga *et al.*, 2006).

## 2.6 Ticks

Two three-month old unfed adult male and female *A. variegatum* ticks were obtained from the animal rearing quarantine unit. The ticks were counted in batches of 10 with each batch consisting of five males and five females and then placed in separate vials. The ticks were marked with artists' paint (Rowenwey Georgian oil paint diluted with linseed oil) with both males and females being marked on the lower quarter of the dorsal side using painters brush. Different batches of ticks were painted with different colours (Maranga *et al.*, 2003). The ticks were then returned to their respective vials and kept in darkness at relative humidity 75% and temperature  $25\pm 1^{\circ}\text{C}$ .

## 2.7 Experimental design and tick release

The semiochemical consisting of a mixture of 2.2mg of AAAP and 16ng of 1-octen-3-ol on filter paper fixed on a Petri-dish was placed on the upper portion of the trap. 500g dry ice was placed in the tube of the trap (Maranga *et al.* 2003). 10% Neem cake extract was formulated using paraffin oil (Mwangi *et al.*, 1995b) and 8 mls of the extract placed in the infecting tray of the trap. Two other doses one 8 mls of 20% neem cake extract and another consisting 30% of neem cake extract were similarly prepared and separately placed in different traps. The control consisted of 8mls liquid paraffin which was also placed in another trap. A trap was then placed at the centre of each of the twelve plots which had earlier been prepared. All experiments were set in triplicates.

Ticks were released as per the method of Maranga *et al.* (2003). In brief, adult male and female ticks marked with different colours were released from 1,2,3,4, and 8m downwind from the centre of the plot. Since the direction of the wind arrived within a range of  $90^{\circ}$  relative to the mean, the ticks were released from three different positions, one being the mean and the other two at  $\pm 45^{\circ}$  relative to the mean. The wind direction was monitored using a thin thread attached to a wooden stick of 1 m long at the centre of the plot. Tick movement was monitored from a down position. Ticks that arrived on all the traps were collected in separate vials and taken to laboratory where they were incubated at  $28 \pm 1^{\circ}\text{C}$  and 75% relative humidity and their mortality monitored and recorded daily for 3 weeks. Each replicate was observed for four days using a fresh source of pheromone,  $\text{CO}_2$  and neem cake extract.

## 2.8 Data analysis

Tick responses to various combined doses of AAAP, 1-octen-3-ol and  $\text{CO}_2$  were recorded and entered on Microsoft Excel. Analysis of Variance (ANOVA) was carried out to test for differences in attraction due to doses, sex or their interaction on the data after square root transformation, using the Statistical Analysis System Software (SAS, 1988). A survival analysis was also performed and differences in the survival curves were analyzed by the Lifetest procedure (SAS)

and the significant level was based on Wilcoxon and Rank tests of equality over strata. Mean values were compared using the Student-Newman-Keuls test at a significance level of 0.05.

### 3.0 Results

The effectiveness of the traps in attracting ticks on the vegetation was assessed. The results showed strong attraction of *A. variegatum* to the blends of AAAP, 1-octen-3-ol and CO<sub>2</sub> ( $p < 0.0001$ ;  $df = 63$ ;  $F = 38.85$ ). The survival curves between the doses were compared and the rank tests for homogeneity indicated a significant difference between the doses ( $p < 0.0001$ ) for the Log-rank test and the Wilcoxon test. The log-rank test, which places more weight on larger survival times, was equally significant as the Wilcoxon test, which places more weight on early survival times. The mean survival time in days (Figure 1) showed that ticks exposed to the NCE concentrations (10% and 20%) lived significantly longer than those exposed to 30% NCE. This study also found that the acaricidal effect of the NCE against *A. variegatum* was concentration-dependent.

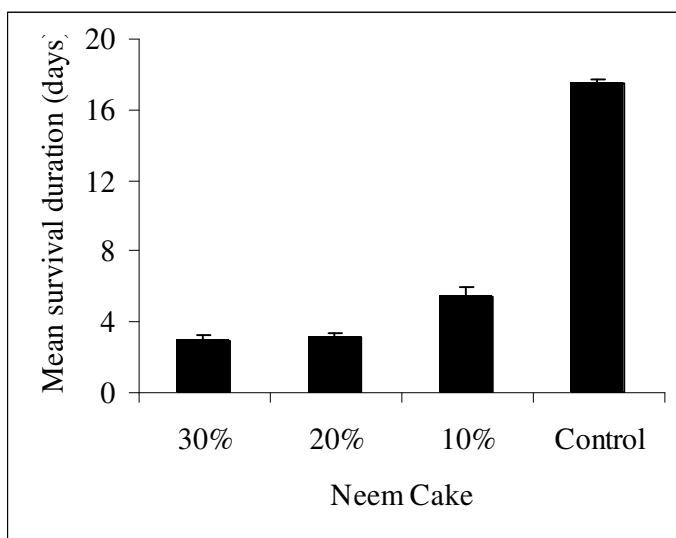


Figure 1: Mean ( $\pm$ SE) survival time of ticks

Higher concentration of NCE produced higher mortalities than the lower concentration and the control (Figure 2). The mortality of the ticks was also time-dependent (Figure 2), with mortalities decreasing from the fourth day. Higher mortality was observed in the first three days of exposure of the ticks to the NCE where 30%, 20% and 10% caused 83%, 79% and 66% of mortality, respectively, during this period.



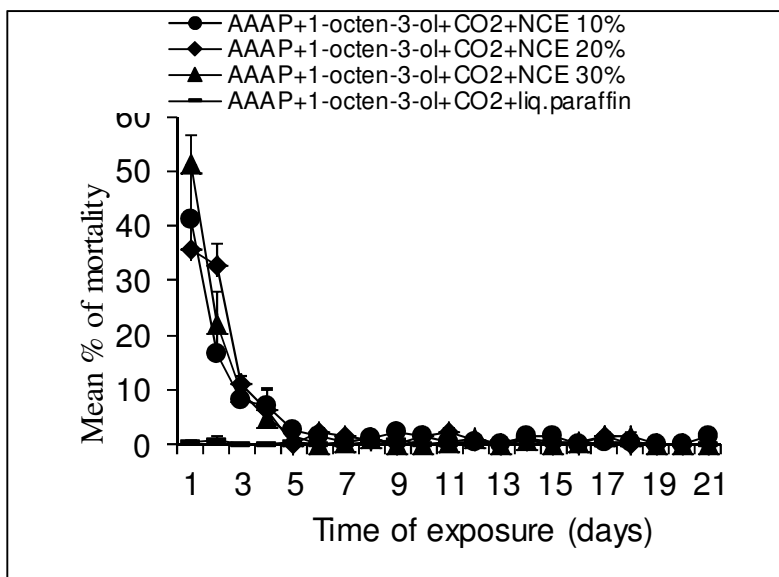


Figure 2: Mean ( $\pm$ SE) percentage of mortality of *A. variegatum* ticks exposed to Neem Cake Extracts after 3 weeks

Figure 3 shows the mean survival duration (days) of the exposed female and male ticks which indicated no significant difference between the males and females ( $p > 0.05$ ).

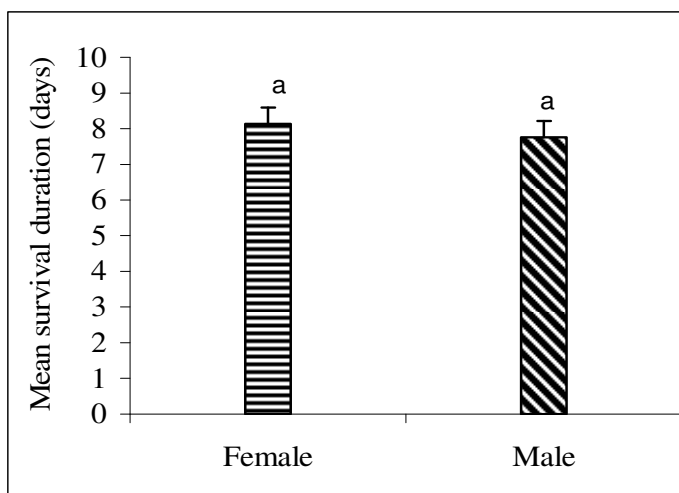


Figure 3: Mean ( $\pm$ SE) survival of male and female *A. variegatum* after 3-week exposure to Neem Cake Extracts. Means bearing the same letter are not significantly different to SNK test ( $P = 5\%$ ).

#### 4.0 Discussion and conclusion

Azadirachtin is the predominant insecticidal active ingredient in the seeds, leaves, and other parts of the Neem tree (Mulla, 1999) and has been reported to have acaricidal properties against *A. variegatum* and other tick species (Ndumu *et al.*, 1999; Ismail *et al.*, 2002; DiefAlla *et al.*, 2003). Long term mortality was expected mainly because of using adult *A. variegatum*, which are less sensitive than larvae and because of using diluted extracts. These results are similar to those of Ndumu *et al.* (1999) who reported that neem oil killed 100% of *A. variegatum* larvae within 48 hours. Similar findings were reported by Ismail *et al.*, (2002) who working on the 3-host tick *Rhipicephalus pulchellus* in Ethiopia, found that 40% neem oil was the most effective in achieving tick mortality which also recorded the highest toxicity compared to 10% neem oil. Investigating the effect of neem on *Hyalomma anaticum*, Abdel-Shafy and Zayed (2002) used a commercial formulation of *A. indica*, neem Azal F, and obtained similar results. Most of the studies investigated only tick larvae which are more susceptible than adults.

The efficacy of neem on *Boophilus microplus* has also been reported (Mansingh and Williams, 1998). These workers investigated the crude ethanol extracts of the Neem leaves on engorged *B. microplus* and found an acaricidal index of 68% and concluded that Neem was very effective against this tick.

This study investigated the effect of different concentration of neem oil using a semiochemical baited trap as an attractant of adult *A. variegatum* and has recorded a similar trend of findings. It is therefore evident that neem extract has a high potential of controlling *A. variegatm* ticks and could be found particularly useful in integrated tick control programmes.

#### Acknowledgements

The authors thank the Ministry for Foreign Affairs of the Netherlands /DSO Programme for a fellowship through the ICIPE African Regional Postgraduate Programme in Insect Science (ARPPIS) to one of the authors. We acknowledge the support of Dr. Ochieng-Odero and Francis Onyango and the technical assistance of Mark Kimondo and Benjamin Omondi. We are also grateful to the National Veterinary Research Centre of Kenya (Muguga) for availing field facilities.

#### References

Abdel-Shafy S. and Zayed A. A. (2002). *In vitro* acaricidal effect of plant extract of Neem seed oil (*Azadirachta indica*) on egg, immature, and adult stages of *Hyalomma anaticum excavatum* (Ixodoidea: Ixodidae). *Veterinary Parasitology*, **106**, pp. 89-96.

DiefAlla H. A., Azzam M. A., Hamdy I. H., Salah, M. K. (2003). Acaricidal effects cardiac glycosides, *Azadirachta indica* and Neem oil against the camel tick, *Hyalomma dromedarii* (Acari: Ixodidae). *Pest Management. Science*, **59**(11), pp. 1250-1254.

Eads R. B., Smith, G. C. and Maupin, G.O (1982). A CO<sub>2</sub> platform trap for taking adult *Dermacentor andersoni* (Acari: Ixodidae). *Proc. Entomol. Soc. Wash.*, **84**, pp. 342-348.

- Gray J. S. (1985). A carbon dioxide trap for prolonged sampling of *Ixodes ricinus* L. populations. *Exp. Appl. Acarol.*, **1**, pp. 35-44.
- Ismail M. H., Chitapa K. and Solomon G. (2002). Toxic effect of Ethiopian Neem Oil on larvae of cattle tick, *Rhipicephalus pulchellus* Gerstaecker. *Kasetsart J. (Nat. Sci.)* **36**, pp. 18-22.
- Kaaya G. P. (2003). Prospects for innovative tick control methods in Africa. *Insect Sci. Applic.*, **23**(1), pp. 59-67.
- Mansingh A. and Williams A. D. L. (1998). Pesticidal potential of tropical plants-II. Acaricidal activity of crude extracts of several Jamaican plants. *Insect Sci. Applic.*, **18**(2), pp. 149-155.
- Maranga R. O., Hassanali A. and Kaaya G. P. Mueke J. M. (2006). Performance of a prototype baited-trap in attracting and infecting the tick *Amblyomma variegatum* (Ixodidae) with the fungi *Beauveria bassiana* and *Metarhizium anisopliae* in field experiments. *Experimental and Applied Acarology*, **38**(2-3), pp. 211-218
- Maranga, R.O., Hassanali, A and Kaaya, G.P. Mueke, J.M. 2005. Effects of combining the fungi *Beauveria bassiana* and *Metarhizium anisopliae*, on the mortality of *Amblyomma variegatum* (Ixodidae) in relation to seasonal changes. *Mycopathologia Vol.*, **159**(4), pp. 527-532.
- Maranga R.O., Hassanali A and Kaaya G. P, Mueke J. M.(2003). Attraction of *Amblyomma variegatum* (ticks) to the attraction-aggregation-attachment-pheromone with or without carbon dioxide. *Experimental and Applied Acarology* ,**29**, pp. 121-130.
- Mulla M. S. (1999). Activity and biological effects of Neem products against arthropods of medical and veterinary importance. *J. Am. Mosq. Control Assoc.*, **15**(2), pp. 133-52.
- Mwangi E. N., Hassanali A., Essuman S., Nyandat E., Moreka L. and Kimondo M. (1995b). Repellent and acaricidal properties of *Ocimum suave* against *Rhipicephalus appendiculatus* ticks. *Exp. and App. Acarol.*, **19**, pp.11-18.
- Ndumu P. A., George J. B. and Choudhury M. K. (1999). Toxicity of neem seed oil (*Azadirachta indica*) against the larvae of *Amblyomma variegatum* a three-host tick in cattle. *Phytother. Res.*, **13** (6), pp. 532-4.
- Norval R. A. I., Butler J. F. and Yunker C. E. (1989). Use of carbon dioxide and natural or synthetic aggregation-attachment pheromone of the bont tick, *Amblyomma hebraeum*, to attract and trap unfed adults in the field. *Exp. App. Acarol.*, **7**, pp. 171-180.
- Norval R. A. I., Yunker C. E., Duncan I. M. and Peter T. (1991). Pheromone/acaricide mixtures in the control of the tick *Amblyomma hebraeum*: Effects of acaricides on attraction and attachment. *Exp. & App. Acarol.*, **11**, pp. 233-240.

Obiri J. A. F., Giathi G. and Massawe, A. (1994). The effect of Cypress Aphid on *Cupressus lusitanica* Orchards in Kenya and Tanzania. *E. Afri. Agric. For. J.* (1994), pp. 227-234.

Punyua D.K. (1992). A review of the development and survival of ticks in tropical Africa. *Insect Sci. Applic.*, **13**, pp. 537-544.

SAS Institute Inc. (1988). SAS/STAT User's guide, Release 6.03 Edition. SAS Institute Inc. Cary, NC.

Schmutterer H. (1990). Properties and potentials of natural pesticides from Neem tree, *Azadirachta indica*. *Annu. Rev. Entomol.*, **35**, pp. 271-297.

Schöni R., Hess E., Blum W. and Ramstein K. (1984). The aggregation-attachment pheromone of tropical bont tick *Amblyomma variegatum* Fabricius (Acari, Ixodidae): isolation, identification and action of its components. *J. Insect. Physiol.*, **30**, pp. 613-618.

## DESIGN AND IMPLEMENTATION OF A MICROPROCESSOR BASED ROOM ILLUMINATION CONTROL SYSTEM

**E. O. Owiti<sup>1</sup>, J. N. Mutuku<sup>1</sup> and R. M. Onger<sup>1</sup>**

<sup>1</sup>*Jomo Kenyatta University of Agriculture and Technology, Nairobi, Kenya*

*E-mail: edwiti16@gmail.com*

### **Abstract**

This paper describes the development of a microprocessor based room illumination control system that offers advantage of improved efficiency in the use of electrical energy and reduced cost of electricity over manually controlled lighting systems. This system is developed to regulate the intensity of light from direct current (DC) bulbs when the presence of a person(s) is detected in the room so that ambient light is always maintained between 135 lux and 300 lux. Lights are however completely turned OFF if the ambient light level is beyond this range. At the heart of this system is an Intel 8085 microprocessor which controls all operations of the system. The infrared and the passive infrared (PIR) sensors are used to detect the occupancy status of the room while the visible light sensor is used to detect the ambient light level in the room. The PIR sensor is mounted at a height of about 2 m which prevents the system from detecting the presence of animals like cats and dogs in the room and therefore avoids turning the lights ON falsely. Analog signals are produced as outputs from the three sensors and are fed to the microprocessor unit (MPU) for processing through the analog-to-digital converter (ADC). The MPU is then capable of controlling all operations and automating the system. The entire hardware functioning is coordinated by a software program written in low level 8085 assembly language and stored in the erasable programmable read only memory (EPROM). Implementing this system improves efficiency in the use of electrical energy and reduces the cost of electricity.

**Key words:** Microprocessor based system, occupancy dependent, illumination control, PIR Sensor, visible light sensor

## 1.0 Introduction

Electrical and light energy management is becoming increasingly popular as means of saving and reducing the cost of energy and electricity. Proper habits like turning lights OFF when there are no person(s) in the room is one of the ways of conserving the electrical energy to avoid energy waste (Athanasios, 2002; Galasiu *et al.*, 2007). In many multifunctional rooms however, poor habits of using the light energy still contribute to an extra cost of electricity, that is, lights are switched ON at full intensity when there is too much natural light and sometimes when there are no person(s) in the room.

Microcontrollers and Microprocessor based systems are increasingly being used to provide solutions where manual systems have failed to provide efficient solutions (Teerasilapa *et al.*, 2002; Shoewu, 2006; Mohamed, 2008; Inderpreet, 2010). Consumption of light energy in appropriate amounts and in the most needed time is desirable to increase the energy efficiency and cost effectiveness. It is desirable that the lights in a room are only turned ON if there is a person(s) in the room, and the intensity of this light be adjusted to a desired level depending on the intensity of the light coming in through the windows and doors. Thus, in this project, a system is designed with transducers for detecting the presence of a person(s) in the room using a PIR sensor (also senses motion) and an infrared sensor and measuring the ambient light level in the room, using a photoconductive detector in form of a light dependent resistor (LDR), before adjusting the bulb intensity to a desired level. An energy saving DC bulb is used to provide the desired level of light in order to supplement the natural light in the room.

The central processing unit (CPU) of the system can only be able to read digital signals. However, the outputs of the three sensors provide analog signals and must first be converted to digital forms by an analog-to-digital converter (ADC) for proper interfacing. The digital data obtained from the infrared sensor and PIR sensor are first added to give a value which is compared to a reference digital value so that if the sum is greater than this reference value, the information is translated to mean that there is a person(s) in the room and lights can be turned ON. In this design, it is desired that the ambient light in the room be maintained between illuminance values of 135 lux and 300 lux which is in the range sufficient for normal reading (Sinclair, 2001). The converted digital data obtained from the light sensor is then compared, continuously, with the digital equivalent of the illuminance range in form of a look-up table to maintain the ambient light as desired.

For the proper working of the microprocessor and other modules and also to ensure adequate and efficient illumination control, a robust software core is essential. The design works with software written in low level-8085 assembly language program which is stored in the EPROM.

## 2.0 Materials and methods

The overall system hardware components are assembled and interfaced as shown in Figure 1.

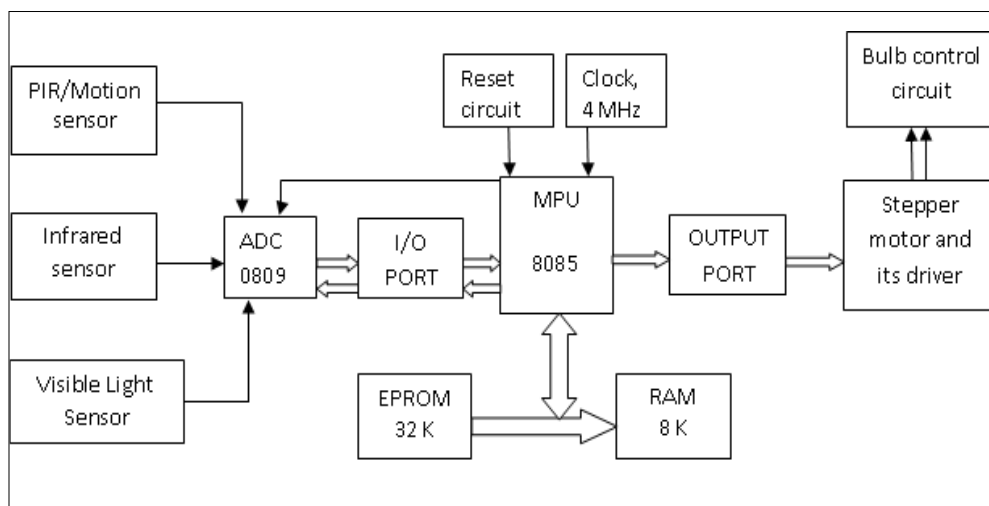


Figure 1: Block diagram showing interface of main components in the design

### 2.1 The Microprocessor Unit (MPU)

The Intel 8085 microprocessor implements the control algorithm by regulating the light intensity from the bulbs according to the amount of natural light coming in through windows and doors. It also determines when information is to be read from the three sensors; infrared sensor, PIR sensor and the visible light sensor. It controls the ADC operation by sending signals to it for start of conversion (SOC), address latch enable (ALE) and receives the end of conversion (EOC) signals. After the MPU processes data in it, it determines the form of operation on the stepper motor through the output port B. The ADC needs to operate at a much slower frequency (500 kHz) compared to the MPU which takes in clock frequency of 4 MHz and gives out a frequency of 2 MHz through its pin 37. It is from this 2 MHz frequency that 500 kHz is obtained through frequency divider circuit designed using D-Flip flops.

### 2.2 The ADC0809 Interface

The ADC needs interfacing through a microprocessor to convert analog data into digital format. The ADC0809 is an 8-bit analog to digital converter having data lines D0-D7 and works on the principle of successive approximation. It has a total of eight analog input channels out of which only one can be selected using address lines A, B and C. Here, in this case, input channels IN4, IN5 and IN6 were set for the visible light sensor, PIR Sensor and infrared sensor and were selected using codes 00H, 04H and 08H respectively. The visible light sensor provides an analog output voltage that is proportional to the ambient light level falling on it. It is this analog

voltage that is fed into the ADC via pin 2 for conversion before the data is taken for processing by the microprocessor. Similarly, the infrared sensor provides an analog output voltage that is proportional to the infrared radiation falling on its surface from human body and is fed into the ADC via its pin 4. The PIR sensor opens its dry contact switch upon detection of any motion and infrared in its field of view. This opened switch is connected to the transistor-relay network to provide a 2.0 V analog voltage for conversion. This value, together with the data from the infrared sensor, is used to determine whether or not the room is occupied.

### 2.3 Memory modules

The two chips used as memory modules are the EPROM and the random access memory (RAM). The EPROM is used to store the program used to run the entire system and must store program codes that are compatible with the Intel 8085 microprocessor. In this project, 27C256B was used as the EPROM to provide a memory space of 32 k. The RAM was used to provide the working space. This includes space for locating the STACK and location for temporary storage of data. This was a 6264 RAM chip which provided 8 k of memory space. Based on this memory space allocation a memory map is as follows,

EPROM:           0000H to 7FFFH

RAM:             8000H to 9FFFH

Unavailable:    A000H to FFFFH

### 2.4 The 8255 Parallel Input Output (PIO) Interface

The main interface chips to this device are the ADC0809, the motor control lines and the ON /OFF relay switch. Two 8255 parallel input output (PIO) ports have been used in this design, one for interfacing the ADC0809 and the stepper motor and the other for interfacing with the relay for turning ON or OFF of the lights as shown in Figure 2. The first PIO is the main link chip and has its port A and port C – upper configured as inputs and ports B and C – lower configured as inputs. The code used to initialize this port is therefore 98H which must be loaded into its control register at the beginning of system program. The second PIO is used with all its ports configured as outputs and therefore code 80H is first loaded to its control register at the beginning of system program.



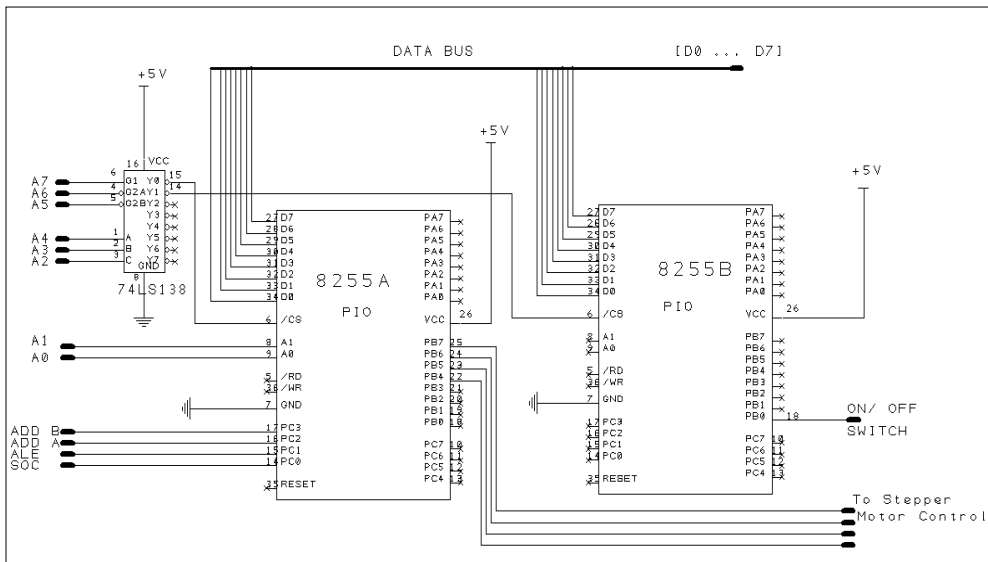


Figure 2: The 8255 PIO interfacing schematic circuit

### 2.5 Bulb Control Unit

The brightness control unit is responsible for the ultimate control of the ambient light in the room. The stepper motor, interfaced with its driver, is the actuator that links the microcomputer system to the bulb control unit. The unit uses a 555 timer integrated circuit (IC) to generate high frequency (150 Hz) pulse width modulated (PWM) signals with varying duty cycles which determine the brightness levels of the bulbs. Duty cycle of 50% and above makes the intensity of the bulbs to be increased whereas a smaller duty cycle makes the DC bulbs dimmer. In Figure 3, the direction of rotation of the stepper motor controls the resistance into the unit through a potentiometer which determines the value of the duty cycle.

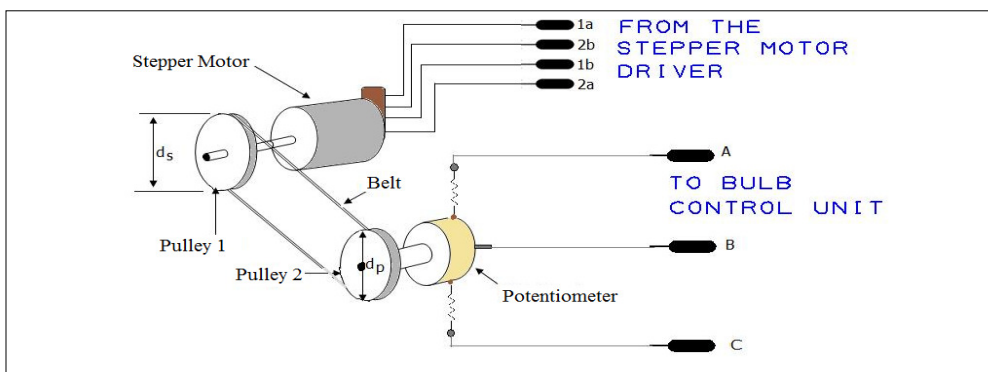


Figure 3: The Stepper motor control of the potentiometer

### 2.6 Software development

One of the most important aspects in this software development is the location of beginning point of different sections of the program and how to synthesize all functions in one program. Basically, the three fundamental procedures in software development were followed. This includes; algorithm design, flowchart design and assembly mnemonics design.

The program is divided into five main parts: PIO port initialization, stack definition and preparation of flag and storage registers; PIR/motion sensing through the ADC and data storage; infrared sensing through the ADC, data retrieval and arithmetic operation; visible light sensing through the ADC; data comparison and action on stepper motor. Figures 4 and 5 show the first two sections.

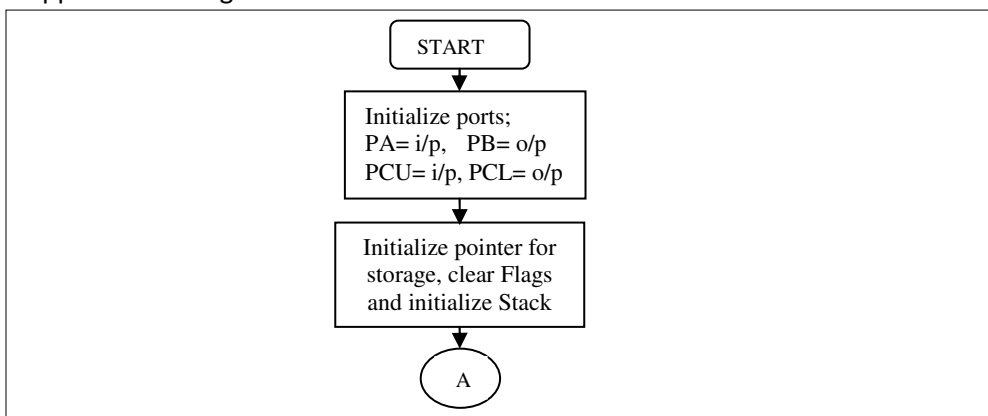


Figure 4: Flowchart showing initialization of ports, flags and stack

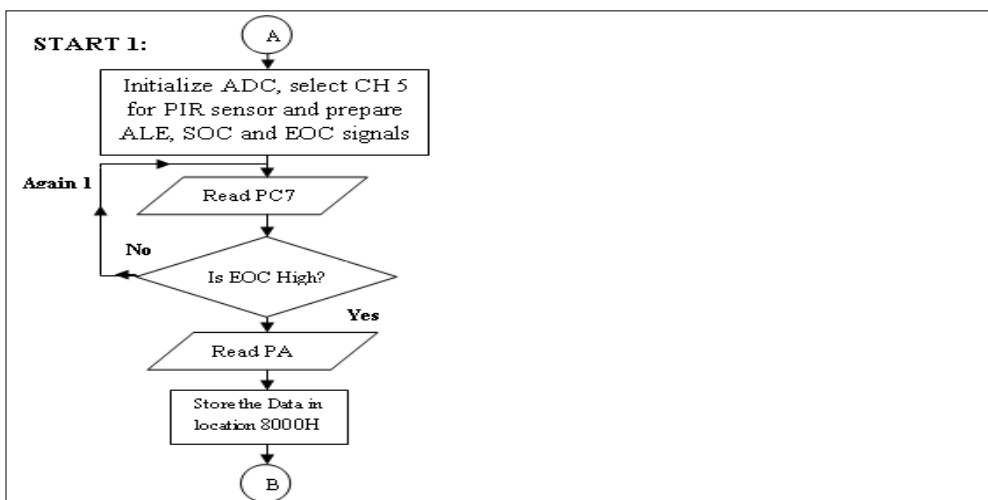


Figure 5: Flowchart showing data flow from PIR Motion sensor through the ADC

Figure 6 shows the third part of the software design which involves reading data from the IR sensor and retrieving the first data from the PIR sensor for addition

before the sum is compared with a minimum threshold of 68H which is an equivalent of 2 V switched ON by the relay

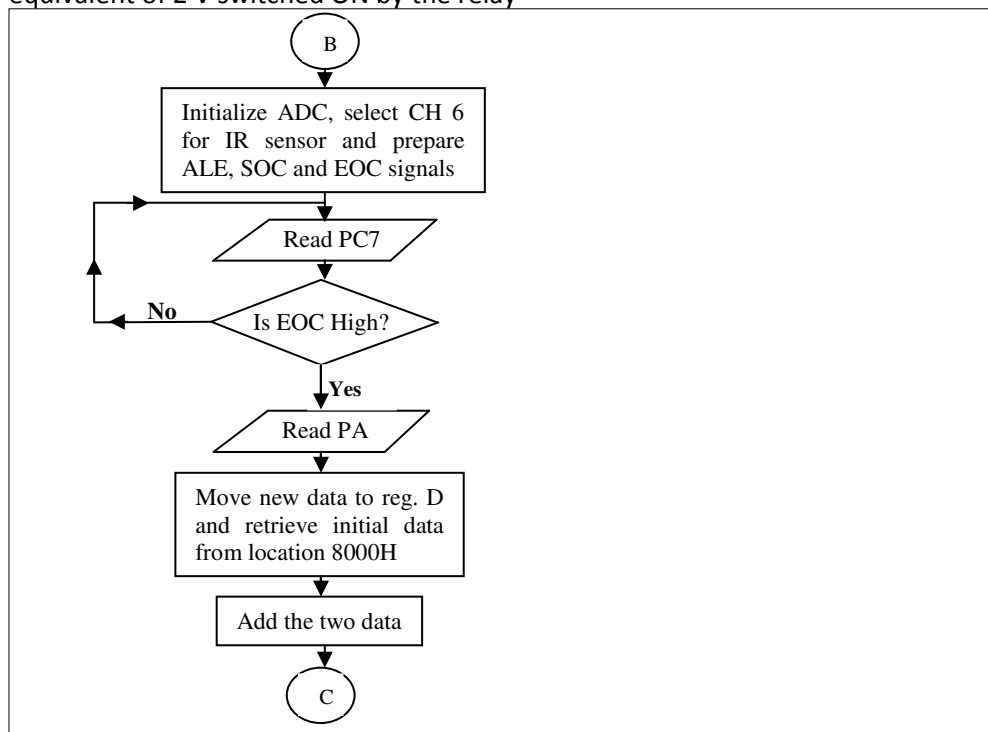


Figure 6: Flowchart showing data acquisition from the IR sensor through the ADC

Figure 6 shows the third part of the software design which involves reading data from the IR sensor and retrieving the first data from the PIR sensor for addition before the sum is compared with a minimum threshold of 68H which is an equivalent of 2 V switched ON by the relay.

The fourth and fifth portions are where the data is read from the visible light sensor and the data is used to determine the amount of light needed from the bulbs. The data that is read is compared with some three threshold values; 1AH, 20H and 30H corresponding to 400 lux, 300 lux and 135 lux respectively as shown in Figures 7 and 8. When data, from the visible light sensor, is less than 20H, the microprocessor unit drives the stepper motor in forward direction to reduce the amount of light. When the data is more than 30H, the microprocessor unit drives the stepper motor in reverse direction to increase the amount light. Data less than 1AH, initiates the relay, ON/OFF switch, to turn OFF the lights. The entire process is repeated continuously until the system is switched OFF.

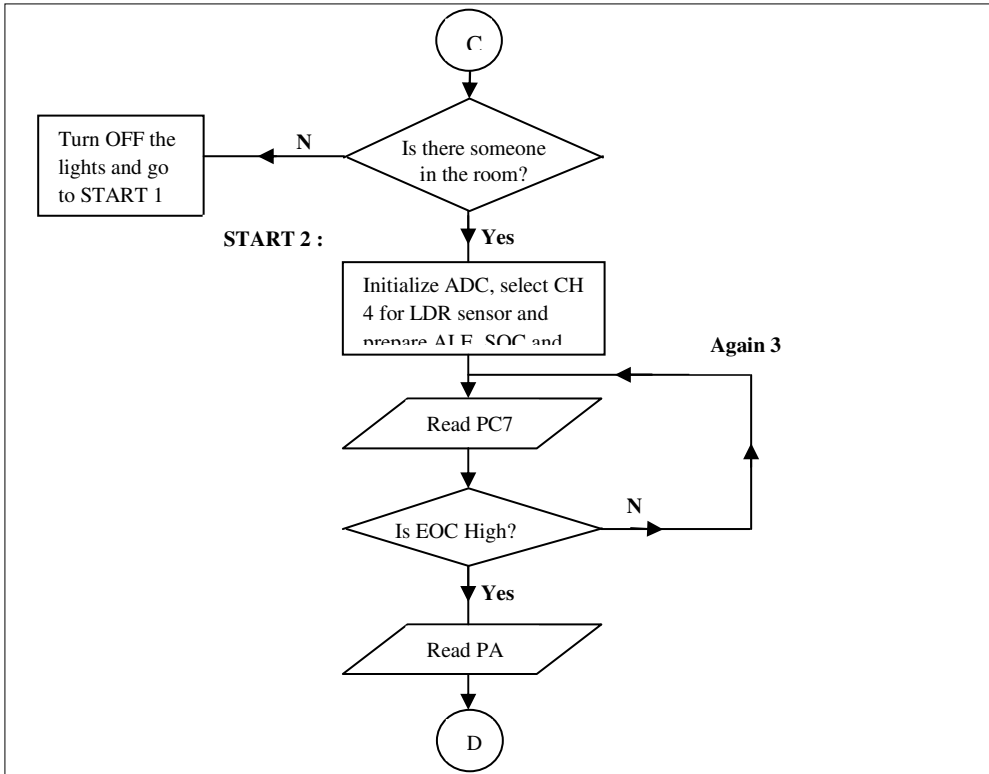


Figure 7: Flowchart showing occupancy determination and LDR data acquisition

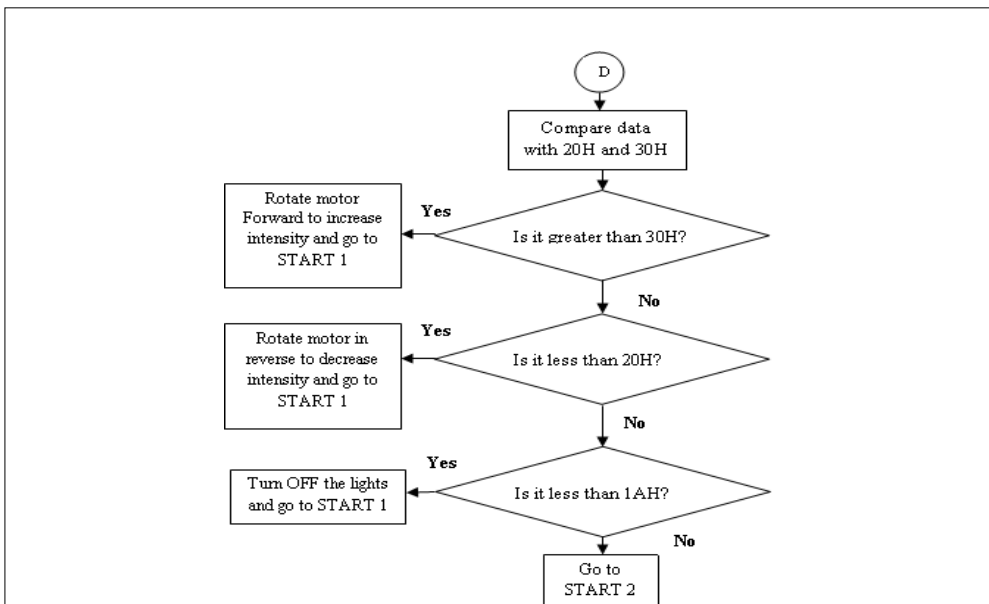


Figure 8: Flowchart showing the outcome of the illumination data obtained

The assembly code representing the individual blocks of the flowcharts was then written using 8085 assembly language.

### 3.0 Results and Discussion

#### 3.1 Illuminance as a function of resistance

The values of LDR resistance were measured with an ohmmeter and the corresponding illuminance values were measured using a luxmeter, under different light levels and presented in a graph. This transducer was positioned at a height of about 1.5 m from the DC bulb and within base area of about 6.25 m<sup>2</sup> (2.5 m<sup>2</sup> X 2.5 m<sup>2</sup>). Only low light levels, from 100 lux to 10 klux, were calibrated using Solar Tex 11W energy saving DC bulb. This bulb has a 6500 K color temperature and resembles the black body radiation. The mathematical relation between the resistance of the sensor and the illuminance was then obtained by drawing the line of best fit as shown in Figure 9.

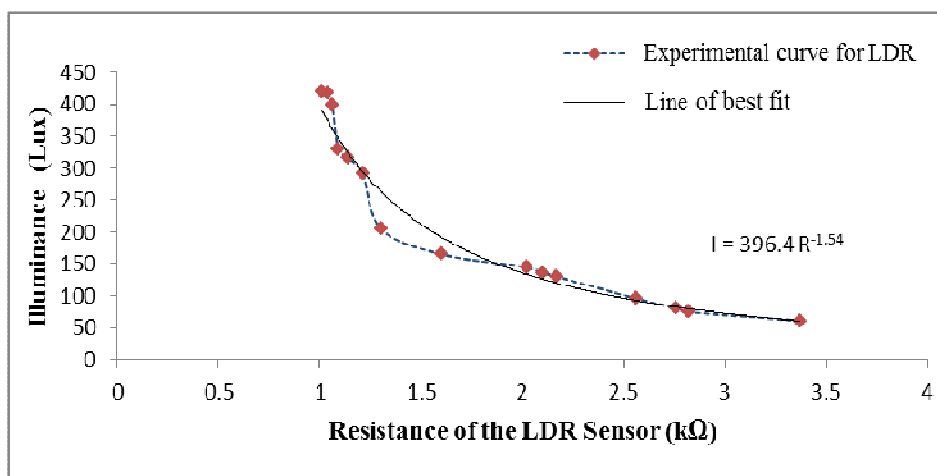


Figure 9: Graph of illuminance against the light sensor resistance

It was observed that the graph of illuminance against the resistance of the LDR followed an exponential decay pattern with minimum illuminance producing maximum resistance across the LDR. Equation 1 below was obtained as the result of the resistance-illuminance relationship of the sensor derived from Figure 9.

$$I = 396.4 R^{-1.54} \dots\dots\dots (1)$$

This equation defines the spectral responsivity of the visible light sensor (LDR) which determines how much of the detector input range is allowed with the corresponding output range (Ciampini *et al.*, 2005).

## 2.7 Calibration of the bulb unit

The potential difference across the bulb was monitored and result recorded using the digital multimeter device. This variation in the potential difference was being effected as a result of varying illumination in the room. The data obtained was recorded and a graph of the potential difference across the load against the illuminance was then drawn as shown in Figure 10. This graph exhibits four regions: In the first region (Region 1) the potential difference decreases from a maximum value of 11.8 V to about 11.2 V with a near zero gradient. In this region the bulbs are turned ON to full intensity; the second region (Region 2) defines the optimum ambient light in the room from 135 lux to 298 lux and the potential difference decreases with increase in illuminance; in the third region (Region 3) the gradient is more steeper compared to regions 1 and 2 up to 400 lux where there is a 'kink'; Region 4 defines the region where the bulb is completely turned OFF when the illuminance is above 400 lux.

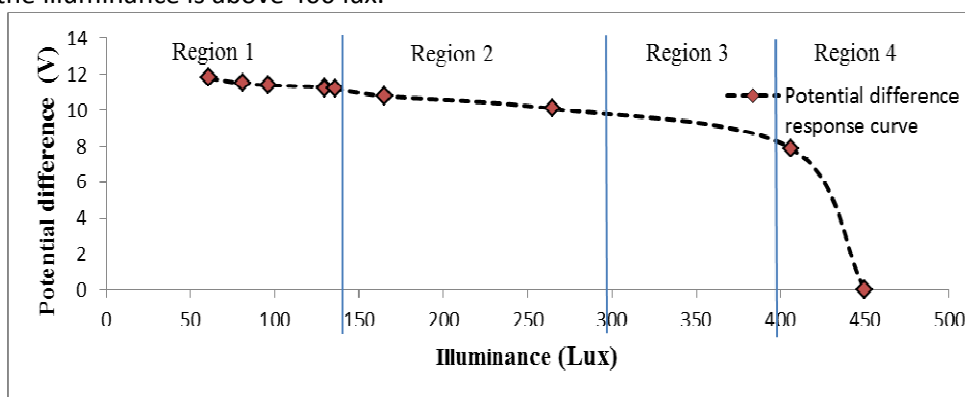


Figure 10: Graph of the potential difference against illuminance of the room

## 2.8 Sample consumption data

After successful calibration of the bulb unit, the system was then subjected to a real test. In this test, the system was set and left to regulate the illumination in a room. The potential differences across the load (bulb) and across the light sensor were recorded using a data logger for about six hours. During the test, the bulb was turned ON after the first 60 minutes. This was done to make it easy to verify whether the data logger was recording the intended data or not. Light falling on the sensor reduced the resistance across it and this produced a regulated potential difference across the bulb as shown in the graph of Figure 11.

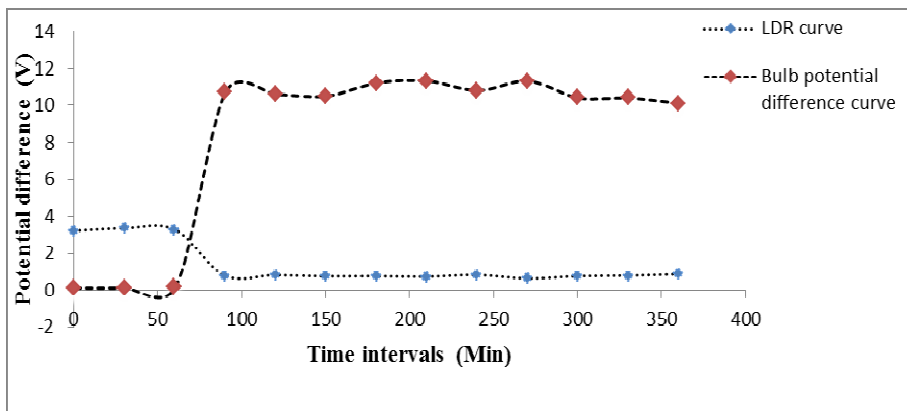


Figure 11: Regulated potential difference across the Bulb

**2.9 Power consumption analysis**

In analysis of the amount of power consumed in a regulated lighting system and unregulated lighting system, the potential difference across the bulb in the two systems is used as the main quantity for comparison i.e. 12.0 V for an unregulated system and 11.2 V average voltage obtained from Figure 11 for a similar and regulated system. Using Equation 2 and a measured resistance of 1860 Ω of the energy saving bulb, the power consumed in the two systems was calculated and recorded as shown in Table 1.

$$P = \frac{V^2}{R} \dots\dots\dots (2)$$

Table 1 Power consumption analysis

	Regulated lighting system (Automated)	Unregulated lighting system (Manual)
Potential difference (V)	11.2	12.0
Bulb resistance (Ω)	1860	1860
Power consumed (W)	0.067	0.077

From Table 1, it is evident that an unregulated lighting control system consumes more electric power than the regulated and automated lighting system. Indeed, this difference is presented as a percentage as follows.

$$\text{percentage difference} = \frac{(0.077 - 0.067)}{0.077} \times 100 = 12.99\%$$

This value means that an automated light control system or the microprocessor based light control system is much more efficient for use as an energy saving strategy by saving about 13% of the energy that would have rather gone to waste.

### **3.0 Conclusion**

The design and implementation of a microprocessor based room illumination control system has been achieved. The design has been tested successfully on a real environment (Physics research laboratory) and produced the expected outcome. In this design, changes in the illumination level outside the room are synchronized with the artificial light from the bulbs. The ambient light detected by the LDR and measured by the luxmeter is a sum total of both the natural light and the artificial light. The relationship between the resistance and illuminance of the LDR sensor was obtained and observed to follow an exponential curve with 396.4 obtained as the proportionality constant and -1.54 as the exponential constant.

The hardware design was developed in modules using six breadboards and fourteen ICs. The software was designed based on the Intel 8085 microprocessor assembly language. Testing of the developed hardware was done by coding and storing a four byte program in the EPROM. A light emitting diode (LED) was then connected on the serial output data (SOD) terminal of the microprocessor, in common cathode mode, to enable the program produce a visible output when it is executed. The LED was turned ON immediately as expected to show that the hardware was properly designed on the breadboards.

In summary, a new automated light control system has been developed based on the 8-bit, Intel 8085, microprocessor with supporting software. This system addresses two main shortcomings in a manually controlled lighting system; lack of light dimming mechanism that controls light intensity from the bulbs depending on the level of natural light in the room and lack of an automated occupancy-dependent light control unit. These challenges introduce a 13% increase in the light energy consumption and to the cost of electricity. A 16-bit or a 32-bit microprocessor based system would function in a similar way and yield same result but would be more preferred when more functions are required in the system. This would also improve the system's operating frequency and computing capability.

### **Acknowledgements**

The authors are grateful to the Physics Department and the Electronics Department of the Jomo Kenyatta University of Agriculture and Technology and the Microelectronics Department of the Kenya Polytechnic University College for their invaluable time and equipment support of this project.



**References**

Athanassios T. (2002). *A methodology for calculating room illuminance distribution and light dimming for a room with a controlled shading device*. MSc Thesis. Concordia University, Quebec, Canada.

Ciampini F., Scarazzato P. S. and Neves A. A. R., (2005). *Low cost data acquisition module for evaluating the quantitative performance of daylight systems*. In: *Passive and Low Energy Architecture*. Proceedings of the 22<sup>nd</sup> conference, November 13-16, Beirut, Lebanon. pp. 1-6.

Galasiu A. D., Guy R. N., Cristian S. and Daniel M. S. (2007). *Energy Saving Lighting Control System for Open-Plan Offices, a field study*, *Journal of Illuminating Engineering Society of North America-Leukos*, **4**, pp.7-29.

Gana J. K, (2007). *Development of a Light Dependent Automatic-Off Timer for House Holds Electronics*, *Leonardo Electronic Journal of Practices and Technologies*, **7**, pp.129 - 138.

Mohamed F., Mounir B. S. and Mouldi B., (2008). *Microcontroller Based Heart Rate Monitor*. *The International Arab Journal of Information Technology*, **5**, pp. 153-157.

Shoewu O. and Baruwa O. T., (2006). *Design of a Microprocessor Based Automatic Gate*, *The Pacific Journal of Science and Technology*, **7**, pp.31-44.

Sinclair I. (2001). *Sensors and Transducers*, Butterworth-Heinemann, London, pp. 58-59.

Teerasilapa D., Sumalee U. and Worapong T., (2002), *Microcontroller based liquid level control Modeling*, *Journal of King Mongkut's Institute of Technology North Bangkok (KMITNB)*, **12**, pp. 1-4.

## **A PROTOTYPE PARABOLIC TROUGH SOLAR CONCENTRATORS FOR STEAM PRODUCTION**

***M. Kawira<sup>1</sup>, R. Kinyua<sup>1</sup> and J. N. Kamau<sup>1</sup>***

*Jomo Kenyatta University of Agriculture and Technology, Kenya*

*Email: kawira.millien@gmail.com*

### **Abstract**

In this work, the potential for a solar-thermal concentrator to produce steam has been studied. Three parabolic trough solar concentrators (PTSCs) of dimensions: - aperture width of 1.2 m, Collector length of 5.8 m and aperture area of 6.95 m<sup>2</sup> were investigated. The absorber pipe was a copper tube which carried water as the heat transfer fluid, were designed, fabricated, characterized and their efficiencies compared when closed and when open. The PTSCs' were made of appropriate materials and were manually tracked. They were designed with principal focus at 0.4 m so that the receiver heat loss is minimized by covering the collectors with glass which was 0.0025 m in thickness. The concentration ratio of the solar concentrators was 128. The concentrator testing was carried out for each of the concentrators. The maximum temperature of steam obtained was 248.3°C while average temperature of steam was produced was 150°C. When closed their efficiencies were: Aluminium sheet reflector PTSC; 55.52 %, Car solar reflector PTSC; 54.65 % and Aluminium foil reflector PTSC; 51.29 %. The open solar concentrator efficiencies were 32.38 %, 34.45 % and 27.74 % respectively. The efficiency of car solar reflector when open was higher than for aluminium sheet since it was less prone to thermal degradation when exposed to weather elements. The results obtained show that production of power using the sun flux is a viable undertaking. The concentrators can be used to provide power to remote areas which are far away from the power transmission gridlines. This will make power readily available to the marginalized rural people. Improvement of the tracking system and optical efficiency can improve the efficiencies of the fabricated concentrator systems.

**Keywords:** Parabolic trough concentrator, solar-thermal, transmittance-absorptance product, thermal and optical efficiency

## 1.0 Introduction

Kenya is endowed with solar power intensity adequate for power electricity generation since the yearly average global irradiation in Nairobi, Lodwar and Mombasa are 5.25 kWh, 6.18 kWh and 5.48 kWh respectively among other areas (SWERA, 2012).

Solar energy is a renewable source of energy. Its use does not contribute to emissions of greenhouse gases and other pollutants to the environment. It is sustainable since it cannot be depleted in a time relevant to the human race. Kenya has an average solar irradiance 6.12 kWh in most of arid and semi- arid regions. Therefore her potential for use of solar collectors for thermal steam production is a viable commercial undertaking. However research efforts to that direction are still wanting. The aim of this study was to use appropriate materials in design, fabrication and characterization of local solar thermal steam producing systems for power generation. Solar collectors transform short wave radiation of the range 0.29  $\mu\text{m}$  - 2.5  $\mu\text{m}$  into long wave radiation and trap this energy in form of heat which is transferred into a heat storage vault by the heat transfer fluid.

Parabolic trough power plants are the only type of solar thermal power plant technology with existing commercial operating systems. A parabolic reflector reflects all the rays that are parallel to its principal axis to a point focus. When this parabola is extrapolated in three dimensions, a parabolic trough is generated, whose focus lies along the axis of the trough. In terms of power capacity solar genix has produced parabolic trough collector modules which are commercially viable and produce 176 Kw of peak energy for dual functions factory roof and for solar heating with an efficiency of 56 % (Cleaveland, 2005). In Africa, a solar thermal plant in Cairo, based on 1,900 m<sup>2</sup> of parabolic trough collector provides steam for pharmaceutical plant, el Nasr project (Ecoworld, 2009). Globally parabolic trough power plants technology with existing commercial operating systems include Nevada solar one which operates on a 250 acre site in Nevada desert and generates 134 MW of power per year. A larger solar based facility already exists in Mojave Desert in USA, generates 354 MW of solar energy power. In Spain Torresol and Arcosol have a 50 MW parabolic trough based plants located in Seville Cadiz. Other Spanish plants using this technology are Andasol 1, 2, 3 in Granada province (Ecoworld, 2009).

## 2 Materials and methods

### 2.1 Fabrication of solar concentrator trough

Angle iron beams of aperture width 1.2 m were bent into parabola with a focus at 0.4 m using Equation 1. These beams have a tensile strength that is able to with stand wind loads of wind speed greater than 10 m/s. Wind loads that are not mitigated cause the collector to be misaligned to the solar beam when the wind blows hence low thermal energy collection. After fabrication the structure was painted to prevent rusting. Equation 1 was used curve the angle iron beams into parabola.

$$y^2 = \frac{x}{4p} \dots \dots \dots (1)$$

Where  $y$  and  $x$  are Cartesian plane coordinates and  $f$  is the predetermined focal length.

Black sheets were folded and welded into angle iron beams on the outside and the ends closed. The black sheets and the angle iron beams were painted to prevent rusting. The edges of the sheets were folded to provide a rail which was lined with rubber sheets so that the glass covers slid smoothly. A rubber sheet was put between glass and metal to prevent the glass from cracking. The length of the collector was 5.8 m and an aperture width of 1.2 m. A manual tracker system was fabricated using a general gears of gear ratio 1:30 and a class B black pipe of external diameter 0.008 m and internal diameter 0.003 m. This pipe was fitted onto one of the bigger diameter slots of the gears while the other slot a winch of radius 0.04 m was fitted to effect minute turning of the collector on the North – South axis. The turning would be affected when a 0.005 m by 0.003 m pin that was placed at the plane of aperture width would cast a shadow. The collector was laminated with three appropriate materials each in its turn i.e. aluminium sheet, car solar reflector and aluminium foil each in its turn. The receiver was a cylindrical copper pipe painted black with appropriate black paint. The paint coat was kept as thin as possible so that there was minimum resistance of flow of heat through the coat to the pipe and to the heat transfer fluid. The collector was covered with a 0.0025 m thick glass cover.

The fabricated collector parameters were: Aperture area = 6.95 m<sup>2</sup>, Collector area = 15.75 m<sup>2</sup>, Aperture width = 1.2 m, Focal length = 0.4 m, Collector length = 5.8 m, Outer diameter of absorber pipe = 0.025 m, Inner diameter of absorber pipe = 0.002 m, Concentration ratio = 128. Figure 1 shows the setup for the fabricated trough solar concentrator used for production of solar thermal steam.



*Figure 1: Fabricated prototype parabolic trough solar concentrator for steam production*

The parabolic trough was laminated with aluminium sheet, car solar reflector and aluminium foil appropriate materials each in its turn.

**2.2 Collector test**

Collector testing was done at Juja which is -1.18333 ° in latitude and 37.1167 ° in longitude. During the collector testing the wind speeds varied between 3.2 m/s and 7.0 m/s.

To perform steady state collector testing: a heat exchanger and a 6 kW heater were fabricated. The testing was done at 2.0 m surface above the ground since the collector was designed for rooftops. The inlet temperatures used were 90° C, 140° C, 190° C and 240 °C. The test times were taken systematically about solar noon, to give a total of sixteen data points.

Testing was carried out for fifteen minutes with a selected fluid inlet temperature. This was followed by further testing with steady state conditions for more fifteen minutes.

The solar irradiance and intercept factor for testing period were found by calorimetric method.

The pressure gauges gave the values of pressure drop across the collector and the thermocouples at both ends of collector mixing joints were read to obtain the fluid inlet temperature, T<sub>1</sub> and the fluid outlet temperature, T<sub>2</sub>.

Direct solar irradiance from the sun was computed from calorimetric method by placing a calorimeter with water and a thermocouple at the plane of collector aperture and continuously recording temperature changes.

**2.3 Measurement of intercept factor**

Four calorimeters with 50 g of water were placed at equidistant points along the receiver and the solar thermal heat they absorbed was determined. The ratio of area of absorbing surface in the direction of the sun to the area of receiver superimposed was also evaluated and Equation 2 and was used to find the irradiance at the collector plane.

$$\alpha\tau AI_b = mc \frac{\Delta\theta}{\Delta t} \dots\dots\dots (2)$$

Where:-

$\alpha\tau$  = beam transmittance-absorptance product, m = mass of water in kg and the density of water = 1000 kg/m<sup>3</sup>, c = specific heat capacity of water J / kg °C, 4200 J/kg °C.  $\frac{\Delta\theta}{\Delta t}$  = temperature change per unit time (°C/s) and A = aperture area and  $I_b$  = 852.5 W/m<sup>2</sup> beam irradiance.

For a black body  $\alpha = 1$ . The absorber was made of copper tube of diameter 0.025 m whose thermal conductivity was taken as  $3.9 \times 10^2$  J/kg/K and absorptance = 0.9 (Hanssan, 1972).

#### 2.4 Average heat absorbed by receiver

To determine the average heat that was absorbed by the receiver per unit time, it was partially filled with water and one end was closed using a control valve and the other end leading to a condenser was left open. The condenser was made of a plastic cylinder in which a coiled copper tube was fixed. The plastic cylinder was then filled with cold water to condense the steam. The collector is placed in the sun, far away from the shades until water in the receiver boiled continuously. The mass of steam condensed was measured using a scale and the time it took to obtain the steam was measured using a stop watch. The temperature at which steam was obtained was also recorded.

#### 2.5 Measurement of solar irradiance

A copper calorimeter of radius 0.03 m was insulated on the outside using aluminium foil and on the inside it was painted black. 0.05 kg of water was poured inside and after waiting for five minutes the probe of thermocouple was used to read initial temperatures of water in the calorimeter and recorded. This calorimeter was left exposed at collector plane of the collector at noon and the time of exposure recorded. This was to done find the amount of solar irradiance incidence on the aperture of the concentrator i.e. at the glass cover. The final temperature reached by water in calorimeter was recorded and Equation 2 was used to determine solar irradiance.

The measurement of solar power intensity was measured throughout the day by recording the temperature changes of the water in the calorimeter every twenty minutes. The calorimeter was placed at the middle of collector plane and secured with a thin cotton thread.

#### 2.6 Thermal efficiency

The efficiency of the concentrators was obtained from Equation 3,

$$\text{Efficiency} = \frac{\text{heat - output}}{\text{heat - input}} = \frac{Q_u}{A_c I_b} \dots\dots\dots (3)$$

Where  $Q_u$  is the heat output,  $A_c$  is the collector area and  $I_b$  is the beam irradiance.

Hottel–Whillier–Bliss equation was also used to find efficiency of the fabricated concentrators as shown in Equation 4.

$$F_R \frac{A_a}{A_c} \left[ I_b \rho \alpha < \alpha T >_b - U_L \frac{(T_1 - T_a)}{I_b} \right]$$

**3 Results and discussion**

**3.1 Intercept factor**

The intercept factor obtained in this work was 0.6. The intercept factors for the Euro trough, Luz collectors and the Sky fuel were 0.69, 0.68 and 0.71 respectively (Suhas, 1992). To find the intercept factor surface area of the calorimeter was obtained as 0.010995 m<sup>2</sup> and the superimposed absorber area was obtained as 5.498 × 10<sup>4</sup> m<sup>2</sup>. The ratio of the two surfaces was found to be 1: 19. The calorimeter with water was exposed to the reflected sun rays at the focal axis and the absorbed solar thermal energy was 1.299 × 10<sup>3</sup> W/m<sup>2</sup>. Intercept factor was found as a ratio of surface area of calorimeter to that of absorber with respect to thermal energy collected. Equation 10 was used to find the intercept factor for the fabricated PTSC

$$\frac{1.22 \times 10^3}{19} = 649.84 \dots\dots\dots (10)$$

The thermal energy that was obtained for four equidistant calorimeter positions of the absorber were: - 649.84 W/m<sup>2</sup>, 591 W/m<sup>2</sup>, 658.7 W/m<sup>2</sup> and 633.1 W/m<sup>2</sup> respectively. The intercept factor obtained as an average was 627.8 W/m<sup>2</sup>. When integration of thermal energy absorbed along the absorber was evaluated, intercept factor was found to be 687.3 W/m<sup>2</sup>.

**3.2 Average heat absorbed by absorber**

The absorber used was painted black with black board paint. The Luz, Euro trough and Sky troughs used absorbers coated with selective surface known as cermet surrounded by a vacuum jacket. To obtain the average heat absorbed, mass of steam used was 0.0778 kg at 150 °C collected in 198 s was used. The average power obtained was 886.9 W/m<sup>2</sup>. Insolation was found to be 852.7 W/m<sup>2</sup> with the collector aperture area of 6.96 m<sup>2</sup>. The power that was collected in one hour was 3.19 × 10<sup>6</sup> W/m<sup>2</sup>. If the PTSC modules of an equivalent area to one acre, the power that would be collected in one hour would be 9.27 × 10<sup>6</sup> MW of steam at 150 °C. The PTSC tracked the sun on a N – S mode. This ensured that the solar image at the absorber was not very much enlarged in the morning and in the evening.

**3.3 Determination of solar irradiance**

The solar power intensity for Juja was obtained as 852.7 W/m<sup>2</sup>. The heat gained by the mass of liquid passing a point in the absorber in time t was obtained using Equation 11.

$$Q = mc_p \frac{\Delta\theta}{\Delta t} \dots\dots\dots (11)$$

(Twidel, *et al*, 1986).

Where  $Q$  = quantity of heat gained,  $m$  = mass of heat transfer fluid,  $\frac{\Delta\theta}{\Delta t}$  was the rate of change of temperature with time and  $c_p$  is the specific heat capacity at constant pressure. The rate of heat gain was found to be 2.4 J/s. The area of the calorimeter base was obtained as  $2.8 \times 10^{-3} \text{ m}^2$  and the solar irradiance for the site found as  $852.7 \text{ W/m}^2$ .

### 3.4 Thermal efficiency

The increase in the temperature across the collector during the collector testing was obtained from the thermocouple thermometers and the pressure drop was obtained from the pressure gauges. Hottel – Whillier – Bliss equation was used to represent collector efficiencies for the fabricated concentrators as shown in the Figures 2, 3 and 4.

The collector efficiency was plotted as a function of  $(T_m - T_a) / I_b \text{ } ^\circ\text{Cm}^2$  for both open and closed fabricated concentrators. Figure 2: Shows characterization of aluminium sheet PTSC when open and when closed.

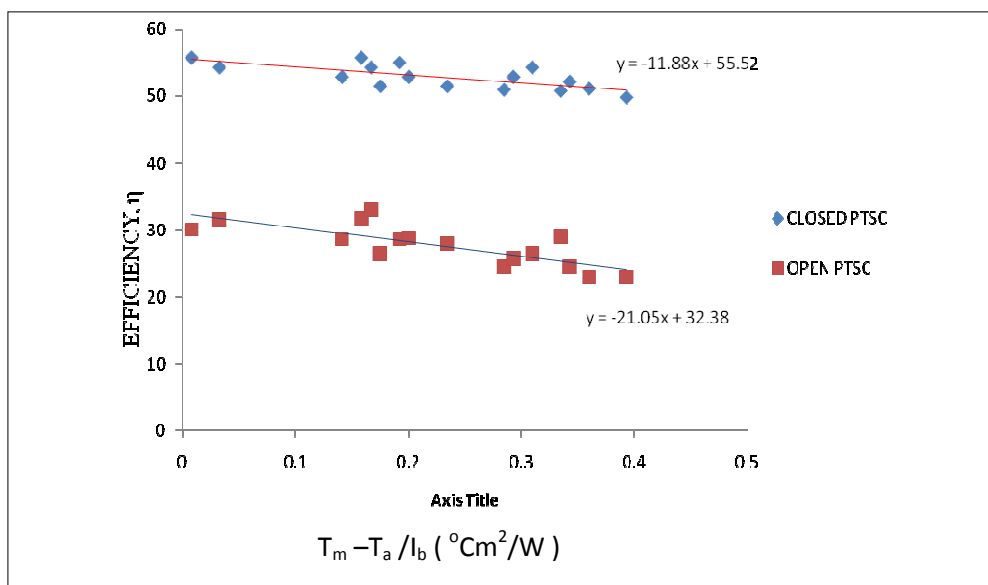


Figure 2: Characterization graph for aluminium sheet solar concentrator when closed and when open.

The following parameters were also used in characterization; - collector heat removal,  $F_R$ ; intercept factor,  $\gamma$ ; reflectance,  $\rho$  and the absorptance – transmittance product,  $\langle \alpha\tau \rangle$ .

The overall heat loss coefficient,  $U_l$  was found to be a weak function of temperature and corresponds to collector heat removal factor. This finding is



similar to the one obtained by John, et, al, 1991. The scatter observed in the data was caused by variations of relative proportions of beam proportion of solar radiation, temperature dependency, wind effects and variations in angle of incidence. In this work the value of efficiency was based on effective aperture area,  $A_a$ . Figure 2 shows efficiency of closed aluminium sheet PTSC as 55.52 %. When experimental variables were used the efficiency was 56.8 %. The heat loss coefficients for the open and closed PTSC were obtained as  $-11.88 \text{ W/m}^2$  and  $-21.05 \text{ W/m}^2$  respectively. The closed fabricated PTSC lost less heat compared to the open PTSC because the closed PTSC had lower speed convectional currents around it due to the enclosure. Therefore the thermal efficiency of the open concentrator was low since it suffered heat losses by convection from the collector to the sky. The thermal efficiency of the closed collector was higher because the collector was covered by glass cover and heat losses by convection were minimum. The experimental efficiency of the collector was lower than one obtained from evaluation of variables. This was because the experimental values were obtained from interaction of environmental factors hence has a higher variability. An example of such an environment factor is wind. When the wind speeds increased between 2.2 m/s to 3.5 m/s the rate of collector heat loss increased. The absorptance transmittance product for aluminium sheet PTSC was found to be 0.8. This was due to the stagnant air mass which formed a blanket around the receiver since it was closed. This caused retention of heat inside the collector; hence the thermal efficiency for the closed collector was 56.8 %. The open collector had a thermal efficiency of 35.73 % due to losses of heat from the absorber. The collector heat removal factor was found to be 0.9, and in agreement with the value obtained by John, et, al, 2005. The collector heat removal factor for the open collector was 0.53. This is an indicator of how low thermal efficiency due to the factors mentioned above. The collector flow factor was obtained as 1.5 for the closed collector and 0.82 for the open collector as can be evaluated using equation 7. The collector efficiency factor of 0.64 was obtained from the closed collector. This was due to the reflectance of aluminium sheet being lowered by scratches and absorber losses. The open PTSC had a collector efficiency of 0.48 due to inaccuracies in position of absorber due to expansion of collector enclosure. Figure 3 shows characterization of car solar reflector PTSC in terms of efficiency when closed with glass of thickness 0.0025 m and when open.

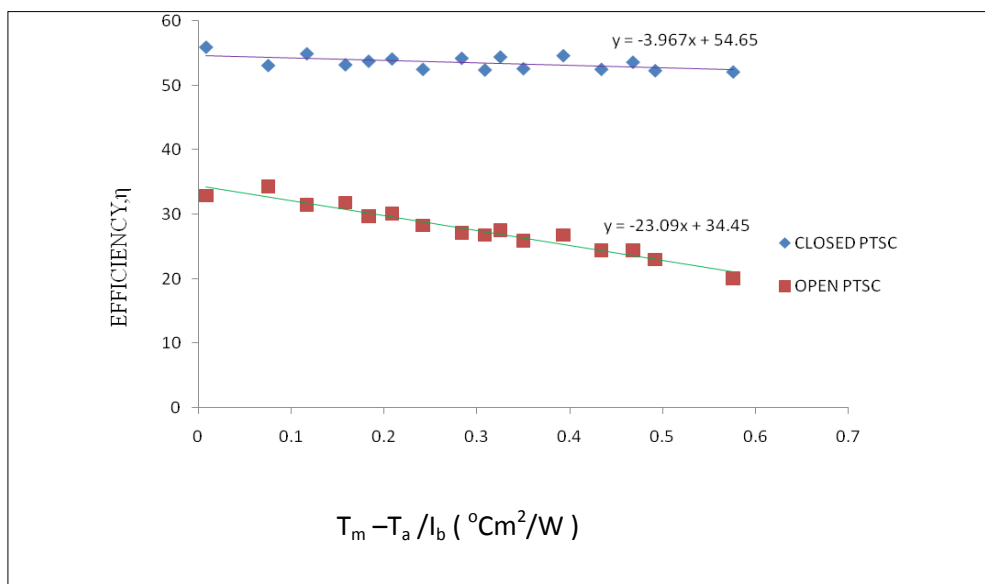


Figure 3: Characterization graph for car solar concentrator when covered with glass and when open

When closed the efficiency was 54.65 %, this value is lower than the one that was obtained by Luz collectors, 68.78 %; Euro trough, 69 % and sky fuel 71 %. This difference is caused by higher reflectivity of Luz collectors of 0.94, absorber surface absorptivity of 0.97 and glass transmittance of 0.965. The efficiency of car solar reflector was higher when open since it was able to resist thermal degradation as compared to both aluminium sheet and aluminium foil PTSC.

When the concentrator was open heat losses due convectional currents caused heat loss on the absorber hence a lower efficiency of utilization of the solar flux. The collector characterization was carried out under the following conditions: -  $\dot{m} = 8.0$  kg/s,  $I_b = 752.1$  W/m<sup>2</sup> and  $\Delta P = 870000$  Pa for the closed collector and  $\dot{m} = 4.78$  kg/s,  $I_b = 803.5$  W/m<sup>2</sup> and  $\Delta P = 463000$  Pa for the open collector. The temperatures that were obtained were: -  $T_m = 210$  °C and  $T_a = 22.7$  °C. When test variables were used to find the efficiency it was obtained as 54.9 %. This was as a result of variability of solar intensity.

The transmittance absorptance product was obtained as 0.78. The air enclosed in the collector enhanced the thermal efficiency of the collector. The heat removal factor was obtained as 0.87 for the closed PTSC and 0.88 for the open PTSC. Over cast sky caused the heat removal factor for the open collector to be higher than for the closed PTSC. The collector efficiency factor that was obtained for the closed PTSC was 0.64 while that for the open one was obtained as 0.42. The heat losses by convection around the open collector contributed to the lower efficiency factor for the open collector. The collector flow factor for the closed PTSC was obtained

as 1.5 since the heat retention in the collector enabled continuous supply of thermal heat to the absorber. The sky trough absorbance was 0.96, emittance of 0.19 and reflectance of 0.95. These factors ensured that the efficiency of the sky trough was 71 %.

The heat loss for the closed PTSC was found to be  $-3.967 \text{ W/m}^2$  due to the insulation of the backside of the collector and the glass covers. The heat loss for the open PTSC was found to be  $-23.09 \text{ W/m}^2$ . This was because of the heat losses by convective currents. Optical efficiency was obtained as 0.56 for this PTSC due to scratches and degradation of the aluminium sheet by the elements of the weather. Figure 4 shows characterization of aluminium foil PTSC when closed and when open.

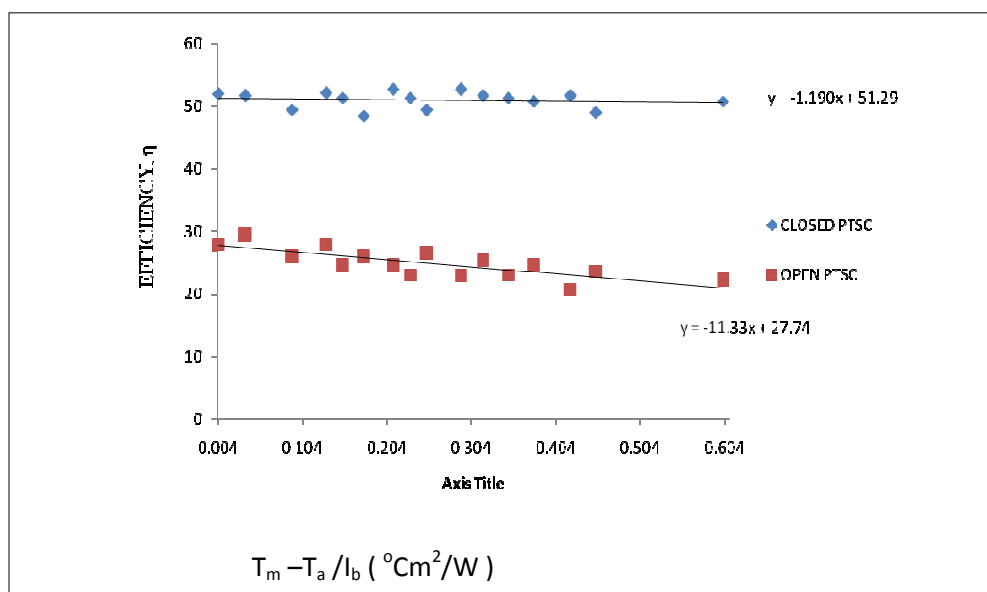


Figure 4: Characterization graph for aluminium foil solar concentrator when covered with glass and when open

The efficiency of aluminium foil PTSC was found to be 53.5 % when closed and 28.7 % when open. This efficiency is lower compared to the efficiency of the Euro trough that was found to be 69.0 %. This is attributed to the evacuated envelop into which the absorber in Euro trough is placed, ensuring minimum heat losses.

During characterization the following conditions were used: -  $\dot{m} = 7.8 \text{ kg/s}$ ,  $I_b = 837.4 \text{ W/m}^2$  and  $\Delta P = 745000 \text{ Pa}$  when closed and when open the conditions under which the collector operated were: -  $\dot{m} = 4.08 \text{ kg/s}$ ,  $I_b = 850 \text{ W/m}^2$  and  $\Delta P = 411000 \text{ Pa}$ . the temperatures achieved for the closed collector were:-  $T_m = 198 \text{ }^\circ\text{C}$ ,  $T_a = 22.5 \text{ }^\circ\text{C}$ . When the wind speed increased from an average of 2.2 m/s to 3.5 m/s the heat losses by convective currents from the glass cover of the collector

increased by  $9.8 \text{ W/m}^2$ . The heat losses contributed to reduced thermal efficiency of the collector. The overall heat loss coefficient for the closed aluminium foil PTSC was  $-1.19 \text{ W/m}^2$  while the one for the open aluminium foil PTSC was found to be  $-11.33 \text{ W/m}^2$ . The wind speeds increased from averages of  $2.2 \text{ m/s}$  in the morning to  $7.0 \text{ m/s}$  in the afternoon. These changes in the wind speeds caused reduced thermal efficiency of the collector. The transmittance absorptance product was obtained as  $0.78$  due to the heat that was trapped in the collector by the glass cover.

The collector heat removal factor was obtained from Equation 5 as  $0.85$  for the closed collector and  $0.57$  for the open collector. This was because the open PTSC lost more thermal heat compared to the closed PTSC.

The collector efficiency factor was obtained as  $0.56$  from Equation 6. This performance is as a result of overcast sky and increased folding on the reflector.

The collector flow factor was obtained as  $1.52$  for the closed concentrator and  $0.73$  for the open concentrator. This was as result of lower thermal absorption performance of the aluminium foil PTSC. The aluminium foil PTSC reflector was more prone to creasing than the other two reflectors. The optical efficiency for aluminium foil PTSC was obtained as  $0.47$ . This is as a result of the diffusion of incident beam radiation by the creases and the folds.

The characterization graphs for the appropriate materials PTSC when closed with glass cover were as follows: - aluminium sheet PTSC,  $55.52 \%$ ; car solar reflector PTSC,  $54.65 \%$ ; and aluminium foil PTSC,  $51.296 \%$  and when open  $32.38 \%$ ,  $34.45 \%$  and  $27.74 \%$  respectively. The Luz collector achieved an efficiency of  $68 \%$ , Euro trough PTSC  $65.2 \%$  and Sky fuel PTSC  $73 \%$ . This difference arises from more advanced absorber surface treatment, evacuation of absorber and use of absorbers with higher reflectance among other factors. It was observed that when operating temperatures of the collector increase the heat losses also increased. The comparison of efficiencies of the open and closed collectors shows that a closed PTSC minimized heat losses by convection. It was also observed that some radiation absorbed by the glass cover slightly raised the temperature of the cover by  $3 \text{ }^\circ\text{C}$  hence reducing the rate of upward heat loss from the receiver. The reduction in the heat losses has an effect in producing some increase in transmittance absorptance product. Reduction of heat losses by introducing covers increased efficiency of each of the collector. The characteristics of the fabricated prototype parabolic trough solar concentrators were as shown in the tables 3, 4 and 5 which played a role in the design of the collector.

#### **4.0 Conclusions and recommendations**

In this paper a study was made to enhance Kenyan research in solar thermal steam generation for steam production by use of appropriate materials. The efficiencies

for the closed PTSC were as follows: Aluminium sheet PTSC, 55.52 %, Car solar reflector 54.65 % Aluminium foil, 51.29 % which is lower than the efficiencies of Luz collector, 68 %, Euro trough, 65.2 % and Sky fuel parabolic trough, 73 %. This is due to evacuation of absorber tube surroundings and automatic tracking systems that they use. The reflectance of the fabricated PTSC was as follows: aluminum sheet PTSC 0.83; car solar reflector PTSC 0.81; Aluminium foil PTSC 0.78; Aluminium for the Luz collector, 0.94 and Euro trough, 0.96. The difference is as a result of the surface treatment of the optical systems, which improves their performance. The glass cover transmittivity of the 0.0025 m glass that was used in fabricated PTSC was 0.8 while the Luz collector has 0.965 and the Euro trough has 0.95. This is because they use selective coatings. The efficiencies observed for closed prototype parabolic trough solar concentrators demonstrates that this technology with appropriate reflector systems can produce solar steam that is hot enough for solar thermal conversion power systems. This can be achieved by use automatic tracking system and smoother reflecting surfaces. In this case higher temperatures and higher efficiencies would be realized. On the other hand use of open parabolic trough systems, where the absorber is exposed, led to high energy losses resulting to low operating efficiencies of the concentrating collectors made from various materials. Enclosing the receiver inside a transparent medium and evacuating it and also surface treatment of receiver as evident with the Euro trough, sky fuel trough, Luz collectors' e.t.c. would significantly improve the efficiencies of the fabricated solar concentrators.

The tables 1, 2, 3, 4 and 5 show a summary of the fabricated concentrator characteristics, which are:- comparison of the pressure difference  $\Delta P$ , mass flow rate  $\dot{m}$  and the average solar power intensity  $I_{bav}$  for the materials that were considered for closed solar concentrators, comparison of the pressure difference, Mass flow rate  $\dot{m}$ , and the average solar power intensity  $I_{bav}$  for the materials that were considered for open solar concentrators, collector flow factor, collector heat removal factor and collector efficiency factor.

Table 1: Comparison of pressure difference  $P$ , mass flow rate and the average solar power intensity  $I_{bav}$  for the materials experimented for closed solar concentrator

Reflector	$\Delta P$ (Pa)	$\dot{m}$ kg/s	$I_{bav}$ (W/m <sup>2</sup> )
Aluminium sheet	921000	8.8	752
Car solar reflector	870000	8.0	752.1
Aluminium foil	745000	7.8	837.4

Table 2: Comparison of pressure difference  $P$ , mass flow rate and the average solar power intensity  $I_{bav}$  for the materials experimented for open solar concentrator.

Reflector	$\Delta P$ (Pa)	$\dot{m}$ kg/s	$I_{bav}$ (W/m <sup>2</sup> )
Aluminium sheet	372000	3.98	749.3
Car solar reflector	463000	4.78	803.5
Aluminium foil	411000	4.08	850

Table 3: Collector flow factor for the fabricated concentrators

PTSC	CLOSED CONCENTRATOR	OPEN CONCENTRATOR
Aluminium sheet	1.50	1.12
Car solar reflector	1.42	0.84
Aluminium foil	1.52	0.73

Table 4: Collector heat removal factor for the fabricated concentrators

PTSC	CLOSED CONCENTRATOR	OPEN CONCENTRATOR
Aluminium sheet	0.90	0.88
Car solar reflector	0.53	0.86
Aluminium foil	0.56	0.81

Table 5: Collector efficiency factor for the fabricated concentrator

PTSC	CLOSED CONCENTRATOR	OPEN CONCENTRATOR
Aluminium sheet	0.64	0.48
Car solar reflector	0.60	0.40
Aluminium foil	0.56	0.34

**References**

Alghoul M. A., Sulaiman M. Y., and Wahab M. A. (2005), *Review of Materials for Solar Thermal Collectors*, Emerald Group Publishers, Malaysia, pp. 200-207.

ASHRAE (American society of Heating, Refrigeration and Air Conditioning Engineers), 1991. *Methods of Testing to Determine the Thermal Performance of Solar Collectors*. ANSI/ASHRAE93-77

Cleaveland T. (2005). Description and Performance of a TRNSYS Model of the Solargenix Tracing Power Roof. in proceedings of ISES solar wind congress, Orlando.

Ecoworld (2009), "Solar Thermal Energy". <http://www.ecoworld.com/energy-fuels/solar> Accessed 22.12.2009, 3.00 a.m.

John D, A. and William B. A. ( 1991 ), *Solar Engineering of Thermal Processes*, John Wiley & Sons Inc., Canada, pp. 3-216, 330-379

John W., Twidel D.S and Anthony D.W. (1986), *Renewable Energy Resources*, ELBSLE and F.N Spon Ltd, London, pp. 17-45

Kalogirou S, Lloyd S and Ward J. ( 1997), *Modeling, Optimization and Performance Evaluation of a Parabolic Trough Solar Steam Generation System*, Sol Energy, London. pp. 49-59

Parabola (2007), "Trough Geometric Design", <http://www.billeoster.com/2007/112/en> Accessed 23.4.2010, 5.30 a.m

Power from the Sun (2009), "Science Encyclopedia," [www.Power from the sun. Net/chapter 2.20/3/2010](http://www.Powerfromthesun.net/chapter2.20/3/2010), 2.00 a.m.

Price H, Lufert E and Kearney D, (2010), *Advances in Parabolic Trough Solar Technology*, Sol Energy-T ASME, London, pp. 109-125.

Rai G.D. (1987). *Solar Energy Utilization*, Kama Publishers, Newdehli, pp. 1 – 19, 160 – 190.

Renewable Energy (2008), "Natural Renewable Energy Laboratory", <http://www.Nrel/.Govl>. Accessed 25.2.2010, 6.00 a.m

Solar and Wind Energy Resource (2006), "Renewable Energy", [http:// www.swera.unep.net](http://www.swera.unep.net) UNEP/Grid-Sioux falls .Accessed 5.5.2010, 11.45 p.m.

Suhas P.S. (1992), *Solar Energy*. Tata Mc Graw Hill Publishing Co. Ltd, Newdehli. Pg. (7- 80).

Solar and Wind Energy Resource Assessment (2012), "Renewable Energy", [http:// www.swera.unep.net](http://www.swera.unep.net). UNEP/Grid-Sioux falls .Accessed 5.5.2012, 11.45 p.m.

Wikipedia Free Encyclopedia (2010), "Solar Thermal Energy Processes", "[http://www wikipedia.org/wiki/ solar thermal](http://www.wikipedia.org/wiki/solarthermal). Accessed 27.1.2010, 11.30 a.

**THERMODYNAMIC MODELLING OF THE EQUILIBRIA IN LAKE BARINGO, KENYA****C. O. Onindo<sup>1</sup> and I. W. Mwangi<sup>1</sup>***Kenyatta University, Kenya**Email: coonindo@yahoo.com***Abstract**

The equilibria that control the composition of a lake is presented using lake Baringo, Kenya, as an example. Lake Baringo (0°37'N, 36°05'E) lies very close to the equator in the Baringo basin in the Eastern Rift Valley, Kenya. Water from the lake was analysed chemically using standard analytical techniques to obtain the stoichiometric concentrations of the major anions and cations. However, this does not indicate how the components are distributed amongst possible species. The speciation calculation was performed using the available equilibrium constants for all the metal – ligand and proton – ligand species identified. At pH 8 the composition of the water of lake Baringo was Ca<sup>2+</sup> (58.88%); CaCO<sub>3</sub> (41.12%); Mg<sup>2+</sup> (97.33%); MgCO<sub>3</sub> (2.88%); HCO<sub>3</sub><sup>-</sup> (98.27%) and SO<sub>4</sub><sup>2-</sup> (99.88%). Sulphate forms very weak complexes of calcium and magnesium and was excluded from the model. MgHCO<sub>3</sub><sup>+</sup>, CaHCO<sub>3</sub><sup>+</sup> and MgSO<sub>4</sub> were found to be minor species.

**Key words:** Speciation, thermodynamic modelling



## 1.0 Introduction

Modelling of the speciation provides an attractive alternative to the often difficult and tedious analytical techniques in speciation studies. All that is required is an extensive data-bank of all conceivable stability constants for a system. This paper reports the use of thermodynamic data to calculate the probable speciation of the major anions and cations present in Lake Baringo, Kenya

Lake Baringo (0°37'N, 36°05'E) lies very close to the equator in the Baringo Basin in the Eastern Rift Valley, Kenya. The lake is roughly 21 kilometres long and 8 kilometres wide with a mean depth of 1.6 metres. It provides a source of fish for the nearby population. The lake has an area of about 130 square kilometres but is variable according to lake levels. Results from previous studies on Lake Baringo (Beadle, 1932, Jenkins 1936, Talling and Talling 1965 and Kallqvist 1980) gave the major species as bicarbonate, chloride, sodium, magnesium and calcium ions while (Alala, 1981) showed no significant heavy metal levels.

Under normal conditions, Lake Baringo, has low alkalinity, but with less rain, the lake has become more saline with an average conductivity of  $660\mu\text{S cm}^{-1}$  while the pH varies between 8.9 and 10.5 (Odada and Olago, 2002). A parallel analysis (Ochieng et.al., 2007) of heavy metals in water and surface sediments in five Rift Valley lakes in Kenya did find some increase in the level of metals due to anthropogenic activities especially in Lake Nakuru.

The analytical data obtained for Lake Baringo however, does not indicate how the components are distributed amongst possible (complex) species. This is achieved *via* speciation calculation that assumes that the system is in equilibrium, that requires the equilibrium constants for all metal-ligand and proton-ligand species at the correct ionic strength and temperature and that accurately defines all the species formed. The speciation calculation was done by Species program (Pettit and Powell, 1999). It calculates and displays speciation curves given the total concentration of reactants and overall stability constants of the complexes considered. It was limited to six components and unable to handle solubility data.

For an aqueous solution phase of a natural water system, the actual composition is given by a set of concentrations. The simplest thermodynamic model for a natural water system is an aqueous solution, which is not subject to physico-chemical reactions with any solid or gaseous phase. Such a system is an idealisation in that water itself and all solutes have some finite escaping tendency, however small. An aqueous solution of electrolyte in a laboratory maintained at constant temperature and exposed to atmospheric pressure represents a common arrangement for studying chemical equilibria. Thermodynamic data obtained from such experimental system can be used to interpret the behaviour of real or model system of a more complex character, e.g. a natural water system (Stumm and Morgan, 1981).

## 2.0 Materials and methods

Water from the lake, was analysed chemically using standard analytical techniques to provide the data to calculate the probable speciation of the major anions and cations present. The procedure followed for the collection and handling of water samples was adopted from those recommended by Ahlers *et al.* (1990) with some modifications. New polythene bottles were used in the sampling process. Sampling was carried out twice in February and July to capture dry season and long rains respectively.

The bottles were first washed with detergent to remove grease then soaked in 2 mol dm<sup>-3</sup> HNO<sub>3</sub> for a minimum of four days. A further soaking for about 24 hours in distilled deionized water followed this. Finally, the bottles were rinsed thoroughly with distilled deionized water. After cleaning, the bottles were filled with leaching solution of 0.01mol dm<sup>-3</sup> analytical grade nitric acid, placed in a separate plastic bag and sealed. The sample bottles were transported in sealed plastic bags taking considerable care to avoid exposure to dust.

On reaching the sampling area, all the bottles were filled partially at least twice and shaken before emptying. Subsequently bottles were filled by hand-dipping (hand protected by wearing plastic hand gloves) empty bottles beneath the water surface. After sampling the bottles were capped and immediately wrapped in polythene bags and later transported to the laboratory.

Samples were drawn from six randomly selected sites along the shore in order to provide a range in water composition. From each site, four aliquots of 500 ml each was withdrawn. Filtration was done as soon as the samples were brought to the laboratory. The filters were first leached with distilled deionized water. Filtration through 0.45 µm nominal pore size membrane filters (Nalgene) was done directly into the acid-cleaned polythene bottles. By convection, whatever passes through the filters is taken to be soluble.

After filtration two 500 ml bottles from each site were preserved for later analysis by the addition of 1 ml concentrated nitric acid per 500 ml of water and kept frozen. The remaining two bottles also stored frozen were left unacidified for the analysis of anions. 2-4 ml of chloroform were added to samples stored for the analysis of nitrite and nitrate to retard bacterial decomposition.

A variety of methods and procedures routinely used in the analysis of natural waters were used, as there were many parameters to be determined. These have a common theme: they involve a physical phenomenon or relationship and its application via appropriate instrumentation. Techniques using these phenomena include potentiometry, voltammetry and spectrometry. These were adopted from various standard textbooks of analytical chemistry (Colterman, 1978, Marr 1983,

Braun, 1982, Vogel, 1961, Midgley 1991 and Linder *et al.*, 1984). Analytical grade reagents (BDH Analar grade) were used in all preparation of reagents using deionised water.

Atomic Absorption Spectrophotometer (901 GBC Scientific Equipment Pty Ltd) was used to determine the levels of iron, calcium, manganese and magnesium. Sodium and potassium were determined by flame photometer (Corning 400) using butane as fuel with air as oxidant. Sulphate and phosphorus were analysed at 530 nm and 426 nm respectively using spectronic 20 spectrometer (Bauch and Lamb). For each element a calibration curve was obtained by drawing a graph of absorbance against the corresponding concentrations of working standard solutions. In most cases, the curves were found to be linear in the concentration ranges used for each element. The reproducibility of each instrument for each element analysed was tested. A standard concentration for each element was analysed four times and a mean absorbance calculated in each case.

The carbonate and bicarbonate concentrations were determined by titrimetric procedures. Fluoride and nitrate were determined using the respective ion selective electrodes. The determination of lead, copper and cadmium were done by stripping voltammetry and concentrations determined by standard addition. A typical instrument setting was: Differential pulse polarography, purging time, 180 seconds; equilibration time, 10 seconds; deposition time, 60 seconds and scan range from -1.00 to -0.15 V (versus Ag/AgCl reference electrode).

### 3.0 Results and discussions

The results of the analysis of the lake are presented in Table 1. The 95% confidence limits for the concentrations were calculated on a sample size of six ( $n=6$ ). The number of significant figures quoted specify the estimate of the precision of the results and the uncertainty in the last figures have been emphasised by having them as subscripts.

The average water temperature of Lake Baringo was moderately high (29°C). This high temperature might facilitate rapid decomposition of organic materials in the lake. The conductivity mean value for the lake water was  $793 \mu\text{S cm}^{-1}$ . High conductivity implies the lake has become more saline (Odada and Olago, 2002). The conductivity of most freshwaters ranges from 10 to  $1000 \mu\text{S cm}^{-1}$  but may exceed  $1000 \mu\text{S cm}^{-1}$  in polluted waters.

The mean pH value of 8.2 was recorded for the lake. This means that the lake can be classified as fresh water lake, which depending on other variables, can be suitable for human consumption. The pH of most natural waters is between 6.0 and 8.5 and therefore it falls within the World Health Organisation (WHO)

recommended values (Meybeck 1990). Lower values can occur in dilute waters high in organic content and higher values in eutrophic water, groundwater, brines and salt lakes. A pH value of 8.2 therefore places Lake Baringo near the alkaline limits for human consumption.

The electroneutrality principle,  $\Sigma(\text{cation charges}) = \Sigma(\text{anion charges})$ , must hold, however a discrepancy was observed in this relationship and the analytical data because organic matter was not included in the analysis. Oxidative decomposition of organic matter will be very rapid at 29°C. Thus although the conjugate bases of simple molecules such as carboxylic acids, amino acids and peptides will contribute to the anion charge, their lifetime will be short. However, the refractory end products of organic oxidation, humic and fulvic acids will persist and will contribute to anion charge.

The salt concentration is high but consistent with water loss by evaporation. Magnesium and Calcium are low, controlled mainly by precipitation of their carbonate salts. Natural waters are dynamic systems. If a sample is returned to the laboratory for analysis, it is important to suppress photosynthesis. The photosynthetic reaction will alter the sample pH by consuming CO<sub>2</sub> and increasing the ratio [CO<sub>3</sub><sup>2-</sup>]/ [HCO<sub>3</sub><sup>-</sup>]. This may promote precipitation of carbonate salts. The high [HCO<sub>3</sub><sup>-</sup>] and high pH are consistent with intensive biodegradation of organic matter and photosynthetic activity. Biodegradation generates inorganic carbon, CO<sub>2</sub> from organic matter. Photosynthesis consumes CO<sub>2</sub> in the production of O<sub>2</sub>. This process lead to the net conversion of HCO<sub>3</sub><sup>-</sup> to CO<sub>3</sub><sup>2-</sup> and hence an increase in pH. Sulphate tends to concentrate in the water because its Ca and Mg salts are reasonably soluble.

Table 1: The concentration in mg L<sup>-1</sup> of the selected water variables

pH	8.2		WHO	EC
	February, 2007	July, 2007	6.5	8.5
Na <sup>+</sup>	307±3.3	280.0±34.0	200	175
K <sup>+</sup>	15.3±3.0	16.0±2.0		
Ca <sup>2+</sup>	1.1±0.1	4.0±1.6		
Mg <sup>2+</sup>	3.0±0.3	3.04±0.2		
CO <sub>3</sub> <sup>2-</sup>	139.3±2.5	154.3±5.0		
HCO <sub>3</sub> <sup>-</sup>	429.1±16.0	448.5±9.0		
PO <sub>4</sub> <sup>3-</sup>	0.56±0.04	0.43±0.06		
SO <sub>4</sub> <sup>2-</sup>	29.2±1.8	20.5±2.8	40	25
NO <sub>2</sub> <sup>-</sup>	0.08±0.02	0.20±0.02		
NO <sub>3</sub> <sup>-</sup>	0.08±0.03	0.09±0.02	45	50

F <sup>-</sup>	2.22±0.09	3.9±0.05	1.5	1.5
Cl <sup>-</sup>	49.3±6.8	59.2±2.9	250	250
DOC	4.3±6.8	4.1±0.8		
COD	nd	18.2±8.1		
Cu <sup>2+</sup>	0.008		1	0.1
Pb <sup>2+</sup>	0.002		0.05	0.05

The thermodynamic data obtained was used to calculate, using the Species computer program (Pettit and Powell, 1999), the probable speciation of the major anions and cations present in lake Baringo, Kenya. The objective of the calculations in the Species program was to determine the most probable chemical model of a system. The program could accept up to six mass balance equations, run on an IBM compatible PC, it had a very simple user interface and a proper graphical output. The results showed a relatively low concentration of lead and copper and these were not included in the species calculations. Lead and copper are also likely to be solubilized by polydentate weak acids ligands which form chelated complexes. The organic ligands were undifferentiated in the DOC.

The concentration of the species in equilibrium is defined in terms of an equilibrium constant:

$$[M_p L_q H_r] = [M]^p [L]^q [H]^r \beta_{pqr}$$

Further, the concentrations of the species in equilibrium are constrained by the law of mass action. For a three component system of a metal ion M, a ligand L and hydrogen ion H<sup>+</sup> with concentrations [M], [L] and [H] (ionic charges are omitted for the sake of generality) the expressions for the mass-balance equations are:

$$T_M = [M] + p \sum \beta_{pqr} [M]^p [L]^q [H]^r$$

$$T_L = [L] + q \sum \beta_{pqr} [M]^p [L]^q [H]^r$$

$$T_H = [H] + r \sum \beta_{pqr} [M]^p [L]^q [H]^r$$

$T_M$ ,  $T_L$  and  $T_H$  are the concentrations in total of metal, ligand and proton respectively. Three component system would give three non-linear equations with [M], [L] and  $[M_p L_q H_r]$  as the only unknowns if the hydrogen ion concentration obtained from the measurement of pH is known.

Using the mass balance equations, the stability constants and the total concentration value of each component were used as input data for the Species program. In the calculations Species program progressively estimates equilibrium

concentrations until all mass balance equations are satisfied. The output may be plotted as percentage versus pH.

In extremely dilute aqueous solutions, such as most rivers and lakes, the major dissolved species can be looked upon as individual free ions. A chemical analysis of such water reported in terms of concentrations of  $\text{Na}^+$ ,  $\text{K}^+$ ,  $\text{Ca}^{2+}$ ,  $\text{Mg}^{2+}$ ,  $\text{Cl}^-$ ,  $\text{SO}_4^{2-}$ ,  $\text{HCO}_3^-$  etc. may provide an entirely satisfactory model of the internal economy of the system. When one considers all the possible binary complexes that might occur in a natural water containing many dissolved elements, the complication seem at first to be overwhelming. However, no complexes need to be considered between cations and chloride ions or between  $\text{K}^+$  and  $\text{HCO}_3^-$  or  $\text{CO}_3^{2-}$ . Alkali metal complexes with  $\text{OH}^-$ ,  $\text{Cl}^-$  and  $\text{NO}_3^-$  are very weak and thermodynamic data for these complexes are highly uncertain. But  $\text{K}^+$  interacts with  $\text{SO}_4^{2-}$ ;  $\text{Na}^+$ ,  $\text{Ca}^{2+}$  and  $\text{Mg}^{2+}$  interact with each of the anions  $\text{SO}_4^{2-}$ ,  $\text{HCO}_3^-$  and  $\text{CO}_3^{2-}$ . The  $\text{OH}^-$  interactions may be neglected because of the generally low concentrations of  $\text{OH}^-$  (Stumm and Morgan (1981).

The important dissolved species may therefore include:  $\text{K}^+$ ,  $\text{KSO}_4^-$ ,  $\text{Na}^+$ ,  $\text{NaCO}_3^-$ ,  $\text{NaHCO}_3^-$ ,  $\text{NaSO}_4^{2-}$ ,  $\text{Ca}^{2+}$ ,  $\text{CaHCO}_3^+$ ,  $\text{CaCO}_3$ ,  $\text{CaSO}_4$ ,  $\text{Mg}^{2+}$ ,  $\text{MgHCO}_3^+$ ,  $\text{MgCO}_3$ ,  $\text{MgSO}_4$ ,  $\text{HCO}_3^-$ ,  $\text{CO}_3^{2-}$ ,  $\text{SO}_4^{2-}$ . The concentrations of the most important species as determined in Lake Baringo (see Table 2) together with the literature values of the stability constants (Table 3) for the major inorganic species most likely to be in solution were fed into the program Species modified to include up to six components simultaneously.

Table 2: Concentrations (mM) of the most important species in Lake-Baringo

	Feb. 2007	July, 2007
$\text{Na}^+$	1.3	1.2
$\text{K}^+$	0.39	0.41
$\text{Ca}^{2+}$	0.028	0.10
$\text{Mg}^{2+}$	0.12	0.12
$\text{CO}_3^{2-}$	2.3	2.6
$\text{SO}_4^{2-}$	0.3	0.21

The reliability of such species calculations in modelling relies heavily on the thermodynamic data available. It follows that very careful judgement is needed in selecting the stability constants available. Much of these are reported at different ionic strengths and temperatures.

Table 3: Stability constants ( $\log K_{ML}$  values) for the important metal-inorganic ligand systems at 25 °C

Ligand	Ca <sup>2+</sup>	Mg <sup>2+</sup>	H <sup>+</sup>
CO <sub>3</sub> <sup>2-</sup>	4.44 <sup>a</sup>	2.984 <sup>c</sup>	9.95 <sup>b</sup>
HCO <sub>3</sub> <sup>-</sup>	1.14 <sup>a</sup>	1.066 <sup>c</sup>	
SO <sub>4</sub> <sup>2-</sup>	1.39 <sup>d</sup>	2.47 <sup>f</sup>	1.10 <sup>e</sup>

<sup>a</sup>Kallqvist (1980) <sup>b</sup>Guyader (1983) <sup>c</sup>Maya (1982) <sup>d</sup>Siebert (1977) <sup>e</sup>Griggs (1979)  
<sup>f</sup>Khoe (1988)

The species distribution curves of the major complexes are shown in Figure 1.

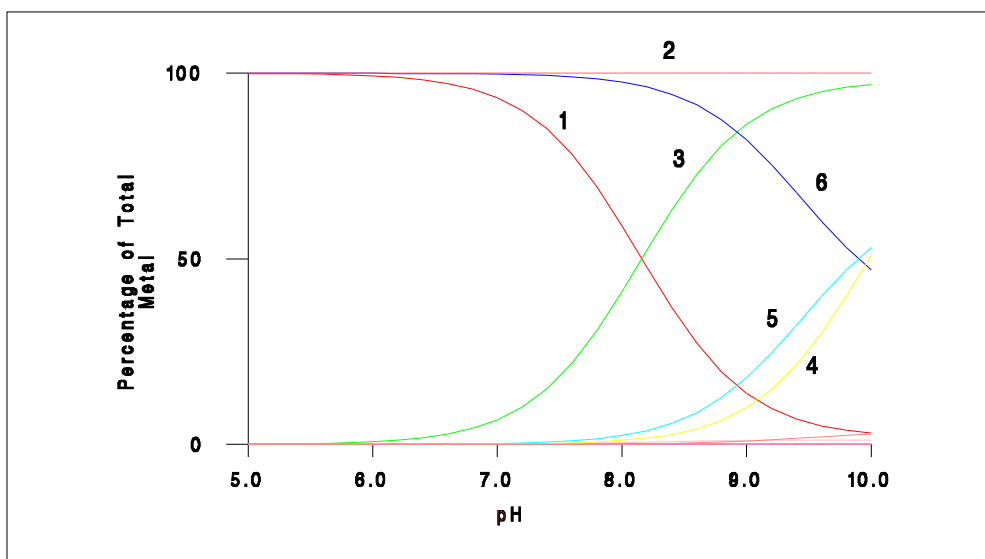


Figure 1: The species distribution curves of the major complexes

where 1= Ca<sup>2+</sup> 2= SO<sub>4</sub><sup>2-</sup> 3= CaCO<sub>3</sub><sup>2+</sup>  
 4= CO<sub>3</sub><sup>2-</sup> 5= MgCO<sub>3</sub> 6= Mg

#### 4.0 Conclusion

Sulphate forms very weak complexes of calcium and magnesium and it can be safely excluded from the model.  $\text{MgHCO}_3^+$ ,  $\text{CaHCO}_3^+$  and  $\text{MgSO}_4$  were also found to be minor species. At pH 8 therefore the composition of the water is as shown in Table 4.

Table 4: Percentage Composition at pH 8

Component	Total Analytical Concentration /mM	Dominant Species pH 8
$\text{Ca}^{2+}$	0.028	$\text{CaCO}_3$ (41.12%) $\text{Ca}^{2+}$ (58.88%)
$\text{Mg}^{2+}$	0.12	$\text{Mg}^{2+}$ (97.33%) $\text{MgCO}_3$ (2.88%) $\text{MgSO}_4$ (0.29%)
$\text{CO}_3^{2-}$	2.3	$\text{HCO}_3^-$ (98.27%)
$\text{SO}_4^{2-}$	0.3	$\text{SO}_4^{2-}$ (99.88%)

#### References

- Ahlers W. W, Reid M. R., Kim J. P. and Hunter, K. A. (1990). *Aust. J. Mar. Freshwater Res*, **41**, pp. 713.
- Alala L. N. N. (1981). MSc Thesis, University of Nairobi, Kenya.
- Beadle L.C., (1932). *J. Limn. Soc. Zool.*, **38**, pp. 157 -211.
- Braun R. D and H. W. Fred H. W. (1982). *Applications of chemical analysis*, McGraw-Hill Company, New York.
- Colterman H. L. (1978). *Methods for Physical and Chemical analysis of Fresh Waters*, International Biological Programme Handbooks; no. 8, Blackwell Scientific Publications, Oxford and Edinburgh.
- Craggs A., Moody G. J. and Thomas J. D. R. (1979). *Analyst*, **104**, pp. 961
- Jenkin P. M. (1936). *Report on the Percy Sladen Expedition to some Rift Valley Lakes in 1929. VIII Summary of the ecological results, with special reference to the alkaline lakes.*
- Kallqvist T. (1980) *Primary production and Phytoplankton in Lakes Baringo and Naivasha, Kenya*, Norwegian Institute for Water Resources, Blindern, Oslo.
- Khoe G. H and Robbins R. G. (1988). *J. Chem. Soc, Dalton Trans.*, 2015



Linder P. W., Torrington R. G. and Williams D. R. (1984). In: *Analysis Using Glass electrodes*, Open University Press.

Marr L. L. (1983). *Environmental Chemical Analysis*. pp. 109-136. International Textbook Company, New York.

Martynova O. I., Vasina L. G. et al. (1975). *Dokl.Akad.Nauk SSSR*, pp. 862

Maya L. (1982). *Inorganic. Chem.*, **21**, pp. 2895.

Meybeck M., Chapman D. V., Helmer R. (eds), (1990). *Global Freshwater Quality*, UNESCO/WHO

Midgley D. and Torrance K. (1991), *Potentiometric Water Analysis*, (2nd Ed.), pp. 313. *John Wiley & Sons* International England.

Ochieng, E.Z., Lalah, J.O. and Wandiga, S.O. (2007): *Bull Environ Contam Toxicol* **79**, pp. 570-576.

Odada E. O and Olago D. O. (eds) (2002):: *Limnology, Palaeolimnology and Biodiversity*. Pp. 335-347. Kluwer Academic Press (Netherlands)

Pettit L. D and Powell K. J.(1999). *SPECIES, Academic Software* in collaboration with RSC, London.

Siebert R. M. and Hostetler P. B. (1977). *Am. J. Sci.*, **277**, pp. 697

Stumm W. and Morgan J. J.(1981). *Aquatic Chemistry: An Introduction Emphasising Chemical Equilibria in Natural Waters*, 2nd ed., Wiley, New York.

Talling J. F. and Talling I. B. (1965). *The Chemical Composition of African Waters*. (Int. Revue Ges. Hydrobiol. 50; 421-463).

Vogel A. I. (1961). *A Textbook of Quantitative Inorganic analysis, including elemental instrumental analysis*, 4th edition. pp. 251 Longman, London.

**EFFECT OF HEXANE TREATMENT AND UNIAXIAL STRETCHING ON BENDING  
ELECTRICITY OF POLYVINYLIDENE FLUORIDE (PVDF)**

**C. M. Mutambi<sup>1</sup>, J. N. Mutuku<sup>1</sup>, and P. K. Karanja<sup>1</sup>**

<sup>1</sup>Jomo Kenyatta University of Agriculture and Technology, Nairobi, Kenya

Email: cmutambi@cuea.edu

**Abstract**

The effect of hexane treatment and uniaxial stretching in polyvinylidene fluoride (PVDF) film was studied. The quantity,  $\beta_{31}$ , defined as the bending piezoelectric stress constant, was calculated. After hexane treatment and uniaxial stretching of the PVDF film, the value of  $\beta_{31}$  was 5.75 mV/m and 8.00 mV/m for draw ratio of 1.5 and 2.5 was recorded. Fourier transform Infra-red (FTIR) spectrophotometry was used for structural investigations.

**Key words:** Polyvinylidene fluoride (PVDF), bending piezoelectric stress constant  $\beta_{31}$ , Fourier Transform infra-red (FTIR) spectrophotometry, iodine doping, hexane treatment, uniaxial stretching.

## 1.0 Introduction

Piezoelectric and pyroelectric polymer electrets (Sessler,1987; Lang,1995) are found more and more in industrial applications . Interest in the electric properties of PVDF began in 1969 when Kawai (Kawai, 1969) showed that thin films that had been poled exhibited a very large piezoelectric coefficient (Kepler and Anderson,1978 ; Luongo,1972) pCN-1, a value which is about ten times larger than had been observed in any other polymer.

PVDF has the advantage of long term stability of its piezoelectricity at room temperature and its mechanical flexibility. Bending (or flexure) piezoelectricity in poled polymer films has been investigated by several authors (Furukawa et al.,1968;Kawai and Heiji,1970;Ibe,1974;Furukawa, 1976; Fukada et al., 1987). These studies were arrived at by determining the piezoelectric activity induced by bending deformation of polymer. While tensile piezoelectricity has been investigated in detail, the origin of bending piezoelectricity is not yet fully understood. When a poled polymer film is subjected to bending deformation, the electrical displacement consists of two components, one proportional to stress (as in the case of elevation) and the other proportional to the stress gradient (Litt et al., 1977; Zoon and Zoon and Liu, 1978; Lang,1974).

The latter effect is characterized by a bending piezoelectric strain constant  $b_{31}$  which depends on the structure of the polymer (Kawai and Heiji, 1970). Commercial polymer films contain various impurities such as antioxidants, residual catalysts, phenanthrene, benzoic acid, aromatic ketone such as benzophenone and some impurities introduced during manufacturer (Umemura et al., 1982; Ronarch and Haridoss, 1981). Hexane has been shown to have greatest permeation rate through polyethylene (Ronarch and Hridoss, 1981). Also it is established that the steady state electrical conductivity in polyethylene is significantly reduced on hexane treatment possibly because of a reduction in the density of impurity hopping sites for the charge carriers (Foss and Dannhauser,1963).

Here we have carried out investigations on untreated and hexane treated PVDF films with the aim of determining the effect of  $\beta_{31}$  on bending piezoelectricity.

Changes in voltage against film bending have been used to establish the effect of the  $\beta_{31}$  on the induced current.

## 1.1 Experimental

Commercial PVDF film of 40mm thickness were obtained from Kureha Industrial Chemical Company; Japan.

Hexane treatment was performed by keeping the PVDF sample in hexane for 24 hours at room temperature. Aluminium electrodes of thickness about 500 Å were vacuum deposited on one surface of the virgin and hexane treated samples.

Fourier transform infra-red (FTIR) spectra of the virgin and hexane treated PVDF films were recorded using a Shimadzu FTIR-8400 Fourier transform infra-red spectrophotometer.

Uniaxial stressing of the samples was performed with the aid of a film stretching frame shown in Fig. 1. Sample specimens of sizes 44 mm x 7 mm were locked at the grips of the stretching frame before being extended. 2 mm portions of the sample under grips were covered by emery cloth to improve the gripping and to prevent heat damage from the hot metal grips. The frame was then placed in an air circulated oven set at 45oC, 55oC and 65oC. The same were left to heat for 5 minutes after which the oven door was partially open and sample stretched at ratios 1.5, 2.0 and 2.5 for the temperature settings of 45oC, 55oC and 65oC respectively by rotating the lever arm of the frame. The samples were then left to cool while under tension.

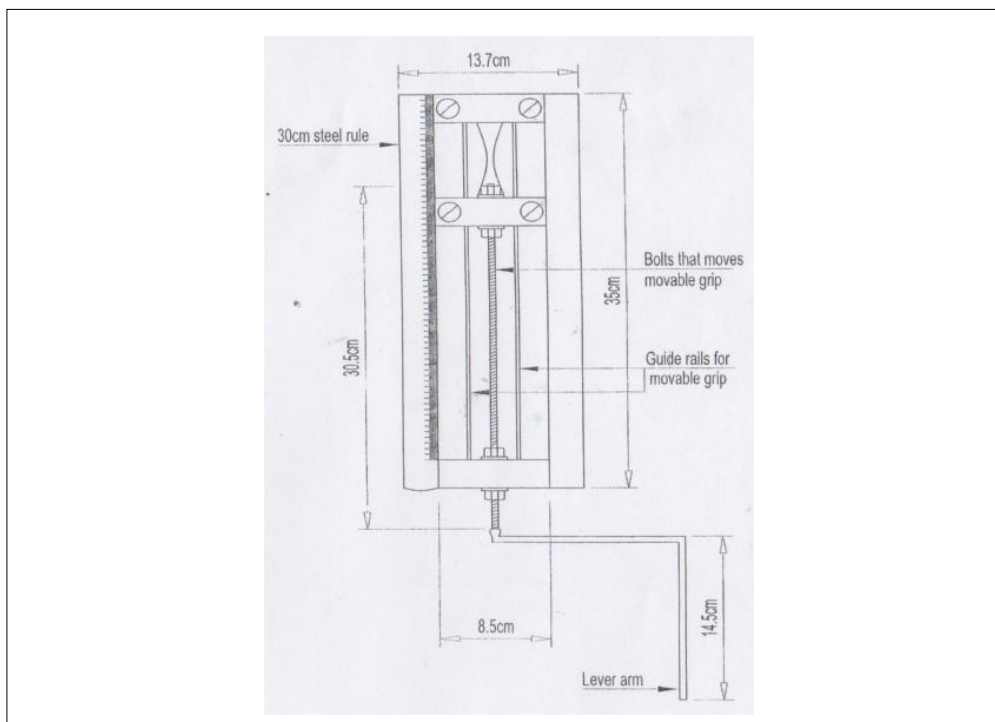


Figure 1: The film-stretching frame

The experiments for the determination of  $\beta_{31}$  values were carried out under room temperature using horizontal deflection of the lower end of the film by eccentrically rotating the micrometer screw gauge. Piezoelectric bending measurements were carried out using a cantilever beam of length 1, width  $w$  and thickness  $t$ . Deflection  $D_2$  is imposed at the end of the beam as shown in Fig. 2.

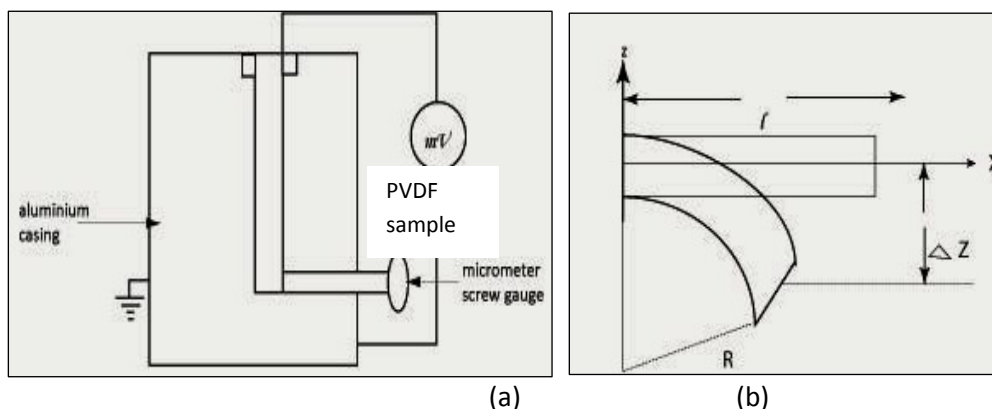


Fig 2. (a) Schematic diagram of the measuring device and (b) geometry of the experiment cantilever beam of length  $l$  and thickness  $t$  deflected by  $\Delta Z$

The induced electric displacement  $D_3$  in the direction of the Z axis is given by

$$D_3 = \epsilon_3 E_3 + \beta_{31} (1/R) \dots \dots \dots (1)$$

$$\frac{dD_3}{dz} = \overline{\epsilon_3 E_3} + \beta_{31} \left( \frac{1}{R} \right) \dots \dots \dots (2)$$

Where  $E_3$  and  $\epsilon_3$  are the z-direction components of electric field intensity and the permittivity of the PVDF film, respectively, and  $R$  is the radius of curvature of the displacement  $D$ . Since  $1/R$  is equal to the thickness gradient of the strain in  $x$ -direction,  $dD_3/dz$ . the quantity  $\beta_{31}$  is defined as the bending piezoelectric stress constant. In a non-uniform polarized dielectric Gauss's law  $dD_3/dz=0$  yields  $D_3 = \text{constant}$  while  $E_3 \epsilon_3$  must be replaced by the average  $E_3 \epsilon_3$ . For constant  $\epsilon_3$  and under short-circuit conditions  $E_3 \epsilon_3 = 0$  and one obtains the electrode charge induced by bending as . Since for small deflections, one obtains

$$\beta_{31} = \frac{l}{2w} \left( \frac{Q}{\Delta Z} \right) \dots \dots \dots (3)$$

But the induced charge  $Q$  is proportional to the voltage  $V$ , i.e, so that

$$\beta_{31} = \frac{l}{2w} \cdot k \cdot \frac{V}{\Delta Z} \dots \dots \dots (4)$$

where  $k$  is a constant

$$\text{Hence } \beta_{31} = \text{constant} \times V / \Delta Z \dots \dots \dots (5)$$

The deflection  $DZ$  of the sample was measured and the corresponding value of

voltage  $v$  was noted. This was repeated for several values of deflection  $DZ$ .

## 2.0 Results and Discussion

Figure 3(a) and Figure 3(b) show the FTIR scans for virgin and hexane treated PVDF films, respectively. Weak peaks in the virgin sample (Figure 3(a)) are eliminated with hexane treatment (Figure 3(b)).

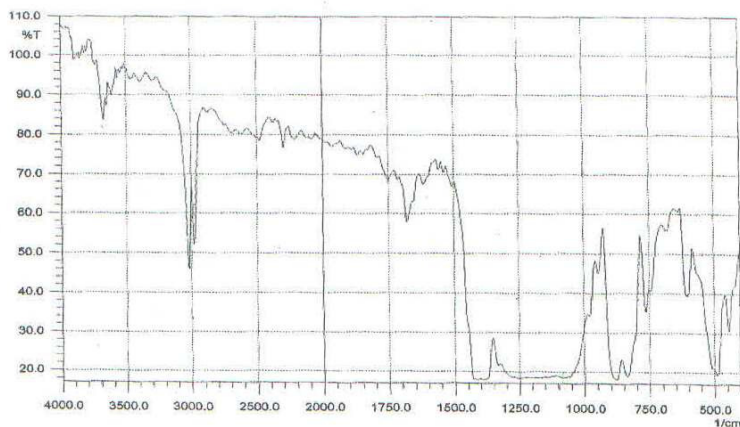


Figure 3(a): FTIR spectrum of virgin PVDF sample

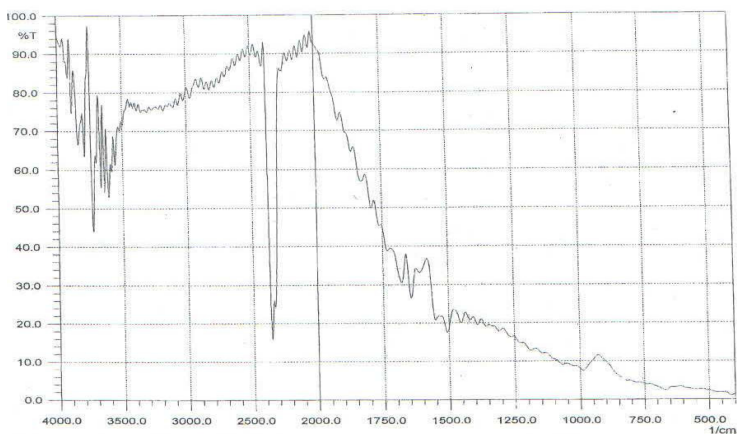


Figure 3(b): FTIR spectrum of hexane treated PVDF sample

Therefore these peaks probably belong to the impurities present in the sample. The impurities could be low molecular weight hydrocarbons, antioxidants and other impurities introduced during the manufacturing process. The exact nature of impurities reached out is uncertain (Umamura *et al.*, 1982; Ronarch and Haridoss, 1981). A shift of  $3019.4 \text{ cm}^{-1}$  peak towards lower wave number is observed after hexane treatment.

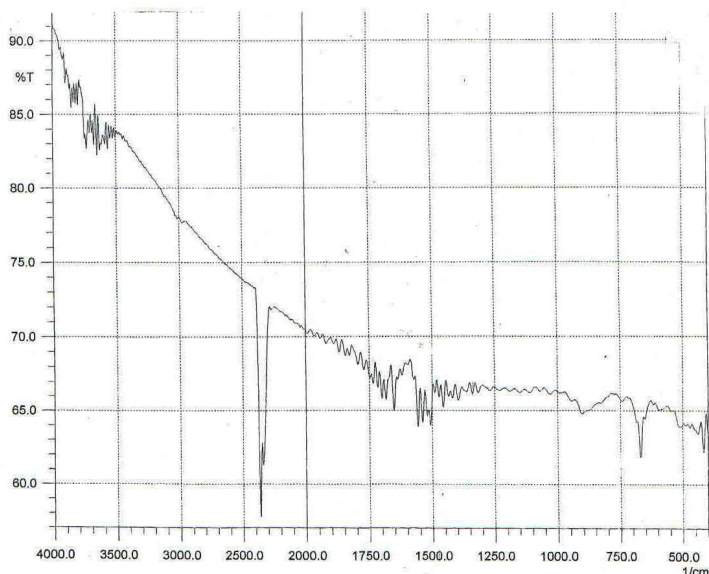


Figure 4: FTIR spectrum of hexane treated and stretched virgin PVDF sample at 45°C and a stretching ratio of 2.5

Figure 4 show FTIR spectrum of hexane treated and stretched PVDF sample at a temperature of 45oC and a stretching ratio of 2.5. Absorption peaks at 3650 and 1653cm<sup>-1</sup> were observed while weak peaks were eliminated. The disappearance of these peaks can be attributed to both hexane treatment and stretching.

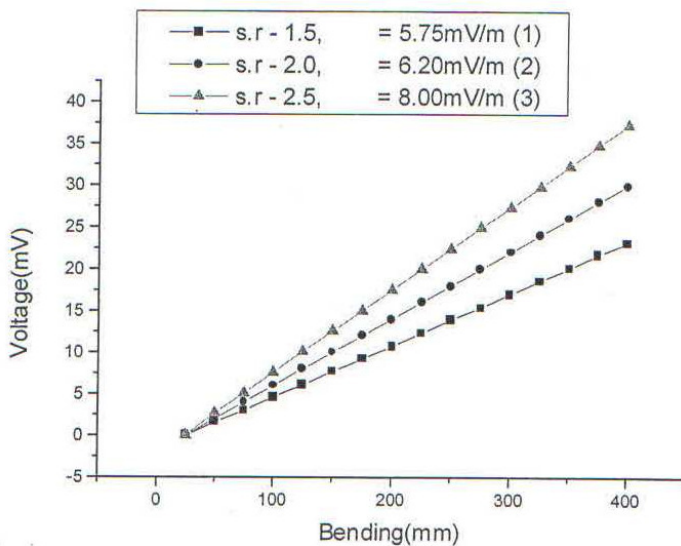


Figure 5: Graph of change in voltage against bending for unpoled stretched PVDF sample at 45°C and stretching ratios 1.5, 2.0 and 2.5

Figure 5 shows a comparison of a change in voltage against bending for a stretched PVDF sample at 45oC with varying stretching ratios of 1.5, 2.0 and 2.5 (plots 1, 2 and 3 respectively). An increase of 2.25 in b31 was observed in plots 1 and 3 respectively.

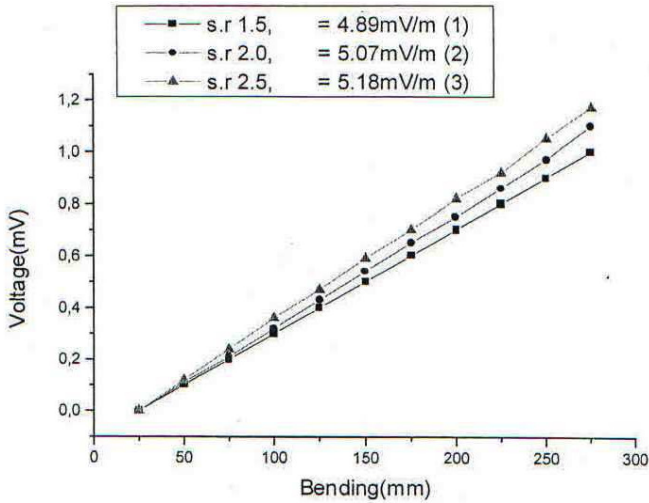


Figure 6: Graph of change in voltage against bending for unpoled stretched PVDF sample at 55°C and stretching ratios 1.5, 2.0 and 2.5

Figure 6 shows a change in voltage against bending for a stretched PVDF sample at a temperature of 55oC and at stretched ratios of 1.5, 2.0 and 2.5 (plots 1, 2 and 3 respectively). The b31 varied from 4.89 mV/m (Plot 1) to 5.18 mV/m (Plot 3).

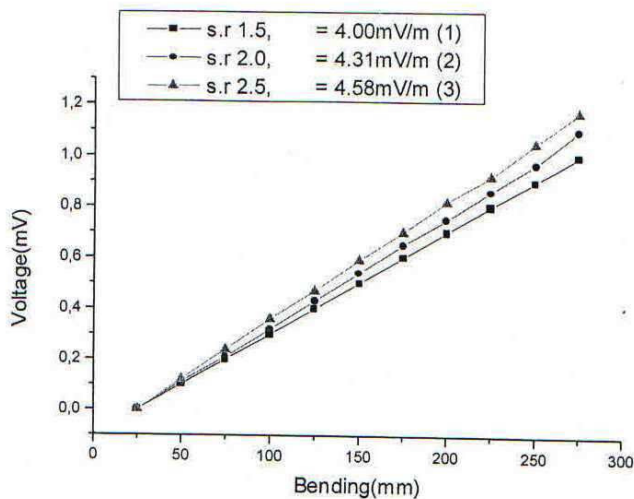


Figure 7: Graph of change in voltage against bending for unpoled stretched PVDF sample at 65°C and stretching ratios 1.5, 2.0 and 2.5



Figure 7 shows a comparison of a change in voltage against bending for a stretched PVDF sample at 65°C with varying stretching ratios of 1.5, 2.0 and 2.5, plots 1, 2 and 3 respectively. The  $b_{31}$  varied from 4.00 mV/m (plot 1) to 4.58 mV/m (plot 3).

### 3.0 Conclusion

Hexane treatment and uniaxial stretching greatly increases the  $b_{31}$  in polyvinylidene fluoride. The elimination of weak peaks and the shift of 3019.4  $\text{cm}^{-1}$  peak towards lower wave number can be attributed to hexane treatment.  $b_{31}$  is optimum at temperature of 45 °C and increases with increase in draw ratios for different temperatures.

### Acknowledgement

One of the authors (C.M. Mutambi) would like to thank Kenya Science Teachers College (KSTC) for a generous scholarship award.

### References

- Foss R. A. and Dannhauser W. (1963) Electrical conduction of polypropylene. *Journal of Applied Polymer Science*, 7, pp. 1015-1021.
- Fukada E., Sessler G. M., West J. M., Berraissoul A. and Günther P. (1987) Bending piezoelectricity in monomorph polymer films, *Journal of Applied Physics*, 62, pp. 3643-3646
- Furukawa T. (1989) Piezoelectricity and pyroelectricity in polymers IEEE transactions on Electrical Insulation, 24, pp. 375-394
- Ibe T. (1974) Bending (or flexural) piezoelectricity. *Japanese Journal of Applied Physics*. 13, 197.
- Kawai H. (1969). The Piezoelectricity of Poly(Vinylidene Fluoride), *Japanese Journal of Applied Physics*, 8, pp. 975-976.
- Kawai H. and Heiji I. (1970) *Oyo Buturi*, 39, 413 in Japanese.
- Kepler R. G. and Anderson R.A. (1978). Ferroelectricity in Polyvinylidene Fluoride, *Japanese Journal of Applied Physics*, 49, pp. 1232-1235.
- Lang S. B. (1989) *Sourcebook of Pyroelectricity* Gordon and Breach Science Publishers London pp. 1-30
- Lang S. B., (1995) *Guide to the literature of piezoelectricity of polymers 1988-1989* *Ferroelectrics* 163 137-377
- Litt M. H., Hsu C. H. and Basu P. (1977) Pyroelectricity and Piezoelectricity in nylon-11 *Journal of Applied Physics* 48 2208-2212

Luongo J. P. (1972) Near infrared spectra of Piezoelectric Polyvinylidene Fluoride. *Journal of Polymer Science*, 10 pp. 1119-1123.

Ronarch D. and Haridoss S. (1981). Depolarization current study of low-density polyethylene containing an Antioxidant. *Journal of Applied Physics*, 52, pp. 5916-5920.

Sessler G. M. (1987) *Electrets*, 2nd enlarged (Ed.). Springer, Berlin

Takamatsu T., Tian R. W and Sasaze H. in proceeding of the 5th International Symposium on electrets, G. M. Sessler and R. Gerhard Mulhaupt (Ed.) IEEE service Centre, Piscataway, NJ 942-946.

Tu, D. M., Wu L. H., Wu X. Z., Cheng C.K. and Kao K.C. (1982). On the Mechanism of Treeing inhibition by additive in polyethylene. *IEEE Electrical Insulation* 17, 539-544.

Umemura T., Suzuki T. and Kashiwazaki T. (1982). Impurity Effect of the Dielectric properties of isotactic polypropylene. *IEEE Transactions on Electrical Insulation* 17 300-305.

Zoon, J.D. and Liu, S.T. (1978) Pyroelectric effects in thin films *Journal of Applied Physics*, 49 4606-4608

**THE EFFECT OF PUMPING WATER FROM WELLS IN AN AQUIFER****K. G. Warui<sup>1</sup>, G.X. Stower<sup>2</sup>, J. K. Sigey<sup>3</sup>**<sup>1</sup>Mombasa Polytechnic University College, Mombasa, Kenya<sup>2</sup>Kenyatta University, Nairobi Kenya<sup>3</sup>Jomo Kenyatta University of Agriculture and Technology, Nairobi Kenya

Email: kennwarui@gmail.com

**Abstract**

Groundwater is sensitive to the climate change and agricultural activities in arid and semi-arid areas. Over the past several decades, human activities, such as groundwater extraction for irrigation, have resulted in aquifer overdraft and disrupted the natural equilibrium in these areas. This study reports research on the effect of pumping water from several wells in a given aquifer. We have considered, for simplicity, an idealized one layer aquifer which has been discretized into 49 identical blocks studied on the middle horizontal row of blocks. We have developed a numerical simulating model by discretizing the equation of continuity which we have converted into computer codes. A program has then been written. This program has successfully generated both hydraulic head and velocity profile distributions. The results reveal that there are less hydraulic head losses on pumpage from blocks which are far apart, the velocities being least in blocks which are far from the pumpage blocks. The results obtained have a high correlation with those from the well-known Theis equation for drawdown. The results would greatly help in limiting the usage of a given aquifer with respect to the maximum number of wells permissible in the aquifer as well as predict the levels of groundwater in a particular aquifer.

**Key words:** Aquifer, piezometric height, velocity profiles and simulation

## 1.0 Introduction

### 1.1 Literature review

Groundwater is often called the forgotten resource. Raudkivi and Callander (1976) define it as all interstitial water below the water table, however deep down it may occur. It lies beneath our feet and supplies wells, bores, springs and flows to our rivers. Groundwater as a source of public water supply has attained considerable importance as a result of its large volume (97%) of occurrence irrespective of climatic conditions. According from The Environment Agency (May, 2012), one third of the water utilized in England, for instance, comes from groundwater. Globally, one third of the world's population is dependent upon groundwater (Evans, 2006). In terms of quality, groundwater is usually low in organic and anthropogeneous pollution except in areas of shallow course aquifers (Ako, 1996).

Groundwater is contained in porous media with substantial quantities found in geologic formations called aquifers. Withdrawal of ground water by pumping is the most significant human activity that alters the amount of groundwater in storage and the rate of discharge from an aquifer. Excessive groundwater level declines have been known to produce serious ecological problems, such as land desertification and soil salinization, displacing inhabitants from their ancestral homeland (Shaoyuan, 2010).

The removal of water stored in geologic materials near the well sets up hydraulic gradients that induce flow from more distant regions of the aquifer. As groundwater storage is depleted within the radius of influence of pumping, water levels in the aquifer decline. The area of water level decline is called the cone of depression, and its size is controlled by the rate and duration of pumping, the storage characteristics of the aquifer, and the ease with which water is transmitted through the geologic materials to the well. The development of a cone of depression can result in an overall decline in water levels of a large geographic area, change the direction of groundwater flow within an aquifer, reduce the amount of base flow to streams, and capture water from a stream or from adjacent aquifers. In areas having a high density of pumped wells, multiple cones of depression can develop within an aquifer (US Geological Survey, 2005). Consequently, it has become extremely important to accurately simulate and predict potential groundwater level changes in these regions so that appropriate water resources management and environmental protection policies can be developed and implemented (Huo *et al.*, 2005).

Due to relative inaccessibility of the aquifers (Napie, 1983), slow pace of subsurface processes and high expenses involved in performing actual ground water experiments, numerical simulation modeling has been found to be one of the most effective techniques of studying ground water flow process (Davis, 1986; Zhao *et al.*, 2005; Matej *et al.*, 2007).

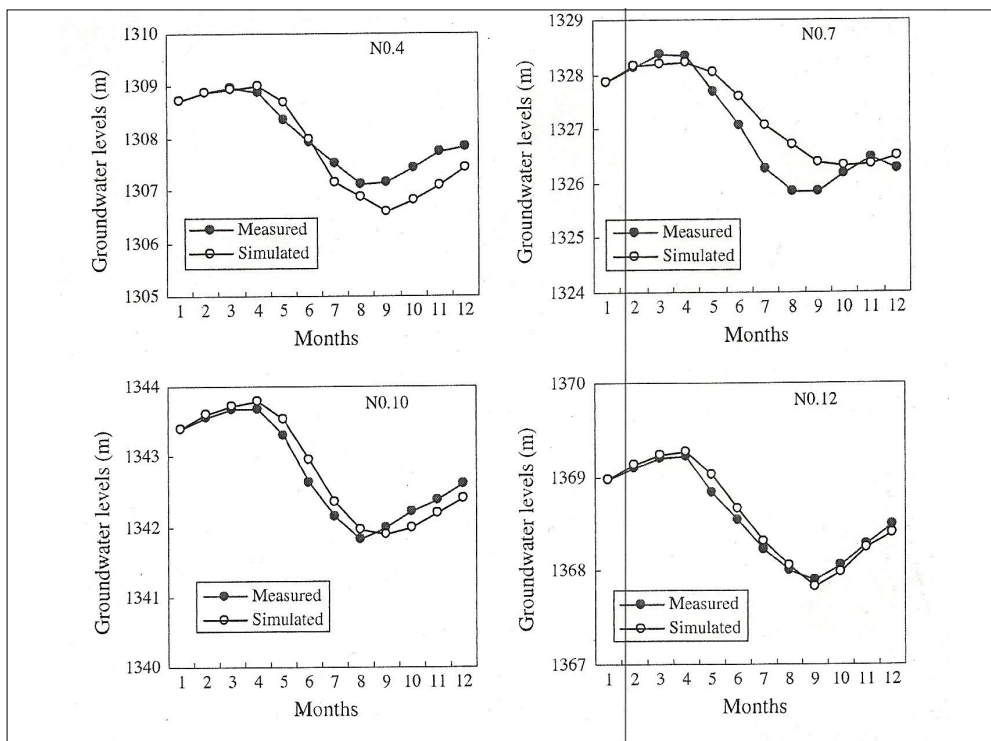


Figure 1: Comparison of simulated and observed groundwater levels for four monitoring wells

Shaoyuan *et al.* (2010) compared simulated and measured groundwater levels from 12 monitoring wells at Minqin oasis in China in 1999. This showed similar groundwater level trends with the hydrogeological situation which indicated that the generalized models of the hydrogeological conditions were reasonable. The models were verified by use of groundwater level data measured in 1999. Figure 1 above shows comparisons between simulated and measured values of groundwater level from four out of 12 monitoring wells in the oasis in 1999. Overall, precision was high for the groundwater with RMSE of 0.71 m, RE of 17.96%, and R2 of 0.84. Overall, the results showed that the trend of changes of simulated groundwater levels basically matched that of the measured values.

Groundwater flow is normally continuous due to hydraulic gradient, pressure gradient or temperature gradient. The flow through the porous medium is governed by the equation of continuity. The velocities in groundwater flow are in general very low; the Reynold's number has generally some value between 1 and 10 for Darcy's law to be valid (Bear, 1988).

The equations governing groundwater flow are partial differential ones (Logan, 1994) whose solutions for non-trivial cases cannot be obtained analytically (Wood, 1993). Fortunately, quite good approximate solutions can be obtained using

computers. In such cases the equations are discretized using methods such as finite differences, finite elements, integrated finite differences, finite volumes and boundary integrals, amongst others. Computer codes can then be developed for the discretized systems of equations and programs written to solve groundwater flow.

In this study, we have developed a model for simulating the effect of pumping out water from several wells in a given idealized aquifer. We have used integrated finite difference method to solve the governing equation. This method is preferred because of the accuracy with which it treats boundaries while maintaining the simplicity differences.

### 1.1 Initial and boundary conditions

Groundwater flow in the aquifer is governed by the boundary conditions of the regional system and the determination of boundary conditions is important for regional groundwater numerical modelling, (Huo *et al.*, 2005). The partial differential elliptic boundary value problem represents the three dimensions in plan aquifer equation for height  $h$  of the water in steady state groundwater flow. This includes second derivatives with reference to the space variables  $x$ ,  $y$ ,  $z$  and it is necessary to have boundary conditions all around the boundary; either known height or known flow. When the groundwater flow is changing with time, the equation representing it becomes parabolic (see equation (2.1)), i.e. it has a first derivative in time and second derivatives in the space coordinates. It is then necessary to have an initial condition as well as boundary conditions all-round the boundary in order to be able to solve our problem represented by the differential equation (2.1) i.e. numerical determination of the hydraulic head distribution within the aquifer as a result of pumping water from some specific points (wells) within the aquifer. The problem is assumed to be well posed, that is the governing equation is formulated so that there is a unique solution and small changes in data make small changes in this solution.

Wood (1993) remarks that to have suitable boundaries, it is often necessary to model a larger area. For this reason we have chosen our model to be an idealized aquifer in form of a rectangular block measuring 3.5 km square with a depth of 10 metres. For the sake of simplicity all the four edges are taken as non-flow boundaries assumed to be bounded by impervious walls. There is therefore no flow into or out of the (confined) aquifer though it must be born in mind that there is actually groundwater movement within the aquifer itself. This is because as stated earlier groundwater is in a continuous flow.

Initially the rate of inflow within the aquifer equals the rate of outflow so that the net velocity is zero. For this reason, initial piezometric height within the aquifer is uniform. In particular the boundary conditions at the four edges are such that the piezometric height is 5 metres. Thus, since in the governing equation, the hydraulic

head,  $h$  is a function of the space coordinates (all restricted to a finite region) and the time  $t$  (unrestricted), we could write  $h(x, y, 0) = 5$  and then proceed to work out  $h(x, y, t)$  subject to  $0 \leq x \leq 3500$ ,  $0 \leq y \leq 3500$ ,  $0 \leq z \leq 10$ ,  $t > 0$ ,  $K > 0$ , the linear measurements being in meters.

The number of blocks, along an edge is chosen odd (in our case 7) in order to have a central block (no.25) through which we can have symmetry either across the aquifer or along its diagonals.

## 2.0 Materials and methods

### 2.1 The governing equation

The governing equation for groundwater flow is the parabolic differential equation in three dimensions given by

$$\nabla^2 h = \frac{S_0}{K} \frac{\partial h}{\partial t} \quad (2.1)$$

$$= \frac{S}{bK} \frac{\partial h}{\partial t} \quad (2.2)$$

$$= \frac{S}{T} \frac{\partial h}{\partial t}, \quad T = bK \quad (2.3)$$

or 
$$T\nabla^2 h = S \frac{\partial h}{\partial t} + Q, \quad Q = \text{net external flow} \quad (2.4)$$

The quantity  $Q$  (Dimensions  $LT^{-1}$ ) represents sinks and sources, or the algebraic sum of extraction flows (pumpage) and replenishment flows (including precipitation, excess irrigation, imported water, stream percolation and artificial recharge).

### 2.2 Discretization of the governing equation

Discretization of a differential equation refers to the process of converting it to discrete components that can be implemented using computer codes (Rice, 1993). This process is necessary for developing a numerical model based on any numerical computing technique. The integrated finite difference method is used to explicitly solve the governing equation. Assuming that the principal components of the hydraulic conductivity, transmissivity and dispersion tensors were aligned in the directions of the Cartesian grid axes, we express equations (2.1) and (2.4) as

$$K_{ij} \frac{\partial^2 h}{\partial x_{ij}^2} = S_0 \frac{\partial h}{\partial t} + Q \quad (2.5)$$

Integrating equation (2.5) over the whole volume since the properties are averaged for each block volume, we obtain:

$$\iiint K_{ij} \frac{\partial^2 h}{\partial x_{ij}^2} dV = \iiint S_0 \frac{\partial h}{\partial t} dV + Q_v \quad (2.6)$$

where  $Q_v$  is summation over volume. However, since we are summing up effects of interaction between block faces, we need to sum over block surfaces instead of block volume. This conversion is done by applying the Gauss divergence theorem to the equation (2.6) above, while assuming that interaction is normal to the block faces. This procedure gives

$$\sum K_{ij} \frac{(h_j^n - h_i^n)}{\Delta x_{ij}} \Delta S_{ij} = V S_0 \left( \frac{h_i^{n+1} - h_i^n}{\Delta t} \right) + Q_v \quad (2.7)$$

where  $V$  is the volume of the block under consideration. The subscript  $i$  refers to the current block,  $1 \leq i \leq 49$  while  $j$  refers to the immediate neighbouring blocks and varies from 1 to 4 depending on the number of block neighbours.  $n$  refers to the current time step while  $n+1$  refers to the next time step. Equation (2.7) can further be rearranged as

$$h_i^{n+1} = h_i^n + \frac{\Delta t}{V S_0} \sum K_{ij} \left( \frac{h_j^n - h_i^n}{\Delta x_{ij}} \right) \Delta S_{ij} - \frac{\Delta t}{V S_0} Q_v \quad (2.8)$$

where  $h_i^{n+1}$  is the hydraulic head we are computing. It is this equation which we have converted into computer codes.

### 2.3 Design of the aquifer

We have considered a model of a confined aquifer of one layer. For the purposes of mathematical calculations of storage and flow of groundwater, we have assumed the aquifer to be homogeneous (hydrologic properties are everywhere identical) and isotropic (hydrologic properties are independent of direction). Moreover, since our aquifer is an idealized one (Lee *et al.*, 1992), we shall take it to be a rectangular block of depth  $b$ . This implies its boundaries are straight. For total independence, the side faces are impervious such that there is no inflow into or outflow from the aquifer. The aquifer is subdivided into 49 identical blocks as illustrated in figure 2 below. Each block measures 500m by 500m by 10m.



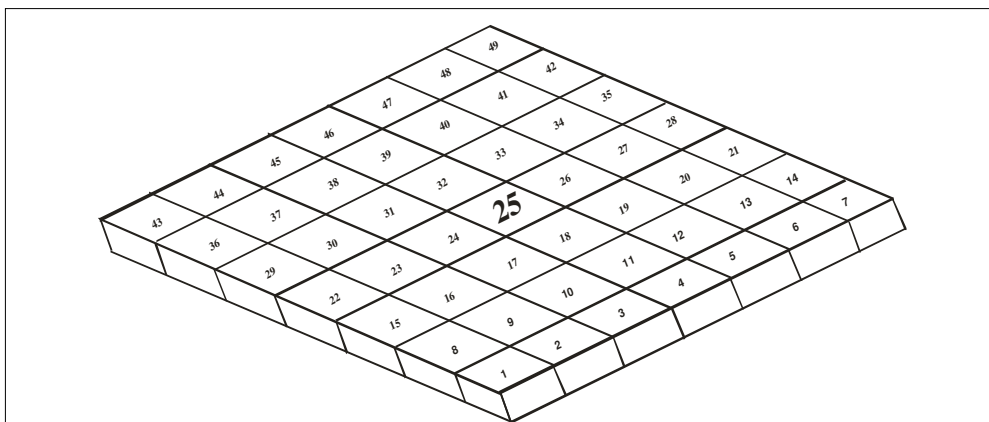


Figure 2.1: Isometric view of an idealized aquifer

The objective of the work is to investigate the variation of the piezometric heights and velocity profiles as time progresses during the pumping process. We have used a time interval of 1.5 days. For the sake of ease in comparison we have considered the wells, drilled in any of the 49 blocks, to be of the same size and the pumping rate to be the same. We have started pumping from the middle block, which is block number 25 (BN25), after which the piezometric heads and velocity profiles in any of the other blocks (BN25 inclusive) can be investigated. Next we pump from the following sets of blocks: {23, 27, 18, 32} and {1, 7, 43, 49}.

### 3.0 Results and discussion

The results of hydraulic heads with respect to time of withdrawal at a constant rate on the two sets of blocks, namely, BN25, BN23, BN27, BN32, BN18 and BN1, BN7, BN43, BN49 are represented in the graphs in figures 3.1a, 3.2a and 3.3a. Now since drawing 49 graphs for each experiment on the same set of axes would lead to too many crowded up graphs on a single page, we have chosen in each case to study the effect of the hydraulic heads and velocity profiles in the middle row only containing block numbers 22, 23, 24, 25, 26, 27 and 28. Thus for each figure there appear seven graphs. Their graphs are found in figures 3.1b, 3.2b and 3.3b respectively.

#### 3.1 Withdrawal on block number 25

In figure 2a, the graphs for the following pairs overlap; 22 and 28, 23 and 27, and 24 and 26. As would be expected, this is due to symmetry with respect to the axis of symmetry passing through block number 25 (BN25). For example (BN22) and (BN28) are three blocks away each from the central block number, (BN25). Consequently, the head loss in BN25 falls drastically to about 3.9 m at the 50<sup>th</sup> day. This is due to the fact that we are pumping directly

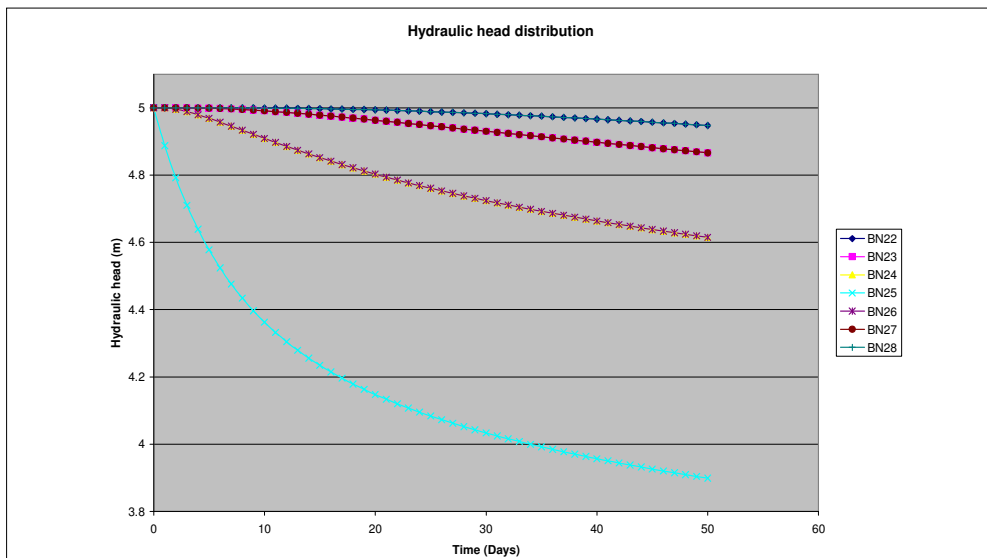


Figure 3.1a: Hydraulic head distribution for withdrawal at a constant rate on block number

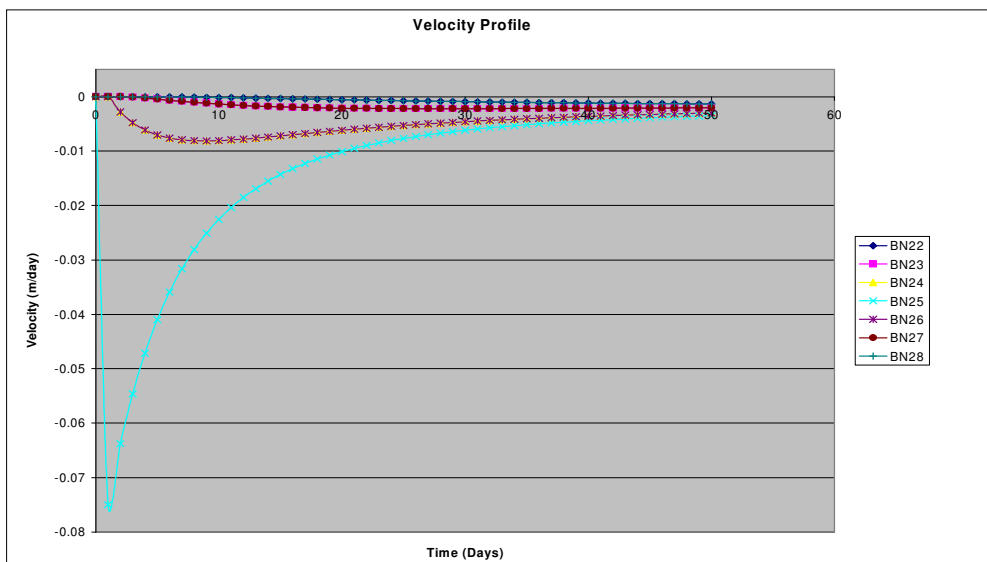


Figure 3.1b: Velocity profiles for withdrawal at constant rate on block number 25

from this block. The velocity for this block drops sharply to approximately -0.075 meters per day as water has to flow faster towards the well due to the great velocity gradient created by the pumpage here. By this reasoning the changes in the hydraulic heads for BN22 and BN28 are least as the blocks are very far from BN25. Similar reasoning explains why the head loss in BN24 and BN26 is more than in BN23 and BN27. As pumping continues the water velocities within the aquifer tend to vanish since the water flow acquires a state of dynamic equilibrium. That is

why the velocity profiles tend to zero after only 50 days. The head loss is greatest in BN23 and BN27 as these are the sources. BN22 and BN28 are affected more than BN24 and BN26 in spite of the two pairs being equidistant from the sources. This is because these two

blocks are bounded on one side by an impervious wall and as such cannot enjoy any replenishment from these walls. On the contrary, BN24 and BN26 can both draw water from BN25, BN32 and BN18, whose equivalence lacks for BN22 and BN28. That is why these pairs of graphs are quite close together. BN25, being farthest from the source, is least affected and for this reason its graph slopes least.

### 3.2 Withdrawal on block numbers 23, 27, 32 and 18

BN23 and BN27 suffer the greatest head losses. This is because; besides being sources they are closest to the impervious boundaries of the aquifer. BN25 is next affected as it is greatly affected by withdrawal on the directly adjacent blocks 18 and 32 apart from being affected, also, by withdrawal on BN23 and BN27 through BN24 and BN26 respectively. BN24 and BN26 are next affected because though directly adjacent to the sources (BN23 and BN27), they are diagonally adjacent to BN18 and BN32. BN22 and BN28 are the least affected because though adjacent to BN23 and BN27 respectively, BN18 and BN32 are too far for their effects to be felt here. Within the first few hours the water velocities towards the wells in BN23 and BN27 are very high (about 0.075 m per day), with their profiles identical with the velocity

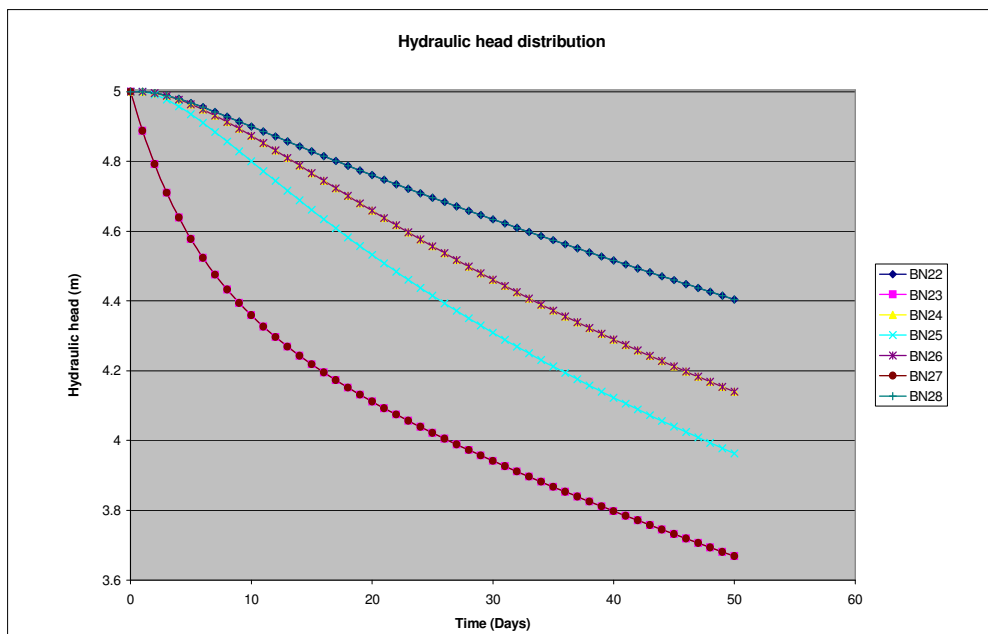


Figure 3.2a: Hydraulic head distribution for withdrawal at a constant rate on block numbers 23, 27, 32 and 18

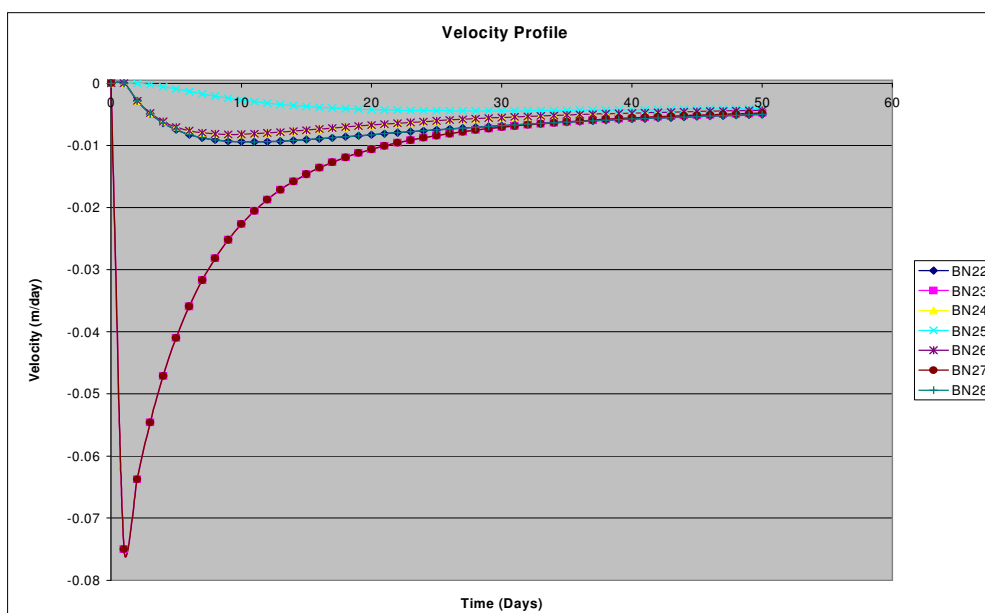


Figure 3.2b: Velocity profiles for withdrawal at a constant rate on block numbers 23, 27, 32 and 18

profile for BN25 in our previous experiment where we were simulating pumpage from BN25 itself. This is because there is pumpage from these two blocks. The velocities in BN25 follow next as water moves to replenish the wells in the directly adjacent blocks 18 and 32. BN22 and BN28 have the least velocity losses due to the fact that apart from being bounded by impervious walls, the water movement is essentially towards BN23 and BN27 only.

#### Withdrawal on corner blocks

BN25, being the farthest from the withdrawal blocks suffers the least hydraulic loss of only 0.004m at the 50th day. By symmetry, BN24 & BN26 follow next, followed by BN23 & BN27. The pair of blocks suffering the greatest head loss is BN22 and BN28 whose piezometric heights stand at only 4.82m at the end of the 50th day. This is because BN22 is closest to withdrawal blocks BN1 and BN43, the same way BN28 is closest to BN7 and BN49.

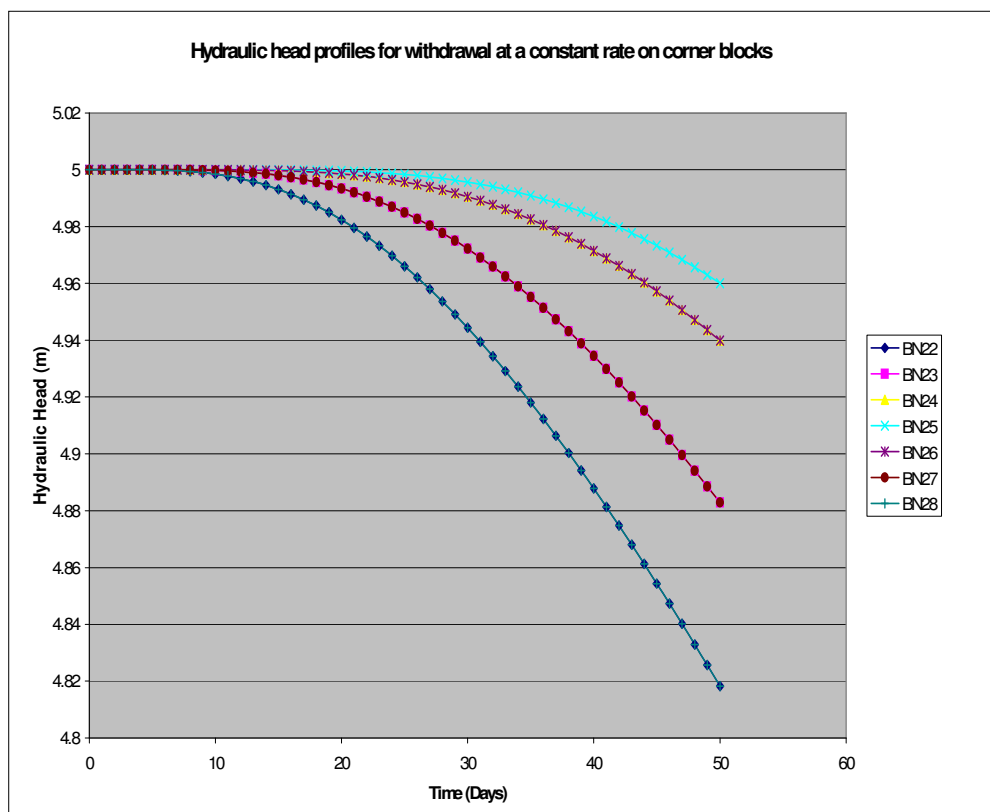


Figure 3.3a: Hydraulic head distribution for withdrawal at a constant rate on block numbers 1,7,43

Incidentally, the head losses in this withdrawal are least compared to the losses in all other experiments as far as the withdrawal effect in the middle row of blocks 22,23,24,25,26,27 and 28 is concerned.

The velocity is least in BN25 due to its great distance from the corner blocks. As would be expected, BN24 and BN26 follow next, followed by BN23 and BN27, the greatest velocities soaring to as high as 0.005m/day being in BN22 & BN28, as these are the closest to the pairs of the corner blocks 1, 43 and 7, 49 respectively.

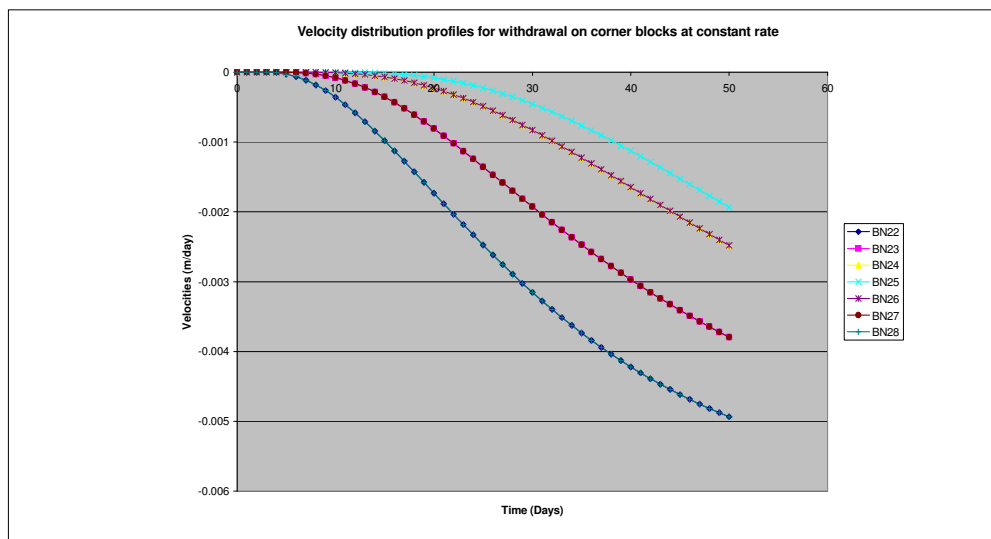


Figure 3.3b: Velocity profiles for withdrawal at a constant rate on block numbers 1, 7, 43 & 49

#### 4.0 Conclusion

The foregoing results do, however, confirm that the discretized governing equation has successfully generated both hydraulic head and velocity profile distributions. These distributions obtained from the model reveal that there is symmetry in the three sets of withdrawal wells. However, in situations lacking symmetry it would be extremely difficult to accurately predict the results. The results in the few selected cases reveal that the more the number of wells of withdrawal, the greater the loss in the hydraulic heads. For instance, withdrawal from corner blocks leads to the least hydraulic head losses on the middle horizontal row as compared to the rest of the withdrawal blocks. This implies that in practice, the wells ought to be drilled being as far apart as is practically possible, subject to their radii of inference.

Ideally, we would have gone ahead to compare the simulated results with actually measured groundwater levels from an actual discretized aquifer. However, as mentioned there earlier, the cost required would be colossal. However the observations discussions done should suffice to validate the results from this model. These results would guide the aquifer users (through the relevant government institutions) on the number of wells that should be drilled in a given aquifer and at what locations within it. This would be done by limiting the usage of the aquifer to a particular acceptable piezometric level. The model can also be used to simulate the effect of agricultural activities on groundwater levels.

**References**

- Ako B., and Osundu, V. (1986). Electrical resistivity survey of the Kerri-Kerri Formation, Darazo, Nigeria. *Journal of African Earth Services*, **5**, pp.527–534.
- Bear J. (1988). *Dynamics of Fluids in Porous Media*. New York: Courier Dover Publications.
- Davis G. D. (1987). *Numerical Methods in Engineering & Science*. London : Chapman and Hall.
- Evans R., Evans R., Jolly P., Barnet S., Hatton T., Merrick N., (2006, November 9). National Groundwater Reform,. <http://www.ncgm.uts.edu.au/media> .
- Huo Z., Feng S., Kang S., Mao X., and Wang F. (2011). Numerically modelling groundwater in an arid area with ANN-generated dynamic boundary conditions. *Hydrological Processes*, **25** (5), 705-713.
- Lee R., Ketelle R., Rizk J., and Rizk T. (1992, July-August). Aquifer Analysis and Modeling in Fractured Heterogeneous Medium. *National Groundwater Association*, **30** (4), pp. 589-597.
- Logan, T. D. (1994). *An Introduction to Linear Partial Differential Equations*. New York: John Wiley & Sons.
- Matej, G., Wemaere, I., & Jan, M. (2007). Regional groundwater model of North-East Belgium. *Journal of Hydrology*, **335** (1-2), pp. 133–139.
- Napier T. L., Scott D., Easter K. W., and Supalla R. (Eds.). (1983). Water resources research. Problems and potentials for agriculture and rural communities. 1983 pp. xii + 247pp. *Problems and Potential for Agriculture and Rural Communities*, 247.
- Raudkivi R. A., and Callander A. J. (1976). , *Analysis of Groundwater Flow*. London: Edward Arnold.
- Rice J. R. ( 1993). *Numerical Methods: Software and Analysis*. San Diego : Academic Press, Inc.
- Shaoyuan F., Huo Z., and Kang S. (2010, May 5). Groundwater simulation using a numerical model under different water resources management scenarios in an arid region of China. *Environ Earth Sci* .
- The Environment Agency | enquiries@environment-agency.gov.uk. (2012, May 22). Groundwater Protection Policy and Practice. *Environment Agency* .
- Wood, W. (1993). *Introduction to Numerical Methods for Water Resources*. New York: Oxford University Press.
- Zhao C., Wan Y., Xi C., and B. G., L. (2005). Simulation of the effects of groundwater level on vegetation change by combining FEFLOW software. *Ecological Modelling*, pp.341–351.

**PARAMETRIC CHANGE POINT ESTIMATION, TESTING AND CONFIDENCE INTERVAL  
APPLIED IN BUSINESS**

**A. W. Gichuhi<sup>1</sup>, J. Franke<sup>2</sup> and J. M. Kihoro<sup>1</sup>**

<sup>1</sup>*Jomo Kenyatta University of Agriculture and Technology*

<sup>2</sup>*University of Kaiserslautern, Kaiserslautern, Germany*

*Email: agwaititu@yahoo.com*

**Abstract**

In many applications like finance, industry and medicine, it is important to consider that the model parameters may undergo changes at unknown moment in time. This paper deals with estimation, testing and confidence interval of a change point for a univariate variable which is assumed to be normally distributed. To detect a possible change point, we use a Schwarz Information Criterion (SIC) statistic whose asymptotic distribution under the null hypothesis is determined. The percentile bootstrap method is used to construct the confidence interval of the estimated change point. The developed tools and methods are applied to the 1987 – 1988 US trade deficit data. Our results show that a significant change in US trade deficit occurred in November 1987. Further, it is shown that the percentile bootstrap confidence intervals are not always symmetrical.

**Key words:** Change point, Schwarz information criterion, percentile bootstrap



## 1.0 Introduction

In many applications of statistics such as the financial, industrial and medical fields, it is important to consider that the model parameters may undergo changes at an unknown moment of time. The time moment when the model has changed is called the change point. Other synonyms are probabilistic diagnostics and disorder problems.

The change point problem is twofold: Change point detection and change point estimation. Depending on whether the probabilistic model of data is known or not, one can distinguish between parametric, semi-parametric and non-parametric methods of change point detection and estimation. Worsley (1983) used the likelihood ratio method to test for a change in probability of a sequence of independent binomial variables.

Non-parametric detection of a change point in a sequence of random variables was studied by many authors. Page (1955) used the cumulative sum technique to test for a possible change point. Worsley (1983) used the cumulative sum statistics to test for a change in probability of a sequence of independent binomial random variables.

Page's CUSUM and Shewhart's control chart are some of the popular procedures used when both the pre-change distribution  $f_0$  and post-change distribution  $f_1$  are completely specified. Yashchin (1997) uses the likelihood ratio strategy. However, in line with statistical quality control, standard procedures assume that the pre-change distribution  $f_0$  is known but the post-change distribution  $f_1$  is unknown and therefore has to be estimated. Such a study has been done in Siegmund and Venkatraman (1995).

The maximum likelihood estimate (MLE) method has been used to estimate a change point when the probabilistic data model is known. Hinkley (1970) applied the MLE method to estimate a change point in a sequence of normally distributed random variables whereby he derived the asymptotic distribution of the estimator using random walk theory. Hinkley and Hinkley (1970) used the MLE method to estimate the change point in a sequence of zero-one variables.

Pettitt (1980) used a Mann-Whitney statistic to estimate a change point when it is known that a change has taken place at an unknown point in a sequence of random variables. In this work, the estimate is compared with MLE using Monte Carlo techniques and is found to be fairly constant over various distributions like normal distribution.

As indicated above, parametric test statistics for a change point are based on the likelihood ratio statistic and the estimation done using maximum likelihood method. More general results can be found in Csörgö, M., and Horvath, L.(1997).

This paper uses the theory of Schwarz Information Criterion (SIC) to detect and estimate a change point for a given sequence of normally distributed random variables.

**2.0 Change Point Model Formulation**

We assume that one is able to observe a sequence of independent normal observations whose distribution possibly changes from  $N(\mu_b, \sigma_b)$  to  $N(\mu_a, \sigma_a)$  at an unknown point in time,  $K$ .

That is

$$X = \begin{cases} X_i \sim N(\mu_b, \sigma_b) & , i = 1, 2, \dots, K \\ X_i \sim N(\mu_a, \sigma_a) & , i = K + 1, K + 2, \dots, n \end{cases}$$

**2.1 Hypotheses**

In this paper, the hypothesis of stability is defined as

$$H_0 : \mu_1 = \mu_2 = \dots = \mu_n = \mu \text{ and } \sigma_1^2 = \sigma_2^2 = \dots = \sigma_n^2 = \sigma^2 \dots \dots \dots (1)$$

The alternative hypothesis is defined as

$$H_1 : \mu_1 = \dots = \mu_K = \mu_b \neq \mu_{K+1} = \dots = \mu_n = \mu_a \text{ and } \sigma_1^2 = \dots = \sigma_K^2 = \sigma_b^2 \neq \sigma_{K+1}^2 = \dots = \sigma_n^2 = \sigma_a^2 \dots \dots \dots (2)$$

Under  $H_0$ , the mle's for  $\mu$  and  $\sigma^2$  are, respectively,

$$\hat{\mu} = \bar{x} = \frac{1}{n} \sum_{i=1}^n x_i \text{ and } \hat{\sigma}^2 = \frac{1}{n} \sum_{i=1}^n (x_i - \bar{x})^2 \dots \dots \dots (3)$$

and under  $H_1$ , the mle's for  $\mu$  and  $\sigma^2$  are, respectively,

$$\begin{aligned} \hat{\mu}_b = \bar{x}_b = \frac{1}{K} \sum_{i=1}^K x_i & \text{ and } \hat{\sigma}_a^2 = \frac{1}{K} \sum_{i=1}^K (x_i - \bar{x}_b)^2 \\ \hat{\mu}_a = \bar{x}_a = \frac{1}{n-K} \sum_{i=K+1}^n x_i & \text{ and } \hat{\sigma}_a^2 = \frac{1}{n-K} \sum_{i=K+1}^n (x_i - \bar{x}_a)^2 \end{aligned}$$

**2.2 Schwarz Information Criteria for the Change Point Inference**

The Schwarz Information Criterion (SIC) was proposed by (Schwarz, 1978) and it is expressed as

$$SIC(m) = -2 \log L(\hat{\Theta}_m) + m \log n, \quad m = 1, 2, \dots, M \dots \dots \dots (4)$$

Where  $m$  is the number of free parameters,  $L(\hat{\Theta}_m)$  is the maximum likelihood function for model( $m$ ) and  $m \log n$  is the penalty term

Using equation (4), the SIC under  $H_0$  has 2 free parameters and it is clearly defined as

$$SIC(n) = n \log 2\pi + n \log \hat{\sigma}^2 + n + 2 \log n \dots \dots \dots (5)$$

where  $\hat{\sigma}^2 = \frac{1}{n} \sum_{i=1}^n (x_i - \bar{x})^2$  is the mle of  $\sigma^2$  under  $H_0$ .

Similarly, using equation (4), the  $SIC$  under  $H_1$  has 4 free parameters and it is defined as

$$SIC(K) = n \log 2\pi + K \log \hat{\sigma}_b^2 + (n - K) \log \hat{\sigma}_a^2 + n + 4 \log n \dots\dots\dots (6)$$

for  $2 \leq K \leq n - 2$

where  $\hat{\sigma}_b^2 = \frac{1}{K} \sum_{i=1}^K (x_i - \bar{x}_b)^2$  and  $\bar{x}_b = \frac{1}{K} \sum_{i=1}^K x_i$  are the mle's of the variance and the mean, respectively, before the change point and

$\hat{\sigma}_a^2 = \frac{1}{n - K} \sum_{i=K+1}^n (x_i - \bar{x}_a)^2$  and  $\bar{x}_a = \frac{1}{n - K} \sum_{i=K+1}^n x_i$  are the mle's of the variance and the mean, respectively, after the change point.

**2.3 Change Point Estimation**

As in Chen and Gupta (2000), we estimate the change point  $K$  by  $\hat{K}$  such that

$$SIC(\hat{K}) = \min_{2 \leq K \leq n-2} SIC(K) \dots\dots\dots (7)$$

**2.4 Change Point Testing**

If  $K$  is not fixed and is unknown, we follow the approach of Chen and Gupta (2000) and fail to reject  $H_0$  iff

$$\Lambda_K = \min_{2 \leq K \leq n-2} (SIC(K) ) + R_n(\alpha) - SIC(n) \dots\dots\dots (8)$$

is positive where  $R_n(\alpha)$  is the critical value associated with the sample size  $n$  and significance level  $\alpha$ .

**2.4.1 Critical Values for SIC,  $R_n(\alpha)$**

Let  $\Delta_{n,K} = \min_{2 \leq K \leq n-K} \{SIC(K) - SIC(n)\} \dots\dots\dots (9)$

Then,

$$\begin{aligned} \Delta_{n,K} &= - \max_{2 \leq K \leq n-K} \{SIC(K) - SIC(n)\} \\ &= - \max_{2 \leq K \leq n-K} (K \log \hat{\sigma}_b^2 + (n - K) \log \hat{\sigma}_a^2 - n \log \hat{\sigma}^2 + 2 \log n) \dots\dots\dots(10) \\ &= -\eta_{n,K}^2 + 2 \log n \end{aligned}$$

$$\text{where } \eta_{n,K} = \left( \max_{2 \leq K \leq n-K} (K \log \hat{\sigma}_b^2 + (n-K) \log \hat{\sigma}_a^2 - n \log \hat{\sigma}^2) \right)^{\frac{1}{2}} \dots\dots\dots(11)$$

From equation (10), one has

$$\eta_{n,K} = \left( 2 \log n - \Delta_{n,K} \right)^{\frac{1}{2}} \dots\dots\dots(12)$$

**Theorem 1** Under  $H_0$ , for all  $x \in \mathbb{R}$ , we have for

$$\lim_{n \rightarrow \infty} P(a(\log n)\eta_{n,K} \leq x + b \log n) = \exp(-2 \exp(-x)) \dots\dots\dots (13)$$

Where  $a(\log n) = (2 \log \log n)^{\frac{1}{2}}$  and  $b(\log n) = 2 \log \log n + \log \log \log n$   
 This result follows immediately from Theorem (2.1) of Gombay and Horvath (1996) and Theorem (2.27) of Chen and Gupta (2000).

Using equation (8) to determine the critical values,  $R_n(\alpha)$ , we note that under theorem (1),

$$\begin{aligned} 1-\alpha &= P(SIC(n) < \min_{2 \leq K \leq n-2} SIC(K) + R_n(\alpha) | H_0) \\ &= P(-\max_{2 \leq K \leq n-2} \{SIC(n) - SIC(K)\} > -R_n(\alpha) | H_0) \\ &= P(\Delta_n > -R_n(\alpha) | H_0) \\ &= P(-\eta_{n,K}^2 + 2 \log n > -R_n(\alpha) | H_0) \\ &= P(0 < \eta_{n,K} < (R_n(\alpha) + 2 \log n)^{0.5} | H_0) \\ &= P(-b(\log n) < a(\log n)\eta_{n,K} - b(\log n) < a(\log n) (R_n(\alpha) + 2 \log n)^{0.5} - b(\log n) | H_0) \\ &\cong \exp\{-2 \exp(b(\log n) - a(\log n) (R_n(\alpha) + 2 \log n)^{0.5})\} - \exp\{-2 \exp(b(\log n))\} \end{aligned} \dots\dots\dots (14)$$

This then implies that

$$\exp\{-2 \exp(b(\log n) - a(\log n) (R_n(\alpha) + 2 \log n)^{0.5})\} \cong 1 - \alpha + \exp\{-2 \exp(b(\log n))\}$$

So that

$$R_n(\alpha) \cong \left[ -\frac{1}{a(\log n)} \log \log \{1 - \alpha + \exp(-2 \exp(b(\log n)))\}^{-0.5} + \frac{b(\log n)}{a(\log n)} \right]^2 - 2 \log n \dots\dots\dots (15)$$

We computed  $R_n(\alpha)$  for  $\alpha = 0.10, 0.05, 0.025, 0.01$  under various sample sizes. The critical values are presented in table 1 below.

Table 1: Asymptotic critical values from equation (15), denoted as  $R_n(\alpha)$ 

n	$\alpha$	$R_n(\alpha)$			
		0.10	0.05	0.025	0.010
7.		7.757992	12.909378	19.63085	35.69935
8.		7.404845	11.925257	17.23230	25.97584
9.		7.262061	11.540438	16.42328	23.94784
10.		7.168499	11.312834	15.99423	23.07060
11.		7.087391	11.138584	15.69148	22.52369
12.		7.010367	10.988932	15.44547	22.10831
13.		6.935751	10.854445	15.23288	21.76289
14.		6.863355	10.731205	15.04386	21.46347
15.		6.793235	10.617091	14.87308	21.19818
16.		6.725433	10.510699	14.71714	20.95987
17.		6.659935	10.410984	14.57361	20.74363
18.		6.596686	10.317120	14.44062	20.54582
19.		6.535604	10.228435	14.31671	20.36366
20.		6.476595	10.144368	14.20073	20.19494
21.		6.419556	10.064448	14.09171	20.03788
22.		6.364386	9.988275	13.98886	19.89103
23.		6.310986	9.915503	13.89152	19.75319
24.		6.259258	9.845834	13.79911	19.62336
25.		6.209112	9.779008	13.71117	19.50068
26.		6.160461	9.714797	13.62728	19.38444
27.		6.113227	9.652998	13.54708	19.27401
28.		6.067332	9.593433	13.47026	19.16885
29.		6.022706	9.535943	13.39655	19.06850
30.		5.979285	9.480385	13.32569	18.97255
40.		5.599685	9.007971	12.736662	18.19266
50.		5.293224	8.639973	12.291699	17.62215
60.		5.036173	8.338068	11.933873	17.17331
70.		4.814683	8.081879	11.634525	16.80384
80.		4.620012	7.859242	11.377170	16.49016
90.		4.446292	7.662302	11.151446	16.21778
100.		4.289397	7.485684	10.950411	15.97721
110.		4.146315	7.325548	10.769185	15.76186
120.		4.014778	7.179053	10.604207	15.56699
130.		3.893040	7.044036	10.452798	15.38910
140.		3.779721	6.918813	10.312891	15.22548
150.		3.673718	6.802049	10.182861	15.07403
160.		3.574131	6.692662	10.061401	14.93309
170.		3.480216	6.589768	9.947450	14.80131

180.	3.391355	6.492633	9.840132	14.67758
190.	3.307024	6.400641	9.738717	14.56097
200.	3.226777	6.313270	9.642588	14.45073

### 3.0 Confidence Interval for the Change Point

Various methods for determining change point confidence intervals exist in literature. One method involves the asymptotic distribution of  $\hat{K} - K$ , where  $K$  is the true change point and  $\hat{K}$  is its estimate. See, for example, Hinkley and Hinkley (1970) and Feder (1975).

Another approximation method involves the use of bootstrap methods. See for instance Hall (1992), Efon and Tibishirani (1993), Davison and Hinkley (1997) and Pastor-Barriuso *et al* (2003).

In this paper, we use the Percentile Bootstrap method to determine the confidence interval for the true change point  $K$ .

### 3.1 Percentile Bootstrap Confidence Interval for the Time of Change

We approximate the distribution of  $\hat{K} - K$  using the percentile bootstrap technique as follows:

1. Given the original sample  $X_i, i = 1, 2, \dots, n$ , estimate the change point  $\hat{K}_n$  and hence the MLEs  $\bar{x}_b, \hat{\sigma}_b, \bar{x}_a, \hat{\sigma}_a$
2. Generate a bootstrap sample  $X_i^*$  such that
 
$$X_i^* = N(1, \bar{x}_{bi}, \hat{\sigma}_{bi})|_{i \leq \hat{K}_n} + N(1, \bar{x}_{ai}, \hat{\sigma}_{ai})|_{i \geq \hat{K}_n + 1}$$

Where  $N(f, g, h)$  is a normal variable of size  $f$ , mean  $g$  and standard deviation  $h$ .

3. Using the bootstrap sample  $\{X_i^*\}_{i=1}^n$ , replicate the estimated time of change,  $\hat{K}_n^*$ .
4. Repeat steps 2 and 3  $B$  times. This step yields  $B$  independent bootstrap samples

$\{X_i^{*1}\}_{i=1}^n, \dots, \{X_i^{*B}\}_{i=1}^n$  from which we get  $\hat{K}_n^{*1}, \dots, \hat{K}_n^{*B}$  bootstrap change points.

From these replicates, we are then able to estimate the distribution function of  $\hat{K}_n^* - \hat{K}_n$  where  $\hat{K}_n^*$  is the time of change estimate of the re-samples.

**Proof**

Suppose that  $K_{\alpha/2}^*$  and  $K_{1-\alpha/2}^*$  are the quartiles of  $K_n^*$  such that

$$P(K_n^* \leq K_{\alpha/2}^*) = P(K_n^* > K_{1-\alpha/2}^*) = \alpha/2 \dots\dots\dots(16)$$

One then has

$$P(K_{\alpha/2}^* \leq K_n^* \leq K_{1-\alpha/2}^*) = 1 - \alpha \dots\dots\dots (17)$$

Equation (16) implies that

$$P(K_{\alpha/2}^* - \hat{K}_n \leq K_n^* - \hat{K}_n \leq K_{1-\alpha/2}^* - \hat{K}_n) = 1 - \alpha \dots\dots\dots (18)$$

Assuming that we can approximate the quartiles of  $\hat{K}_n - K$  by the quartiles of  $K_n^* - \hat{K}_n$ , we have

$$P(K_{\alpha/2}^* - \hat{K}_n \leq \hat{K}_n - K \leq K_{1-\alpha/2}^* - \hat{K}_n) \approx 1 - \alpha \dots\dots\dots (19)$$

So that

$$P(\hat{K}_n - (K_{1-\alpha/2}^* - \hat{K}_n) \leq K \leq \hat{K}_n - (K_{\alpha/2}^* - \hat{K}_n)) \approx 1 - \alpha \dots\dots\dots (20)$$

As noted in Efon and Tibshirani (1993), transforming equation (20) can give better a confidence interval. We therefore transform the random variable  $\hat{K}_n$  using a symmetrical function say,  $t(\cdot)$ , denote as:

$$\hat{\omega}_n = t(\hat{K}_n) \dots\dots\dots (21)$$

Using equations (20) and (21), one has

$$P(\hat{\omega}_n - (\omega_{1-\alpha/2}^* - \hat{\omega}_n) \leq \omega \leq \hat{\omega}_n - (\omega_{\alpha/2}^* - \hat{\omega}_n)) \approx 1 - \alpha \dots\dots\dots(22)$$

Due to symmetry,  $(\omega_{1-\alpha/2}^* - \hat{\omega}_n) = -(\omega_{\alpha/2}^* - \hat{\omega}_n)$  so that equation (22) can be written as

$$P(\hat{\omega}_n + (\omega_{\alpha/2}^* - \hat{\omega}_n) \leq \omega \leq \hat{\omega}_n + (\omega_{1-\alpha/2}^* - \hat{\omega}_n)) \approx 1 - \alpha \dots\dots\dots (23)$$

So that

$$P(\omega_{\alpha/2}^* \leq \omega \leq \omega_{1-\alpha/2}^*) \approx 1 - \alpha \dots\dots\dots (24)$$

Transforming equation (24) back to the original scale gives

$$P(K_{\alpha/2}^* \leq K \leq K_{1-\alpha/2}^*) \approx 1 - \alpha \dots\dots\dots (25)$$

That is

$$P(K_{n,((B+1)\alpha/2)}^* \leq K \leq K_{n,((B+1)(1-\alpha/2))}^*) \approx 1 - \alpha \dots\dots\dots (26)$$

Therefore, the  $\alpha$  – percentile bootstrap confidence interval is given by:

$$\left( K_{n,((B+1)\alpha/2)}^*, K_{n,((B+1)(1-\alpha/2))}^* \right) \dots\dots\dots (27)$$

**4.0 Empirical Results**

**4.1 The Data**

Table (2) shows US trade deficit data from 1987 to 1988 in billions of dollars. The data is from Wheeler (1993).

Table 2: US Trade Deficits 1987-1988 (\$ billions)

Year	Jan	Feb	Mar	Apr	May	Jun	Jul	Aug	Sep	Oct	Nov	Dec
1987	10.7	13.0	11.4	11.5	12.5	14.1	14.8	14.1	12.6	16.0	11.7	10.6
1988	10.0	11.4	7.9	9.5	8.0	11.8	10.5	11.2	9.2	10.1	10.4	10.5

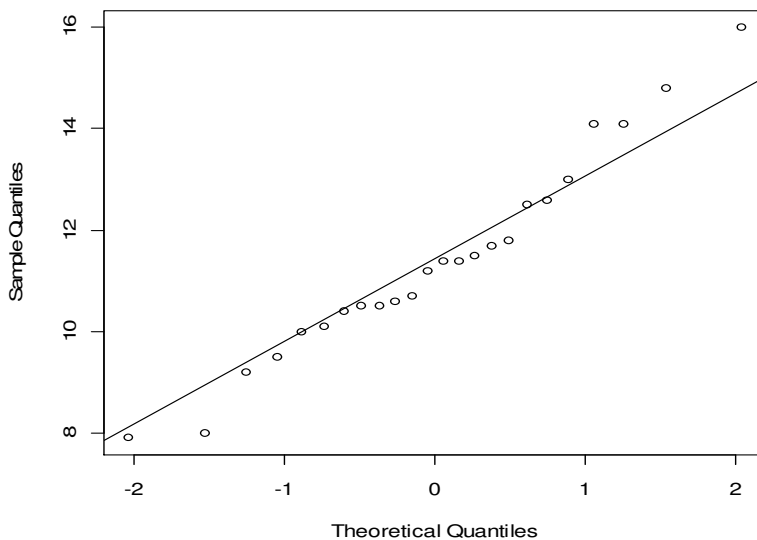


Figure 1: Normal Q-Q plot for the data in table 2

From figure 1, the US Trade Deficits from 1987-1988 were approximately normal in distribution.

**4.2 Change Point Detection**

Using equation (6), the  $SIC(K)$  for  $2 \leq K \leq n - 2$  was computed and the results presented in figure 2. Using equation (7), the change point was detected at  $\hat{K} = 11$ . This implies that a change of deficits was detected to have occurred in November 1987.



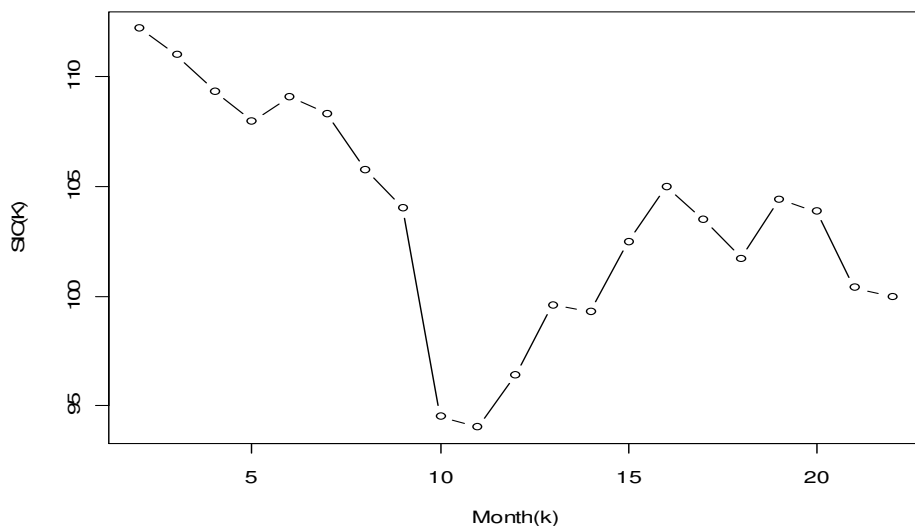


Figure 2: Change point detection for the US 1987-1988 trade deficits

This finding agrees with that of Taylor(2000) who analyzed the same data using a different change point tool and detected the change point to have occurred in November 1987.

**4.2 Change Point Testing**

Under section (2.4), equation (8), table 1 and figure 2, the following values were computed:

Table 3:  $\min_{2 \leq K \leq 22} \{SIC(K), R_{24}(\alpha) \text{ and } SIC(24)\}$  for the 1987-1988 US Trade Deficits

$\min_{2 \leq K \leq 22} \{SIC(K)\}$	$R_{24}(\alpha)$				$SIC(24)$
	0.1	0.05	0.025	0.01	
94.02100	6.25926	9.84583	13.79911	19.62336	106.8370

From table 3 and using equation (8), we reject  $H_0$  (equation(1)) at  $\alpha = 0.05$ . We therefore confirm that a change in mean and variance did actually occur in November 1987 at 5% significance level.

**4.3 Confidence Interval for the Change Point**

Figure 3 shows the bootstrap change points computed in line with section 3.1. 10,000 bootstraps for the change point were computed.

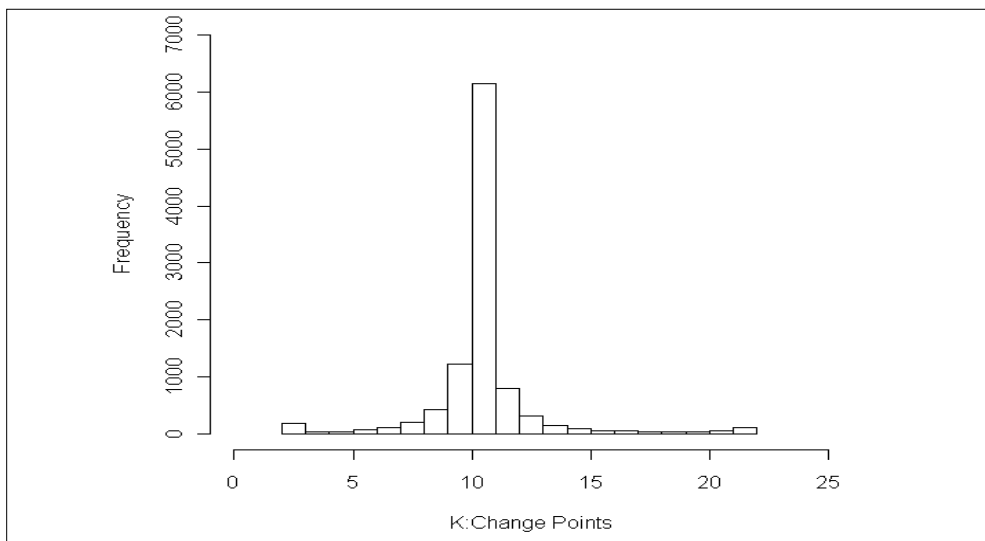


Figure 3: Histogram of bootstrap change points

Table 4: Confidence Interval results for  $B = 10000$  bootstrap replications of the change point  $\hat{K}_{24} = 11$  for the 1987-1988 US Trade Deficits

$\hat{K}_{24} = 11$	
Confidence Level	Confidence Interval
90%	8 - 14
95%	6 - 17

Our results indicate that the percentile bootstrap confidence intervals for the change point are not always symmetrical. These results are supported by Cook and Weisberg (1990).

### 5.0 Conclusion

In this paper, we have used the SIC criterion to detect a possible change point. This method has been applied to the 1987-1988 US Trade Deficits data and the results agreed with those of other authors. A table of critical values was computed for reference purposes.

The authors of this paper considered the case where only one change point was assumed to have occurred. More research should be done to model the case where two or more change points are assumed to have occurred.

**References**

- Chen J. and Gupta A. K. (2000) *Parametric Change Point Analysis*, Birkhäuser, Boston
- Cobb G. W. (1978). The problem of the Nile: conditional solution to a change point problem. *Biometrika*, **65(2)**, pp. 243-251.
- Cook R. D. and Weisberg S. (1990). Confidence curves in nonlinear regression. *J. Amer. Statist. Assoc.* **85(410)**, pp. 544 - 551.
- Csörgö, M. and Horvath, L.(1997) *Limit Theorems in Change-Point Analysis*.Wiley, New York.
- Davison A. C. and Hinkley D. V. (1997) *Bootstrap methods and their application*, 1 of Cambridge Series in Statistical and Probabilistic Mathematics. Cambridge University Press, Cambridge.
- Efron, B. and Tibshirani, R. J. (1993) *An introduction to the bootstrap*, 57 of Monographs on Statistics and Applied Probability. Chapman and Hall.
- Feder P. I. (1975). The log likelihood ratio in segmented regression. *Annals of Statistics*, **3**, pp. 84 – 97.
- Gombay E. and Horvath L. (1996). On the rate of approximations for maximum likelihood tests in change-point models. *J. Multivariate Anal.* **56(1)**, pp. 120 - 152.
- Hall P. (1992). *The bootstrap and Edgeworth expansion*. Springer Series in Statistics. Springer-Verlag, New York.
- Hinkley D. V. (1970). Inference about the change-point in a sequence of random variables. *Biometrika*, **57**, pp. 1 - 17.
- Hinkley D. V. and Hinkley E. A. (1970). Inference about the changepoint in a sequence of binomial variables. *Biometrika*, **57** , pp. 477 - 488.
- Page E. S. (1955). A test for a change in a parameter occurring at an unknown point. *Biometrika*, **42**, pp. 523 - 527.
- Pastor-Barriuso R. Guallar E. and Coresh J. (2003). Transition models for change-point estimation in logistic regression. *Statist. Med.*, **22** , pp. 1141 - 1162.
- Pettitt A. N. (1980). A simple cumulative sum type statistic for the changepoint problem with zero-one observations. *Biometrika*, **67(1)**, pp. 79 - 84.
- Schwarz G. (1978). Estimating the dimension of a model. *Annals of Statistics*, **6**, pp. 461 - 464.

Siegmund D. and Venkatraman E. S. (1995). Using the generalized likelihood ratio statistic for sequential detection of a change-point. *Annals of Statistics*, **23(1)**, pp. 255 - 271.

Taylor Wayne A. (2000), Change Point Analysis: A Powerful New Tool For Detecting Changes, WEB: <http://www.variation.com/cpa/tech/changepoint.html>.

Wheeler D. (1993). *Understanding Variation – The Key to Managing Chaos*, SPC Press, Knoxville, Tennessee.

Worsley K. J (1983). The power of likelihood ratio and cumulative sum tests for a change in a binomial probability. *Biometrika*, **70(2)**, pp. 455 - 464.

Yashchin, E.(1997) . Change-point models in industrial applications. In Proceedings of the Second World Congress of Nonlinear Analysts, Part 7 **30**, pp. 3997- 4006.

**A COMPARISON OF SPATIAL RAINFALL ESTIMATION TECHNIQUES: A CASE STUDY  
OF NYANDO RIVER BASIN KENYA**

***\*Re-published***

***F. Mutua and D. Kuria***

*Jomo Kenyatta University of Agriculture and Technology*

*E-mail: felix.mutua@gmail.com*

**Abstract**

Many hydrological models for watershed management and planning require rainfall as an input in a continuous format. This study analyzed four different rainfall interpolation techniques in Nyando river basin, Kenya. Interpolation was done for a period of 30 days using 19 rainfall stations. Two geostatistical interpolation techniques (kriging and cokriging) were evaluated against inverse distance weighted (IDW) and global polynomial interpolation (GPI). Of the four spatial interpolators, kriging and cokriging produced results with the least root mean square error (RMSE). A digital elevation model (DEM) was introduced into the cokriging method and this improved the results considerably. The results demonstrate that for low-resolution rain gauge networks, geostatistical interpolation methods perform better than other techniques that ignore spatial dependence patterns. The use of secondary information improved the prediction results, as demonstrated by the inclusion of the DEM in this study.

**Key words:** DEM, GPI, IDW, kriging, rainfall

## **1.0 Introduction**

Watershed models are powerful tools for water resources planning and management. Models may be used to predict how conditions are expected to change over time, to understand the nature and scope of a problem and to evaluate alternative management options. Precipitation is the primary input to hydrological models and is characterized by spatial variations. This is brought about by differences in the type and scale of development of precipitation producing processes, and strongly influenced by local or regional factors, such as topography and wind direction at the time of precipitation (Sumner, 1998). Rainfall data is traditionally presented as point data. However, hydrological modelling requires spatial representation of rainfall and thus the gauge measurements need to be transformed into areal coverages.

Several methodologies exist for spatial interpolation of climate and weather parameters. These include; inverse distance weighting (Englund and Weber, 1994), Thiessen polygon method, isohyetal method, and more sophisticated statistical methods such as kriging, and its various extensions, also known as geostatistical methods (Symeonakis, 2008). Recent advances in the fields of geographic information systems (GIS) and remote sensing have made satellite-based rainfall estimates readily available in coverage forms. However, the scales, temporal and spatial resolutions are usually coarse for application at a basin scale.

Several attempts have been made to compare these methods with most of the studies suggesting that geostatistical methods provide the most accurate estimates. Goovaerts (2000) used geostatistical algorithms to include elevation into the interpolation procedure at the South of Portugal. Johansson and Chen (2003) developed a regression model that included the wind variable for Sweden. Marquínez et al. (2003) used a regression model performed with topographic variables for Cantabria (Spain). Vicente-Serrano et al. (2003) concluded that the best results were achieved by geostatistical methods and a regression model formed by four geographic variables for the Ebro Valley (Spain). Subyani (2004) used geostatistical methods in the study of annual and seasonal rainfall patterns in south west Arabia; whilst Eulogio (1998) used geostatistical methods in estimating areal climatological rainfall mean using data and precipitation in southern Spain.

Majority of these studies focused on interpolating precipitation for small to regional scale applications emphasizing the need for similar research over larger areas to support the respective work on hydrological processes, such as surface runoff and soil erosion (Symeonakis, 2008). This study attempts to evaluate four geostatistical interpolation techniques and compare their performance in generating spatial distributions of rainfall in Nyando river basin. Section 2) provides a brief discussion of spatial interpolation methods, section 3) discusses methods, data, and tools while results are presented in section 4.

**2.0 Interpolation methods**

**2.1 Inverse Distance Weighting (IDW)**

Inverse Distance Weighting (IDW) is an interpolation technique in which interpolated estimates are made based on values at nearby locations, weighted only by distance from the interpolation location. IDW explicitly implements the assumption that things that are close to one another are more alike than those that are farther apart. In the IDW approach, the values to be interpolated  $Z_{IDW}^*$  are estimated as a linear combination of several surrounding observations, with the weights being inversely proportional to the distance between observations and location  $u$  to the power of  $p$ .

$$Z_{IDW}^*(u) = \frac{\sum_{\alpha=1}^{n(u)} \lambda_{\alpha}(u) Z(u_{\alpha})}{\sum_{\alpha=1}^{n(u)} \lambda_{\alpha}(u)}, \text{ with } \lambda_{\alpha}(u) = \frac{1}{|u - u_{\alpha}|^p} \dots\dots\dots(1)$$

Where  $n(u)$  is the number of the points at location  $u$  considered for the estimation and  $\lambda_{\alpha}(u)$  is the weight.

**2.2 Global polynomial interpolation (GPI)**

Global Polynomial interpolation (GPI) is a quick and smooth deterministic interpolator. A first-order global polynomial (GP) fits a single plane through the data; a second-order fits a surface with a bend in it, allowing the calculation of surfaces representing valleys; a third-order allows for 2 bends; and so forth. However, when a surface has a different shape, as in a landscape that slopes, levels out, and then slopes again, a single GP will not fit well (Johnston et al., 2001).

**2.3 Kriging**

Kriging is a moderately quick interpolator that can be exact or smoothed depending on the measurement error model. Kriging uses statistical models that allow a variety of map outputs including predictions, standard errors and probability. Kriging assigns weights according to a (moderately) data-driven weighting function, rather than an arbitrary function, but it is still an interpolation algorithm and will give very similar results to others in many cases (Isaaks and Srivastava, 1992). Kriging estimators are variants of the basic linear regression estimator:

$$Z^*(u) - m(u) = \sum_{\alpha=1}^{n(u)} \lambda_{\alpha}(u) [Z(u_{\alpha}) - m(u_{\alpha})] \dots\dots\dots(2)$$

Where  $n(u)$  is the number of the points at location  $u$  and  $\lambda_{\alpha}(u)$  is the weight assigned to the datum  $z(u_{\alpha})$  interpreted as a realization of the random variable  $Z(u_{\alpha})$ . The values  $m(u)$  and  $m(u_{\alpha})$  are the expected values of the random variables  $Z(u)$  and  $Z(u_{\alpha})$  respectively.

Kriging estimators are required to be unbiased and to minimize error variance, i.e.  $\sigma_E^2(u) = \text{Var}\{Z^*(u) - Z(u)\}$  under the constraint that the expected error is zero:  $E\{Z^*(u) - Z(u)\} = 0$ . Each random function is usually decomposed into a residual component and a trend component:  $Z(u) = R(u) + m(u)$ . The residual component is modeled as a stationary random function with zero mean and covariance function.

$$C_R(h) : E\{R(u)\} = 0$$

$$\text{cov}\{R(u), R(u+h)\} = E\{R(u).R(u+h)\} = C_R(h)$$

The expected value of the random variables  $Z$  at a certain location  $u$  is the value of the trend component at that location  $E\{Z(u)\} = m(u)$ . Three Kriging variants can be distinguished according to the model considered for the trend: Simple, ordinary and universal. Simple kriging (SK) considers the mean  $m(u)$  to be known and constant through the study area. The SK estimator is expressed mathematically by equation 3.

$$Z_{SK}^*(u) = \sum_{\alpha=1}^{n(u)} \lambda_{\alpha}^{SK}(u) Z(u_{\alpha}) + \lambda_m^{SK}(u) m, \text{ with } \lambda_{\alpha}^{SK}(u) = 1 - \sum_{\alpha=1}^{n(u)} \lambda_{\alpha}^{SK}(u) \tag{3}$$

The SK weights are determined such as to minimize the error variance, while ensuring the unbiasedness of the estimator. More detailed discussion on kriging methods can be found in Goovaerts (2000).

**2.4 Cokriging**

The addition of cross-related information reduces the variance of estimation error by using the cokriging method. In this case, the primary data  $\{z_1(u_{\alpha_1}), \alpha_1 = 1, 2, \dots, n_1\}$  is supplemented by secondary data related to  $(N_v - 1)$  continuous attributes  $Z_i, \{z_i(u_{\alpha_i}), \alpha_i = 1, 2, \dots, n_i, i = 2, \dots, N_v\}$  at  $N$  possible different locations. The linear kriging estimator (equation 2) is extended to incorporate such additional information.

$$Z_1^*(u) - m_1(u) = \sum_{\alpha_1=1}^{n_1(u)} \lambda_{\alpha_1}(u) [z_1(u_{\alpha_1}) - m_1(u_{\alpha_1})] + \sum_{i=2}^{N_v} \sum_{\alpha_i=1}^{n_i(u)} \lambda_{\alpha_i}(u) [z_i(u_{\alpha_i}) - m_i(u_{\alpha_i})] \tag{4}$$



Where  $\lambda_{\alpha_i}(u)$  is the weight assigned to the primary datum  $z_1(u_{\alpha_i})$  and  $\lambda_{\beta_i}(u)$ ,  $i > 1$  is the weight assigned to the secondary datum  $z_i(u_{\beta_i})$ . The terms  $m_1(u_{\alpha_i})$  and  $m_i(u_{\beta_i})$  are the expected values for the random variables  $z_1(u_{\alpha_i})$  and  $z_i(u_{\beta_i})$  respectively.

Cokriging estimators are required to be unbiased and to minimize error variance  $\sigma_E^2(u) = \text{Var}\{z_1^*(u) - z_1(u)\}$  under the constraint that the expected error is zero:  $E\{z_1^*(u) - z_1(u)\} = 0$ . Each random function can be written as the sum of a residual component plus a trend component:  $Z_i(u) = R_i(u) + m_i(u), i = 1, \dots, N_v$ .

The residual component is modeled as a stationary random function with zero mean and covariance function  $C_i^R(h) : E\{R_i(u)\} = 0$  and  $\text{cov}\{R_i(u), R_i(u+h)\} = E\{R_i(u) \cdot R_i(u+h)\} = C_i^R(h)$ . The cross variance is given by  $C_{ij}^R(h) = \text{cov}\{R_i(u), R_j(u+h)\}$ . According to the trend model  $m_i(u)$ , three cokriging models can be distinguished: Simple, ordinary and universal. The Simple cokriging (SCK) method considers each local mean, known and constant within the study area. The SCK estimator is expressed mathematically by equation 5.

$$\sum_{j=1}^{N_v} \sum_{\beta_j=1}^{n_j(u)} \lambda_{\beta_j}^{sck}(u) C_{ij}(u_{\alpha_i} - u_{\beta_j}) = C_{i1}(u_{\alpha_i} - u), \dots, \alpha_i = 1, \dots, n_i(u), i = 1, \dots, N_v \dots [5]$$

### 3.0 Materials and methods

#### 3.1 Study area

Nyando basin (Figure 1) is located on the western region of Kenya and is a part of the greater Lake Victoria Basin. It's geographically located along the equator bounded by latitudes  $0^{\circ}7'N$  and  $0^{\circ}24'S$ ; longitudes  $34^{\circ}25'E$  and  $35^{\circ}43'E$ . It covers an area of about  $3500 \text{ km}^2$ .

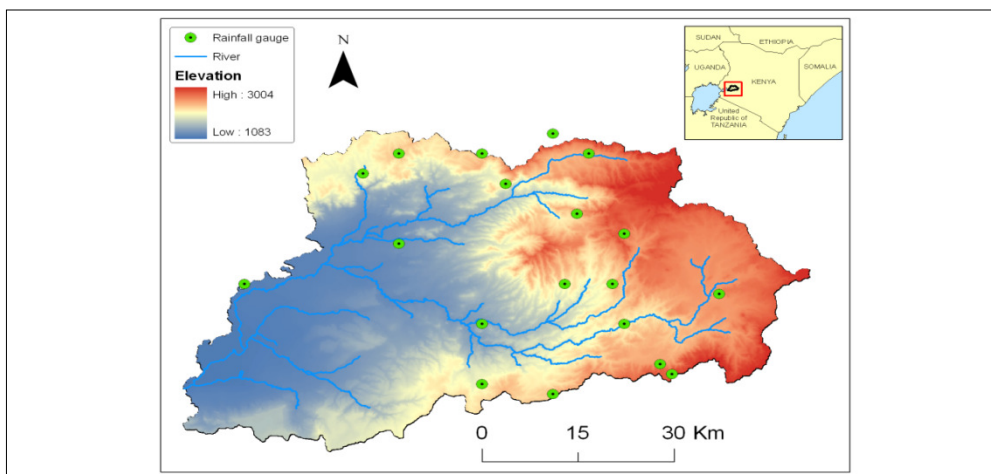


Figure 1: Study Area

Rainfall in the region is mainly influenced by the migration of the Inter tropical Convergence zone (ITCZ) and exhibits a bi-modal pattern with peaks in the long rains season March-April-May (MAM) and short rains October-November-December (OND). The mean annual rainfall varies from 1,000 mm near Lake Victoria to approximately 1,600 mm in the highlands. Land use and property rights vary across the basin. The upper part of the basin is comprised of gazetted forests, commercial tea production, and small-scale agriculture on steep hillsides that were de-gazetted as forests during the last 40 years. Mid-altitude land uses are composed of a mixture of smallholder farms (with maize, beans and some coffee, bananas, sweet potatoes and dairy activities) and large-scale commercial farms (mostly sugar cane).

### 3.2 Data

Table 1 shows a summary of the datasets used in this study

Table 1: Datasets

Dataset	Type	Source	Specifications
Rainfall data	Rain gauge data, tabular	Kenya Meteorological Department	Primary data(mm/day)
DEM	Elevation(Raster)	USGS	Secondary data (90 m resolution)
Nyando Basin boundary	GIS File (shapefile)	Department of Biomechanical and Engineering Department (BEED), Jomo Kenyatta University of Agriculture Technology (JKUAT)	Secondary data (Shapefile)

Others: Roads, river network, boundaries	GIS files(Shapefile)	Department of Geomatic Engineering and Geospatial Information Systems (GEGIS), Jomo Kenyatta University of Agriculture Technology	Auxiliary data (Shapefile)
---	----------------------	---	-------------------------------

Data preparation and analysis was carried out using Ms Office Excel® and ArcGIS 9.3®. ArcGIS 9.3 provided the GIS platform for visualization, manipulation of data production of maps. The ArcGIS Geostatistical Analyst® tool was used for interpolation, production of maps and error plots. The tool provides advanced statistical tools for surface generation, analysis and mapping of continuous datasets. It includes exploratory spatial data analysis tools providing insights about data distribution, global and local outliers, global trends, levels of spatial autocorrelation, and variation among multiple datasets (ESRI, 2007).

Rainfall data was obtained from the Kenya meteorological department. There are 25 rainfall stations near the Nyando river basin and only 19 stations are within the basin. This data was characterized by gaps (~40%) and a period of 30 days was chosen partly because of this challenge.

Table 2: Rainfall Stations in Nyando Basin

Station ID	Station Name (stn)	Latitude (N/S)	Longitude (E)	Year Opened	Height (M)
9035002	Londiani Forest Station	-0.150	35.600	1908	2316
9035020	Kipkelion Railway Station	-0.200	35.467	1904	1931
9035042	Equator Barguat Estate	-0.017	35.400	1932	2012
9035068	Kipkelion Morau Company Ltd.	-0.133	35.450	1938	1920
9035075	Kaisugu House, Kericho	-0.317	35.367	1939	2134
9035102	S.Kalya's Farm, Kedowa	-0.267	35.517	1946	2286
9035148	Koru Bible School	-0.200	35.267	1960	1707
9035150	Tinderet Estate	-0.133	35.383	1959	2134
9035199	Ainamoi Chiefs Camp, Kericho	-0.300	35.267	1960	1981
9035240	Keresoi Forest Station, Londiani	-0.283	35.533	1961	2682

9035256	Maragat Forest Station	-0.050	35.467	1965	2134
8935001	Kabagendui Kibet Farm	0.033	35.300	1920	1890
8935013	Nandi,Koisagat Tea Estate	0.083	35.267	1921	2073
8935033	Nandi Hills, Savani Estate	0.050	35.100	1929	1829
8935148	Kipkurere Forest Station	0.083	35.417	1959	2256
8935159	Cerengoni Forest Station	0.117	35.367	1964	2438
8935161	Nandi Hills,Kibweri Tea Estate	0.083	35.150	1958	2103
9035046	Chemelil Plantation	-0.067	35.150	1932	1229

The 30 days were selected randomly across the years considering days when rainfall was recorded at all the stations. This eliminated the skewedness that would be introduced by stations with no rainfall.

### 3.3 IDW and GPI interpolation

In these two methods, few decisions were made with regards to interpolation parameters. In both cases, the power  $p$  (equation 1) for the weighting function was varied whilst for IDW; the neighborhood search was also specified. Some tests were made and three different models for each interpolation procedure chosen as below:

IDW with  $p=1$  ; GPI with  $p=1$

IDW with  $p=2$  ; GPI with  $p=2$

IDW with  $p=3$  ; GPI with  $p=3$

### 3.4 Kriging and cokriging interpolation

Kriging methods involve many decisions and specification of several parameters. The flow of activities is summarized below:

#### 3.4.1 Model fitting

Kriging, like most interpolation techniques, is built on the basis that things that are close to one another are more alike than those farther away (quantified here as spatial autocorrelation). The empirical semivariogram is a means to explore this relationship. Pairs that are close in distance should have a smaller difference than those farther away from one another. The extent that this assumption is true can be examined in the empirical semivariogram. Empirical Semivariograms were computed for each of the 30 days. Depending on the shape of the variograms,

appropriate models were selected. Fitting a model was done by defining a line that provided the best fit through the points.

### **3.4.2 Neighborhood search**

Kriging equations are defined by matrices and vectors that depend on the spatial autocorrelation among the measured sample locations and prediction location. The autocorrelation values come from the semivariogram model. The matrices and vectors determine the kriging weights that are assigned to each measured value in the neighborhood search. All stations were included in the neighborhood search for interpolation at any point in the basin.

### **3.4.3 Making a prediction**

From the kriging weights and the measured values, predictions were computed for locations with unknown values. Maps were produced and cross validation parameters used to assess the accuracy of the predicted values.

### **3.5 Interpolator evaluation**

For IDW and GPI, only two measures were possible i.e. Mean and RMSE. For the kriging methods, additional measures were used and a brief discussion of these is provided below:

Standardized mean (MS): is a measure of biasness, the mean prediction error should be near zero.

Prediction error = measured – predicted

Root-mean-squared prediction error(RMSE)

Average standard error (ASE): measure of variability in the predictions. If ASE >RMSE, then the system is overestimating variability and vice versa

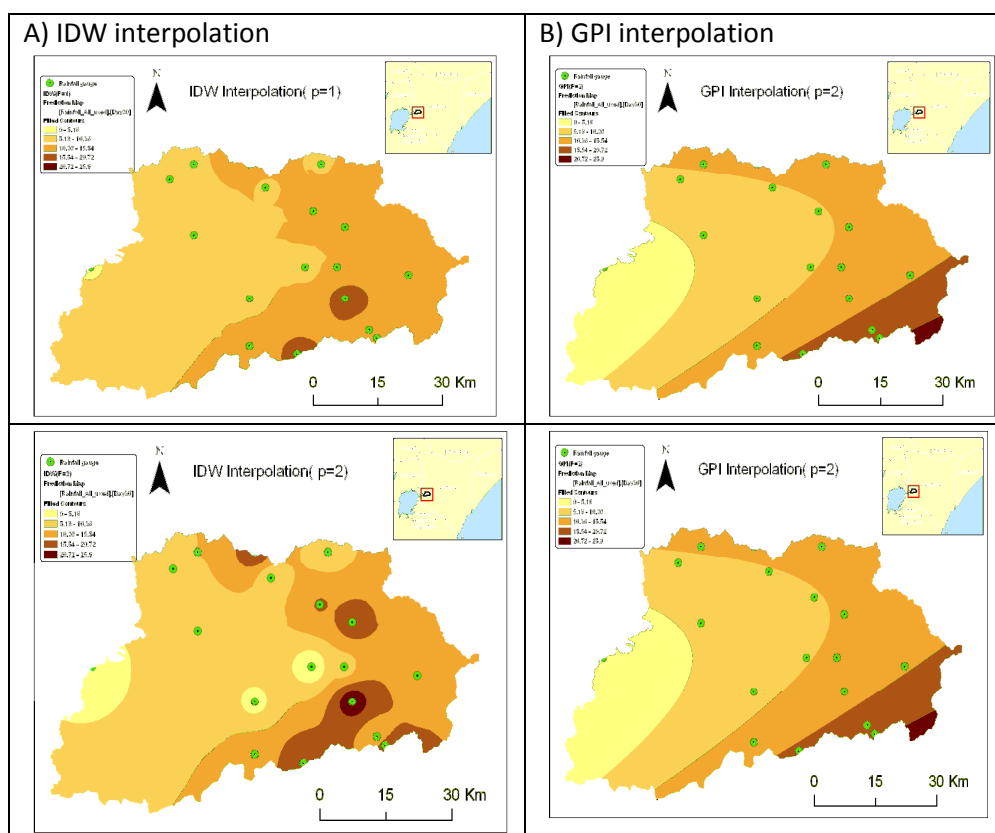
Standardized root-mean-squared prediction (RMSS): If the root-mean-squared standardised errors are greater than 1, then there's underestimating of variability in the predictions; if the root-mean-squared standardized errors are less than 1, then the system is overestimating variability in the predictions.

## **4.0 Results**

Due to lack of adequate data, cross validation was used in which each of the stations was omitted from the interpolation, new values for the same station were derived and then compared to the true (observed) value. This was done for all the stations iteratively. Results presented as map and charts are for 30<sup>th</sup> April 1968 (day 30) while tables are used to present the remaining days.

### 4.1 IDW and GPI interpolations

The IDW method required two levels of decision to implement, the power ( $p$ ) and neighborhood search. Figure 2 shows the IDW (A) and GPI (B) interpolated surfaces with ( $p=1, 2, 3$ ) respectively. The south west section of the basin has only one station and this explains the uniform gradual decrease in rainfall around this region for all the interpolators. In contrast to the  $p=1$  interpolation, IDW interpolation with  $p=2$  produces smoother surfaces with gradual transition of rainfall. A “hull effect” (circle around the data) forms in the interpolated surfaces for the IDW. It was clearly demonstrated that the larger the value of  $p$  the larger the RMSE. Interpolation for the rest of the study period was implemented with  $p=1$  for IDW.



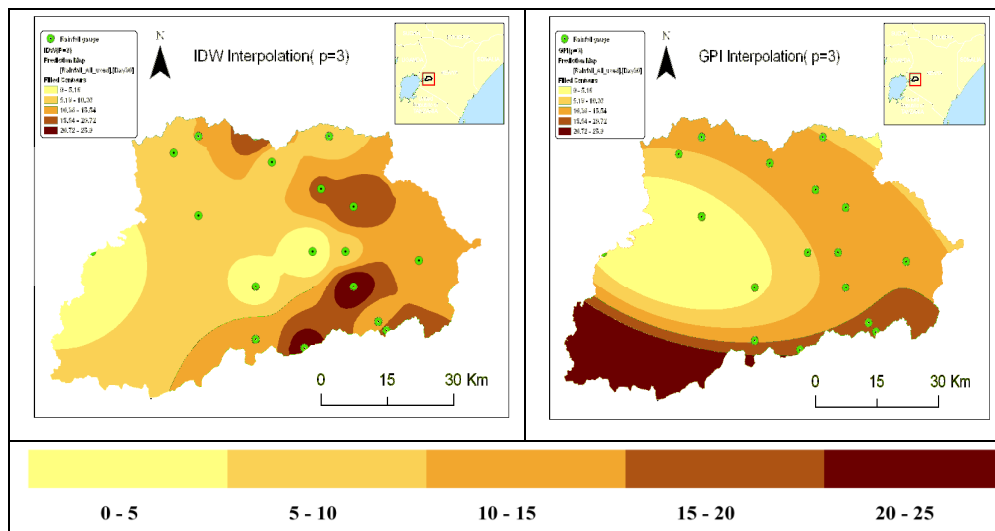


Figure 2: IDW (A) and GPI (B) interpolation surfaces generated using different values of power  $p$ . From top to bottom,  $p = 1, 2, 3$

The GPI method required the least of decisions to implement; only power ( $p$ ). The interpolation method produced surfaces characterized by stripping and devoid of the hull effect. However, the transition from one value to the other is drastic and quite unrealistic. Unlike when  $p=1$ , the GPI interpolator with  $p=2$  tends to smoothen the surface and captures the trend in the rainfall observations, with the low amounts recorded to the south west location of the basin. Transition is extremely uniform and quite unrealistic. GPI with  $p=3$  produced the poorest results with the largest error (RMSE=11.37). The method over-estimates rainfall over the southern parts of the basin where the stations recorded the least amounts of rainfall. For the remaining interpolations, GPI was implemented using  $p=2$ .

#### 4.2 Kriging

Figure 3 shows a scatter plot (prediction versus observations) for the kriging method on day 30.

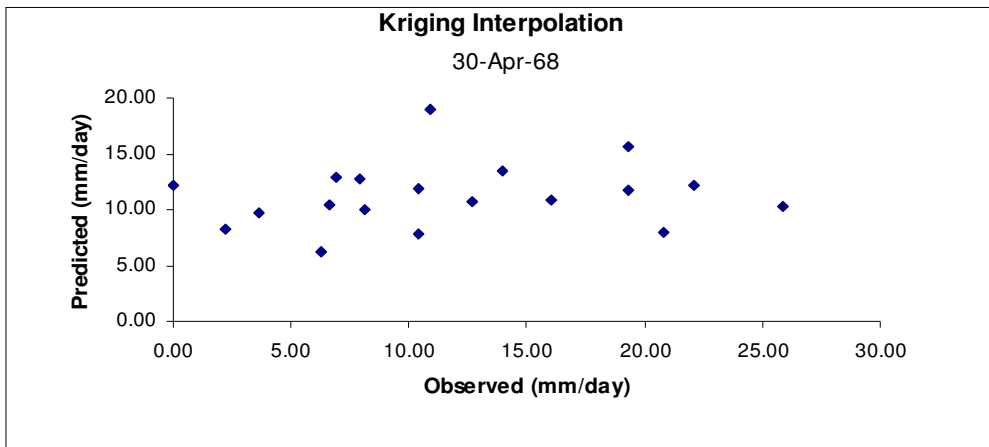


Figure 3: Kriging interpolation: predicted versus observed for 30<sup>th</sup> April 1968

The RMSE for the selected day 30 is 7.016, ASE=6.856 and Mean=0.009. A comparison was also done between the Gaussian and Spherical models (figure 4).

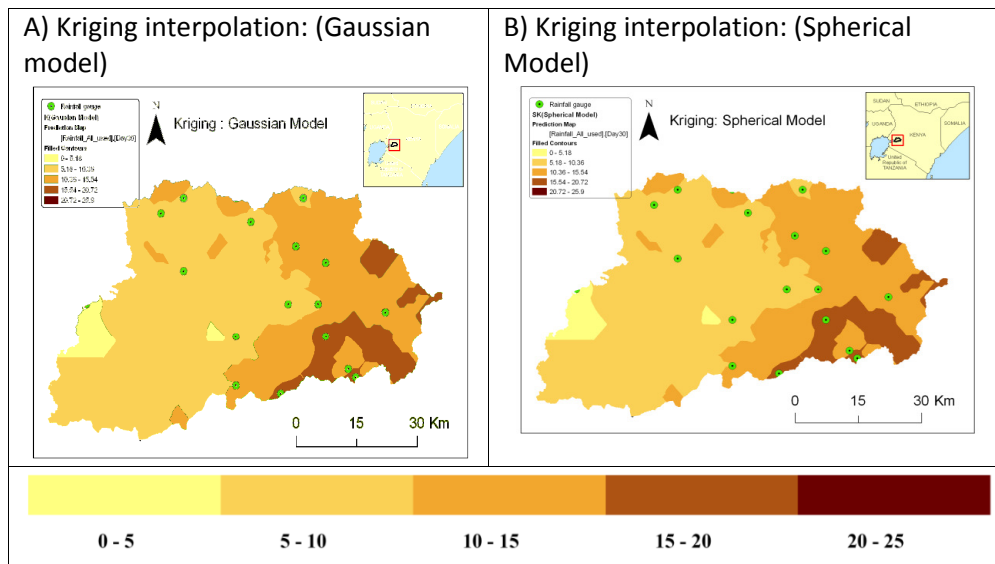


Figure 4: Kriging interpolation (A) using Gaussian model and (B) using spherical model

The difference between the two is minimal and in both cases the RMSE was the same. The Gaussian model was then used for the rest of the interpolations.

#### 4.4 Cokriging

Cokriging works by coupling primary data and secondary data.



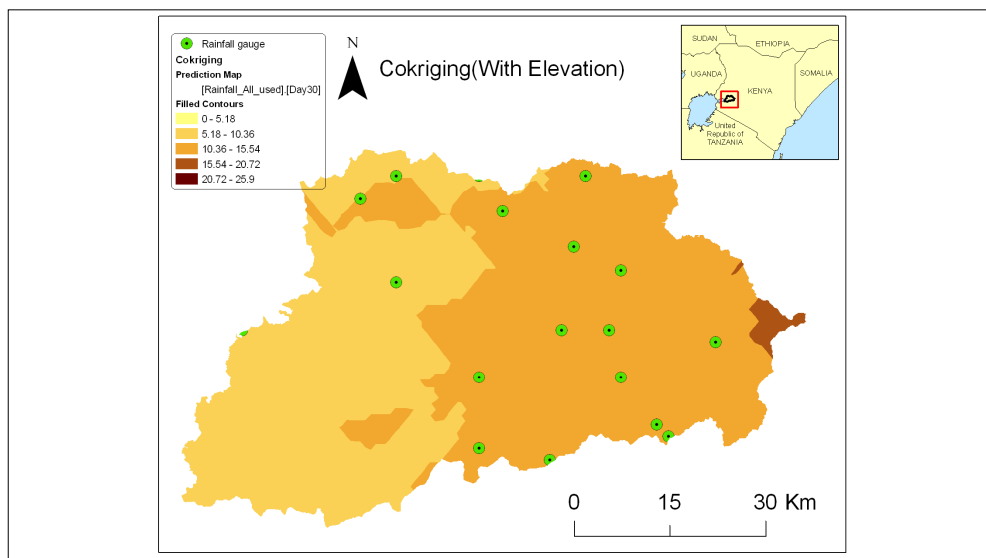


Figure 5: Cokriging interpolation (Day 30)

Figure 5 shows the output from the cokriging interpolator using gauge data coupled with 90m elevation data (DEM). The method produces similar results to kriging though it has a rugged spatial representation and gives the interpolation a more natural appearance. The interpolator does not reproduce high rainfall amounts but produces moderately averaged estimates.

#### 4.5 Comparison between the Interpolation Techniques

Generally, the best model is the one that has the standardized mean nearest to zero, the smallest root-mean-squared prediction error, the average standard error nearest the root-mean-squared prediction error, and the standardized root-mean-squared prediction error nearest to one.

##### 4.5.1 IDW versus GPI

The results produced by GPI are simple, and somehow unrealistic. The method does not reproduce the natural pattern that a rainfall event would exhibit. IDW on the other hand produces slightly better results but is highly affected by the hull effect around the stations. This is because more weight is given to the closest station. Comparatively, IDW produced better results than the GPI interpolator.

##### 4.5.2 Kriging versus Cokriging

Comparison between the two kriging methods was done using error statistics. This is because the spatial surfaces produced were similar and visual interpretation would be insufficient. Figure 6 summarizes error parameters.

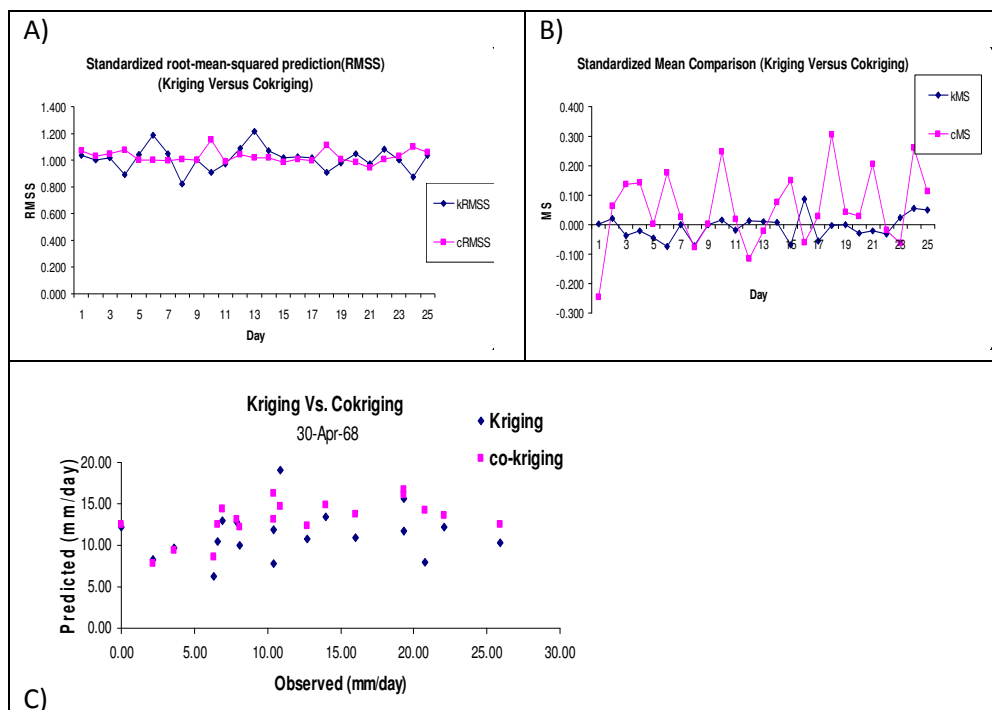


Figure 6: Comparison of RMSS (A) and RMSE (B) for kriging and cokriging; and (C) predicted versus measured rainfall for day 30

Cokriging produced better RMSE (cRMSE) (figure 6A) compared to kriging (kRMSE) for most of the days under investigation. This improvement is attributed to the inclusion of elevation data as secondary source of information. Kriging interpolation represents rainfall well with most of the standardized mean (Figure 6(B)) values close to 0 compared to cokriging whose values are above 0.1. In terms of variability, cokriging scores better than kriging because all its RMSS values are close to 1 as shown in figure 6(A). Figures 6 (C) shows a scatter plot for the two geostatistical interpolators for day 30.

### 4.5.3 Overall evaluation

Evaluation for all the interpolation techniques was only possible by comparing the common measures of reliability. Table 3 summarizes the RMSE for all the interpolators.

Table 3: RMSE values for all the Interpolators

Date	IDW	Kriging	Cokriging	GPI
5-Jan-88	6.88	7.31	6.00	45.00
14-Jun-91	10.71	9.62	8.70	51.24
13-Jun-91	12.88	13.20	11.13	53.09
1-Mar-62	5.82	5.23	5.23	53.14

18-Apr-73	7.44	5.82	5.24	25.08
25-Jun-91	3.42	3.77	2.58	50.23
21-Aug-70	5.60	5.18	4.86	25.13
19-Feb-62	5.18	4.34	5.43	44.46
24-Jun-91	6.69	5.71	5.07	50.08
17-Aug-70	8.15	7.84	7.77	26.13
13-Apr-73	1.23	1.14	1.09	23.69
6-Jan-88	5.39	5.14	4.57	44.25
26-Jan-62	0.95	0.99	0.84	52.84
9-May-73	9.76	9.21	8.64	37.56
14-Aug-70	6.33	7.69	6.75	27.49
15-Dec-81	9.75	9.72	8.11	35.48
21-Apr-73	8.45	6.41	5.83	25.16
23-Aug-70	5.36	5.00	5.26	26.08
22-Apr-73	8.59	7.51	7.22	25.85
28-Feb-62	2.28	2.05	1.80	43.91
19-Aug-70	10.54	9.71	8.10	27.51
25-Aug-70	8.58	7.60	7.06	26.09
4-Jan-88	2.31	2.06	1.93	43.54
24-Aug-70	7.31	6.53	6.66	26.28
Average	6.65	6.19	5.66	37.05

GPI produced the largest values of RMSE for all the days under investigation. IDW, Kriging and cokriging produced comparable results with cokriging producing the best results (least RMSE).

#### 4.6 Discussion and conclusions

This study aimed at interpolating rain gauge observations into spatial surfaces using IDW, GPI, Kriging, and cokriging interpolators. Thirty days of study were selected and spatial surfaces generated. The performance of the interpolators was evaluated by visual inspection of the generated surfaces as well as analysis of reliability measures. GPI produced the poorest results with surfaces characterized by massive stripping and large values of RMSE. IDW on the other hand produced better results compared to GPI but was limited due to the "hull effect". For this purpose, they are quite unsuitable for rainfall interpolation especially if the gauge stations are sparsely located. Though IDW produced better results than GPI, it placed more weight to the nearest stations. The cokriging interpolator was used by combining observations with a 90m DEM as secondary information. While it was impossible to differentiate between kriging and cokriging from the interpolated surfaces visually, evaluation of measures of reliability showed that cokriging produced the best results. It produced the least values of RMSE and the best values of the standardized root-mean-squared prediction error nearest to one, implying that cokriging represented variability well in the interpolation.

While these findings suggest better performance of co-kriging using elevation, further research is recommended to incorporate more days in the study and investigate the inherent relationship between rainfall and elevation. Research on the incorporation of other sources of secondary spatial data into cokriging (e.g radar) to improve the interpolations would be useful.

### Acknowledgement

The authors would like to thank the department of Biomechanical and Environmental Engineering (BEED), Jomo Kenyatta University of Agriculture (JKUAT) for the provision of data. We appreciate the department of Geospatial Engineering and Geospatial Information Systems (GEGIS) for the provision of GIS tools. We are grateful to the editor and anonymous reviewers for their constructive and valuable comments which greatly improved the quality of this paper.

### References

- Ali M. Subyani (2005). Geostatistical study of annual and seasonal mean rainfall patterns in southwest Saudi Arabia. *Hydrological Sciences–Journal–des Sciences Hydrologiques*, **49**(5).
- Borga M. and Vizzaccaro A. (1997). On the interpolation of hydrological variables: formal equivalence of multiquadratic. *Journal of Hydrology*, **195**, pp. 160–171.
- Chen. D. and Johansson. B. (2003). The influence of wind and topography on precipitation distribution in Sweden: statistical analysis and modelling. *International Journal of Climatology*, **23**, pp. 1523-1535.
- Englund E. J. and Weber D. D. (1994). Evaluation and comparison of spatial Interpolators. *Mathematical Geology*, pp. 589 -603.
- ESRI. (2007). *ArcGIS 9.2 help*. Retrieved December 16, 2008, from ESRI: <http://webhelp.esri.com/arcgisdesktop/9.2/index.cfm?>
- Eulogio Pardo-igu' Zquiza (1998). Comparisons of geostatistical methods for estimating areal average climatological rainfall mean using data on precipitation and topography. *International journal of climatology, Int. J. Climatol.*, **18**, pp. 1031–1047
- Goovaerts P. (2000). Geostatistical approaches for incorporating elevation into the spatial interpolation of rainfall. *Journal of Hydrology*, pp. 113–129.
- Isaaks E. and Srivastava R. (1992). *An Introduction to Applied Geostatistics*. New York: Oxford University Press.
- Johnston K., Ver Hoef J., Krivoruchko. K. and Lucas. N. (2001). *Using ArcGIS Geostatistical Analyst*. Redlands CA: ESRI.
- Marquínez J., Lastra J. and García, P. (2003). Estimation models for precipitation in mountainous regions: the use of GIS and multivariate analysis. *Journal of Hydrology*. **270**, pp. 1-11.

Nalder I. and Wein R. (1998). Spatial interpolation of climatic normals: test of a new method in the Canadian boreal. *Agricultural and Forest Meteorology*, **92**, pp. 211–225.

Vicente-serrano S.M., Saz-sánchez. M.A. and Cuadrat. J.M. (2003). Comparative analysis of interpolation methods in the middle Ebro Valley (Spain): application to annual precipitation and temperature. *Climate research.*, **24**, pp. 161-180.

Sumner G. (1998). *Precipitation: Process and Analysis*. New York: John Wiley.

Swallow B., Onyango. L. and Meinzen-Dick. R. (2005). *Catchment Property Rights and the Case of Kenya's Nyando Basin*. Nairobi: World Agroforestry Agro forestry Centre.

Symeonakis E. (2008). A comparison of Rainfall estimation techniques for sub saharan Africa. *International Journal of Applied Earth observation Geoinformatics*.